

LIFE IN A BUBBLE

Host cell refurbishment by the malaria parasite

Joachim Michael Matz

Cover: *Plasmodium berghei* expressing cytoplasmic GFP (green) and mCherry-labelled translocon component heat shock protein 101 (red).
Printed by: Off Page
ISBN: 978-94-6182-722-7

© Joachim Michael Matz, 2016

All rights reserved. No parts of this publication may be reproduced or transmitted in any form or by any means without prior written permission of the author and the publisher holding the copyrights of the published articles.

The research described in this thesis was performed at the Department of Medical Microbiology, Radboud University Medical Center, Radboud Institute for Molecular Life Sciences, Nijmegen, The Netherlands, and in the Max Plack Institute for Infection Biology, Parasitology Unit, Berlin, Germany. The publication of this thesis was financially supported by the Radboud University Nijmegen.

LIFE IN A BUBBLE

Host cell refurbishment by the malaria parasite

Proefschrift

ter verkrijging van de graad van doctor
aan de Radboud Universiteit Nijmegen
op gezag van de rector magnificus prof. dr. J.H.J.M. van Krieken
volgens besluit van het college van decanen

en

ter verkrijging van de graad van doctor rerum naturalium
in de biologie / parasitologie
aan de Humboldt-Universität zu Berlin
op gezag van de president prof. dr.-Ing. habil. dr. S. Kunst

in het openbaar te verdedigen op donderdag 17 november 2016
om 10:30 uur precies

door

Joachim Michael Matz
geboren op 20 juli 1987
te Potsdam, Duitsland

Promotoren: prof. dr. Robert W. Sauerwein
prof. dr. Kai Matuschewski (Humboldt-Universität zu Berlin,
Duitsland)

Copromotor: dr. Taco W.A. Kooij

Manuscriptcommissie: prof. dr. Mike S.M. Jetten
prof. dr. Andreas Herrmann (Humboldt-Universität zu
Berlin, Duitsland)
prof. dr. Mike J. Blackman (London School of Hygiene and
Tropical Medicine, London, Verenigt Koninkrijk)

LIFE IN A BUBBLE

Host cell refurbishment by the malaria parasite

Doctoral Thesis

to obtain the degree of doctor
from Radboud University Nijmegen on the authority of
the rector magnificus prof. dr. J.H.J.M. van Krieken
according to the decision of the council of deans
and
to obtain the degree of doctor rerum naturalium
in biology / parasitology
from Humboldt-Universität zu Berlin
on the authority of the president prof. dr.-Ing. habil. dr. S. Kunst

to be publicly defended on Thursday, November 17, 2016
at 10:30 hours

by

Joachim Michael Matz
born on July 20, 1987
in Potsdam, Germany

Supervisors: prof. dr. Robert W. Sauerwein
 prof. dr. Kai Matuschewski (Humboldt-Universität zu Berlin,
 Germany)

Co-supervisor: dr. Taco W.A. Kooij

Thesis Committee: prof. dr. Mike S.M. Jetten
 prof. dr. Andreas Herrmann (Humboldt-Universität zu
 Berlin, Germany)
 prof. dr. Mike J. Blackman (London School of Hygiene and
 Tropical Medicine, London, United Kingdom)

LIFE IN A BUBBLE

Host cell refurbishment by the malaria parasite

Inauguraldissertation

zur Erlangung der Doktorwürde

von der Radboud Universiteit Nijmegen

im Namen des Rector magnificus Prof. Dr. J.H.J.M. van Krieken,

nach dem Beschluss des Kollegiums der Dekane

und

zur Erlangung des Grades Doktor rerum naturalium

im Fach Biologie / Parasitologie

von der Humboldt-Universität zu Berlin

im Namen der Präsidentin Prof. Dr.-Ing. habil. Dr. S. Kunst

öffentlich zu verteidigen am Donnerstag, dem 17. November 2016

um 10:30 Uhr

von

Joachim Michael Matz

geboren am 20. Juli 1987

in Potsdam, Deutschland

Betreuer: Prof. Dr. Robert W. Sauerwein
Prof. Dr. Kai Matuschewski (Humboldt-Universität zu Berlin,
Deutschland)

Co-Betreuer: Dr. Taco W.A. Kooij

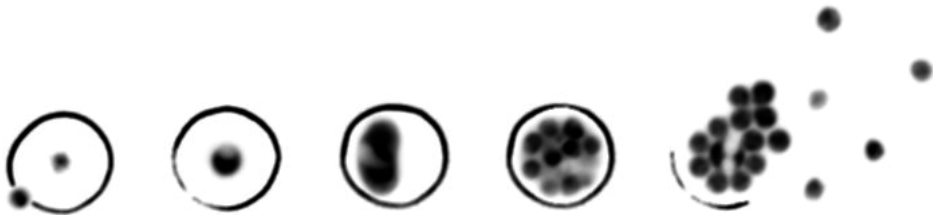
Prüfungskommission: Prof. Dr. Mike S.M. Jetten
Prof. Dr. Andreas Herrmann (Humboldt-Universität zu
Berlin, Deutschland)
Prof. Dr. Mike J. Blackman (London School of Hygiene and
Tropical Medicine, London, Großbritannien)

TABLE OF CONTENTS

Chapter 1	Host cell remodeling by the malaria parasite	11
Chapter 2	Towards genome-wide experimental genetics in the <i>in vivo</i> malaria model parasite <i>Plasmodium berghei</i>	39
Chapter 3	Two putative protein export regulators promote <i>Plasmodium</i> blood stage development <i>in vivo</i>	71
Chapter 4	<i>In vivo</i> function of PTEX88 in malaria parasite sequestration and virulence	107
Chapter 5	The <i>Plasmodium berghei</i> translocon of exported proteins reveals spatiotemporal dynamics of tubular extensions	131
Chapter 6	General discussion	169
Abstract	Summary	213
	Samenvatting	214
	Zusammenfassung	215
Acknowledgements	217
List of publications and cover images	219

Chapter 1

Host cell remodeling by the malaria parasite



THE *PLASMODIUM* LIFE CYCLE

Parasites of the genus *Plasmodium* are the causative agent of malaria. These unicellular organisms pose a major threat to global health and significantly affect the economics of developing countries. In 2015, approximately 438,000 people died of malaria, with most deaths occurring in children under five years of age. Roughly 90% of malaria-related deaths occur in sub-Saharan Africa.¹ *Plasmodium falciparum* is the most deadly species of the human malaria parasites and due to its high virulence, accounts for most malaria-related deaths. Though extremely dangerous, *Plasmodium* parasites are highly fascinating organisms. They progress through a very complex life cycle, in which they alternate between a vertebrate and an arthropod host. During its sexual and asexual development, this remarkable organism faces different environments and stage transition periods. Consequently, malaria parasites have evolved a multitude of specific adaptations to ensure their survival, transmission and genetic recombination.

Plasmodium parasites are transmitted during the blood meal of an infected female *Anopheles* mosquito. During the initial phase of proboscis probing, the infectious sporozoites are deposited into the skin via the saliva of the mosquito.² Here, the motile sporozoites become activated and migrate actively into blood vessels, by which they are transported to the hepatic circulatory system.³ Upon arrival in the liver sinusoids, the sporozoite breaches both liver resident macrophages (the so-called Kupffer cells) and several hepatocytes by a mechanism called cell traversal.^{4,5} While the sporozoite is a motile, non-proliferative and extracellular form, its final invasion of a liver cell initiates a prolonged period of intracellular growth and proliferation. During this clinically silent stage of development, the parasite divides into thousands of daughter merozoites, usually between 10,000 and 30,000.⁶ Additionally, some malaria parasite species like the human pathogens *P. vivax* and *P. ovale* form dormant liver stages, the so-called hypnozoites. These parasite forms persist for many years and can eventually re-establish blood infection.⁷

Upon final segregation, the newly formed merozoites are released into the blood stream, where they subsequently invade the vastly available erythrocytes.⁸ In these cells they thrive by digesting hemoglobin and by fermenting blood glucose, passing through the ring, trophozoite and schizont stage. The intraerythrocytic parasite divides into 8 to 36 merozoites in a process called merogony. Eventually, the newly

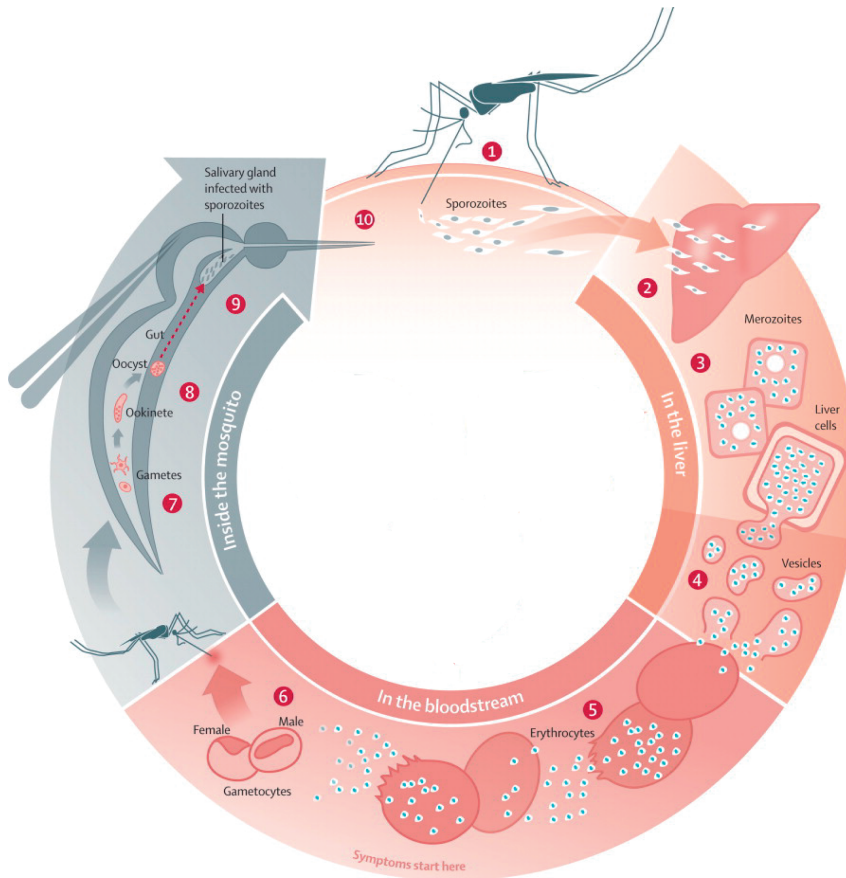


Figure 1 | Life cycle of the malaria parasite (after Crawley *et al.*, 2010).¹⁸ During the blood meal of an infected female *Anopheles* mosquito (1), the salivary gland sporozoites are released into the blood stream of the intermediate host, where they first invade liver cells (2). Inside the hepatocytes the parasites replicate by schizogony and form many merozoites (3), which are released in vesicles called merozoites (4). After the merozoites egress from the merozoites, they invade red blood cells, in which they undergo repeated cycles of replication, causing the symptoms of malaria (5). Some parasites develop into sexually differentiated gametocytes (6), which are taken up by a female mosquito during a blood meal. Inside the *Anopheles* midgut, the male gametocytes exflagellate, giving rise to the motile microgametes. The microgametes then fuse with the female macrogametes, which develop from the female gametocytes (7). The zygote differentiates into a motile ookinete, which traverses the midgut epithelium and encysts at the basal lamina (8). In the developing oocyst, sporozoites are formed by the process of sporogony. When released into the hemolymph, they migrate to the salivary glands of the mosquito (9) to be injected during the next blood meal (10).

formed daughter merozoites rupture their old host cell and invade new erythrocytes.⁹ As opposed to the liver stage development, these repeated cycles of erythrocyte invasion, growth and lysis elicit a multitude of adverse effects and are the sole cause for the symptoms of malaria, which include severe anemia and fever.¹⁰

While this cycle of asexual blood stage propagation continues, some intraerythrocytic parasites commit to sexual differentiation by forming gametocytes. Gametocytes do not give rise to a new generation of daughter merozoites but differentiate in preparation for the mosquito stage of infection.¹¹ Once taken up during a blood meal, the gametocytes are activated by a change in temperature, pH and chemical composition of the extracellular milieu.¹² Upon activation, the gametocytes egress from their host cells.¹³ While the female gametocyte transforms into the rather static female macrogamete, the male gametocyte undergoes a spectacular transformation: during the process of exflagellation, eight whip-like microgametes are formed in a matter of minutes, each harboring its own nucleus. Under rapid movement the microgametes disconnect from the male gametocyte and swim freely in the lumen of the midgut.¹⁴ Once they encounter a macrogamete they attach and fuse, thereby forming the diploid zygote. In order to escape the adverse midgut environment, the zygote transforms into the motile crescent-shaped ookinete, which traverses the midgut epithelium and establishes mosquito infection.¹⁵ Once the basal lamina is reached, the ookinete encapsulates to form a continuously growing oocyst. Behind the thick oocyst wall, the parasite multiplies by a process called sporogony, giving rise to a multitude of sporozoites. Once, maturation is complete, the oocyst wall is lysed in a protease dependent manner and the sporozoites enter the hemocoel.¹⁶ Here, they gain access to the mosquito salivary glands, which are invaded in preparation of a new vertebrate host infection.¹⁷ For an overview of all *Plasmodium* life cycle stages, the reader is referred to Figure 1 of this chapter and Figure 1 of chapter 2.

CHALLENGES OF RED BLOOD CELL INFECTION

As is obvious from its complex life cycle, the malaria parasite has to face different challenging environments and has evolved complex strategies to survive in both its vertebrate and invertebrate host. Probably most astonishing is the parasite's ability

to develop and multiply inside of red blood cells (RBCs), especially since neither viruses, nor bacteria are able to thrive in this terminally differentiated cell type. The human erythrocyte can easily be regarded as a 'metabolic wasteland', because it consists almost entirely of hemoglobin. Although it is efficiently digested by the parasite,¹⁹ hemoglobin is devoid of isoleucin. In addition, other amino acids like proline, cysteine, methionine and glutamate are not very abundant and cannot cover the parasite's metabolic requirements. Furthermore, several other essential compounds, like pantothenic acid, are scarcely available.²⁰

The RBC exhibits a rather tuned-down metabolism that mainly serves to maintain the plasma membrane potential, but does not allow for any biosynthetic activity or major ATP generation.²¹ Therefore, the erythrocyte does not offer any renewable pools of nutrients, carbon scaffolds or energy, that can be exploited by the parasite. However, like most rapidly growing and multiplying cells, the *Plasmodium* parasite requires enormous amounts of organic molecules, both for efficient biomass production and energy generation.²² The parasite's central carbon metabolism relies almost entirely on the fermentation of glucose to lactate,^{23,24} and strategies for efficient nutrient uptake and waste product disposal need to be in place. Consequently, the parasite needs to enhance the permeability of the RBC membrane to meet the metabolic demands of rapid cell proliferation.

Given the circumstances, it becomes clear that survival inside the erythrocyte requires an extensive array of parasite-derived mechanisms, by which the properties of the RBC can be altered. However, classical trafficking pathways are absent from the erythrocyte and cannot be exploited to that end, posing a logistical challenge for the parasite. The transport of proteins and lipids through the infected cell first requires the *de novo* genesis of an extraparasitic trafficking machinery in the RBC cytosol, underlining the necessity for the parasite to extensively refurbish its environment as a means of enabling efficient host cell manipulation.

***PLASMODIUM*-INDUCED MEMBRANE SPACES**

The parasitophorous vacuole and the tubovesicular network

During the invasion of a RBC, the first compartment of the parasite-derived trafficking pathway is formed. The free merozoite attaches tightly to its new host

cell and invaginates the erythrocyte membrane. By a complex interplay of parasite motility and protein secretion, the merozoite glides through a ring-shaped protein complex, the so-called moving junction, that connects both parasite surface and host plasma membrane. After the merozoite has entered the erythrocyte, it resides inside a membranous compartment, known as the parasitophorous vacuole (PV).²⁵⁻

27

Throughout its whole intraerythrocytic development, the parasite thrives within the boundaries of the PV membrane (PVM). Studies have shown that most material of the early PVM is derived from the erythrocytic plasma membrane.^{28,29} However, as the parasite matures, the surface of the PVM increases, suggesting that lipids and proteins are actively incorporated into the growing membrane. The PVM is in close proximity to the plasma membrane of the parasite, suggesting a rather small volume of the PV lumen. However, during parasite maturation large membrane whorls emerge from the surface of the vacuole, forming a tubovesicular network (TVN).³⁰⁻³² This network has been implied in the delivery of nutrients, since blocking TVN assembly with a specific inhibitor diminished the incorporation of exogenously supplied fluorescent dyes, amino acids and nucleosides into *P. falciparum* parasites.³³ These results lead to the idea that temporary junctions between the TVN and the RBC membrane may act as a molecular sieve that allows entry of several nutrients and low molecular weight compounds into the PVM and subsequently into the parasite.³³ A competing model has suggested the presence of a permanent connection between PV-derived extensions and the RBC membrane, the highly controversial 'parasitophorous duct'.³⁴ However, formal proof for a transient or permanent continuity of serum and PV has not been presented, leaving the mechanism of TVN-mediated nutrient import unknown.

Maurer's clefts

In the human malaria parasite *P. falciparum*, the infected RBC shows additional membranous features, the so-called Maurer's clefts (MCs). MCs are parasite-derived discoid cisternae, which are bound by a single membrane. They are approximately 500 nm wide and usually underlie the erythrocyte surface (Figure 2 b and c).³⁵⁻³⁷ These structures are believed to originate from the PVM.³⁸ However, there is still debate, whether the MCs form a continuum with the PV/TVN or if they are detached from their origin of genesis. While some studies using lipid dyes and

electron microscopy, suggest a highly connected membrane network, which includes the PV, TVN and the MCs,^{36,39} a multitude of other studies did not observe any protein or lipid exchange between MCs and the PV lumen.^{37,38,40,41} MCs are formed rather early and their number remains constant already 8 hours post invasion.⁴² During the early phase of infection, the newly formed MCs are highly dynamic and their position inside the RBC changes frequently. However, with the onset of the trophozoite stage (~20 hours post invasion), the MCs appear to become fixed at specific sites under the erythrocyte plasma membrane, where they remain until shortly before merozoite egress.^{42,43} Indeed, tether-like structures appear to immobilize the MCs by attaching them to the subpellicular RBC cytoskeleton.^{37,41,44} The MCs have an important function in trafficking parasite derived virulence factors to the erythrocyte surface, which will be discussed in more detail below.

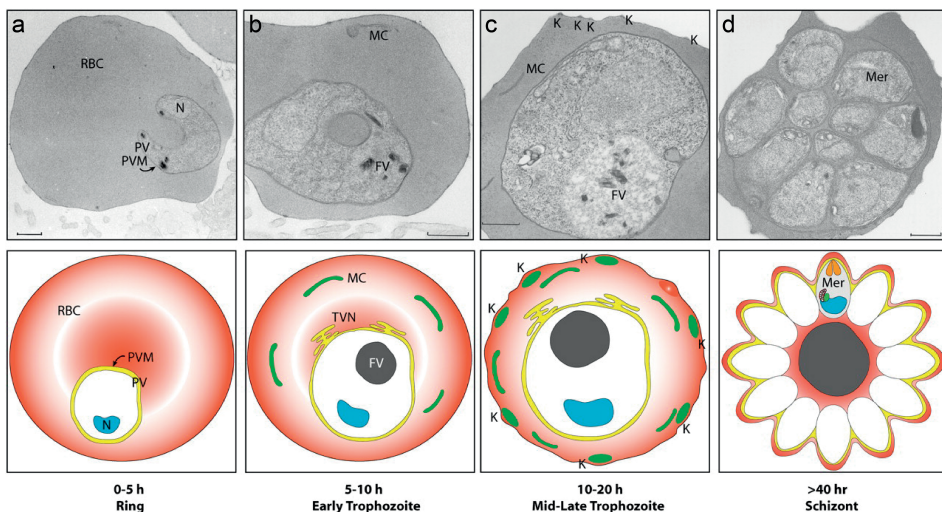


Figure 2 | Refurbishment of the infected erythrocyte by *Plasmodium falciparum* (after Marti *et al.*, 2005).⁴⁵ (a) During intraerythrocytic development, the malaria parasite resides within the parasitophorous vacuole (PV), which is bound by the parasitophorous vacuole membrane (PVM). (b) While growing inside the red blood cell (RBC), the parasite induces the formation of a tubovesicular network (TVN), which originates from the PV. During the early trophozoite stage, the Maurer's clefts (MC) emerge and detach from the PV. (c) These compartments become fixed beneath the RBC surface during the mid to late trophozoite stage and participate in the genesis of the knobs (K) and the cytoadherence complex. (d) During merozoite (Mer) formation, TVN and MCs become less apparent. Transmission electron micrographs and schematic representations of the respective developmental stages are shown. N, nucleus; FV, food vacuole; Bars, 0.5 μ m.

EXPORTED PROTEINS AND THEIR FUNCTIONS

During its asexual development, the *Plasmodium* parasite creates multiple complex membrane spaces inside the erythrocyte in order to establish new reaction compartments in the otherwise desolate host cell (Figure 2). However, it is clear that the alteration of RBC properties cannot simply rely on the biogenesis of membranous features, but is in most parts carried out by parasite-derived proteins. In order to manipulate the RBC, the parasite releases these proteins into the space of the PV by the action of its default secretory pathway.⁴⁶ From this highly specialized host-parasite interface, the cargo is transported to diverse locations inside the host cell, including the erythrocyte cytoplasm, plasma membrane, cytoskeleton, the MCs, and several small dynamic vesicles. Indeed, ~10% of all *P. falciparum* proteins are believed to be exported into the infected RBC.⁴⁷⁻⁴⁹

New permeability pathways

As mentioned above, the *Plasmodium* parasite needs to alter the permeability of the RBC to accommodate its metabolic demands. It has been shown in several studies, that the permeability of multiple compounds, including carbohydrates, amino acids and nucleosides, is significantly increased upon *Plasmodium* infection.^{20,50-53} This phenomenon has been termed the new permeability pathway (NPP, Figure 3). While the TVN and the ominous parasitophorous duct have been implicated in this process,^{33,34} there is growing evidence that parasite-encoded channels in the erythrocyte membrane are responsible for the altered uptake profile of the infected cell. This has been elegantly shown by Baumeister and colleagues (2006):⁵⁴ chymotrypsin treatment of infected erythrocytes completely abolished NPP activity. Strikingly, erythrocyte permeability increased progressively after removal of the protease. Since the RBC has lost its ability of *de novo* synthesis, parasite-derived surface proteins appear to be responsible for the increased conductance of the host cell. Even though the phenomenon of enhanced permeability has long been recognized, only the different isoforms of exported cytoadherence-linked asexual protein 3 (CLAG3) were shown to enhance the uptake properties of the RBC.⁵⁵ Other exported proteins involved in the NPP are yet to be identified. After crossing the host cell membrane, imported solutes are transported across the PVM *via* unspecific pores, which display an exclusion size

of approximately 1.4 kDa.⁵⁶ The nature of these pores is yet unknown and remains to be determined. Further import into the parasite is thought to be catalyzed by an array of transporters on the parasite plasma membrane.^{57,58}

A competing, but not exclusive, scenario favors the modulation of endogenous erythrocyte transporters by the parasite.²⁰ Nonetheless, export of parasite-derived proteins to the RBC surface would still be a prerequisite for the manipulation of the erythrocytic permeability. It remains a matter of speculation, how the modulation of host cell transporters could be achieved. However, the export of protein kinases by the parasite might offer a plausible mechanism, since transporter kinetics have been shown to be phosphorylation-sensitive.⁵⁹ Indeed, most of the apicomplexan-specific FIKK kinases of *P. falciparum* are predicted to be exported,⁶⁰ and the kinase FIKK4.1 was shown to efficiently phosphorylate erythrocyte dematin.⁶¹ While FIKK4.1 and many other members of this family are most likely involved in cytoskeletal alterations,^{61,62} it is possible that other exported kinases serve to manipulate erythrocyte transporter characteristics.

The cytoadherence complex

Although it is essential for the parasite to alter the erythrocyte's properties, it also counteracts the only advantage of RBC infection: staying invisible. RBCs do not express molecules of the major histocompatibility complex (MHC) at their surface, nor do they have the capacity to actively process pathogenic proteins and display them to T-lymphocytes. Therefore, the parasite would remain undetectable during its intraerythrocytic growth, if it were not for the changes it inflicts upon its host cell. Due to its continuous growth and the massive rearrangements of the host cell surface and cytoskeleton, the RBC loses its flexibility, which is required to pass through the tiny capillaries of the peripheral tissues and through the interendothelial slits of the spleen.⁶³⁻⁶⁵ As a consequence of the increased rigidity, the infected erythrocyte is no longer invisible to the host and is filtered out by the spleen as a measure of RBC quality control.^{66,67} This phenomenon has led to highly complex counteradaptations which serve to avoid splenic passage of the infected cell.

The clinically most significant and remarkable adaptation of *P. falciparum* against splenic clearance is the biogenesis of the cytoadherence complex (Figure 4b). This highly organized protein apparatus is located beneath the erythrocyte surface and

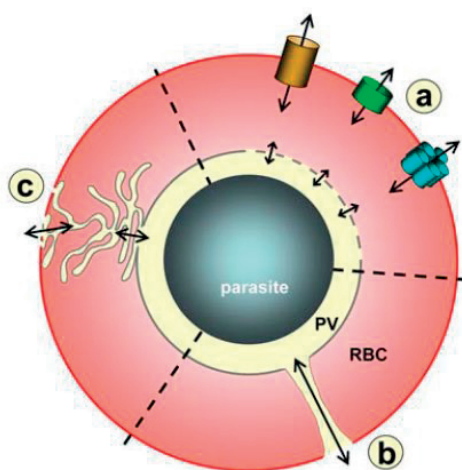


Figure 3 | Possible strategies of nutrient acquisition by the malaria parasite (after Baumeister *et al.*, 2010).²⁰ During blood infection, *Plasmodium* parasites enhance the permeability of the infected red blood cell (RBC) for several metabolites. Three possible mechanisms are shown. (a) The parasite exports transporters to the red blood cell surface or modulates endogenous host cell transporters to enhance permeability. (b) A 'parasitophorous duct' forms a

constant connection between the erythrocyte membrane and the membrane of the parasitophorous vacuole (PV), thereby promoting direct access to metabolites in the host serum. (c) Processes of the tubovesicular network transiently connect with the erythrocyte plasma membrane and act as a nutrient import network. In all scenarios, nutrient import across the plasmodial plasma membrane is carried out by transporters on the parasite surface.

serves to display the major virulence factor *P. falciparum* erythrocyte membrane protein 1 (*PfEMP1*) on the host cell plasma membrane. *PfEMP1* tethers the infected cell to endothelial ligands, thereby immobilizing the erythrocyte and avoiding splenic clearance.⁶⁸ By this mechanism, most parasites sequester to peripheral tissues, as they progress from the trophozoite to the schizont stage, during which form and physical properties of the infected RBC become increasingly aberrant.⁶⁹ Due to their immobilization in peripheral tissues, mature schizonts are rarely observed in the circulation.

PfEMP1 is an adhesion factor of 200 – 300 kDa, which is encoded by the ~59 genes of the *var* gene family, each giving rise to a different variant of this crucial virulence factor.⁷⁰⁻⁷² Because of its prominent exposure on the infected RBC surface, *PfEMP1* is an immunodominant antigen, that can elicit significant immune responses.^{73,74} The parasite is able to switch the expression of *PfEMP1* from one *var* gene to another, once a specific immune response is initiated, thereby confronting the host with a yet unknown antigen variant and rendering the generated immune response powerless. Consequently, *P. falciparum* parasites express only one *PfEMP1* variant at a time.^{75,76}

In conclusion, antigenic variation promotes the evasion of both the immune system and splenic clearance by means of cytoadherence. Depending on the variant, *PfEMP1* can bind to different endothelial receptors, like ICAM1, CD36, chondroitin sulfate and endothelial protein C receptor, often leading to completely different pathologies.^{77,78} Not only can the activation of endothelial ligands trigger pro-inflammatory responses in the endothelium,⁷⁹⁻⁸¹ but the physical clogging of the microvasculature by sequestering infected erythrocytes may cause ischemia, edema and hemorrhages. Depending on the site of sequestration, this can lead to acute organ failure and in the case of the brain to coma and to the clinical picture of cerebral malaria.⁸²⁻⁸⁴

The genesis of the cytoadherence complex and the presentation of *PfEMP1* are tightly linked to the export of several virulence factors to the RBC surface. In close association with other exported proteins, *PfEMP1* localizes to specific sites of the erythrocyte membrane, known as knobs. These knobs are parasite-induced small protrusions that cover the surface of infected erythrocytes and serve as sites of *PfEMP1* presentation and cytoadherence.⁸⁵⁻⁸⁷ Right beneath the RBC surface, the knob-associated histidine-rich protein (KAHRP) is a highly abundant component that amongst other exported proteins, interacts with the intracellular domain of *PfEMP1* and with the cytoskeleton of the erythrocyte.⁸⁸⁻⁹⁰ Therefore, *PfEMP1* is strongly anchored in the host cell, and during ligand binding, shear forces are communicated to the erythrocytic cytoskeleton. In agreement with such a scenario, parasites expressing truncated KAHRP display a reduced binding phenotype under flow conditions.⁹¹

For a long time, the virulence factor *PfEMP1* has been the main focus of cytoadherence-related research. However, more recent insights progressively uncover the role of additional surface antigens in the manipulation of the RBC binding properties. These antigens include members of the subtelomeric variable open reading frame family (STEVORs),⁹² the repetitive interspersed gene family (RIFINs), surface-associated interspersed gene family (SURFINs), the *Plasmodium* helical interspersed sub-telomeric (PHIST) gene family,⁹³ and the Maurer's cleft 2 transmembrane domain proteins (*PfMC-2TM*).⁹⁴ Future research will uncover their yet poorly understood contributions to cytoadherence and malarial pathology.

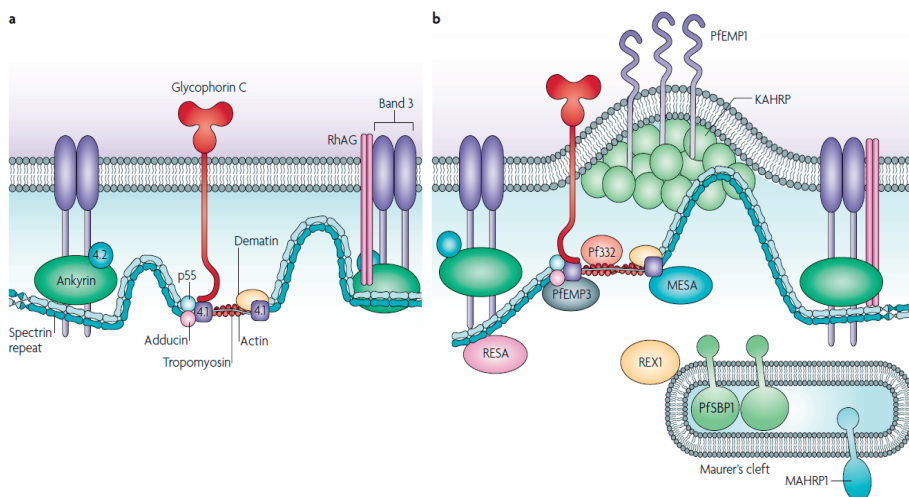


Figure 4 | *Plasmodium*-induced reorganization of the host cell surface (after Maier *et al.*, 2009)¹⁰².

The malaria parasite alters the organization of the erythrocytic cytoskeleton and surface. (a) Native state of the red blood cell surface. The subpellicular cytoskeletal network consists of spectrin, actin and several junctional proteins. It is closely tethered to the erythrocyte membrane and conveys flexibility to the cell. (b) *Plasmodium*-infected erythrocytes harbor Maurer's clefts which participate in the export of virulence factors to the red blood cell surface. Several of these factors associate strongly with the cytoskeletal proteins and can disrupt endogenous protein interactions. Thereby, the parasite alters the mechanical properties of the erythrocyte, leading to an increased stiffness and decreased deformability of the cell. The knob-associated histidine-rich protein (KAHRP) is exported to the plasma membrane and serves to form the protrusions known as knobs and to expose the major virulence factor *P. falciparum* erythrocyte membrane protein 1 (PfEMP1). PfEMP1 tethers the infected red blood cell to the endothelium, thereby avoiding spleen passage and elimination of the infected cell. RhAG, Rh-associated glycoprotein; RESA, ring-infected erythrocyte surface antigen; PfEMP3, *P. falciparum* erythrocyte membrane protein 3; MESA, mature erythrocyte surface antigen; REX1, ring exported protein 1, PfSBP1, *P. falciparum* skeleton-binding protein 1; MAHRP1, Membrane-associated histidine-rich protein 1.

Due to the outstanding pathogenicity of *P. falciparum*, research has predominantly focused on the cytoadhesion-phenotype of this most virulent parasite species. However, there is growing evidence that the sequestration of infected RBCs might be a conserved feature among hematozoan parasites. Indeed, *P. vivax* was shown to mediate cytoadhesion of infected RBCs to the lung, brain and placental endothelium, engaging the same receptors as *P. falciparum*-infected erythrocytes, though to a lesser extent. Interestingly, as in *P. falciparum*, cytoadhesion in *P. vivax* is partly mediated by members of a large subtelomeric multigene family, the VIR

proteins.⁹⁵⁻⁹⁷ The fact that similar phenotypes are also observed in rodent malaria parasite species^{98,99} and even in the piroplasmid parasite *Babesia*^{100,101} argues for the plesiomorphic nature of malaria parasite sequestration.

Manipulation of the host cytoskeleton

Apart from nutrient acquisition, cytoadherence and immune evasion, exported parasite proteins are heavily involved in the modulation of the RBC cytoskeleton. The erythrocyte has a subpellicular network of actin and spectrin filaments, which in its physiological state promotes a high level of cellular flexibility and deformability (Figure 4a). These physical properties are of utmost importance for passing the narrow capillaries in the peripheral tissues.¹⁰³⁻¹⁰⁵ As outlined above, the parasite rigidifies the RBC, to aid efficient cytoadherence.⁶³⁻⁶⁵ To this end, exported parasite proteins bind and stabilize certain junctional sites of the cytoskeleton, while simultaneously dissociating others, thereby altering the mechanical properties of the RBC (Figure 4b). Interestingly, such interactions might also facilitate the egress of newly formed merozoites from their used up host cells.¹⁰⁶ *P. falciparum* erythrocyte membrane protein 3 (*PEMP3*) can bind and disrupt sites of spectrin / actin interaction, thereby loosening up the cytoskeletal framework.¹⁰⁷ It has been speculated that this might facilitate the destabilization of the host cell during merozoite egress, a scenario that contrasts the predominant paradigm of protease-initiated host cell break down,¹⁰⁸⁻¹¹¹ but which might be a complementing mechanism during merozoite egress.¹⁰⁶

THE ROUTE OF EXPORTED PROTEINS

Connectivity of Plasmodium-induced membrane spaces

As reviewed above, the *Plasmodium* parasite rearranges the erythrocyte by two major processes: (1) by establishing novel membranous compartments and (2) by trafficking proteins to different locations in the RBC. How these two aspects of host cell refurbishment relate, has long been a matter of vivid controversy.¹¹²⁻¹¹⁷ The presence of several consecutive membrane compartments is suggestive of protein transport between the PV, the TVN, the MCs and the erythrocyte surface. Based on

their findings in electron microscopic serial sections, Wickert *et al.* (2003) concluded that all these compartments represent different aspects of the same highly interconnected and intertwined membrane continuum.³⁹ This scenario would offer a simple explanation, how secreted parasite proteins are trafficked from the PV to the MCs by simply diffusing through the membrane network. Furthermore, temporal or permanent contacts of this network with the erythrocytic membrane could offer a delivery route to the RBC surface. However, the idea of a membrane continuum and its connectivity with the erythrocyte surface is highly controversial, and there are many reports that provide evidence for a lack of protein diffusion between the PV/TVN and the MCs (see above).^{37,38,40,41} Furthermore, this model does not provide any explanation for the export of proteins destined for the RBC cytosol. In conclusion, it is highly unlikely that the export of proteins exclusively occurs by means of a PVM-delineated network.

Maurer's clefts as a central hub during protein export

The presence of multiple membrane spaces in the infected erythrocyte has evoked ideas of an exported secretory pathway, suggesting vesicular transport mechanisms like those occurring between the endoplasmic reticulum, the Golgi apparatus and the plasma membrane. Indeed, the MCs have long been regarded as an exported Golgi apparatus, due to their appearance and function in the trafficking of virulence factors to the erythrocyte surface.¹¹⁸⁻¹²¹ Components of the cytoadherence complex and other exported surface antigens first associate with the MCs before being transferred to their final destination. This is exemplified by the dynamic localization of the major virulence factor *PfEMP1* to the MCs and the erythrocyte membrane.¹²² It is worth of note, that the onset of *PfEMP1* surface exposure coincides with the timing of MC fixation beneath the erythrocyte membrane.^{42,43,123} Other parasite proteins, like *PfEMP3* and KAHRP, also transiently associate with the cytoplasmic face of the MCs before reaching the erythrocyte surface.¹²⁴ In contrast, specific constituents like membrane-associated histidine-rich protein 1 (MAHRP1), skeleton-binding protein 1 (SBP1), and ring-exported protein 1 (REX1) and 2 (REX2) exclusively localize to the MCs and disruption of their functions can heavily impair protein trafficking.¹²⁴ Depletion of REX1 was shown to cause aggregation and stacking of MCs. As a consequence, *PfEMP1* exposure and cytoadherence to CD36 were significantly reduced, consolidating the function of

MCs as a central hub during protein export to the RBC surface.¹²⁵⁻¹²⁷

Similar membrane-bound compartments are also observed in other malaria parasite species. The so-called Schüffner's dots (SDs) are found in RBCs infected with the human pathogens *P. vivax* and *P. ovale*, and a variety of non-human primate malaria parasites.¹²⁸⁻¹³¹ As of yet, it remains unclear if the MCs and the SDs are functional equivalents, since they differ significantly in size, number, and membrane organization.¹³² However, the exclusive localization of the PEXEL-positive protein PHIST/CVC-8195 to the SDs of *P. vivax* and *P. cynomolgi*, might suggest a similar interconnection with the protein export pathway.^{132,133}

Vesicular transport vs. protein translocation

It is conceivable that the exchange of proteins between the membranous spaces of the infected erythrocyte might occur by means of vesicular transport. The PVM and the whorls of the TVN were shown to serve as a membrane pool for detached PV-derived lumina in the infected erythrocyte, which include several vesicular structures and the MCs.^{38,46,134} Furthermore, proteins that are first present in the confines of the PV were shown to be passively transported during the budding of the nascent MCs.³⁸ It is therefore possible that membrane fissions of the PVM and the TVN are an efficient way of transporting secreted parasite proteins across the RBC cytoplasm to distinct locations of the infected cell. However, several virulence factors and exported proteins destined to the host cell surface are expressed much later during intraerythrocytic development, long after MC genesis, suggesting an additional route of protein delivery.⁴³

There is growing evidence that vesicle-mediated transport might be the underlying mechanism of protein exchange between the MCs and the host cell membrane. Experiments using immuno-electron microscopy demonstrated an association of *PfEMP1* and *PfEMP3* with electron-dense vesicles of 60-100 nm width, which were often found to be located beneath the erythrocyte membrane, suggesting that virulence factors can be transferred by these vesicles from the MCs to the RBC surface.^{42,115,135} Even though MCs and the erythrocyte membrane are closely associated, there is no lipid continuum³⁷ and a vesicular transport pathway appears plausible. Indeed, the electron-dense vesicles seem to fuse with the erythrocyte membrane, giving rise to cup-shaped areas that have been interpreted as sites of knob formation.¹¹⁵

As mentioned above, the fixation of the MCs beneath the host cell membrane coincides with the onset of *PfEMP1* exposure.^{42,43,123} Therefore, close apposition of the MCs appears to be a prerequisite for efficient protein transfer to the RBC surface. Consequently, one could speculate, that electron-dense vesicles carry their cargo proteins by using the tethers of the MCs as some sort of rail, in analogy to the dynein- and kinesin-mediated vesicle movement along microtubules. Indeed, cargo-transporting vesicles were found to be associated with the rearranged actin cytoskeleton that connects MCs and the erythrocytic membrane.¹³⁶

The comparison of the MCs with the Golgi apparatus has been largely over-interpreted in the past. While specific Golgi markers are absent from the MCs, they are detected in intraparasitic structures, suggesting the presence of a classical Golgi apparatus in *Plasmodium* parasites.¹³⁷ In contrast to the secretory pathway,¹³⁸ protein export to the MCs has never been demonstrated to depend on vesicular trafficking. Surprisingly, the exact opposite appears to be the case. There is evidence that parasite-derived cargo proteins traverse the RBC cytosol *via* soluble chaperoned aggregates, as has been demonstrated for *PfEMP1*.^{40,139}

This route of protein transport has a very fundamental consequence: it requires the presence of a translocation machinery that is able to unfold the secreted cargo proteins in the PV and transport them across the boundary of the PVM. Indeed, the export of virulence factors has been shown to depend upon unfolding of the cargo.¹⁴⁰ Fusions of exported proteins to a dihydrofolate reductase (DHFR) domain were readily exported under normal conditions. However, addition of the inhibitor WR99210 specifically causes the DHFR domain to stabilize around this compound, thereby interfering with the unfoldase activity of a putative translocase by 'plugging' the pore. Strikingly, the inhibition of cargo unfolding lead to the accumulation of the proteins in the parasite periphery and to their strong association with the PVM.¹⁴⁰

These key experiments marked a paradigm shift in the understanding of protein export in the malaria parasite and paved the way for the identification of a PVM-resident complex that catalyzes the transposition of virulence factors across the parasite-host interface: the *Plasmodium* translocon of exported proteins (PTEX).¹⁴¹ The characterization of this highly specialized protein complex is the subject of my thesis.

AIM AND OUTLINE OF THE THESIS

Since the initial description of a putative protein export translocon,¹⁴¹ several studies have provided important new insights into the arrangement and function of this complex.¹⁴²⁻¹⁴⁴ Surprisingly, only very few studies have looked beyond the edge of the Petri dish. The human pathogen *P. falciparum* is still at the center of protein export-related research in malaria parasites, due to the vast expansion of its exportome and the clinical consequences thereof. However, it remains questionable, if conclusions drawn from *in vitro* experimentation hold true during *in vivo* infection. While molecular aspects can be studied with relative ease, *P. falciparum* cultivation does not allow for an assessment of host-pathogen interactions. This is particularly problematic, since the protein export machinery has evolved as a means to promote such interactions, enabling nutrient salvage,²⁰ cytoadherence,⁷⁰⁻⁷² and evasion of the spleen and the immune system.^{66,67,75} The interplay between parasite and host is at the heart of *Plasmodium* pathology. Therefore, an investigation of the protein export translocon during infection is desperately needed. In this thesis, I aim to gain new insights into the organization of the protein export translocon and evaluate the consequences of impairing PTEX function *in vivo*, focussing on host-parasite interactions on a microscopic and macroscopic level.

The upcoming chapters will demonstrate, how a highly versatile rodent *in vivo* malaria model can be used to explore the organization and function of the parasite protein export machinery. Using advanced experimental genetics approaches, I set out to uncover yet unrecognized features of the complex which is responsible for the export of an enormous array of parasite proteins. This *in vivo* approach will greatly contribute to our understanding of *Plasmodium*-induced erythrocyte makeover and will shed light on the significance of the PTEX translocon for parasite virulence, pathology and infection outcome.

Chapter 2 of my thesis will offer a comprehensive overview of the techniques and molecular tools that are available for the genetic dissection of *Plasmodium berghei*, and will reflect upon the relevance of this rodent model system. Furthermore, I will provide new ideas for future improvements, in order to bring *P. berghei* experimental genetics to a genome-wide scale.

In chapter 3, I aim to assess the importance of the PTEX translocon during *in vivo*

blood stage propagation by systematic gene targeting. To that end, new genetic tools and powerful phenotyping techniques for *P. berghei* are developed and applied.

The role of the PTEX translocon in parasite-host interactions will be addressed in chapter 4. A combination of reverse genetics, in depth parasite phenotyping and a detailed examination of host pathology will help uncover functional links between the protein export machinery and malaria parasite virulence.

In chapter 5, the spatiotemporal dynamics of the PTEX translocon will be investigated. Advanced live and electron microscopic techniques serve to elucidate the expression and localization profile of the individual PTEX components throughout blood stage development and life cycle progression *in vivo*. In addition, these methods will help to obtain novel insights into the ultrastructure of protein export-competent regions of the PV and the interconnection of protein translocation and membrane organization.

In chapter 6, the implications of my findings will be discussed and put into an evolutionary perspective.

REFERENCES

- 1 World Malaria Report 2015, World Health Organization.
- 2 Sinnis P, Zavala F. The skin: where malaria infection and the host immune response begin. *Semin Immunopathol.* 2012;34(6):787-92.
- 3 Douglas RG, Amino R, Sinnis P, Frischknecht F. Active migration and passive transport of malaria parasites. *Trends Parasitol.* 2015;31(8):357-62.
- 4 Tavares J, Formaglio P, Thiberge S, Mordelet E, Van Rooijen N, Medvinsky A, *et al.* Role of host cell traversal by the malaria sporozoite during liver infection. *J Exp Med.* 2013;210(5):905-15.
- 5 Cha SJ, Park K, Srinivasan P, Schindler CW, van Rooijen N, Stins M, *et al.* CD68 acts as a major gateway for malaria sporozoite liver infection. *J Exp Med.* 2015;212(9):1391-403.
- 6 Prudêncio M, Rodriguez A, Mota MM. The silent path to thousands of merozoites: the *Plasmodium* liver stage. *Nat Rev Microbiol.* 2006;4(11):849-56.
- 7 Markus MB. The hypnozoite concept, with particular reference to malaria. *Parasitol Res.* 2011;108(1):247-52.
- 8 Sturm A, Amino R, van de Sand C, Regen T, Retzlaff S, Rennenberg A, *et al.* Manipulation of host hepatocytes by the malaria parasite for delivery into liver sinusoids. *Science.* 2006;313(5791):1287-90.
- 9 Glushakova S, Humphrey G, Leikina E, Balaban A, Miller J, Zimmerberg J. New stages in the program of malaria parasite egress imaged in normal and sickle erythrocytes. *Curr Biol.* 2010;20(12):1117-21.
- 10 Haldar K, Murphy SC, Milner DA, Taylor TE. Malaria: mechanisms of erythrocytic infection and pathological correlates of severe disease. *Annu Rev Pathol.* 2007;2:217-49.
- 11 Kooij TW, Matuschewski K. Triggers and tricks of *Plasmodium* sexual development. *Curr Opin Microbiol.* 2007;10(6):547-53.
- 12 Kuehn A, Pradel G. The coming-out of malaria gametocytes. *J Biomed Biotechnol.* 2010;2010:976827.
- 13 Sologub L, Kuehn A, Kern S, Przyborski J, Schillig R, Pradel G. Malaria proteases mediate inside-out egress of gametocytes from red blood cells following parasite transmission to the mosquito. *Cell Microbiol.* 2011;13(6):897-912.
- 14 Sinden RE, Talman A, Marques SR, Wass MN, Sternberg MJ. The flagellum in malarial parasites. *Curr Opin Microbiol.* 2010;13(4):491-500.
- 15 Angrisano F, Tan YH, Sturm A, McFadden GI, Baum J. Malaria parasite colonisation of the mosquito midgut – placing the *Plasmodium* ookinete centre stage. *Int J Parasitol.* 2012;42(6):519-27.
- 16 Aly AS, Matuschewski K. A malarial cysteine protease is necessary for *Plasmodium* sporozoite egress from oocysts. *J Exp Med.* 2005;202(2):225-30.
- 17 Akaki M, Dvorak JA. A chemotactic response facilitates mosquito salivary gland infection by malaria sporozoites. *J Exp Biol.* 2005;208(Pt 16):3211-8.
- 18 Crawley J, Chu C, Mtove G, Nosten F. Malaria in children. *Lancet.* 2010;375(9724):

- 1468-81.
- 19 Francis SE, Sullivan DJ, Goldberg DE. Hemoglobin metabolism in the malaria parasite *Plasmodium falciparum*. *Annu Rev Microbiol*. 1997;51:97-123.
- 20 Baumeister S, Winterberg M, Przyborski JM, Lingelbach K. The malaria parasite *Plasmodium falciparum*: cell biological peculiarities and nutritional consequences. *Protoplasma*. 2010;240(1-4):3-12.
- 21 Yachie-Kinoshita A, Nishino T, Shimo H, Suematsu M, Tomita M. A metabolic model of human erythrocytes: practical application of the E-Cell Simulation Environment. *J Biomed Biotechnol*. 2010;2010:642420.
- 22 Salcedo-Sora JE, Caamano-Gutierrez E, Ward SA, Biagini GA. The proliferating cell hypothesis: a metabolic framework for *Plasmodium* growth and development. *Trends Parasitol*. 2014;30(4):170-5.
- 23 Bryant C, Voller A, Smith MJ. The incorporation of radioactivity from (¹⁴C) glucose into the soluble metabolic intermediates of malaria parasites. *Am J Trop Med Hyg*. 1964;13:515-9.
- 24 Jensen MD, Conley M, Helstowski LD. Culture of *Plasmodium falciparum*: the role of pH, glucose, and lactate. *J Parasitol*. 1983;69(6):1060-7.
- 25 Paul AS, Egan ES, Duraisingh MT. Host-parasite interactions that guide red blood cell invasion by malaria parasites. *Curr Opin Hematol*. 2015;22(3):220-6.
- 26 Koch M, Baum J. The mechanics of malaria parasite invasion of the human erythrocyte - towards a reassessment of the host cell contribution. *Cell Microbiol*. 2016;18(3):319-29.
- 27 Weiss GE, Crabb BS, Gilson PR. Overlaying molecular and temporal aspects of malaria parasite invasion. *Trends Parasitol*. 2016;32(4):284-95.
- 28 Dluzewski AR, Mitchell GH, Fryer PR, Griffiths S, Wilson RJ, Gratzer WB. Origins of the parasitophorous vacuole membrane of the malaria parasite, *Plasmodium falciparum*, in human red blood cells. *J Cell Sci*. 1992;102 (Pt 3):527-32.
- 29 Ward GE, Miller LH, Dvorak JA. The origin of parasitophorous vacuole membrane lipids in malaria-infected erythrocytes. *J Cell Sci*. 1993;106 (Pt 1):237-48.
- 30 Elmendorf HG, Haldar K. Secretory transport in *Plasmodium*. *Parasitol Today*. 1993;9 (3):98-102.
- 31 Behari R, Haldar K. *Plasmodium falciparum*: protein localization along a novel, lipid-rich tubovesicular membrane network in infected erythrocytes. *Exp Parasitol*. 1994;79(3):250-9.
- 32 Elmendorf HG, Haldar K. *Plasmodium falciparum* exports the Golgi marker sphingomyelin synthase into a tubovesicular network in the cytoplasm of mature erythrocytes. *J Cell Biol*. 1994;124(4):449-62.
- 33 Lauer SA, Rathod PK, Ghori N, Haldar K. A membrane network for nutrient import in red cells infected with the malaria parasite. *Science*. 1997;276(5315):1122-5.
- 34 Pouvelle B, Spiegel R, Hsiao L, Howard RJ, Morris RL, Thomas AP, *et al*. Direct access to serum macromolecules by intraerythrocytic malaria parasites. *Nature*. 1991;353(6339):73-5.
- 35 Atkinson CT, Aikawa M. Ultrastructure of malaria-infected erythrocytes. *Blood Cells*. 1990;16(2-3):351-68.

- 36 Wickert H, Göttler W, Krohne G, Lanzer M. Maurer's cleft organization in the cytoplasm of *Plasmodium falciparum*-infected erythrocytes: new insights from three-dimensional reconstruction of serial ultrathin sections. *Eur J Cell Biol.* 2004;83(10):567-82.
- 37 Hanssen E, Sougrat R, Frankland S, Deed S, Klonis N, Lippincott-Schwartz J, *et al.* Electron tomography of the Maurer's cleft organelles of *Plasmodium falciparum*-infected erythrocytes reveals novel structural features. *Mol Microbiol.* 2008;67(4):703-18.
- 38 Spycher C, Rug M, Klonis N, Ferguson DJ, Cowman AF, Beck HP, *et al.* Genesis of and trafficking to the Maurer's clefts of *Plasmodium falciparum*-infected erythrocytes. *Mol Cell Biol.* 2006;26(11):4074-85.
- 39 Wickert H, Wissing F, Andrews KT, Stich A, Krohne G, Lanzer M. Evidence for trafficking of PfEMP1 to the surface of *P. falciparum*-infected erythrocytes via a complex membrane network. *Eur J Cell Biol.* 2003;82(6):271-84.
- 40 Knuepfer E, Rug M, Klonis N, Tilley L, Cowman AF. Trafficking of the major virulence factor to the surface of transfected *P. falciparum*-infected erythrocytes. *Blood.* 2005;105(10):4078-87.
- 41 Hanssen E, Carlton P, Deed S, Klonis N, Sedat J, DeRisi J, *et al.* Whole cell imaging reveals novel modular features of the exomembrane system of the malaria parasite, *Plasmodium falciparum*. *Int J Parasitol.* 2010;40(1):123-34.
- 42 McMillan PJ, Millet C, Batinovic S, Maiorca M, Hanssen E, Kenny S, *et al.* Spatial and temporal mapping of the PfEMP1 export pathway in *Plasmodium falciparum*. *Cell Microbiol.* 2013;15(8):1401-18.
- 43 Grüning C, Heiber A, Kruse F, Ungefehr J, Gilberger TW, Spielmann T. Development and host cell modifications of *Plasmodium falciparum* blood stages in four dimensions. *Nat Commun.* 2011;2:165.
- 44 Pachlatko E, Rusch S, Müller A, Hemphill A, Tilley L, Hanssen E, *et al.* MAHRP2, an exported protein of *Plasmodium falciparum*, is an essential component of Maurer's cleft tethers. *Mol Microbiol.* 2010;77(5):1136-52.
- 45 Marti M, Baum J, Rug M, Tilley L, Cowman AF. Signal-mediated export of proteins from the malaria parasite to the host erythrocyte. *J Cell Biol.* 2005;171(4):587-92.
- 46 Adisa A, Rug M, Klonis N, Foley M, Cowman AF, Tilley L. The signal sequence of exported protein-1 directs the green fluorescent protein to the parasitophorous vacuole of transfected malaria parasites. *J Biol Chem.* 2003;278(8):6532-42.
- 47 Hiller NL, Bhattacharjee S, van Ooij C, Liolios K, Harrison T, Lopez-Estraño C, *et al.* A host-targeting signal in virulence proteins reveals a secretome in malarial infection. *Science.* 2004;306(5703):1934-7.
- 48 Marti M, Good RT, Rug M, Knuepfer E, Cowman AF. Targeting malaria virulence and remodeling proteins to the host erythrocyte. *Science.* 2004;306(5703):1930-3.
- 49 Spielmann T, Gilberger TW. Critical steps in protein export of *Plasmodium falciparum* blood stages. *Trends Parasitol.* 2015;31(10):514-25.
- 50 Overmann RR. Reversible cellular permeability alterations in disease; *in vivo* studies on sodium, potassium and chloride concentrations in erythrocytes of the malarious monkey. *Am J Physiol.* 1948;152(1):113-21.
- 51 Ginsburg H, Krugliak M, Eidelman O, Cabantchik ZI. New permeability pathways

- p induced in membranes of
- Plasmodium falciparum*
- infected erythrocytes. Mol Biochem Parasitol. 1983;8(2):177-90.
- 52 Ginsburg H, Kutner S, Krugliak M, Cabantchik ZI. Characterization of permeation pathways appearing in the host membrane of *Plasmodium falciparum* infected red blood cells. Mol Biochem Parasitol. 1985;14(3):313-22.
 - 53 Desai SA. Why do malaria parasites increase host erythrocyte permeability? Trends Parasitol. 2014;30(3):151-9.
 - 54 Baumeister S, Winterberg M, Duranton C, Huber SM, Lang F, Kirk K, *et al.* Evidence for the involvement of *Plasmodium falciparum* proteins in the formation of new permeability pathways in the erythrocyte membrane. Mol Microbiol. 2006;60(2):493-504.
 - 55 Nguitragool W, Bokhari AA, Pillai AD, Rayavara K, Sharma P, Turpin B, *et al.* Malaria parasite clag3 genes determine channel-mediated nutrient uptake by infected red blood cells. Cell. 2011;145(5):665-77.
 - 56 Desai SA, Rosenberg RL. Pore size of the malaria parasite's nutrient channel. Proc Natl Acad Sci U S A. 1997;94(5):2045-9.
 - 57 Martin RE, Henry RI, Abbey JL, Clements JD, Kirk K. The 'permeome' of the malaria parasite: an overview of the membrane transport proteins of *Plasmodium falciparum*. Genome Biol. 2005;6(3):R26.
 - 58 Martin RE, Ginsburg H, Kirk K. Membrane transport proteins of the malaria parasite. Mol Microbiol. 2009;74(3):519-28.
 - 59 Stolarczyk EI, Reiling CJ, Paumi CM. Regulation of ABC transporter function *via* phosphorylation by protein kinases. Curr Pharm Biotechnol. 2011;12(4):621-35.
 - 60 Schneider AG, Mercereau-Puijalon O. A new Apicomplexa-specific protein kinase family: multiple members in *Plasmodium falciparum*, all with an export signature. BMC Genomics. 2005;6:30.
 - 61 Brandt GS, Bailey S. Dematin, a human erythrocyte cytoskeletal protein, is a substrate for a recombinant FIKK kinase from *Plasmodium falciparum*. Mol Biochem Parasitol. 2013;191(1):20-3.
 - 62 Nunes MC, Okada M, Scheidig-Benatar C, Cooke BM, Scherf A. *Plasmodium falciparum* FIKK kinase members target distinct components of the erythrocyte membrane. PLoS One. 2010;5(7):e11747.
 - 63 Nash GB, O'Brien E, Gordon-Smith EC, Dormandy JA. Abnormalities in the mechanical properties of red blood cells caused by *Plasmodium falciparum*. Blood. 1989;74(2):855-61.
 - 64 Paulitschke M, Nash GB. Membrane rigidity of red blood cells parasitized by different strains of *Plasmodium falciparum*. J Lab Clin Med. 1993;122(5):581-9.
 - 65 Maier AG, Rug M, O'Neill MT, Brown M, Chakravorty S, Szeszak T, *et al.* Exported proteins required for virulence and rigidity of *Plasmodium falciparum*-infected human erythrocytes. Cell. 2008;134(1):48-61.
 - 66 Engwerda CR, Beattie L, Amante FH. The importance of the spleen in malaria. Trends Parasitol. 2005;21(2):75-80.
 - 67 Del Portillo HA, Ferrer M, Brugat T, Martin-Jaular L, Langhorne J, Lacerda MV. The role of the spleen in malaria. Cell Microbiol. 2012;14(3):343-55.
 - 68 Pasternak ND, Dzikowski R. PfEMP1: an antigen that plays a key role in the

- pathogenicity and immune evasion of the malaria parasite *Plasmodium falciparum*. *Int J Biochem Cell Biol.* 2009;41(7):1463-6.
- 69 Smith JD, Rowe JA, Higgins MK, Lavstsen T. Malaria's deadly grip: cytoadhesion of *Plasmodium falciparum*-infected erythrocytes. *Cell Microbiol.* 2013;15(12):1976-83.
 - 70 Baruch DI, Pasloske BL, Singh HB, Bi X, Ma XC, Feldman M, *et al.* Cloning the *P. falciparum* gene encoding PfEMP1, a malarial variant antigen and adherence receptor on the surface of parasitized human erythrocytes. *Cell.* 1995;82(1):77-87.
 - 71 Smith JD, Chitnis CE, Craig AG, Roberts DJ, Hudson-Taylor DE, Peterson DS, *et al.* Switches in expression of *Plasmodium falciparum* var genes correlate with changes in antigenic and cytoadherent phenotypes of infected erythrocytes. *Cell.* 1995;82(1):101-10.
 - 72 Su XZ, Heatwole VM, Wertheimer SP, Guinet F, Herrfeldt JA, Peterson DS, *et al.* The large diverse gene family var encodes proteins involved in cytoadherence and antigenic variation of *Plasmodium falciparum*-infected erythrocytes. *Cell.* 1995;82(1):89-100.
 - 73 Oguariri RM, Borrmann S, Klinkert MQ, Kremsner PG, Kun JF. High prevalence of human antibodies to recombinant Duffy binding-like alpha domains of the *Plasmodium falciparum*-infected erythrocyte membrane protein 1 in semi-immune adults compared to that in nonimmune children. *Infect Immun.* 2001;69(12):7603-9.
 - 74 Krause DR, Gatton ML, Frankland S, Eisen DP, Good MF, Tilley L, *et al.* Characterization of the antibody response against *Plasmodium falciparum* erythrocyte membrane protein 1 in human volunteers. *Infect Immun.* 2007;75(12):5967-73.
 - 75 Scherf A, Lopez-Rubio JJ, Riviere L. Antigenic variation in *Plasmodium falciparum*. *Annu Rev Microbiol.* 2008;62:445-70.
 - 76 Guizetti J, Scherf A. Silence, activate, poise and switch! Mechanisms of antigenic variation in *Plasmodium falciparum*. *Cell Microbiol.* 2013;15(5):718-26.
 - 77 Kraemer SM, Smith JD. A family affair: var genes, PfEMP1 binding, and malaria disease. *Curr Opin Microbiol.* 2006;9(4):374-80.
 - 78 Ochola LB, Siddondo BR, Ocholla H, Nkya S, Kimani EN, Williams TN, *et al.* Specific receptor usage in *Plasmodium falciparum* cytoadherence is associated with disease outcome. *PLoS One.* 2011;6(3):e14741.
 - 79 Hollestelle MJ, Donkor C, Mantey EA, Chakravorty SJ, Craig A, Akoto AO, *et al.* von Willebrand factor propeptide in malaria: evidence of acute endothelial cell activation. *Br J Haematol.* 2006;133(5):562-9.
 - 80 Tchinda VH, Tadem AD, Tako EA, Tene G, Fogako J, Nyonglema P, *et al.* Severe malaria in Cameroonian children: correlation between plasma levels of three soluble inducible adhesion molecules and TNF-alpha. *Acta Trop.* 2007;102(1):20-8.
 - 81 Moxon CA, Chisala NV, Wassmer SC, Taylor TE, Seydel KB, Molyneux ME, *et al.* Persistent endothelial activation and inflammation after *Plasmodium falciparum* infection in Malawian children. *J Infect Dis.* 2014;209(4):610-5.
 - 82 Ponsford MJ, Medana IM, Prapansilp P, Hien TT, Lee SJ, Dondorp AM, *et al.* Sequestration and microvascular congestion are associated with coma in human cerebral malaria. *J Infect Dis.* 2012;205(4):663-71.
 - 83 Castillo P, Menéndez C, Mayor A, Carrilho C, Ismail MR, Lorenzoni C, *et al.* Massive *Plasmodium falciparum* visceral sequestration: a cause of maternal death in Africa.

- Clin Microbiol Infect. 2013;19(11):1035-41.
- 84 Milner DA, Lee JJ, Frantzreb C, Whitten RO, Kamiza S, Carr RA, *et al.* Quantitative assessment of multiorgan sequestration of parasites in fatal pediatric cerebral malaria. J Infect Dis. 2015;212(8):1317-21.
- 85 Nakamura K, Hasler T, Morehead K, Howard RJ, Aikawa M. *Plasmodium falciparum*-infected erythrocyte receptor(s) for CD36 and thrombospondin are restricted to knobs on the erythrocyte surface. J Histochem Cytochem. 1992;40(9):1419-22.
- 86 Crabb BS, Cooke BM, Reeder JC, Waller RF, Caruana SR, Davern KM, *et al.* Targeted gene disruption shows that knobs enable malaria-infected red cells to cytoadhere under physiological shear stress. Cell. 1997;89(2):287-96.
- 87 Horrocks P, Pinches RA, Chakravorty SJ, Papakrivos J, Christodoulou Z, Kyes SA, *et al.* PfEMP1 expression is reduced on the surface of knobless *Plasmodium falciparum* infected erythrocytes. J Cell Sci. 2005;118(Pt 11):2507-18.
- 88 Pei X, An X, Guo X, Tarnawski M, Coppel R, Mohandas N. Structural and functional studies of interaction between *Plasmodium falciparum* knob-associated histidine-rich protein (KAHRP) and erythrocyte spectrin. J Biol Chem. 2005;280(35):31166-71.
- 89 Weng H, Guo X, Papoin J, Wang J, Coppel R, Mohandas N, *et al.* Interaction of *Plasmodium falciparum* knob-associated histidine-rich protein (KAHRP) with erythrocyte ankyrin R is required for its attachment to the erythrocyte membrane. Biochim Biophys Acta. 2014;1838(1 Pt B):185-92.
- 90 Ganguly AK, Ranjan P, Kumar A, Bhavesh NS. Dynamic association of PfEMP1 and KAHRP in knobs mediates cytoadherence during *Plasmodium* invasion. Sci Rep. 2015; 5:8617.
- 91 Rug M, Prescott SW, Fernandez KM, Cooke BM, Cowman AF. The role of KAHRP domains in knob formation and cytoadherence of *P. falciparum*-infected human erythrocytes. Blood. 2006;108(1):370-8.
- 92 Sanyal S, Egée S, Bouyer G, Perrot S, Safeukui I, Bischoff E, *et al.* *Plasmodium falciparum* STEVOR proteins impact erythrocyte mechanical properties. Blood. 2012; 119(2):e1-8.
- 93 Oberli A, Zurbrugg L, Rusch S, Brand F, Butler ME, Day JL, *et al.* *Plasmodium falciparum* PHIST proteins contribute to cytoadherence and anchor PfEMP1 to the host cell cytoskeleton. Cell Microbiol. 2016. Accepted article. DOI: 10.1111/cmi.12583
- 94 Chan JA, Fowkes FJ, Beeson JG. Surface antigens of *Plasmodium falciparum*-infected erythrocytes as immune targets and malaria vaccine candidates. Cell Mol Life Sci. 2014;71(19):3633-57.
- 95 Carvalho BO, Lopes SC, Nogueira PA, Orlandi PP, Bargieri DY, Blanco YC, *et al.* On the cytoadhesion of *Plasmodium vivax*-infected erythrocytes. J Infect Dis. 2010;202 (4):638-47.
- 96 Bernabeu M, Lopez FJ, Ferrer M, Martin-Jaular L, Razaname A, Corradin G, *et al.* Functional analysis of *Plasmodium vivax* VIR proteins reveals different subcellular localizations and cytoadherence to the ICAM-1 endothelial receptor. Cell Microbiol. 2012;14(3):386-400.
- 97 Marín-Menéndez A, Bardaji A, Martínez-Espinosa FE, Bôtto-Menezes C, Lacerda MV, Ortiz J, *et al.* Rosetting in *Plasmodium vivax*: a cytoadhesion phenotype associated with anaemia. PLoS Negl Trop Dis. 2013;7(4):e2155.

- 98 Franke-Fayard B, Fonager J, Braks A, Khan SM, Janse CJ. Sequestration and tissue accumulation of human malaria parasites: can we learn anything from rodent models of malaria? *PLoS Pathog.* 2010;6(9):e1001032.
- 99 Fonager J, Pasini EM, Braks JA, Klop O, Ramesar J, Remarque EJ, *et al.* Reduced CD36-dependent tissue sequestration of *Plasmodium*-infected erythrocytes is detrimental to malaria parasite growth *in vivo*. *J Exp Med.* 2012;209(1):93-107.
- 100 Parrodi F, Wright IG, Bourne AS, Dobson C. *In vitro* adherence of bovine erythrocytes infected with *Babesia bovis* to thrombospondin and laminin. *Int J Parasitol.* 1989;19(5):567-9.
- 101 O'Connor RM, Long JA, Allred DR. Cytoadherence of *Babesia bovis*-infected erythrocytes to bovine brain capillary endothelial cells provides an *in vitro* model for sequestration. *Infect Immun.* 1999;67(8):3921-8.
- 102 Maier AG, Cooke BM, Cowman AF, Tilley L. Malaria parasite proteins that remodel the host erythrocyte. *Nat Rev Microbiol.* 2009;7(5):341-54.
- 103 Li J, Lykotrafitis G, Dao M, Suresh S. Cytoskeletal dynamics of human erythrocyte. *Proc Natl Acad Sci U S A.* 2007;104(12):4937-42.
- 104 Mohandas N, Gallagher PG. Red cell membrane: past, present, and future. *Blood.* 2008;112(10):3939-48.
- 105 Nans A, Mohandas N, Stokes DL. Native ultrastructure of the red cell cytoskeleton by cryo-electron tomography. *Biophys J.* 2011;101(10):2341-50.
- 106 Millholland MG, Chandramohanadas R, Pizzarro A, Wehr A, Shi H, Darling C, *et al.* The malaria parasite progressively dismantles the host erythrocyte cytoskeleton for efficient egress. *Mol Cell Proteomics.* 2011;10(12):M111.010678.
- 107 Pei X, Guo X, Coppel R, Mohandas N, An X. *Plasmodium falciparum* erythrocyte membrane protein 3 (PfEMP3) destabilizes erythrocyte membrane skeleton. *J Biol Chem.* 2007;282(37):26754-8.
- 108 Dowse TJ, Koussis K, Blackman MJ, Soldati-Favre D. Roles of proteases during invasion and egress by *Plasmodium* and *Toxoplasma*. *Subcell Biochem.* 2008;47:121-39.
- 109 Blackman MJ. Malarial proteases and host cell egress: an 'emerging' cascade. *Cell Microbiol.* 2008;10(10):1925-34.
- 110 Wirth CC, Pradel G. Molecular mechanisms of host cell egress by malaria parasites. *Int J Med Microbiol.* 2012;302(4-5):172-8.
- 111 Roiko MS, Carruthers VB. New roles for perforins and proteases in apicomplexan egress. *Cell Microbiol.* 2009;11(10):1444-52.
- 112 Gormley JA, Howard RJ, Taraschi TF. Trafficking of malarial proteins to the host cell cytoplasm and erythrocyte surface membrane involves multiple pathways. *J Cell Biol.* 1992;119(6):1481-95.
- 113 Oliaro P, Castelli F. *Plasmodium falciparum*: an electronmicroscopy study of caveolae and trafficking between the parasite and the extracellular medium. *Int J Parasitol.* 1997;27(9):1007-12.
- 114 Foley M, Tilley L. Protein trafficking in malaria-infected erythrocytes. *Int J Parasitol.* 1998;28(11):1671-80.
- 115 Taraschi TF, Trelka D, Martinez S, Schneider T, O'Donnell ME. Vesicle-mediated trafficking of parasite proteins to the host cell cytosol and erythrocyte surface

- membrane in *Plasmodium falciparum* infected erythrocytes. *Int J Parasitol.* 2001;31(12):1381-91.
- 116 Taraschi TF, O'Donnell M, Martinez S, Schneider T, Trelka D, Fowler VM, *et al.* Generation of an erythrocyte vesicle transport system by *Plasmodium falciparum* malaria parasites. *Blood.* 2003;102(9):3420-6.
- 117 Haeggström M, Kironde F, Berzins K, Chen Q, Wahlgren M, Fernandez V. Common trafficking pathway for variant antigens destined for the surface of the *Plasmodium falciparum*-infected erythrocyte. *Mol Biochem Parasitol.* 2004;133(1):1-14.
- 118 Albano FR, Berman A, La Greca N, Hibbs AR, Wickham M, Foley M, *et al.* A homologue of Sar1p localises to a novel trafficking pathway in malaria-infected erythrocytes. *Eur J Cell Biol.* 1999;78(7):453-62.
- 119 Adisa A, Albano FR, Reeder J, Foley M, Tilley L. Evidence for a role for a *Plasmodium falciparum* homologue of Sec31p in the export of proteins to the surface of malaria parasite-infected erythrocytes. *J Cell Sci.* 2001;114(Pt 18):3377-86.
- 120 Wickert H, Rohrbach P, Scherer SJ, Krohne G, Lanzer M. A putative Sec23 homologue of *Plasmodium falciparum* is located in Maurer's clefts. *Mol Biochem Parasitol.* 2003;129(2):209-13.
- 121 Tilley L, Sougrat R, Lithgow T, Hanssen E. The twists and turns of Maurer's cleft trafficking in *P. falciparum*-infected erythrocytes. *Traffic.* 2008;9(2):187-97.
- 122 Wickham ME, Rug M, Ralph SA, Klonis N, McFadden GI, Tilley L, *et al.* Trafficking and assembly of the cytoadherence complex in *Plasmodium falciparum*-infected human erythrocytes. *EMBO J.* 2001;20(20):5636-49.
- 123 Kriek N, Tilley L, Horrocks P, Pinches R, Elford BC, Ferguson DJ, *et al.* Characterization of the pathway for transport of the cytoadherence-mediating protein, PfEMP1, to the host cell surface in malaria parasite-infected erythrocytes. *Mol Microbiol.* 2003;50(4):1215-27.
- 124 Sam-Yellowe TY. The role of the Maurer's clefts in protein transport in *Plasmodium falciparum*. *Trends Parasitol.* 2009;25(6):277-84.
- 125 Hanssen E, Hawthorne P, Dixon MW, Trenholme KR, McMillan PJ, Spielmann T, *et al.* Targeted mutagenesis of the ring-exported protein-1 of *Plasmodium falciparum* disrupts the architecture of Maurer's cleft organelles. *Mol Microbiol.* 2008;69(4):938-53.
- 126 Dixon MW, Kenny S, McMillan PJ, Hanssen E, Trenholme KR, Gardiner DL, *et al.* Genetic ablation of a Maurer's cleft protein prevents assembly of the *Plasmodium falciparum* virulence complex. *Mol Microbiol.* 2011;81(4):982-93.
- 127 McHugh E, Batinovic S, Hanssen E, McMillan PJ, Kenny S, Griffin MD, *et al.* A repeat sequence domain of the ring-exported protein-1 of *Plasmodium falciparum* controls export machinery architecture and virulence protein trafficking. *Mol Microbiol.* 2015;98(6):1101-14.
- 128 Schüffner W. Beitrag zur Kenntnis der Malaria. *Deutsch. Arch. f. Klin. Med.* 1899;64:428
- 129 Aikawa M, Hsieh CL, Miller LH. Ultrastructural changes of the erythrocyte membrane in ovale-type malarial parasites. *J Parasitol.* 1977;63(1):152-4.
- 130 Matsumoto Y, Matsuda S, Yoshida Y. Ultrastructure of human erythrocytes infected with *Plasmodium ovale*. *Am J Trop Med Hyg.* 1986;35(4):697-703.
- 131 Coatney GR. The simian malarias: zoonoses, anthroponoses, or both? *Am J Trop Med*

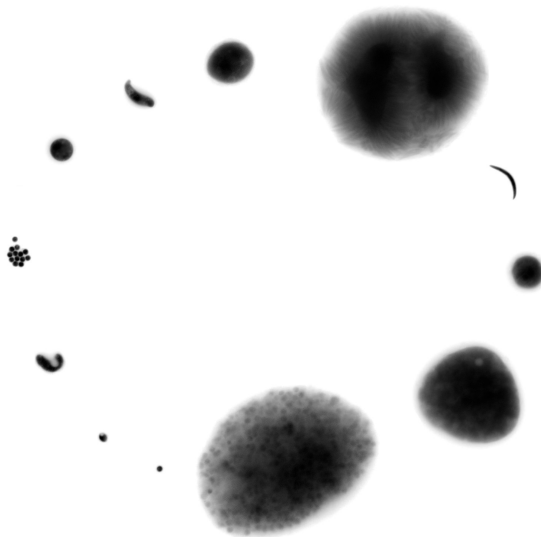
- Hyg. 1971;20(6):795-803.
- 132 Akinyi S, Hanssen E, Meyer EV, Jiang J, Korir CC, Singh B, *et al.* A 95 kDa protein of *Plasmodium vivax* and *P. cynomolgi* visualized by three-dimensional tomography in the caveola-vesicle complexes (Schüffner's dots) of infected erythrocytes is a member of the PHIST family. *Mol Microbiol.* 2012;84(5):816-31.
 - 133 Barnwell JW, Ingravallo P, Galinski MR, Matsumoto Y, Aikawa M. *Plasmodium vivax*: malarial proteins associated with the membrane-bound caveola-vesicle complexes and cytoplasmic cleft structures of infected erythrocytes. *Exp Parasitol.* 1990;70(1):85-99.
 - 134 Meibalan E, Comunale MA, Lopez AM, Bergman LW, Mehta A, Vaidya AB, *et al.* Host erythrocyte environment influences the localization of exported protein 2, an essential component of the *Plasmodium* translocon. *Eukaryot Cell.* 2015;14(4):371-84.
 - 135 Trelka DP, Schneider TG, Reeder JC, Taraschi TF. Evidence for vesicle-mediated trafficking of parasite proteins to the host cell cytosol and erythrocyte surface membrane in *Plasmodium falciparum* infected erythrocytes. *Mol Biochem Parasitol.* 2000;106(1):131-45.
 - 136 Cyrklaff M, Sanchez CP, Kilian N, Bisseye C, Simpoire J, Frischknecht F, *et al.* Hemoglobins S and C interfere with actin remodeling in *Plasmodium falciparum*-infected erythrocytes. *Science.* 2011;334(6060):1283-6.
 - 137 Adisa A, Frankland S, Rug M, Jackson K, Maier AG, Walsh P, *et al.* Re-assessing the locations of components of the classical vesicle-mediated trafficking machinery in transfected *Plasmodium falciparum*. *Int J Parasitol.* 2007;37(10):1127-41.
 - 138 Tonkin CJ, Pearce JA, McFadden GI, Cowman AF. Protein targeting to destinations of the secretory pathway in the malaria parasite *Plasmodium falciparum*. *Curr Opin Microbiol.* 2006;9(4):381-7.
 - 139 Papakrivovs J, Newbold CI, Lingelbach K. A potential novel mechanism for the insertion of a membrane protein revealed by a biochemical analysis of the *Plasmodium falciparum* cytoadherence molecule PfEMP-1. *Mol Microbiol.* 2005;55(4):1272-84.
 - 140 Gehde N, Hinrichs C, Montilla I, Chapien S, Lingelbach K, Przyborski JM. Protein unfolding is an essential requirement for transport across the parasitophorous vacuolar membrane of *Plasmodium falciparum*. *Mol Microbiol.* 2009;71(3):613-28.
 - 141 de Koning-Ward TF, Gilson PR, Boddey JA, Rug M, Smith BJ, Papenfuss AT, *et al.* A newly discovered protein export machine in malaria parasites. *Nature.* 2009;459(7249):945-9.
 - 142 Bullen HE, Charnaud SC, Kalanon M, Riglar DT, Dekiwadia C, Kangwanrangsan N, *et al.* Biosynthesis, localization, and macromolecular arrangement of the *Plasmodium falciparum* translocon of exported proteins (PTEX). *J Biol Chem.* 2012;287(11):7871-84.
 - 143 Elsworth B, Matthews K, Nie CQ, Kalanon M, Charnaud SC, Sanders PR, *et al.* PTEX is an essential nexus for protein export in malaria parasites. *Nature.* 2014;511(7511):587-91.
 - 144 Beck JR, Muralidharan V, Oksman A, Goldberg DE. PTEX component HSP101 mediates export of diverse malaria effectors into host erythrocytes. *Nature.* 2014;511(7511):592-5.

Chapter 2

Towards genome-wide experimental genetics in the
in vivo malaria model parasite *Plasmodium berghei*

Matz JM, Kooij TWA. Pathog. Glob. Health. 2015; 109:46–60.

(invited review, cover image, editor's choice)



ABSTRACT

Plasmodium berghei was identified as a parasite of thicket rats (*Grammomys dolichurus*) and *Anopheles duren*i mosquitoes in African highland forests. Successful adaptation to a range of rodent and mosquito species established *P. berghei* as a malaria model parasite. The introduction of stable transfection technology, the first and most efficient in any malaria parasite, permitted classical reverse genetics strategies and thus systematic functional profiling of the gene repertoire. In the past ten years following the publication of the *P. berghei* genome sequence, many new tools for experimental genetics approaches have been developed and existing ones have been improved. The infection of mice is the principal limitation towards a genome-wide repository of mutant parasite lines. The past few years, there have been some promising and most welcome developments that allow rapid selection and isolation of recombinant parasites while simultaneously minimizing animal usage. Here, we will provide an overview of all the currently available tools and methods.

INTRODUCTION

Since the first description of the malaria parasite by Alphonse Laveran,¹ researchers have been trying to gain insights into the biology of *Plasmodium* parasites. While initial studies solely focused on observation of wild-type parasites, the ability to genetically manipulate *Plasmodium* spp., revolutionized the field of malaria research. Successful transfection was first demonstrated in the avian pathogen *Plasmodium gallinaceum*.² Since then, a diverse repertoire of *Plasmodium* parasites proved to be accessible to genetic manipulation, including human,^{3,4} primate,^{5,6} and rodent⁷⁻⁹ malaria parasites. The availability of many complete or near-complete genome sequences¹⁰⁻¹⁵ has been another huge advance towards a more profound understanding of *Plasmodium* biology. Genome sequence data have been key to the scope and success of experimental genetics approaches in malaria research.

Despite the ability to introduce foreign DNA molecules into a variety of malaria parasite species, there are profound differences in the level of accessibility, ease, and efficiency of genetic manipulation. For example, despite recent advances that enable the use of zinc-finger nucleases to modify the *P. vivax* genome more effectively,¹⁶ all genetic manipulation of this human malaria parasite is severely hampered by the inability to continuously culture these parasites *in vitro*, thus necessitating *in vivo* infections in non-human primates.¹⁷ *P. falciparum* is the deadliest and most devastating human malaria parasite and has been adapted to long-term *in vitro* growth. As such, it has become the most extensively studied *Plasmodium* species. For long, inefficiency of transfection technology slowed down progress as the generation of stable genetic mutants could easily last many months (see Limenitakis & Soldati-Favre for a comprehensive overview¹⁸). The recent successful adaptation of the CRISPR/Cas9 system,¹⁹ however, has the potential to once more revolutionize the field by providing an unprecedented ease and speed of generating recombinant *P. falciparum* lines. On the other hand, experimentation with *P. falciparum* is predominantly performed in *in vitro* blood-stage cultures. This is due to obvious issues with maintenance of the complete *in vivo* life cycle as well as the inability to complete the life cycle *in vitro*. Suitable *in vivo* models that highlight the relevance of the findings during an infection should complement the *in vitro* model.

Rodent malaria parasites, in particular *P. berghei* and *P. yoelii*, provide such model

systems. They combine fast and efficient experimental genetics techniques with access to the complete *in vivo* life cycle (Figure 1). In addition, the evolutionary distances of the rodent malaria parasite clade to either *P. falciparum* or *P. vivax* are in the same order of magnitude as the evolutionary distance between *P. falciparum* and *P. vivax*.¹³ All these factors render *P. berghei* and *P. yoelii* practical and relevant model species to study common principles of *Plasmodium* biology. They allow the examination of parasite-host-interactions *in vivo*, including clinically relevant phenomena like parasite sequestration,²⁰ experimental cerebral malaria,^{21,22} host immune responses,²³ and parasite immune evasion.²⁴ This is exemplified by the use of intravital imaging techniques, which have proven useful for the investigation of sequestered blood-stage parasites in the brain,²⁵ sporozoite migration,²⁶ and liver-stage development.²⁷ Another great advantage, especially when working with infected anopheline mosquitoes, is the inability of *P. berghei* and *P. yoelii* to cause malaria in humans. Indeed, much of our knowledge on the *Plasmodium* mosquito stages stems from findings in *P. berghei*. For the purpose of this review, we will focus on *P. berghei*, a versatile and highly amendable malaria model parasite species and the first malaria parasite for which stable genetic manipulation was established.

TRANSFECTION

Successful genetic manipulation relies on efficient transfer of modifying DNA constructs into the nucleus and on sufficient parasite survival during the transfection procedure. Asexual blood-stage parasites are the most straightforward to accumulate in large quantities and are haploid negating the need for crossing heterozygotes to achieve homozygote mutants. However, in order to modify the parasite genome, the targeting DNA construct would have to pass four membranes: (i) the erythrocyte plasma membrane, (ii) the parasitophorous vacuolar membrane, (iii) the parasite plasma membrane, and (iv) the nuclear envelope. This is further complicated by the blood-stage parasite's dependence on the integrity of the host erythrocyte for survival. During *P. berghei* transfections, both matters are overcome by electroporating mature merozoites, the invasive, briefly extracellular forms that establish infection of new erythrocytes. This may partly explain the differences in transfection efficiencies between *P. berghei* and *P. falciparum*. For the latter, either developing, intracellular ring-stage parasites are

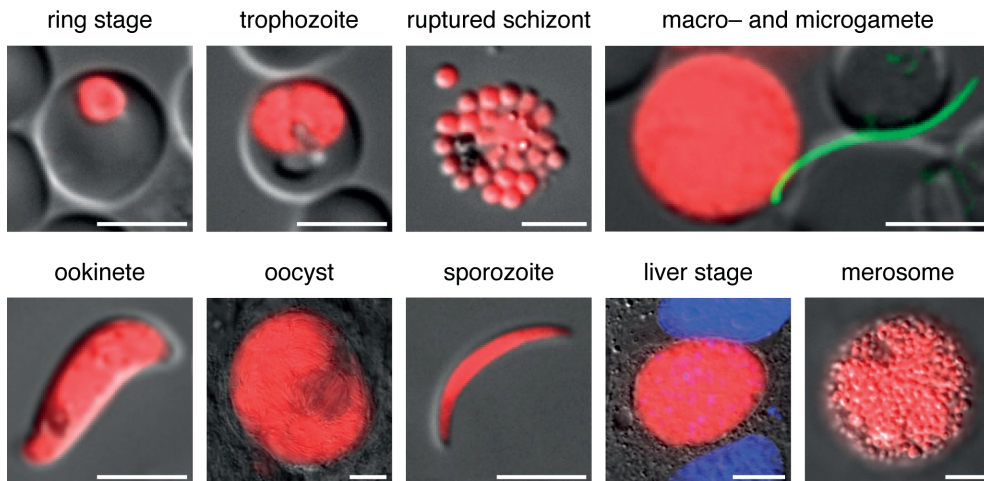


Figure 1 | Live imaging of the complete *Plasmodium berghei* life cycle using the Berred reference strain.⁶⁴ Berred expresses high levels of the red fluorescent protein mCherry in all stages under the control of the *P. berghei* heat shock protein 70 promoter. Shown are asexual blood stages (a ring-stage parasite, a trophozoite, and mature blood-stage merozoites from a ruptured schizont); *in vitro* activated sexual stage parasite (a male Berggreen microgamete – which expresses high levels of GFP – attaching to a female Berred macrogamete); a cultured ookinete; mosquito stages from *in vivo* infections (an oocyst at day 14 after the mosquito blood meal and a salivary gland-associated sporozoite); and *in vitro* cultured liver stages (a liver-stage trophozoite at 48 hours after infection and mature liver-stage merozoites in a merosome released from the hepatocyte). Bars for oocyst, liver stage, and merosome, 10 μ m; all others, 5 μ m.

used or uninfected erythrocytes are preloaded with targeting DNA prior to parasite invasion.²⁸ The parasite purification for transfection is based on the phenomenon, that *P. berghei* parasites develop normally into merozoites in *in vitro* culture, but cannot egress from the erythrocyte without additional mechanical shear stress.^{29,30} Consequently, *ex vivo* cultivation of mixed blood stages for 16–18 h is sufficient for the accumulation of large numbers of enclosed viable merozoites, which can be purified by a subsequent one-step density gradient centrifugation.³¹ Since the first successful transfections of *P. berghei*, nearly 20 years ago,⁷ electroporation protocols have steadily improved. The latest method uses the Nucleofector® technology, which yields transfection efficiencies in the range of 10^{-3} and 10^{-2} .³²

INTEGRATION

There are different strategies available to genetically manipulate *P. berghei*: (i) episomal transfections, (ii) single crossover/ends-in, and (iii) double crossover/ends-out homologous recombination (Figure 2). The choice of which strategy to employ is determined by the required genetic stability of the recombinant parasites and whether the loss of genetic information is unwanted or rather desirable. Even the anticipated difficulties in cloning the parasite's extremely AT-rich DNA, in particular larger fragments of non-coding regions like promoter and terminator sequences, influence the choice of strategy.

Circular transfection plasmids will not be integrated in the parasite genome but instead will be maintained episomally as long as drug pressure is applied. Such transfections do not lead to the loss of any genetic information, however, the episomes will be lost rapidly in the absence of a selecting drug. Furthermore, the introduction of episomally coded sequences for protein expression and/or localization harbors the risk of artifacts, e.g. variant plasmid copy numbers between individual parasites. An early study has demonstrated maintenance of as many as 15 plasmid copies per parasite during drug pressure.³³ Recently, this concept was utilized to control expression levels of a GFP::actin 2 fusion protein through drug-regulated episomal copy numbers.³⁴ The use of a *Plasmodium* artificial chromosome, harboring functional centromere and telomere sequences, allows the introduction of a multitude of transgenes simultaneously in a more controlled manner, i.e. with efficient replication and transfer of single copies to daughter cells.³⁵ Using these artificial chromosomes, a high-coverage genomic library has previously been cloned and transfected in *P. berghei*, with fragment sizes ranging from 10 to 50 kb.³⁶

Stable integration can be achieved using linearized DNA constructs with left and right homology arms that target the construct to a specific locus in the parasite genome. Potential issues with varying copy numbers and the need for continuous drug pressure may be avoided with this technique. The most efficient approach is through single crossover/ends-in homologous recombination (Figure 2A), for which 250 – 300 bp of homologous sequence can be sufficient for integration.³⁷ Typically, however, homology arms of 0.5 – 1 kb are used to increase the efficiency of recombination. For the generation of the transfection construct, a single fragment of target DNA is cloned into a suitable vector and a unique restriction site in the

fragment is used for plasmid linearization. To study gene function, this strategy can be used to disrupt the coding sequence of a gene of interest. The downside of such an approach is that both N- and C-terminal truncated versions of the gene remain present in the genome. Hence, this approach also harbors the danger of recombination-mediated reversion in the absence of a positive selection drug. This is especially true in cases where insertion of the transfection vector led to a reduced fitness of the parasites. Although less appropriate to generate gene deletion mutants, the single crossover approach has been applied extensively to generate at least 50% of the endogenously tagged parasite lines (Figure 2C).³⁸ Advantages of this strategy include the requirement for only a single molecular cloning step and a ~10-fold increase in integration efficiency resulting in the transgenic parasites to emerge at least one day earlier (personal observations and C.J. Janse, personal communications). Another possible advantage is that one can apply insertional mutagenesis to duplicate a gene at its endogenous locus, e.g. when tagging of an endogenous gene is detrimental for its function but the presence of an additional tagged copy is tolerated.³⁹ Naturally, one should always be cautious interpreting such results as the requirement for an untagged copy of the protein may well suggest that functionality and localization of the tagged protein are affected.

Despite marginally lower integration efficiency and the need for at least two cloning steps to generate the transfection construct, double crossover/ends-out homologous recombination is nonetheless the method of choice (Figure 2B and C). The efficiency of integration is greatly dependent on the length of the homologous sequence.⁴⁰ Interestingly, homology arms that differ ~4% from the targeted nucleotide sequence are still sufficient to drive integration.⁴¹ Double crossover/ends-out homologous recombination is the only way to permanently and stably modify the *P. berghei* genome, since it completely removes the entire coding sequence of a gene of interest. Hence, parasites cannot revert to wild-type genotypes. This is particularly important in cases where parasites are to be cycled through mosquito stages where no drug pressure can be applied, when generating reference parasite lines, or when studying loss-of-function mutants. It is therefore not surprising that >90% of the reported gene deletion mutants have been generated using a double crossover strategy (Figure 2C). The generation of stable genetic mutants is furthermore a prerequisite when aiming to generate parasite lines with multiple genetic modifications, e.g. through recycling of the drug selectable cassette (see below).

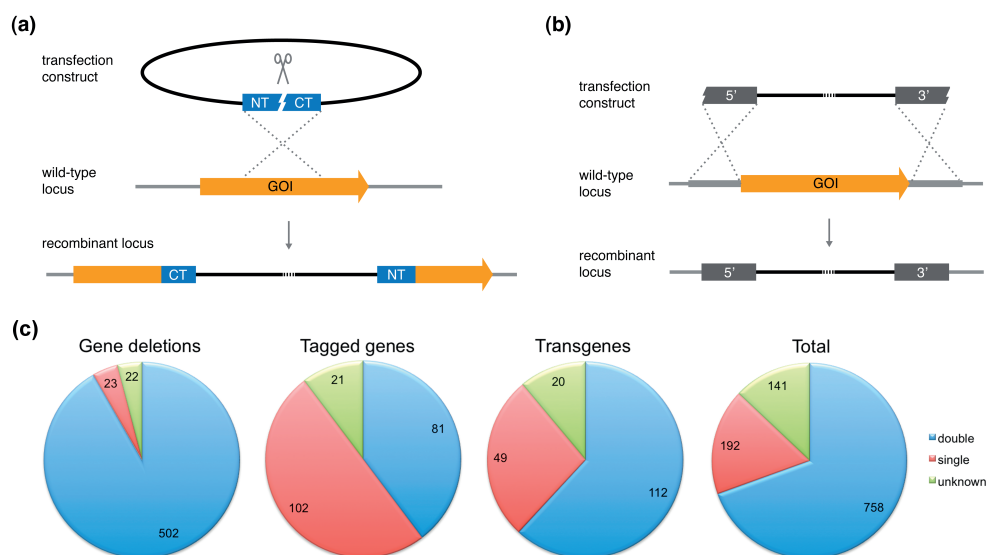


Figure 2 | Generation of recombinant parasites using homologous recombination. (a) Schematic representation of a gene deletion approach by single crossover, ends-in homologous recombination. The transfection plasmid is linearized roughly in the middle of the single targeting sequence. Successful integration into the wild-type locus leads to the disruption of the gene of interest (GOI) and partial sequence duplication. Two gene fragments remain that are truncated at the carboxy-terminus (CT) or the amino-terminus (AT). This strategy can also be used to introduce tag fusions or to duplicate complete coding sequences. (b) Schematic representation of a gene deletion approach by double crossover, ends-out homologous recombination. The linearized transfection construct harbors two targeting sequences, one upstream (5') and one downstream (3') of the target gene. Successful integration into the wild-type locus leads to deletion of the GOI. This strategy can also be used to introduce tag fusions. (c) Distribution of the approaches used (when known) to generate recombinant parasites harboring gene deletions, endogenously tagged genes, or transgenes. Data have been extracted from the Rodent Malaria genetically modified Parasites database, RMgMDB, as on 28-11-2014 (A. van Wigcheren & C.J. Janse, personal communications).³⁸ The vast majority of gene deletions mutants (>90%) were generated using double crossover recombination (blue), while at least half of the recombinant parasites expressing endogenously tagged genes were created through single crossover recombination (red). Numbers indicate the total number of mutant parasite lines in each category.

Another important consideration when manipulating the parasite genome is the site of integration. The most direct way to study the function of a gene is by targeted disruption or deletion of the endogenous locus. Alternatively, genetic material may be introduced elsewhere as a transgene. For the latter, genes have been employed

that were empirically identified to have dispensable roles during normal life cycle progression; e.g. the gene encoding the gamete surface antigen P230P⁴² and the *P. yoelii* S1 locus.⁴³ Furthermore, the loci of the ribosomal RNA C- and D-units have been used extensively in *P. berghei*. However, a small defect in oocyst development was observed after gene disruption, which should be considered when planning experiments with transgenic mosquito stage parasites.⁴¹ Although disruptions of several loci had no detectable effects on life cycle progression, it is conceivable that new phenotypic methods may reveal as yet undetected deficits. Furthermore, synergistic effects of additional genetic modification cannot be excluded. To avoid these issues, we have started to employ a silent intergenic locus on *P. berghei* chromosome 6 (SIL6) that is devoid of genes and transcriptionally silent for stable integration through double crossover.⁴⁴

SELECTION

After electroporation, the parasites are injected intravenously into naïve recipient mice. Successfully transfected parasites are usually selected by applying drug pressure. Positive selection of transgenic *P. berghei* parasites is based on the antifolates pyrimethamine or WR99210.^{45,46} Both serve as inhibitory substrate analogues of the parasite's bifunctional dihydrofolate reductase-thymidylate synthase (DHFR-TS) enzyme.⁴⁷ Pyrimethamine can be administered orally with drinking water, whereas WR99210 needs to be injected repeatedly intraperitoneally or subcutaneously. The most commonly used selection cassettes encode drug-insensitive variants of *DHFR-TS* from *Toxoplasma gondii* or *P. berghei*, which confer resistance to pyrimethamine.^{7,48-50} Human *DHFR* confers resistance to pyrimethamine and WR99210,⁵¹ thus allowing its use as a second selectable marker. An additional reason why *hDHFR* has become more commonly used is its relative small size. This facilitates the generation of more complex^{44,52,53} or PCR-based⁵⁴ transfection vectors. To date, these two drugs are the only efficient compounds for positive selection in *P. berghei* that can be used sequentially without the need to recycle the selection cassette (see below). Development of novel selection markers is hampered by two closely related problems: (i) positive selection of transfected parasites cannot be performed *in vitro* due to the inefficient reinvasion in culture and (ii) drugs must therefore be suited for *in vivo* application and should be non-toxic to the rodent host.

The *P. falciparum* chloroquine resistance transporter gene (*CRT*) has been tested as a potential new resistance marker. It has been demonstrated that mutations in *PfCRT* promote resistance towards the antimalarial chloroquine *in vitro*⁵⁵ and *in vivo*,⁵⁶ resulting in elevated IC₅₀ values of up to 17-fold.⁵⁷ Unfortunately, cross-species complementation in *P. berghei* did not increase resistance towards the drug during infection, omitting the use of mutant *PfCRT* as an additional positive selection marker.⁵⁸ There are no reports on the application, successful or unsuccessful, of any other selection markers functional in *P. falciparum*.^{59,60}

ISOLATION

Positive drug-selection is usually not completely effective, resulting in mixtures of transgenic, spontaneously mutated, and wild-type parasites, thus necessitating the purification of transgenic parasites. Traditionally, transfectants have been isolated by limiting dilution,³² through the injection of single parasites from the parental population into several naïve mice (usually ten). The success of this method relies strongly on the ratio of wild-type to mutant parasites and is therefore very inefficient when working with slow growing mutants. To circumvent this problem, parasites may be passaged through several animals under pyrimethamine pressure, resulting in the favored growth and enrichment of the transfectants prior to cloning. However, this method is labor intensive and requires a large number of experimental animals.

The development of flow cytometry-based isolation methods significantly reduced workload and animal usage (Figure 3A). The method depends on the introduction of a fluorescent protein expression cassette and subsequent isolation of the fluorescent transgenic parasites by FACS. Initial methods employed the eEF1 α promoter to drive GFP expression.^{61,62} However, due to regular wild-type contaminations of sorted populations, repeated cycles of flow-cytometric isolation or a subsequent cloning step by limiting dilution were recommended. A novel approach uses the significantly stronger HSP70 promoter, resulting in cytosolic fluorescence levels that are an order of magnitude higher, thus resulting in an almost absolute separation of wild-type and fluorescent mutant parasites.^{44,63} This method has been shown to be efficient even in the presence of a 100-fold excess of wild-type parasites, provided that the parasitaemia of the donor mice does not exceed 1%. At higher parasitaemias, sorting efficiencies decline due to the

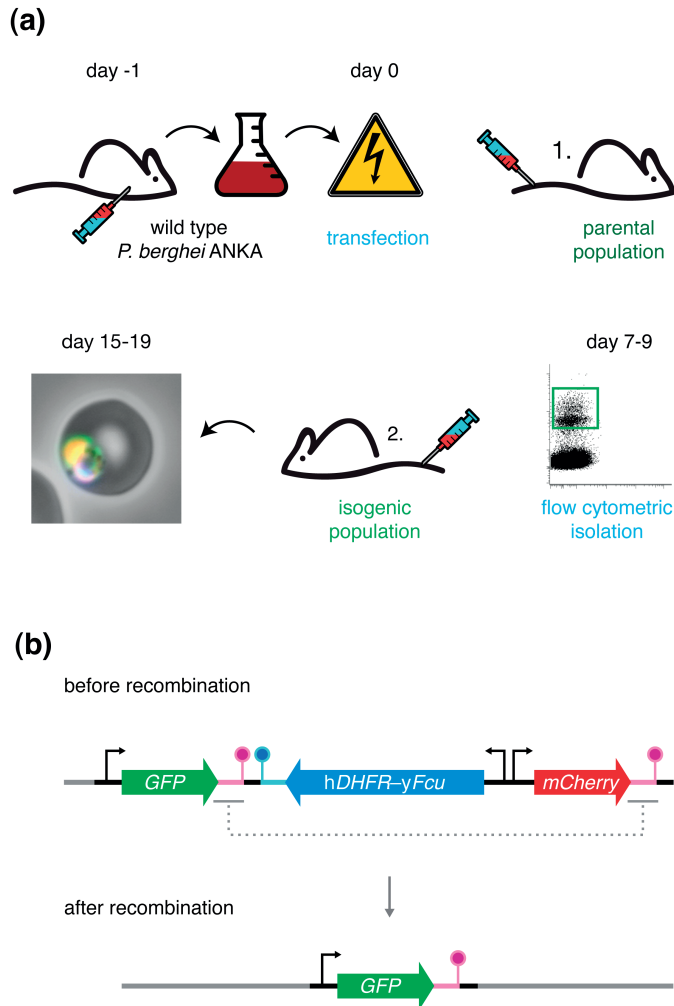


Figure 3 | Flow cytometry-based methods reduce workload and animal usage. (a) Schematic representation of the *P. berghei* transfection and mutant isolation protocol. Blood of a mouse infected with wild-type parasites is harvested by cardiac puncture and cultured overnight. Following maturation, the parasites fail to egress and arrest at the schizonts stage. These schizonts are purified and transfected with the targeting constructs. Transfected merozoites are injected intravenously into a naïve mouse. Administration of pyrimethamine in the drinking water favors the growth of successfully modified parasites, which now also express a fluorescent protein. When the parasitaemia is 0.1-1.0% (typically 7-9 days after transfection), 50 mutant parasites are isolated by flow cytometry and transferred to a naïve mouse. 8-10 days after injection, the isogenic parasite line can be harvested, stored or transferred, and tested. (b) Schematic representation of the “Gene Out

Marker Out" strategy exemplifying recycling of the *hDHFR-yFcu* drug-selectable cassette.⁶⁸ Successfully transfected and isolated parasites harbor a fluorescent cassette (GFP; green), a drug-selectable cassette (*hDHFR-yFcu*; blue), and a second fluorescent cassette (mCherry; red). After intravenous injection into a naïve mouse, 5-fluorocytosine is administered in the drinking water. This favors the growth of parasites that have successfully lost *yFcu* by homologous recombination of the duplicated sequences flanking the drug-selectable cassette and the mCherry marker (magenta). Finally, recycled parasites can be isolated using flow cytometry through the selection of GFP-positive, mCherry-negative parasites.

presence of double-infected erythrocytes harboring a transfected and a wild-type parasite. Complications resulting from the maintenance of episomal transfection vector copies were overcome through more efficient linearization protocols.⁶³ In addition to GFP, other fluorophores may be used to isolate parasites, including yellow (YFP), red (mCherry),⁶⁴ and cyan (CFP) fluorescent proteins (unpublished data). The high levels of fluorescence also facilitate imaging of live and fixed parasites in all life cycle stages, even of the extremely thin and highly motile male microgametes.⁴⁴ Most importantly though, the flow-cytometric isolation of mutant parasite lines leads to an 80-90% reduction in the use of experimental animals.

SEQUENTIAL GENETIC MODIFICATION

The availability of just two selectable markers prevents repeated rounds of genetic manipulation. The generation of double mutants is feasible, although the requirement for repeated intraperitoneal or subcutaneous administration of WR99210 is undesirable. Nonetheless, the sequential introductions of (i) *Pb* or *TgDHFR-TS* with pyrimethamine-selection and (ii) *hDHFR* with WR99210 can verify loss-of-function phenotypes through recovery of wild-type behavior by complementation. Thus, the circumsporozoite gene was reintroduced after deletion.⁵¹ Such a strategy is desirable not only for the generation of revertant strains but also for providing definitive proof for gene essentiality. This could be achieved by introducing an additional copy of the gene of interest either episomally or as a transgene by means of positive selection with pyrimethamine and insensitive *Pb* or *TgDHFR-TS*. If the subsequent deletion of the endogenous locus using WR99210 and *hDHFR* is successful in this strain but not in wild type parasites, this provides proof for the accessibility of the genomic locus and essential functions of the gene. However, when attempting to delete an essential

gene following introduction of a compensatory second copy of the gene one has to consider the requirement to use heterologous regulatory sequences. Failure to replace at least one of the up- or downstream flanking regions may lead to the preferred deletion of the transgene instead of the original target gene. It is also important to keep in mind that the hDHFR cassette must always be used as the second selectable marker when attempting the generation of double mutant parasites, since it also confers resistance to pyrimethamine. An additional issue limiting the use of WR99210 is its selective capacity. Introduction of hDHFR in the *P. berghei* genome only resulted in a 5-fold increase in WR99210 resistance,⁵¹ demonstrating the limitations of this positive selection marker when targeted integration is attempted. In contrast, WR99210 resistance was increased 1,000-fold when the hDHFR cassette was maintained episomally, due to an elevated copy number per parasite. Perhaps, this is one of the reasons why so far only two studies have reported the use of sequential gene deletions using this strategy.^{65,66}

Alternatively, flow cytometric isolation has been used as selection method, *i.e.* without the use of a drug-selectable cassette.^{32,62} Despite being relatively inefficient compared to traditional methods using drug selection, this method was employed to generate the widely used reference strain GFP_{CON}. Though largely untested, one might speculate that the improved isolation tools and methods^{44,63} might facilitate a more reliable use of flow-cytometry based isolation in the absence of drug pressure. Such an approach could even be expanded to multiple manipulation rounds by using multiple fluorescent markers with different colours.⁶⁴ Still, it remains questionable whether slow growing mutants can be isolated without additional drug pressure.

Recycling of the drug cassette would allow a virtually unlimited number of subsequent transfections. To achieve this, a positive/negative selection cassette was created containing a fusion of hDHFR and the yeast cytosine deaminase/uracil phosphoribosyltransferase gene (*yFcu*). *yFcu* metabolizes 5-fluorocytosine (5-FC) into a toxic metabolite.⁵³ Thus, this selection cassette first allows the positive selection of successfully transfected parasites by pyrimethamine or WR99120 selection, and may next be completely removed again following selection with 5-FC. This loss occurs by means of homologous recombination, using duplicated sequences flanking the selectable marker (Figure 3B). Though, 5-FC had previously to be administered through intraperitoneal injection, a protocol has been established enabling oral administration through the drinking water, thus facilitating

the procedure for both experimenter and mouse.⁶⁷ A disadvantage is the need for a subsequent cloning step by limiting dilution to isolate parasites that have lost their resistance cassette in order to use them as a recipient strain in a subsequent transfection. This issue has been elegantly solved by introducing a second, red fluorescent marker in the drug-selectable cassette in an approach that was termed “gene-out, marker-out” (GOMO).⁶⁸ Following successful integration of the transfection construct, parasites are both GFP- and mCherry-positive and can be isolated by flow cytometry. Subsequent negative selection leads to a loss of the drug-selectable cassette along with the mCherry expression cassette. Hence, successfully recycled parasites can now be isolated by sorting green-only fluorescent parasite while excluding double fluorescent parental parasites (Figure 3B).

The “gene-insertion, marker-out” (GIMO) strategy allows the fast generation of drug-selectable marker free parasites expressing a transgene.⁶⁹ This method relies on the loss of a stably integrated *hDHFR/lyFcu* drug-selectable cassette from a reference strain or gene deletion mutant through its replacement by a new marker-free transfection construct. Parasites that have successfully replaced the drug-selectable cassette are selected by administration of 5-FC. The method allows the fast generation of marker-free *P. berghei* or *P. yoelii* mutants expressing transgenes. Unfortunately, the application possibilities of GIMO are limited to recipient strains with the adopted drug-selectable cassette integrated without flanking repeat sequences.

Despite the advances and successes in generating double mutant parasite lines, we observed that off-target integrations are relatively common, when using the same vector system repeatedly, favoring integration into the sites of the initial recombination (unpublished data). We would therefore recommend the use of different vector systems for the subsequent transfections. When using an episomal construct in the second transfection, such problems should not be observed.

Double mutants may also be obtained by a classical *in vivo* cross-fertilization of two transgenic parasite lines. Mice infected with two different genetically engineered parasite lines are fed to female anopheline mosquitoes where homozygous and heterozygous fertilizations occur. In heterozygous offspring, chromosomal reorganization or recombination may yield double mutant parasites, which can be isolated after transmission to a naïve recipient mouse. This method was employed to enable conditional mutagenesis using site-specific recombination by combining

two transgenic lines, one harboring the Flp recombinase, and the other containing the *FRT* recombination sites (see below).⁵² At least three double gene-deletion mutant parasite lines have been generated using *in vivo* genetic crossing of two single gene-deletion clones.^{70,71} The efficiency of this method is highly dependent on the loci of integration. New combinations of two loci on separate chromosomes should occur at high frequencies due to chromosomal redistribution. However, loci on the same chromosome are recombined less frequently. Their uncoupling relies solely on crossing-over and interchromosomal recombination and depends largely on the distance between the two loci. Recently, we demonstrated the generation of a double mutant parasite line, expressing the endogenously tagged translocon components HSP101 and PTEX88, both of which are located at chromosome 9 and separated by approximately 360 kb (unpublished data). Loci that are associated more closely may prove difficult to recombine by meiotic crossing. Flow cytometry may help to isolate recombined parasites, when crossing mutant lines that have different fluorescent markers integrated in their respective genetically engineered loci.

In vivo crossing also offers the possibility of employing a larger number of subsequent recombination rounds, thus facilitating the generation of parasites with a multitude of mutations. However, with increasing numbers of mutations, the number of possible combinations increases even more rapidly. Hence, repeated rounds of *in vivo* crossing require diligent isolation and testing procedures of the offspring after transmission. The application of *in vivo* crossing is further limited by potential synergistic effects of the mutations that might lead to an impairment of the parasites' ability to complete the life cycle. This restriction renders meiotic crossing useless for the generation of a much desired, safe, late liver-stage arrested vaccine candidate strain.⁷²⁻⁷⁴ Ideally, a safe genetically attenuated parasite line would lack a number of genes, e.g. *LISP1*,⁷⁵ *PALM*,^{76,77} and *ZIPCO*,⁷⁸ that would allow a nearly complete maturation of liver stage parasites including the expression of blood-stage antigens. Parasites lacking any one of these genes can cause breakthrough infections, however, one can hope to eliminate these by combining multiple gene deletions. Hence, when behaving as desired, no blood-stage parasites can be obtained upon sporozoite infection. To generate such double mutant parasites, recycling of the drug-selectable cassette is required. Following negative selection, parasites deficient in the liver-stage gene *B9*⁶⁹ were rendered drug-sensitive. Next, deletion of a second liver-stage gene, *SLARP*,⁷⁹ was achieved. This proof of concept provided a safe, but early arrested genetically attenuated whole parasite

vaccine strain.⁸⁰

CONDITIONAL APPROACHES

The possibilities of analyzing genes essential for *P. berghei* blood-stage development have been limited. The establishment of a robust inducible knockdown system has been hindered by the requirements of an *in vivo* system, e.g. the administered inducers should not be toxic, be taken up efficiently, and have a prolonged systemic half-life. RNAi mediated knockdown strategies, one of the most powerful inducible systems, cannot be exploited, due to the lack of functioning RNAi machinery in *Plasmodium* parasites.⁸¹ Systems that reduce protein stability by fusion of a destabilization domain have been successfully applied to *in vitro* cultures of *P. falciparum*,⁸² but thus far no functioning system for *P. berghei* has been established.

Despite these limitations, there are a number of strategies to further characterize genes with a crucial role during blood-stage growth. Two approaches rely on differential endogenous promoter activities without the need for exogenous inducing or repressing compounds. These approaches are well suited to study gene function in an *in vivo* model, notably during transmission stages. Firstly, conditional gene ablation can be achieved by exploiting the Flp/*FRT* system of site-specific recombination (Figure 4A).⁵² This technology has been applied to study the function of the essential merozoite surface protein 1 (MSP1) during liver-stage development.⁸³ The recombinase gene was integrated into the genome under the control of a promoter that is silent during blood-stage development and is active when DNA excision is required. By using the thermolabile FlpL recombinase undesired activity during blood-stage development was further minimized. In a second transfection, *FRT* sites are inserted at both sides of the target sequence to be deleted from the genome. When the promoter is active, the recombinase is expressed and excises the *FRT* flanked locus. Therefore, the choice of promoter sequence is critical for the success of this approach.⁸⁴

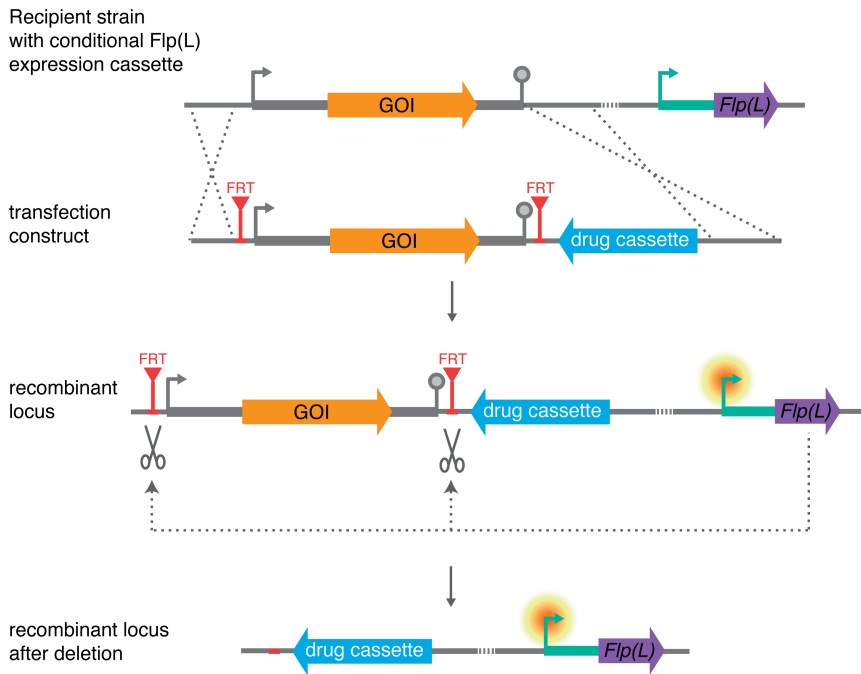
Secondly, gene function in specific stages can also be studied by exchanging the promoter sequence using homologous recombination. The strategy harnesses promoters that display expression during blood-stage development, but which are inactive during other phases of the life cycle. This has been demonstrated for the

unconventional class XIV myosin A,⁸⁵ which is essential during asexual blood-stage development. The endogenous promoter was replaced with the apical membrane antigen 1 (*AMA1*) promoter, which is active in blood stages but not in ookinetes. This results in functional levels of myosin A permitting normal blood-stage development. During the ookinete stage, however, the promoter swap resulted in a complete loss of myosin A and an impaired ookinete motility.⁸⁵ Following a similar strategy, central roles in the formation of fertile male gametes and during early mosquito-stage development were demonstrated for the putative histone chaperone FACT-L, which is essential during blood-stage development.⁸⁶

To study genes refractory to gene deletion during a blood-stage infection, a tetracycline repressor (TetRep)-based system has been established (Figure 4B).⁸⁷ It is based on an inducible promoter containing a *tet* operator. The endogenous promoter of the target gene drives the expression of a fusion of a TetRep protein and a parasite-specific activating domain (TRAD4). This fusion protein can trans-activate the *tet* operator upstream of the gene of interest. Anhydrotetracycline (ATc) binds to the trans-activator thus preventing transcription of the target gene. Administration of ATc in the drinking water led to a ~90% downregulation of transcription, as shown for the knockdown of the essential actin binding protein profilin.⁸⁷ The significance of this technical achievement notwithstanding, downregulation during mosquito stage development was not observed. Potentially, this was due to problems with ATc administration or due to the inefficiency of the described genetic components during this parasite life cycle stage. During liver-stage development, however, the system proved to be fully functional again. Very recently, this system has been used to confirm the perceived essentiality of the putative PTEX translocon component heat shock protein 101 (HSP101) in the translocation and export of cargo proteins.⁸⁸

Despite all recent advances, the described technologies share a common problem; actual proof of gene essentiality during blood-stage development is difficult to obtain. The possibility to first introduce a second copy of a gene and then remove the endogenous gene is hampered by (i) the unavailability of multiple selection markers, (ii) the need to use heterologous regulatory elements, and (iii) potential dominant negative effects of the genetic duplication. Apart from that, conditional systems all have their own limitations, e.g. incomplete levels of knock down and restrictions on the stages that can be studied.

(a)



(b)

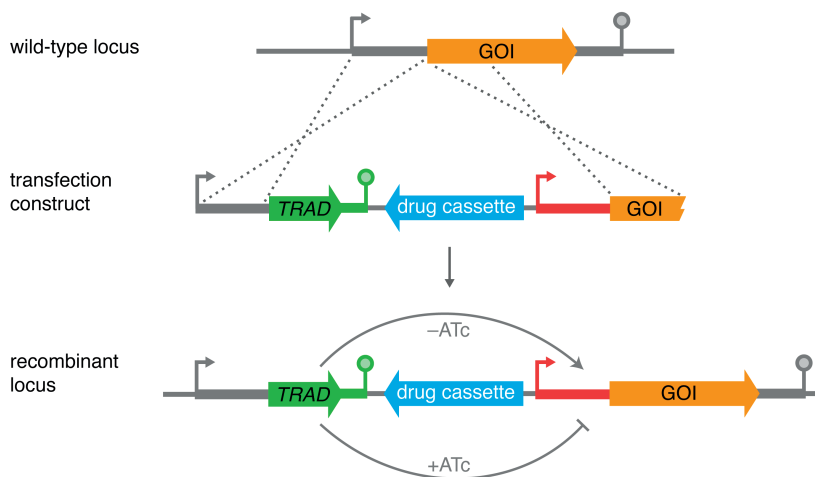


Figure 4 | Conditional gene deletion and knockdown strategies. (a) Schematic representation of conditional gene deletion using the Flp/*FRT* system. This approach requires the previous integration of a cassette driving the expression of Flp recombinase or its thermolabile variant FlpL under the control of a differentially active promoter (turquoise). By targeted integration, *FRT* sites are inserted upstream and downstream of the gene of interest (GOI). During asexual blood-stage propagation, the promoter driving *Flp(L)* transcription is silent and the recombinase is not expressed. When the promoter becomes active during other life cycle stages, Flp(L) is expressed and excises the GOI at the *FRT* sites. The resultant mutants have now lost the gene and its function can be analyzed in subsequent life cycle stages. (b) Schematic representation of conditional knockdown using a tetracycline-repressible system. An inducible promoter (red) is inserted upstream of the GOI. Additionally, the coding sequence of a tetracycline repressor protein containing a parasite-specific activating domain (TRAD) is inserted adjacent to the endogenous promoter of the GOI. Expression of TRAD in the absence of anhydrotetracycline (ATc) leads to a trans-activation of the inducible promoter by means of TRAD binding, and the GOI is transcribed. However, when ATc is present it induces conformational changes in TRAD, thereby preventing transcription.

VISUALIZATION

To date, the most efficient way to test essentiality is the independent transfection with a disruptive and a non-disruptive construct, providing proof for the accessibility of the locus and thus indirectly of gene essentiality.

Such a non-disruptive construct can be used for protein localization studies. One homology arm is derived from the 3' sequence, equivalent to that used for the disruptive construct. The second arm is derived from the carboxy-terminal coding sequence of the target gene, cloned directly adjacent to and in frame with a tag sequence. Thus, in addition to providing a positive control for transfection efficiency and accessibility of the target locus, protein expression levels and subcellular localization can be studied. Recently, we have introduced the *Berghei* Adaptable Transfection (pBAT) plasmid system that allows the generation of deletion and tagging constructs from the same intermediate construct.⁴⁴ These plasmids have been optimized for size and ease of cloning and combine (i) a recyclable, drug-selectable cassette and (ii) a bright fluorescence cassette flanked by multiple cloning sites and transgene targeting sequences. A variety of plasmids are available that include amino- or carboxy-terminal tagging sequences. One of these transfection plasmids was used to provide support for the apicoplast localizations and essential roles of four of the five sulfur utilization factors (SUF).⁸⁹ Using a comparable strategy but an alternative transfection vector system,^{90,91} the distinct spatio-temporal distribution of two alveolins was visualized.⁹² Refractoriness to

gene-deletion in combination with accessibility of the loci provided convincing evidence for essential functions during asexual blood-stage development, while conversely the efficient establishment of a blood infection following the endogenous tagging of the proteins leans support to the correct localization and functionality of these GFP-tagged proteins. This may be further confirmed by assuring that parasite growth rates and protein integrity also remain unaltered.⁶⁴

Needless to say that microscopy is central to the studying of malaria parasites. Arguably some of the most exciting recent developments are in the intravital imaging of murine malaria parasites during an infection, *e.g.* using bioluminescence⁹³ or fluorescence. The latter has been used to visualize mosquito-to-mouse transition,⁹⁴⁻⁹⁶ liver-stage development,^{26,97} the transition from liver to blood-stage infection,²⁷ and parasites in the brain.^{25,98} Such studies can provide profound insights in pathology and virulence of the parasites, the host immune defenses against the pathogen, and host-parasite interactions. The continuous developments in experimental genetics aid these studies by providing a range of genetically engineered parasite lines expressing luciferases or fluorescent proteins. Furthermore, there are reference parasite lines that have fluorescent markers targeting to specific organelles and other subcellular localizations such as the parasitophorous vacuole (unpublished data).^{99,100} These lines facilitate cell biological studies of this ancient eukaryotic single cell pathogen. For much more extensive reviews of the many exciting developments in various aspects of visualizing malaria parasites, we refer the readers to a special issue of *Parasitology International*.¹⁰¹⁻¹⁰⁶

NEXT GENERATION

Ten years after the publication of the nearly complete genome sequence, and twenty years after the development of techniques for stable genetic engineering, the time has come to make the next big leap in our understanding of *Plasmodium* biology. One way of doing so is by utilizing random mutagenesis through site-specific transposable elements. The first method in *Plasmodium* was developed using a mini-Tn5 derivative to mutagenize an *Escherichia coli* library of *P. berghei* DNA.¹⁰⁷ More recently, a system relying on the insertion of the lepidopteran transposable element *piggyBac* developed in *P. falciparum*¹⁰⁸ has been adapted to *P. berghei* and employed to generate 127 insertions.¹⁰⁹ The nature of the target

sequence, *i.e.* AATT, leads to the transposon integrating predominantly in non-coding sequences, making this method particularly useful for regulatory mutations.

There have been a number of studies employing standard *P. berghei* transfection technology to study multiple genes. The first and still the third largest study to date targeted 20 genes encoding putative secreted proteins of the ookinete.¹¹⁰ In 2010, the landmark paper by Tewari and colleagues, described the largest functional characterization of 66 putative protein kinases encoded in the *P. berghei* genome.¹¹¹ The generation and characterization of 23 loss-of-function mutants enabled the identification of some essential regulators of mosquito transmission. In a complementary approach, published four years later, the essentiality of 16 of 30 targeted phosphatases during asexual blood-stage growth was shown, with distinct roles of the other phosphatases during life cycle progression and differentiation.¹¹² No more than nine additional studies attempting the deletion of ≥ 5 genes have provided insights in the functions of a variety of gene/protein families, pathways, and complexes. These include studies of genes encoding exported proteins,^{113,114} components of the *Plasmodium* translocon of exported proteins,^{64,115} 6-Cys proteins,⁴² rhomboid proteases,¹¹⁶ protein S-acyl transferases,¹¹⁷ sulfur utilization factors of the apicoplast,⁸⁹ and *P. yoelii* early transcribed membrane proteins.¹¹⁸ Currently, 427 genes have been targeted of which 175 (39%) proved refractory to gene deletion and the remaining 252 (59%) have been deleted successfully (Figure 5).³⁸ Recent years have also seen a steady increase of parasite lines expressing endogenously tagged genes bringing the total at 178 while 2 genes were refractory to tagging (Figure 5). Despite all the progress made, it would take until the end of the century to target all *P. berghei* genes, if continued at the current pace.

Before we can bring targeted, non-random experimental genetics to a truly genome-wide scale, a number of hurdles need to be overcome. The first is the construction of the thousands of transfection constructs needed to target the ~5,000 genes.¹⁵ Some advances have been made to facilitate the transfection vector construction. PCR-based construction of replacement vectors can be scaled relatively easily, but is limited to small constructs.⁵⁴ Another PCR-based solution was used to generate *P. yoelii* transfection vectors, however, still requires a single enzymatic cloning step.¹¹⁹ A huge advance has been the establishment of the *PlasmoGEM* system, a pipeline for the genome-scale production of linear replacement vectors with large homology arms.^{40,120} Utilization of these vectors in combination with signature tagged mutagenesis enables the reproducible

generation of a pool of up to 90 gene-deletion mutants in a single mouse.¹²¹ Each individual mutant can be identified by a unique barcode sequence flanked by a standard sequencing primer annealing site. Thus dispensable gene functions during asexual blood-stage replication and growth rates of the gene deletion mutants can be assessed, however, the method is not compatible with the isolation of the generated mutants. Therefore a combination of the *Plasmo*GEM system with flow cytometry-assisted sorting procedures that have tackled the bottleneck of isolating successfully modified parasites would be particularly useful.^{63,68}

Transfection efficiency improved substantially since the establishment of the AMAXA transfection technology.³² Genetic manipulation efficiency has increased to the point where there is little room for further improvement. Nonetheless, the recent report that the CRISPR/Cas9 system is also functional in *P. yoelii*¹²² is a useful step forward. CRISPR/Cas9 will be particularly useful to introduce a multitude of small point mutations, which are much harder to generate with the more conventional methods. Perhaps this technology can also be utilized when considering a genome-wide gene deletion effort.

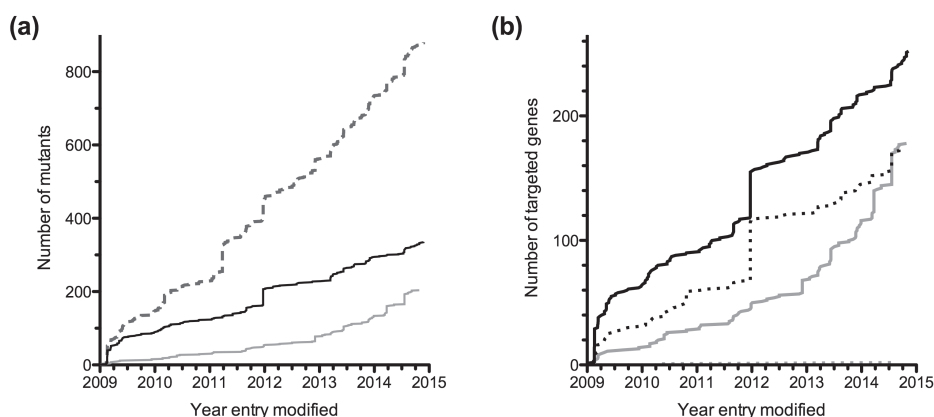


Figure 5 | Progress of experimental genetics efforts in rodent malaria parasites. Data have been extracted from the Rodent Malaria genetically modified Parasites database, RMgmDB, as on 28-11-2014 (A. van Wigcheren & C.J. Janse, personal communications).³⁸ Note that the date indicated for each entry is the date when the entry was last modified in the database. Therefore, no entries precede the year 2009 in which the database was initiated. (a) Total number of successfully generated mutants (dashed line) including loss-of-function (black) and endogenously tagged (gray) parasite lines. (b) Number of targeted unique genes. Indicated are successful (solid) and unsuccessful (dotted) attempts to delete (black) or endogenously tag (gray) the genes of interest.

However, in spite of all these improvements, the phenotypic characterization of the generated mutants arguably remains the main limiting factor of *Plasmodium* genome-wide functional genetics. Streamlining analysis and standardizing the various checkpoints of life cycle progressions would be a first step to expedite phenotypic characterization. The introduction of a number of bioluminescence-based methods enables faster and less subjective quantification of the *P. berghei* burden when compared to traditional microscopy based approaches.¹²³⁻¹²⁶ These methods, however, do not permit the comparison of multiple mutants simultaneously. A flow cytometry-based *in vivo* competition assay has been developed that enables the analysis of blood-stage development of three differently colored fluorescent parasite lines within a single mouse.⁶⁴ Introduction of additional fluorescent markers should further increase the number of mutants that might be analyzed simultaneously. Unfortunately, no methods enabling the quantification of multiple mutant parasite lines simultaneously in other life cycle stages are yet available.

CONCLUDING REMARKS

The malaria research community has made some major advances in experimental genetics approaches in the *in vivo* murine malaria model systems. These improvements had a profound impact on our understanding of malaria parasite biology and infections. Continuous progress, e.g. through the development of methods to generate and isolate multiple recombinant parasite lines simultaneously, will hopefully bring a genome-wide repository of mutant and transgenic parasite lines within our grasp. The efficiency of generating multi-mutant parasite strains including the analyses of gene essentiality through complementation approaches needs improvement. Perhaps the biggest challenge will be the design of efficient and informative methods to analyze these recombinant parasite lines throughout the complex *Plasmodium* life cycle.

REFERENCES

- 1 Laveran A. Un nouveau parasite trouvé dans le sang de malades atteints de fièvre palustre. Origine parasitaire des accidents de l'impaludisme. Bull Mem Soc Med Hopitaux Paris. 1881;17:158–64.
- 2 Goonewardene R, Daily J, Kaslow D, Sullivan TJ, Duffy P, Carter R, *et al.* Transfection of the malaria parasite and expression of firefly luciferase. Proc Natl Acad Sci USA. 1993;90:5234–6.
- 3 Wu Y, Sifri CD, Lei HH, Su XZ, Wellems TE. Transfection of *Plasmodium falciparum* within human red blood cells. Proc Natl Acad Sci USA. 1995;92:973–7.
- 4 Pfahler JM, Galinski MR, Barnwell JW, Lanzer M. Transient transfection of *Plasmodium vivax* blood stage parasites. Mol Biochem Parasitol. 2006;149:99–101.
- 5 van der Wel AM, Tomas AM, Kocken CH, Malhotra P, Janse C, Waters AP, *et al.* Transfection of the primate malaria parasite *Plasmodium knowlesi* using entirely heterologous constructs. J Exp Med. 1997;185:1499–503.
- 6 Kocken CH, Van Der Wel A, Thomas AW. *Plasmodium cynomolgi*: transfection of blood-stage parasites using heterologous DNA constructs. Exp Parasitol. 1999;93:58–60.
- 7 van Dijk MR, Waters AP, Janse C. Stable transfection of malaria parasite blood stages. Science. 1995;268:1358–62.
- 8 Mota MM, Thathy V, Nussenzweig RS, Nussenzweig V. Gene targeting in the rodent malaria parasite *Plasmodium yoelii*. Mol Biochem Parasitol. 2001;113:271–8.
- 9 Reece SE, Thompson J. Transformation of the rodent malaria parasite *Plasmodium chabaudi* and generation of a stable fluorescent line PcGFP_{CON}. Malar J. 2008;7:183.
- 10 Gardner MJ, Hall N, Fung E, White OR, Berriman M, Hyman RW, *et al.* Genome sequence of the human malaria parasite *Plasmodium falciparum*. Nature. 2002;419:498–511.
- 11 Carlton JM, Angiuoli SV, Suh BB, Kooij TWA, Perteu M, Silva JC, *et al.* Genome sequence and comparative analysis of the model rodent malaria parasite *Plasmodium yoelii yoelii*. Nature. 2002;419:512–9.
- 12 Hall N, Karras M, Raine JD, Carlton JM, Kooij TWA, Berriman M, *et al.* A comprehensive survey of the *Plasmodium* life cycle by genomic, transcriptomic, and proteomic analyses. Science. 2005;307:82–6.
- 13 Carlton JM, Adams JH, Silva JC, Bidwell SL, Lorenzi H, Caler E, *et al.* Comparative genomics of the neglected human malaria parasite *Plasmodium vivax*. Nature. 2008;455:757–63.
- 14 Pain A, Böhme U, Berry A, Mungall K, Finn RD, Jackson AP, *et al.* The genome of the simian and human malaria parasite *Plasmodium knowlesi*. Nature. 2008;455:799–803.
- 15 Otto TD, Böhme U, Jackson AP, Hunt M, Franke-Fayard B, Hoeijmakers WAM, *et al.* A comprehensive evaluation of rodent malaria parasite genomes and gene expression. BMC Biol. 2014;12:86.
- 16 Moraes Barros RR, Straimer J, Sa JM, Salzman RE, Melendez-Muniz VA, Mu J, *et al.* Editing the *Plasmodium vivax* genome, using zinc-finger nucleases. J Infect Dis. 2014;;jiu423.

- 17 Udomsangpetch R, Kaneko O, Chotivanich K, Sattabongkot J. Cultivation of *Plasmodium vivax*. Trends Parasitol. 2008;24:85–8.
- 18 Limenitakis J, Soldati-Favre D. Functional genetics in Apicomplexa: potentials and limits. FEBS Lett. 2011;585:1579–88.
- 19 Ghorbal M, Gorman M, Macpherson CR, Martins RM, Scherf A, Lopez-Rubio J-J. Genome editing in the human malaria parasite *Plasmodium falciparum* using the CRISPR-Cas9 system. Nat Biotechnol. 2014;32:819–21.
- 20 Franke-Fayard B, Fonager J, Braks A, Khan SM, Janse C. Sequestration and tissue accumulation of human malaria parasites: can we learn anything from rodent models of malaria? PLoS Pathog. 2010;6:e1001032.
- 21 Engwerda C, Belnoue E, Grüner AC, Rénia L. Experimental models of cerebral malaria. Curr Top Microbiol Immunol. 2005;297:103–43.
- 22 Hansen DS. Inflammatory responses associated with the induction of cerebral malaria: lessons from experimental murine models. PLoS Pathog. 2012;8:e1003045.
- 23 Hafalla JC, Silvie O, Matuschewski K. Cell biology and immunology of malaria. Immunol Rev. 2011;240:297–316.
- 24 Jemmely NY, Niang M, Preiser PR. Small variant surface antigens and *Plasmodium* evasion of immunity. Future Microbiol. 2010;5:663–82.
- 25 Nacer A, Movila A, Baer K, Mikolajczak SA, Kappe SHI, Frevert U. Neuroimmunological blood brain barrier opening in experimental cerebral malaria. PLoS Pathog. 2012;8:e1002982.
- 26 Frevert U, Engelmann S, Zougbedé S, Stange J, Ng B, Matuschewski K, *et al.* Intravital observation of *Plasmodium berghei* sporozoite infection of the liver. PLoS Biol. 2005;3:e192.
- 27 Sturm A, Amino R, van de Sand C, Regen T, Retzlaff S, Rennenberg A, *et al.* Manipulation of host hepatocytes by the malaria parasite for delivery into liver sinusoids. Science. 2006;313:1287–90.
- 28 Rug M, Maier AG. Transfection of *Plasmodium falciparum*. Methods Mol Biol. 2013; 923:75–98.
- 29 Mons B, van der Kaay HJ. The effect of cryopreservation on gametocytogenesis of *Plasmodium berghei berghei*: a preliminary report. Acta Leiden. 1982;48:9–16.
- 30 Mons B, Janse C, Boorsma EG, van der Kaay HJ. Synchronized erythrocytic schizogony and gametocytogenesis of *Plasmodium berghei* *in vivo* and *in vitro*. Parasitology. 1985;91 (Pt 3):423–30.
- 31 Waters AP, Thomas AW, van Dijk MR, Janse C. Transfection of malaria parasites. Methods. 1997;13:134–47.
- 32 Janse C, Franke-Fayard B, Mair GR, Ramesar J, Thiel C, Engelmann S, *et al.* High efficiency transfection of *Plasmodium berghei* facilitates novel selection procedures. Mol Biochem Parasitol. 2006;145:60–70.
- 33 van Dijk MR, Vinkenoog R, Ramesar J, Vervenne RA, Waters AP, Janse C. Replication, expression and segregation of plasmid-borne DNA in genetically transformed malaria parasites. Mol Biochem Parasitol. 1997;86:155–62.
- 34 Andreadaki M, Morgan RN, Deligianni E, Kooij TWA, Santos JM, Spanos L, *et al.* Genetic crosses and complementation reveal essential functions for the *Plasmodium* stage-specific actin2 in sporogonic development. Cell Microbiol. 2014;16:751–67.

- 35 Iwanaga S, Khan SM, Kaneko I, Christodoulou Z, Newbold CI, Yuda M, *et al.* Functional identification of the *Plasmodium* centromere and generation of a *Plasmodium* artificial chromosome. *Cell Host Microbe*. 2010;7:245–55.
- 36 Iwanaga S, Kaneko I, Yuda M. A high-coverage artificial chromosome library for the genome-wide screening of drug-resistance genes in malaria parasites. *Genome Res*. 2012;22:985–92.
- 37 Nunes A, Thathy V, Bruderer T, Sultan AA, Nussenzweig RS, Ménard R. Subtle mutagenesis by ends-in recombination in malaria parasites. *Mol Cell Biol*. 1999;19:2895–902.
- 38 Janse C, Kroeze H, van Wigcheren A, Mededovic S, Fonager J, Franke-Fayard B, *et al.* A genotype and phenotype database of genetically modified malaria-parasites. *Trends Parasitol*. 2011;27:31–9.
- 39 Kooij TWA, Franke-Fayard B, Renz J, Kroeze H, van Dooren MW, Ramesar J, *et al.* *Plasmodium berghei* α -tubulin II: a role in both male gamete formation and asexual blood stages. *Mol Biochem Parasitol*. 2005;144:16–26.
- 40 Pfander C, Anar B, Schwach F, Otto TD, Brochet M, Volkmann K, *et al.* A scalable pipeline for highly effective genetic modification of a malaria parasite. *Nat Methods*. 2011;8:1078–82.
- 41 van Spaendonk RM, Ramesar J, van Wigcheren A, Eling WMC, Beetsma AL, van Gemert G-J, *et al.* Functional equivalence of structurally distinct ribosomes in the malaria parasite, *Plasmodium berghei*. *J Biol Chem*. 2001;276:22638–47.
- 42 van Dijk MR, van Schaijk BCL, Khan SM, van Dooren MW, Ramesar J, Kaczanowski S, *et al.* Three members of the 6-cys protein family of *Plasmodium* play a role in gamete fertility. *PLoS Pathog*. 2010;6:e1000853.
- 43 Jacobs-Lorena VY, Mikolajczak SA, Labaied M, Vaughan AM, Kappe SHI. A dispensable *Plasmodium* locus for stable transgene expression. *Mol Biochem Parasitol*. 2010;171:40–4.
- 44 Kooij TWA, Rauch MM, Matuschewski K. Expansion of experimental genetics approaches for *Plasmodium berghei* with versatile transfection vectors. *Mol Biochem Parasitol*. 2012;185:19–26.
- 45 Childs GE, Lambros C. Analogues of N-benzyloxydihydrotriazines: *in vitro* antimalarial activity against *Plasmodium falciparum*. *Ann Trop Med Parasitol*. 1986;80:177–81.
- 46 Canfield CJ, Milhous WK, Ager AL, Rossan RN, Sweeney TR, Lewis NJ, *et al.* PS-15: a potent, orally active antimalarial from a new class of folic acid antagonists. *Am J Trop Med Hyg*. 1993;49:121–6.
- 47 Yuvaniyama J, Chitnumsub P, Kamchonwongpaisan S, Vanichthanankul J, Sirawaraporn W, Taylor P, *et al.* Insights into antifolate resistance from malarial DHFR-TS structures. *Nat Struct Biol*. 2003;10:357–65.
- 48 Ferone R, Burchall JJ, Hitchings GH. *Plasmodium berghei* dihydrofolate reductase. Isolation, properties, and inhibition by antifolates. *Mol Pharmacol*. 1969;5:49–59.
- 49 Ferone R. Dihydrofolate reductase from pyrimethamine-resistant *Plasmodium berghei*. *J Biol Chem*. 1970;245:850–4.
- 50 Donald RG, Roos DS. Stable molecular transformation of *Toxoplasma gondii*: a selectable dihydrofolate reductase-thymidylate synthase marker based on drug-resistance mutations in malaria. *Proc Natl Acad Sci USA*. 1993;90:11703–7.

- 51 de Koning-Ward TF, Fidock DA, Thathy V, Ménard R, van Spaendonk RM, Waters AP, *et al.* The selectable marker human dihydrofolate reductase enables sequential genetic manipulation of the *Plasmodium berghei* genome. *Mol Biochem Parasitol.* 2000;106:199–212.
- 52 Carvalho TG, Thiberge S, Sakamoto H, Ménard R. Conditional mutagenesis using site-specific recombination in *Plasmodium berghei*. *Proc Natl Acad Sci USA.* 2004;101:14931–6.
- 53 Braks JAM, Franke-Fayard B, Kroeze H, Janse C, Waters AP. Development and application of a positive–negative selectable marker system for use in reverse genetics in *Plasmodium*. *Nucleic Acids Res.* 2006;34:e39–9.
- 54 Ecker A, Moon R, Sinden RE, Billker O. Generation of gene targeting constructs for *Plasmodium berghei* by a PCR-based method amenable to high throughput applications. *Mol Biochem Parasitol.* 2006;145:265–8.
- 55 Lakshmanan V, Bray PG, Verdier-Pinard D, Johnson DJ, Horrocks P, Muhle RA, *et al.* A critical role for PfCRT K76T in *Plasmodium falciparum* verapamil-reversible chloroquine resistance. *EMBO J.* 2005;24:2294–305.
- 56 Picot S, Olliaro P, de Monbrison F, Bienvenu A-L, Price RN, Ringwald P. A systematic review and meta-analysis of evidence for correlation between molecular markers of parasite resistance and treatment outcome in *falciparum* malaria. *Malar J.* 2009;8:89.
- 57 Sidhu ABS, Verdier-Pinard D, Fidock DA. Chloroquine resistance in *Plasmodium falciparum* malaria parasites conferred by PfCRT mutations. *Science.* 2002;298:210–3.
- 58 Ecker A, Lakshmanan V, Sinnis P, Coppens I, Fidock DA. Evidence that mutant PfCRT facilitates the transmission to mosquitoes of chloroquine-treated *Plasmodium* gametocytes. *J Infect Dis.* 2011;203:228–36.
- 59 Mamoun CB, Gluzman IY, Goyard S, Beverley SM, Goldberg DE. A set of independent selectable markers for transfection of the human malaria parasite *Plasmodium falciparum*. *Proc Natl Acad Sci USA.* 1999;96:8716–20.
- 60 Ganesan SM, Morrissey JM, Ke H, Painter HJ, Laroia K, Phillips MA, *et al.* Yeast dihydroorotate dehydrogenase as a new selectable marker for *Plasmodium falciparum* transfection. *Mol Biochem Parasitol.* 2011;177:29–34.
- 61 Franke-Fayard BMD, Trueman HE, Ramesar J, Mendoza J, van der Keur M, van der Linden R, *et al.* A *Plasmodium berghei* reference line that constitutively expresses GFP at a high level throughout the complete life cycle. *Mol Biochem Parasitol.* 2004;137:23–33.
- 62 Janse C, Franke-Fayard BMD, Waters AP. Selection by flow-sorting of genetically transformed, GFP-expressing blood stages of the rodent malaria parasite, *Plasmodium berghei*. *Nat Protoc.* 2006;1:614–23.
- 63 Kenthirapalan S, Waters AP, Matuschewski K, Kooij TWA. Flow cytometry-assisted rapid isolation of recombinant *Plasmodium berghei* parasites exemplified by functional analysis of aquaglyceroporin. *Int J Parasitol.* 2012;42:1185–92.
- 64 Matz JM, Matuschewski K, Kooij TWA. Two putative protein export regulators promote *Plasmodium* blood stage development *in vivo*. *Mol Biochem Parasitol.* 2013;191:44–52.
- 65 Jobe O, Lumsden J, Mueller A-K, Williams J, Silva-Rivera H, Kappe SHI, *et al.* Genetically attenuated *Plasmodium berghei* liver stages induce sterile protracted

- protection that is mediated by major histocompatibility complex Class I-dependent interferon-gamma-producing CD8+ T cells. *J Infect Dis*. 2007;196:599–607.
- 66 Annoura T, van Schaijk BCL, Ploemen IHJ, Sajid M, Lin J-W, Vos MW, *et al*. Two *Plasmodium* 6-Cys family-related proteins have distinct and critical roles in liver-stage development. *FASEB J*. 2014;28:2158–70.
- 67 Orr RY, Philip N, Waters AP. Improved negative selection protocol for *Plasmodium berghei* in the rodent malarial model. *Malar J*. 2012;11:103.
- 68 Manzoni G, Briquet S, Risco-Castillo V, Gaultier C, Topçu S, Ivănescu ML, *et al*. A rapid and robust selection procedure for generating drug-selectable marker-free recombinant malaria parasites. *Sci Rep*. 2014;4:4760.
- 69 Lin J-W, Annoura T, Sajid M, Chevalley-Maurel S, Ramesar J, Klop O, *et al*. A novel “gene insertion/marker out” (GIMO) method for transgene expression and gene complementation in rodent malaria parasites. *PLoS ONE*. 2011;6:e29289.
- 70 Moon RW, Taylor CJ, Bex C, Schepers R, Goulding D, Janse C, *et al*. A cyclic GMP signalling module that regulates gliding motility in a malaria parasite. *PLoS Pathog*. 2009;5:e1000599.
- 71 Tremp AZ, Dessens JT. Malaria IMC1 membrane skeleton proteins operate autonomously and participate in motility independently of cell shape. *J Biol Chem*. 2011;286:5383–91.
- 72 Vaughan AM, Wang R, Kappe SHI. Genetically engineered, attenuated whole-cell vaccine approaches for malaria. *Hum Vaccin*. 2010;6:107–13.
- 73 Borrmann S, Matuschewski K. Targeting *Plasmodium* liver stages: better late than never. *Trends Mol Med*. 2011;17:527–36.
- 74 Nganou-Makamdop K, Sauerwein RW. Liver or blood-stage arrest during malaria sporozoite immunization: the later the better? *Trends Parasitol*. 2013;29:304–10.
- 75 Ishino T, Boisson B, Orito Y, Lacroix C, Bischoff E, Loussert C, *et al*. LISP1 is important for the egress of *Plasmodium berghei* parasites from liver cells. *Cell Microbiol*. 2009;11:1329–39.
- 76 Haussig JM, Matuschewski K, Kooij TWA. Inactivation of a *Plasmodium* apicoplast protein attenuates formation of liver merozoites. *Mol Microbiol*. 2011;81:1511–25.
- 77 Haussig JM, Burgold J, Hafalla JCR, Matuschewski K, Kooij TWA. Signatures of malaria vaccine efficacy in ageing murine immune memory. *Parasite Immunol*. 2014;36:199–206.
- 78 Sahu T, Boisson B, Lacroix C, Bischoff E, Richier Q, Formaglio P, *et al*. ZIPCO, a putative metal ion transporter, is crucial for *Plasmodium* liver-stage development. *EMBO Mol Med*. 2014;6:1387–97.
- 79 Silvie O, Goetz K, Matuschewski K. A sporozoite asparagine-rich protein controls initiation of *Plasmodium* liver stage development. *PLoS Pathog*. 2008;4:e1000086.
- 80 van Schaijk BCL, Ploemen IHJ, Annoura T, Vos MW, Lander F, van Gemert G-J, *et al*. A genetically attenuated malaria vaccine candidate based on *P. falciparum* *b9/slarp* gene-deficient sporozoites. *eLife*. 2014;3.
- 81 Baum J, Papenfuss AT, Mair GR, Janse C, Vlachou D, Waters AP, *et al*. Molecular genetics and comparative genomics reveal RNAi is not functional in malaria parasites. *Nucleic Acids Res*. 2009;37:3788–98.
- 82 Russo I, Oksman A, Vaupel B, Goldberg DE. A calpain unique to alveolates is

- essential in *Plasmodium falciparum* and its knockdown reveals an involvement in pre-S-phase development. *Proc Natl Acad Sci USA*. 2009;106:1554–9.
- 83 Combe A, Giovannini D, Carvalho TG, Späth S, Boisson B, Lousset C, *et al*. Clonal conditional mutagenesis in malaria parasites. *Cell Host Microbe*. 2009;5:386–96.
 - 84 Lacroix C, Giovannini D, Combe A, Bargieri DY, Späth S, Panchal D, *et al*. FLP/FRT-mediated conditional mutagenesis in pre-erythrocytic stages of *Plasmodium berghei*. *Nat Protoc*. 2011;6:1412–28.
 - 85 Siden-Kiamos I, Ganter M, Kunze A, Hliscs M, Steinbüchel M, Mendoza J, *et al*. Stage-specific depletion of myosin A supports an essential role in motility of malarial ookinetes. *Cell Microbiol*. 2011;13:1996–2006.
 - 86 Laurentino EC, Taylor S, Mair GR, Lasonder E, Bártfai R, Stunnenberg HG, *et al*. Experimentally controlled downregulation of the histone chaperone FACT in *Plasmodium berghei* reveals that it is critical to male gamete fertility. *Cell Microbiol*. 2011;13:1956–74.
 - 87 Pino P, Sebastian S, Kim EA, Bush E, Brochet M, Volkmann K, *et al*. A tetracycline-repressible transactivator system to study essential genes in malaria parasites. *Cell Host Microbe*. 2012;12:824–34.
 - 88 Elsworth B, Matthews K, Nie CQ, Kalanon M, Charnaud SC, Sanders PR, *et al*. PTEX is an essential nexus for protein export in malaria parasites. *Nature*. 2014;511:587–91.
 - 89 Haussig JM, Matuschewski K, Kooij TWA. Identification of vital and dispensable sulfur utilization factors in the *Plasmodium* apicoplast. *PLoS ONE*. 2014;9:e89718.
 - 90 Tremp AZ, Khater EI, Dessens JT. IMC1b is a putative membrane skeleton protein involved in cell shape, mechanical strength, motility, and infectivity of malaria ookinetes. *J Biol Chem*. 2008;283:27604–11.
 - 91 Carter V, Shimizu S, Arai M, Dessens JT. PbSR is synthesized in macrogametocytes and involved in formation of the malaria crystalloids. *Mol Microbiol*. 2008;68:1560–9.
 - 92 Tremp AZ, Al-Khattaf FS, Dessens JT. Distinct temporal recruitment of *Plasmodium* alveolins to the subpellicular network. *Parasitol Res*. 2014;113:4177–88.
 - 93 Franke-Fayard BMD, Waters AP, Janse C. Real-time *in vivo* imaging of transgenic bioluminescent blood stages of rodent malaria parasites in mice. *Nat Protoc*. 2006;1:476–85.
 - 94 Frischknecht F, Baldacci P, Martin B, Zimmer C, Thiberge S, Olivo-Marin J-C, *et al*. Imaging movement of malaria parasites during transmission by *Anopheles* mosquitoes. *Cell Microbiol*. 2004;6:687–94.
 - 95 Vanderberg JP, Frevert U. Intravital microscopy demonstrating antibody-mediated immobilisation of *Plasmodium berghei* sporozoites injected into skin by mosquitoes. *Int J Parasitol*. 2004;34:991–6.
 - 96 Amino R, Thiberge S, Martin B, Celli S, Shorte S, Frischknecht F, *et al*. Quantitative imaging of *Plasmodium* transmission from mosquito to mammal. *Nat Med*. 2006;12:220–4.
 - 97 Tarun AS, Baer K, Dumpit RF, Gray S, Lejarcegui N, Frevert U, *et al*. Quantitative isolation and *in vivo* imaging of malaria parasite liver stages. *Int J Parasitol*. 2006;36:1283–93.
 - 98 Zhao H, Aoshi T, Kawai S, Mori Y, Konishi A, Ozkan M, *et al*. Olfactory plays a key role in spatiotemporal pathogenesis of cerebral malaria. *Cell Host Microbe*. 2014;15:551–

- 63.
- 99 Stanway RR, Witt T, Zobiak B, Aepfelbacher M, Heussler VT. GFP-targeting allows visualization of the apicoplast throughout the life cycle of live malaria parasites. *Biol Cell*. 2009;101:415–30.
- 100 Stanway RR, Mueller N, Zobiak B, Graewe S, Froehlke U, Zessin PJM, *et al*. Organelle segregation into *Plasmodium* liver stage merozoites. *Cell Microbiol*. 2011;13:1768–82.
- 101 Vanderberg JP. Imaging mosquito transmission of *Plasmodium* sporozoites into the mammalian host: immunological implications. *Parasitol Int*. 2014;63:150–64.
- 102 Lawton JC, Benson RA, Garside P, Brewer JM. Using lymph node transplantation as an approach to image cellular interactions between the skin and draining lymph nodes during parasitic infections. *Parasitol Int*. 2014;63:165–70.
- 103 Frevert U, Nacer A, Cabrera M, Movila A, Leberl M. Imaging *Plasmodium* immunobiology in the liver, brain, and lung. *Parasitol Int*. 2014;63:171–86.
- 104 Claser C, Malleret B, Peng K, Bakocevic N, Gun SY, Russell B, *et al*. Rodent *Plasmodium*-infected red blood cells: imaging their fates and interactions within their hosts. *Parasitol Int*. 2014;63:187–94.
- 105 Ferrer M, Martin-Jaular L, De Niz M, Khan SM, Janse C, Calvo M, *et al*. Imaging of the spleen in malaria. *Parasitol Int*. 2014;63:195–205.
- 106 Lima FA, Gómez-Conde I, Videira PA, Marinho CRF, Olivieri DN, Tadokoro CE. Intravital microscopy technique to study parasite dynamics in the labyrinth layer of the mouse placenta. *Parasitol Int*. 2014;63:254–9.
- 107 Sakamoto H, Thiberge S, Akerman S, Janse C, Carvalho TG, Ménard R. Towards systematic identification of *Plasmodium* essential genes by transposon shuttle mutagenesis. *Nucleic Acids Res*. 2005;33:e174–4.
- 108 Balu B, Shoue DA, Fraser MJ, Adams JH. High-efficiency transformation of *Plasmodium falciparum* by the lepidopteran transposable element *piggyBac*. *Proc Natl Acad Sci USA*. 2005;102:16391–6.
- 109 Fonager J, Franke-Fayard BMD, Adams JH, Ramesar J, Klop O, Khan SM, *et al*. Development of the *piggyBac* transposable system for *Plasmodium berghei* and its application for random mutagenesis in malaria parasites. *BMC Genomics*. 2011;12:155.
- 110 Ecker A, Bushell ESC, Tewari R, Sinden RE. Reverse genetics screen identifies six proteins important for malaria development in the mosquito. *Mol Microbiol*. 2008;70:209–20.
- 111 Tewari R, Straschil U, Bateman A, Böhme U, Cherevach I, Gong P, *et al*. The systematic functional analysis of *Plasmodium* protein kinases identifies essential regulators of mosquito transmission. *Cell Host Microbe*. 2010;8:377–87.
- 112 Guttery DS, Poulin B, Ramaprasad A, Wall RJ, Ferguson DJP, Brady D, *et al*. Genome-wide functional analysis of *Plasmodium* protein phosphatases reveals key regulators of parasite development and differentiation. *Cell Host Microbe*. 2014;16:128–40.
- 113 van Ooij C, Tamez P, Bhattacharjee S, Hiller NL, Harrison T, Liolios K, *et al*. The malaria secretome: from algorithms to essential function in blood stage infection. *PLoS Pathog*. 2008;4:e1000084.
- 114 Pasini EM, Braks JA, Fonager J, Klop O, Aime E, Spaccapelo R, *et al*. Proteomic and genetic analyses demonstrate that *Plasmodium berghei* blood stages export a large

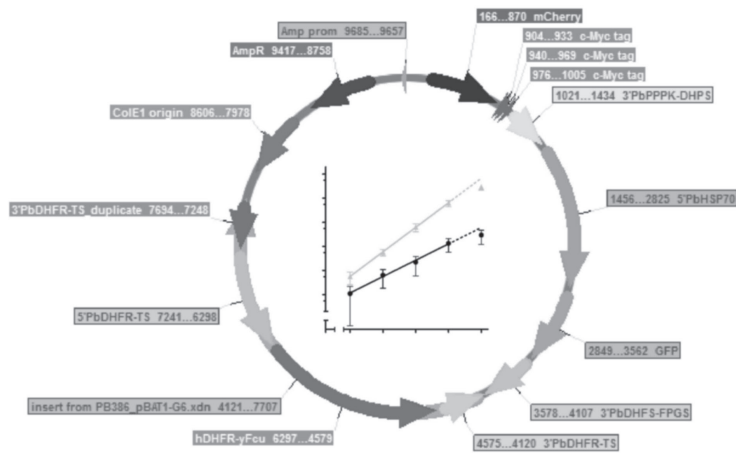
- and diverse repertoire of proteins. *Mol Cell Proteomics*. 2013;12:426–48.
- 115 Matthews K, Kalanon M, Chisholm SA, Sturm A, Goodman CD, Dixon MWA, *et al*. The *Plasmodium* translocon of exported proteins (PTEX) component thioredoxin-2 is important for maintaining normal blood-stage growth. *Mol Microbiol*. 2013;89:1167–86.
 - 116 Lin J-W, Meireles P, Prudencio M, Engelmann S, Annoura T, Sajid M, *et al*. Loss-of-function analyses defines vital and redundant functions of the *Plasmodium* rhomboid protease family. *Mol Microbiol*. 2013;88:318–38.
 - 117 Frénal K, Tay CL, Mueller C, Bushell ES, Jia Y, Graindorge A, *et al*. Global analysis of apicomplexan protein S-acyl transferases reveals an enzyme essential for invasion. *Traffic*. 2013;14:895–911.
 - 118 MacKellar DC, Vaughan AM, Aly ASI, DeLeon S, Kappe SHI. A systematic analysis of the early transcribed membrane protein family throughout the life cycle of *Plasmodium yoelii*. *Cell Microbiol*. 2011;13:175567.
 - 119 Mikolajczak SA, Aly ASI, Dumpit RF, Vaughan AM, Kappe SHI. An efficient strategy for gene targeting and phenotypic assessment in the *Plasmodium yoelii* rodent malaria model. *Mol Biochem Parasitol*. 2008;158:213–6.
 - 120 Schwach F, Bushell E, Gomes AR, Anar B, Girling G, Herd C, *et al*. PlasmoGEM, a database supporting a community resource for large-scale experimental genetics in malaria parasites. *Nucleic Acids Res*. 2015;43:D1176–82.
 - 121 Gomes AR, Bushell ESC, Schwach F, Girling G, Anar B, Quail MA, *et al*. A genome scale vector resource enables high throughput reverse genetic screening in a malaria parasite. *Cell Host Microbe*. 2015;17:404–13.
 - 122 Zhang C, Xiao B, Jiang Y, Zhao Y, Li Z, Gao H, *et al*. Efficient editing of malaria parasite genome using the CRISPR/Cas9 system. *MBio*. 2014;5:e01414–4.
 - 123 Franke-Fayard BMD, Djokovic D, Dooren MW, Ramesar J, Waters AP, Falade MO, *et al*. Simple and sensitive antimalarial drug screening *in vitro* and *in vivo* using transgenic luciferase expressing *Plasmodium berghei* parasites. *Int J Parasitol*. 2008;38:1651–62.
 - 124 Ploemen IHJ, Prudencio M, Douradinha BG, Ramesar J, Fonager J, van Gemert G-J, *et al*. Visualisation and quantitative analysis of the rodent malaria liver stage by real time imaging. *PLoS ONE*. 2009;4:e7881.
 - 125 Miller JL, Murray S, Vaughan AM, Harupa A, Sack B, Baldwin M, *et al*. Quantitative bioluminescent imaging of pre-erythrocytic malaria parasite infection using luciferase expressing *Plasmodium yoelii*. *PLoS ONE*. 2013;8:e60820.
 - 126 Zuzarte-Luis V, Sales-Dias J, Mota MM. Simple, sensitive and quantitative bioluminescence assay for determination of malaria pre-patent period. *Malar J*. 2014;13:15.

Chapter 3

Two putative protein export regulators promote *Plasmodium* blood stage development *in vivo*

Matz JM, Matuschewski K, Kooij TWA. Mol. Biochem. Parasitol. 2013; 191:44–52.

(cover image)



ABSTRACT

Protein export is considered an essential feature of malaria parasite blood stage development. Here, we examined five components of the candidate *Plasmodium* translocon of exported proteins (PTEX), a complex thought to mediate protein export across the parasitophorous vacuole membrane into the host cell. Using the murine malaria model parasite *Plasmodium berghei*, we succeeded in generating parasite lines lacking *PTEX88* and thioredoxin 2 (*TRX2*). Repeated attempts to delete the remaining three translocon components failed, suggesting essential functions for EXP2, PTEX150, and heat shock protein 101 (HSP101) during blood stage development. To analyze blood infections of the null-mutants, we established a flow cytometry-assisted intravital competition assay using three novel high fluorescent lines (Berggreen, Beryellow, and Berred). Although blood stage development of parasites lacking *TRX2* was affected, the deficit was much more striking in *PTEX88* null-mutants. The multiplication rate of *PTEX88*-deficient parasites was strongly reduced resulting in out-competition by wild-type parasites. Endogenous tagging revealed that *TRX2::tag* resides in distinct punctate organelles of unknown identity. *PTEX88::tag* shows a diffuse intraparasitic pattern in blood stage parasites. In trophozoites, *PTEX88::tag* also localized to previously unrecognized extensions reaching from the parasite surface into the erythrocyte cytoplasm. Together, our results indicate auxiliary roles for *TRX2* and *PTEX88* and central roles for EXP2, PTEX150, and HSP101 during *P. berghei* blood infection.

INTRODUCTION

The genus *Plasmodium* comprises hundreds of apicomplexan parasites that infect a variety of host species and includes the causative agents of human malaria. During invasion of a liver or red blood cell, the parasites form an intracellular membrane bound compartment, termed the parasitophorous vacuole (PV), in which they grow and replicate while hiding from the host immune defense. In order to develop within this protective niche, the parasite needs to remodel the host cell by exporting a variety of proteins across the parasitophorous vacuole membrane (PVM).¹⁻⁴ The involvement of the *Plasmodium falciparum* erythrocyte membrane protein 1 (PfEMP1) in cytoadherence and sequestration of infected red blood cells has long been recognized⁵⁻⁷ and many other exported proteins are required for PfEMP1 trafficking.⁸ The link between protein export and *P. falciparum* pathogenicity is further exemplified by the finding that human polymorphic hemoglobins S and C, which protect carriers against severe malaria, interfere with parasite-induced host-actin remodeling.⁹ Parasite-derived proteins expressed at the red blood cell surface were also shown to mediate nutrient uptake.¹⁰

Many proteins destined for export into the host cell are tagged with a specific motif, which makes them accessible to translocation. The *Plasmodium* export element (PEXEL) or vacuolar transport signal (VTS) is a short sequence with the consensus RxLxE/Q/D.^{11,12} An amino-terminal hydrophobic signal peptide ensures the entry into the secretory pathway of the parasite by translocation into the endoplasmic reticulum (ER). Here, the PEXEL/VTS motif binds phosphatidylinositol 3-phosphate (PI3P)¹³ prior to cleavage behind the leucine residue by the ER-resident protease plasmepsin V.^{14,15} The matured PEXEL/VTS protein becomes acetylated at its amino-terminus¹⁶ and is now flagged for transposition across the PVM. In recent years, a growing number of PEXEL/VTS negative exported proteins (PNEPs) has been identified, suggesting the existence of multiple processes and peptide motifs involved in cargo protein recognition.^{17,18}

Indeed, other *Plasmodium* spp. harbor lower numbers of PEXEL/VTS containing proteins than *P. falciparum*, in which malaria protein export has been studied most extensively. The *P. falciparum* exportome encompasses >500 PEXEL/VTS-positive proteins,^{11,12} many of which belong to large, often subtelomeric, gene families. Likewise, the majority of the >100 unique sequences is located in non-syntenic regions^{19,20} and initial orthology-based estimates of PEXEL/VTS containing proteins

in the murine model malaria parasite *P. berghei* ranged from 9 to 33 proteins.²¹⁻²³ Recently, *de novo* identification using hidden Markov model analysis revealed at least 75 unique PEXEL/VTs-positive sequences in *P. berghei*.²⁴ Functional genetics studies in *P. berghei* demonstrated that 19 of 33 orthologous genes were refractory to gene deletion indicating important functions for many of the conserved *Plasmodium* exported proteins.^{22,25}

When secreted into the PV lumen, soluble cargo proteins are thought to associate with a putative *Plasmodium* translocon of exported proteins (PTEX),²⁶ a large multimeric complex of >1230 kDa,²⁷ which resides at the PVM. This complex constitutes an important interface between the parasite-derived microenvironment and the host cell cytoplasm and is thought to be responsible for the unfolding and translocation of parasite proteins.^{28,29} Unfolding of proteins is required for the export of soluble as well as transmembrane proteins.^{17,30} For transmembrane PNEPs, a preceding translocation step at the parasite plasma membrane has also been demonstrated, though molecular details on this process are currently missing.¹⁷ The PTEX translocon is hypothesized to consist of at least five components:²⁶ (i) EXP2 (PBANKA_133430), a small PVM-associated protein, which is likely to form a membrane spanning pore; (ii) heat shock protein 101 (HSP101; PBANKA_093120), a member of the ClpA/B chaperone family that is thought to unfold the cargo proteins by the action of its AAA+ ATPase domains; (iii) PTEX150 (PBANKA_100850), a protein of unknown function that shows a similar stoichiometry as HSP101;²⁷ (iv) PTEX88 (PBANKA_094130), another protein of unknown function, and (v) thioredoxin 2 (TRX2; PBANKA_135800).

Although the importance of protein export is obvious, virtually no data are available about the putative PTEX translocon from any other *Plasmodium* spp. We used the rodent malaria model parasite *P. berghei* to evaluate the putative PTEX translocon by a systematic gene deletion approach. We recently developed transfection vectors³¹ and flow cytometry-based isolation methods for recombinant parasite lines.³² Here, we applied these techniques to generate recombinant parasite lines lacking *PTEX88* and *TRX2* or expressing fluorescently tagged proteins for live cell imaging. We further expanded our approaches with a flow cytometry-based intravital competition assay that we employed to demonstrate a reduced blood stage development most prominent in *ptex88*⁻ parasites.

MATERIALS AND METHODS

Experimental animals

This study was carried out in strict accordance with the German 'Tierschutzgesetz in der Fassung vom 22. Juli 2009' and the Directive 2010/63/EU of the European Parliament and Council 'On the protection of animals used for scientific purposes'. The protocol was approved by the ethics committee of the Berlin state authority ('Landesamt für Gesundheit und Soziales Berlin', permit number G0469/09). C57BL/6 mice were used for sporozoite infections. All other parasite infections were conducted with NMRI mice.

Generation of recombinant parasite lines

We used advanced experimental genetic techniques to generate^{31,33} and isolate³² all recombinant parasite lines. Further details on vector construction and genotyping strategies including primer sequences and restriction endonuclease recognition sites used for molecular cloning are provided in Figure 1, Supplementary Table S1 and Supplementary Figures S2-4.

To generate the three isogenic, strongly fluorescent reference parasite lines, Bergreen, Beryellow, and Berred, that express high levels of GFP, YFP, and mCherry, respectively, we removed the mCherry-3xMyc carboxy-terminal tagging sequence from the original pBAT-SIL6 vector³¹ by restriction digestion with BlnI and HpaI followed by Klenow fill-in and religation of the plasmid. The resulting vector pBAT-G6 harbors the GFP-expression and recyclable drug-selectable cassettes along with integration sequences targeting the silent, intergenic locus on *P. berghei* chromosome 6. We exchanged GFP from the high-expressing fluorescent protein cassette for YFP and mCherry to yield pBAT-Y6 and pBAT-M6, respectively. The plasmids were verified by commercial Sanger sequencing and linearized with ApaLI and AhdI before transfection into wild-type *P. berghei* strain ANKA parasites. Isolation of fluorescent parasites was performed as described,³² with the following adaptation to sort in three different channels. We used excitation wavelengths of 488 nm for GFP and YFP and 561 nm for mCherry parasites. Fluorescence was detected using the following band pass filters: GFP, 513/17 nm; YFP, 530/30nm; mCherry, 610/20 nm.

For the generation of vectors targeting the five components of the *P. berghei* PTEX translocon, 3' fragments were amplified from gDNA (ranging in size from 498 to 848 bp) and cloned into the pBAT vector³¹ using XhoI and KpnI to generate five intermediate constructs (pPTEX-IM). For the generation of the five gene deletion vectors (pPTEX-KO), 5' promoter regions were amplified from ANKA gDNA (ranging in size from 1,094 to 1,593 bp) and fused directly upstream of the mCherry-3xMyc tag in the five pPTEX-IM vectors using SacII and HpaI. For the two tagging constructs, termed pPTEX88-tag and pTRX2-tag, fragments of the carboxy-terminal coding regions were amplified from gDNA (699 and 652 bp, respectively) and fused in frame to the mCherry-3xMyc tag in pPTEX88-IM and pTRX2-IM using SacII and HpaI. The carboxy-terminal coding sequences cloned into the tagging plasmids were verified by commercial Sanger sequencing. All vectors targeting the putative PTEX translocon components were linearized with AhdI and ApaLI before transfection into wild-type *P. berghei* strain ANKA parasites.

Genotypic characterization of recombinant parasite lines

To demonstrate correct integration of the transfection vectors and absence of contaminating WT parasites in the isogenic, recombinant parasite lines, primer combinations were used as indicated in Supplementary Table S1, Figure 1 and Supplementary Figures S2 and S4.

Southern blot analysis using the PCR DIG Probe Synthesis kit and the DIG Luminescent Detection kit (Roche) was used, according to the manufacturer's instructions, to confirm the correct genotype of the *ptex88*⁻ and *trx2*⁻ lines. Probes were amplified using primers that were used to generate the 3' integration sequences of the respective transfection constructs (see Supplementary Table S1) and hybridized to BsmI (*ptex88*⁻) or HpaI (*trx2*⁻) restriction-digested gDNA (Figure 1).

We further confirmed inactivation of *PTEX88* and *TRX2* in the respective loss-of-function lines through RT-PCR. Total RNA was isolated from asynchronous blood stage parasites using the RNeasy Mini kit (Qiagen) following the manufacturer's instructions. To remove contaminating genomic DNA, RNA samples were treated with Turbo-DNA-free (Ambion). cDNA was synthesized by a two-step PCR reaction using oligo(dT) primers and random hexamers (Ambion). For the detection of *PTEX88* and *TRX2* transcripts, cDNA samples were tested using gene specific

primers CT-PTEX88-F-SacII and CT-PTEX-R-HpaI (699 bp), and CT-TRX2-F-SacII and CT-TRX2-R-HpaI (gDNA: 652 bp; cDNA: 279 bp). Primers specific for heat shock protein 70 (HSP70, PbHSP70-F and PbHSP70-R, 164 bp) were used to control cDNA load. All primer sequences are listed in Supplementary Table S1.

Intravital competition assay for analyzing malaria blood infection

To study blood stage development of *ptex88⁻* and *trx2⁻* parasites, we developed a new competitive growth assay. We determined parasitemia of donor mice infected with reference or recombinant parasites by flow cytometry using the gating strategies depicted in Supplementary Figure S3. A drop of tail blood was collected in 1 ml of Alsever's solution (Sigma) containing 1 μ l of Hoechst 33342. The cells were collected by centrifugation for 5 min at 1500 x g, resuspended in 1 ml PBS, and passed through 30 μ m CellTrics filters (Partec) to remove cell aggregates. All flow cytometric analyses were performed on a BD Biosciences LSR Fortessa analyzer at 10,000 to 20,000 events per second, counting a total of 10^6 cells per sample. Forward and side scatter gating was used to exclude small particles (such as blood platelets and debris), overly large cells (predominantly leukocytes), and cell doublets and triplets. The following excitation wavelengths were used: mCherry, 561 nm; GFP and YFP, 488 nm; Hoechst 33342, 405 nm. Fluorescence was detected with the photomultiplier tube voltage set to its maximum sensitivity using the following band pass filters: Hoechst 33342, 450/50 nm; GFP, 513/17 nm; YFP, 525/50 nm; mCherry, 610/20 nm. Since GFP and YFP signals are detectable in both channels, the following compensation values were used: GFP-YFP: 55%; YFP-GFP: 48%.

When donor mice had reached parasitemia that were readily detectable but not exceeding 1.0%, hence parasites were still within the exponential growth phase (ideally between 0.1% and 1.0%), blood from donor mice was collected. The blood was diluted and mixed to inject 500 reference parasite- and 500 recombinant parasite-infected erythrocytes in a final volume of 100 μ l RPMI 1640 intravenously into naïve recipient NMRI mice. The progress of the infection was monitored from day 3 to day 7 using flow cytometry.

Note that this method reduces experimental variation as well as animal usage from a minimum of 8 mice (2 donor mice, 3 WT-infected mice, and 3 mutant-infected mice), when using conventional Giemsa-based determination of parasitemia, to 3

mice (2 donor mice, 1 co-infected mouse) per experimental replicate.

Analysis of the Plasmodium life cycle

Monitoring of exflagellation activity, evaluation of mosquito stage development, *i.e.* determination of midgut oocyst and salivary gland sporozoite numbers, testing of sporozoite infectivity to naïve recipient C57BL/6 mice, and determination of liver stage development *in vitro* were all performed as described.³⁴

Western blot analysis

Whole protein extracts of mixed blood stages of parasites expressing endogenously tagged proteins were separated on 8% (*ptex88::tag*) or 15% (*trx2::tag*) SDS-polyacrylamide gels. Proteins were transferred on a PVDF membrane, incubated with rat monoclonal anti-mCherry antibodies (1:5000; ChromoTek) and detected with horseradish peroxidase coupled goat anti-rat antibodies (1:5000; Jackson ImmunoResearch).

Image acquisition

All images were recorded on a Zeiss AxioObserver Z1 epifluorescence microscope and processed minimally with ImageJ. Minimum and maximum intensities were optimized to use the full dynamic range of the look-up-tables. No gamma adjustments or thresholds were applied.

RESULTS

PTEX components share between 32 and 98% amino acid sequence identity

A brief bioinformatical analysis confirmed earlier findings that the five components are conserved within and unique to the *Plasmodium* genus.²⁶ The amino acid identity levels, however, do vary greatly for the different components (Supplementary Figure S1). HSP101 is very well conserved sharing >80%

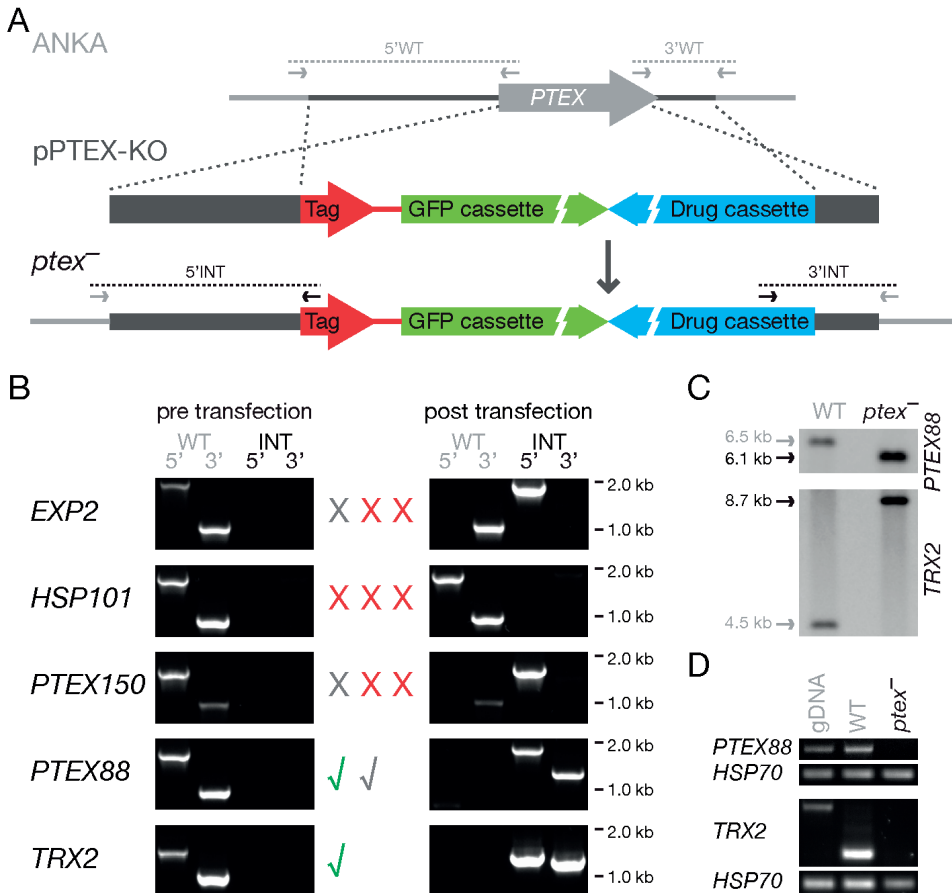


Figure 1 | Systematic gene targeting of putative *P. berghei* PTEX components. (A) Replacement strategy to delete the five genes encoding putative components of the *P. berghei* PTEX translocon. The respective loci (*PTEX*) were targeted with replacement plasmids containing 5' and 3' regions (dark gray bars) flanking the open reading frames (light gray arrow), a high-expressing GFP cassette (green), and the drug-selectable cassette (blue). The 5' integration sequences consisted of complete promoter sequences and were fused directly to an mCherry-3xMyc tag (red). Primer combinations specific for integration (5' and 3'INT) and WT (5' and 3'WT) as well as the expected fragments are indicated (Supplementary Table S1). (B) Overview of all transfection experiments. For each target gene, diagnostic PCRs of the WT locus, the outcome of up-to three independent transfection experiments (green tick, successful gene deletion and isolation of recombinant parasites; black tick, successful gene deletion but no isolation of recombinant parasites; black "X", 5' integration of transfection construct but no gene deletion; red "X", selection of pyrimethamine-resistant parasites but unsuccessful gene deletion), and diagnostic PCRs of the drug-selected and

isolated parasites are shown. (C) Southern blot analysis of the *ptex88*⁻ (top) and *trx2*⁻ (bottom) lines. Probes were amplified from pPTEX-KO vectors, using the 3' integration sequence primers, and hybridized to BsmI or HpaI restriction-digested gDNA, respectively, revealing the expected size shifts. (D) Transcript detection in blood stage WT, *ptex88*⁻, and *trx2*⁻ parasites confirms the successful ablation of *PTEX88* (top) and *TRX2* (bottom) in the knockout lines. Quality of cDNA preparations was controlled using *HSP70*-specific primers.

sequence identity between any pair of sequences and 98% between *P. berghei* and *P. yoelii*. Conservation levels of the different EXP2 sequences exceed >60% identity, while sequences of the two potentially accessory components PTEX88 and TRX2 are clearly more diverse. Perhaps most surprisingly, the third component considered a core part of the PTEX translocon, PTEX150, was the least conserved with identity levels dropping to 32% (between *P. falciparum* and *P. chabaudi*). Indeed, the *P. berghei* and *P. chabaudi* PTEX150 amino acid sequences were only 68% identical, compared to 83% for EXP2 and 94% for HSP101.

Systematic experimental genetics of the candidate PTEX translocon components

We explored the essentiality and functionality of the five components suggested to build the *P. berghei* PTEX translocon using experimental genetics. We used an approach where, upon successful integration, the promoter regions of the target genes would be linked directly to the mCherry-3xMyc tag (Figure 1A). Hence, loss-of-function mutants should express the red fluorescent protein during all stages where the corresponding promoter is active.

We generated and isolated recombinant parasite lines deficient in *PTEX88* and *TRX2* (Figure 1B-D). Note that we had to repeat the sorting procedure to obtain a *ptex88*⁻ population devoid of wild type (WT) contamination, because this parasite appeared to grow rather poorly. Three attempts to ablate the three suggested PTEX translocon core components, *i.e.* *EXP2*, *HSP101*, and *PTEX150*, were unsuccessful (Figure 1B). In one transfection experiment, however, we observed a weak presence of 5' but not 3' integration of the constructs targeting *EXP2* and *PTEX150*. After flow cytometry-assisted sorting of these parental populations, we were able to demonstrate 5' integration and 3' WT PCR in the isolated 5' *exp2::tag* and 5' *ptex150::tag* lines. We postulated that the larger, roughly 1.5 kb homologous 5' integration sequence had recombined, but that the chromosome was

subsequently repaired through a rare event of non-homologous end-joining. According to this model, which we could confirm by PCR (Supplementary Figure S2), the resulting parasites have become insensitive to pyrimethamine, express high levels of green fluorescent protein (GFP), and retained a functional copy of the targeted gene, *i.e.* *EXP2* or *PTEX150*. An insertion of undigested transfection plasmid was ruled out (Supplementary Figure S2).

Generation of three new “Bercolor” reference strains

Already during the isolation procedure of *ptex88*⁻ parasites, we observed that this line developed poorly during blood infection. Therefore, we decided to establish a flow cytometry-based method to quantify these recombinant parasites growing in competition with highly fluorescent reference strains in multiply infected mice. We removed the carboxy-terminal tagging element from the original *P. berghei* adaptable transfection vector pBAT-SIL6³¹ to generate a vector, termed pBAT-G6 (Supplementary Figure S3), containing (i) a recyclable, drug-selectable cassette, (ii) a high expressing GFP cassette, (iii) two extensive multiple cloning sites, and (iv) two sequences for stable transgene integration into an silent intergenic locus (SIL6).³¹ We then exchanged the gene encoding GFP with genes encoding yellow fluorescent protein (YFP) and the red fluorescent protein mCherry, resulting in two additional vectors, pBAT-Y6 and pBAT-M6 (Supplementary Figure S3).

We used these vectors to generate three reference parasite lines expressing high levels of GFP (Bergreen), YFP (Beryellow), or mCherry (Berred) under the control of the *PbHSP70* promoter through double crossover/ends-out homologous recombination in SIL6 (Supplementary Figure S4A). Recombinant parasites were isolated by flow cytometry-assisted cell sorting (Supplementary Figure S4B).³² As reported previously for other recombinant parasites expressing high levels of GFP integrated in SIL6, life cycle progression of the Bercolor parasite lines was within the WT range (data not shown). Live imaging of these parasites showed bright fluorescent parasites in blood, mosquito, and liver stages (Figure 2A).

Establishing an intravital competition assay

We examined blood stage growth of the Bercolor lines by flow cytometry after intravenous injection of 1,000 parasites in NMRI mice (Supplementary Figure S5).

All three lines grew with indistinguishable dynamics (Supplementary Figure S6A). The same was true when we co-injected a total of 1,000 parasites with equal numbers of each reference line into single recipient NMRI mice (Figure 2B). The overall parasitemia of the competitively growing parasites equaled the growth dynamics of the individual infections (Supplementary Figure S6A). We also compared our method with conventional determination of blood stage parasitemia using Giemsa-stained thin blood films for mice infected with Beryellow only (Supplementary Figure S6B) or with all three Bercolor lines (Figure 2C) and observed no significant differences. We further validated the intravital competition

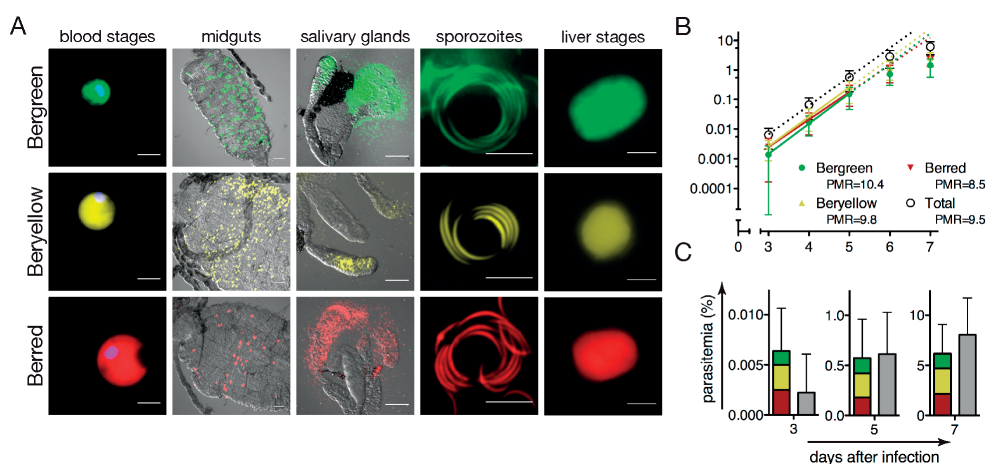


Figure 2 | An intravital competition assay using three “Bercolor” reference lines. (A) Live imaging of “Bercolor” (Bergreen, Beryellow, and Berred) asexual blood stages (nuclei were stained with Hoechst 33342; bars, 2 μm), infected mosquito midguts and salivary glands (10 and 25 days after blood meal, respectively; bars, 100 μm), salivary gland sporozoites performing circular gliding locomotion (bars, 10 μm), and liver stage parasites at 48 hours after infection of cultured hepatoma cells (bars, 10 μm). (B) In three independent experiments, parasitemia of mice infected with a total of 1,000 parasites (equal numbers of Bergreen, Beryellow, and Berred parasites) were established using flow cytometry (see Materials and Methods and Supplementary Figure S5 for further details). Data from the exponential growth phase, *i.e.* with parasitemia <1%, fitted a linear regression well ($r^2 \geq 0.999$) and allowed the calculation of the parasite multiplication rate (PMR). Blood stage development and PMRs of the three reference strains did not differ significantly ($P > 0.05$; two-way ANOVA). The total parasitemia (black dashed line) compared well with those of mice infected with single reference strains from Supplementary Figure S6A. (C) Giemsa-stained blood film-based determination of parasitemia (gray bars) at days 3, 5, and 7 after inoculation did not differ significantly from flow cytometry-based total parasitemia (triple colored bars) of mice infected with three reference lines ($P > 0.05$; paired, two-tailed student’s T-test).

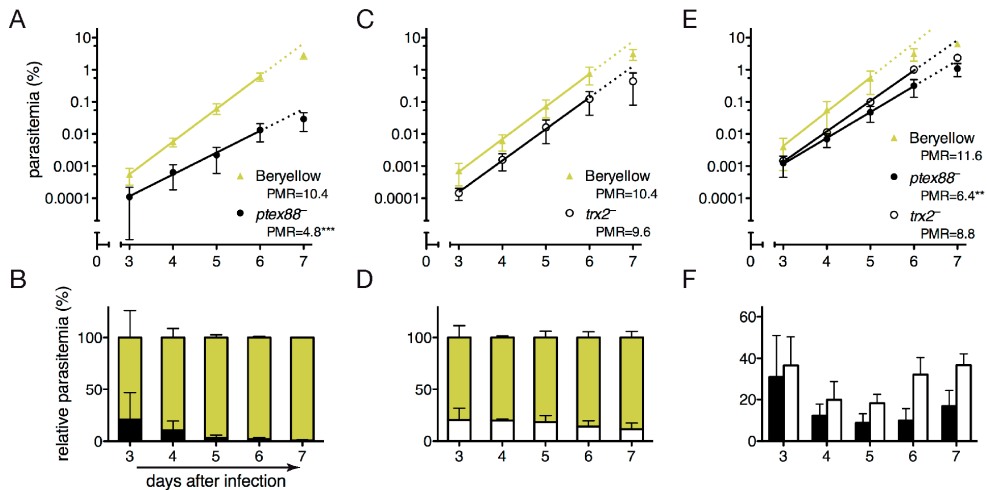


Figure 3 | In vivo blood infection is affected in *trx2*⁻ and particularly *ptex88*⁻ parasites. In three independent experiments, parasitemia of mice infected with 500 Beryellow parasites and 500 *ptex88*⁻ (A and B) or 500 *trx2*⁻ (C and D) parasites were assessed by the intravital competition assay. Data from the exponential growth phase, i.e. with parasitemia <1%, fitted a linear regression well ($r^2 \geq 0.995$) and allowed the calculation of the parasite multiplication rate (PMR). (A) Blood stage growth of Beryellow and *ptex88*⁻ differ significantly ($P < 0.01$; two-way ANOVA). The PMR of *ptex88*⁻ parasites is 54% lower than Beryellow ($P < 0.001$). (B) Relative parasitemia of Beryellow and *ptex88*⁻ demonstrate that the loss-of-function mutants get outcompeted fast, dropping to ~20% on day 3 to under 1% after one week. (C) Blood stage growth of Beryellow and *trx2*⁻ differ significantly ($P < 0.05$; two-way ANOVA). However, the PMR of *trx2*⁻ parasites is not significantly different from Beryellow ($P > 0.05$). (D) Relative parasitemia of Beryellow and *trx2*⁻ demonstrate that WT-like parasites outcompete the loss-of-function mutants, which drop to 12% of total parasitemia after one week. (E) Blood stage development in mice infected with a single parasite line (Beryellow, *ptex88*⁻, or *trx2*⁻) differ significantly ($P < 0.01$; two-way ANOVA). The PMR of *ptex88*⁻ parasites is 45% lower than Beryellow ($P < 0.01$), the difference in PMR of *trx2*⁻ is not significant ($P > 0.05$). (F) Relative parasitemias of mice infected with *ptex88*⁻ (black) or *trx2*⁻ (white) parasites in comparison to Beryellow-infected mice. From 3 to 5 days after inoculation the slower growth of *trx2*⁻ and particularly *ptex88*⁻ is evident. Recovery of relative parasite levels from day 6 onwards are attributable to Beryellow parasites not growing exponential anymore while having reached parasitemias >1%.

assay by re-examining the blood stage growth of two previously published recombinant parasite lines,³² lacking aquaglyceroporin (*aqp*⁻) and expressing an mCherry-tagged AQP protein (*aqp::tag*) (Supplementary Figure S6C-F). For monitoring competitive growth of dual labeled parasites expressing cytoplasmic GFP and mCherry tagged protein, we used the Beryellow reference line.

PTEX88 and TRX2 promote in vivo blood infection

We employed the intravital competition assay to show that blood stage development of the *ptex88*⁻ and *trx2*⁻ lines was significantly different from the co-injected Beryellow reference strain (Figure 3A and C). Though the effect was less striking, the reduced blood stage development of both parasite lines was confirmed in single infection experiments (Figure 3E and F). The 24 h parasite multiplication rate (PMR) of exponentially growing *ptex88*⁻ was significantly reduced by ~50% (Figure 3A and E). At day 7 following co-injection, less than 1% *ptex88*⁻ parasites remained (Figure 3B).

A trend towards out-competition by Beryellow parasites was also evident in mice co-infected with *trx2*⁻ parasites (Figure 3D). However, PMRs of *trx2*⁻ parasites did not differ significantly from Beryellow (Figure 3C and E), indicative of an early defect that likely occurs during blood transfusion rather than during parasite replication.

A natural transmission experiment confirmed successful life cycle progression of both knockout parasite lines, as shown by flow cytometric blood analysis three days after mosquito challenge (Supplementary Figure S7). Furthermore, the numbers of oocysts, midgut and salivary gland-associated sporozoites, and cultured liver stages were comparable to WT parasites (data not shown).

Promoter activities of different PTEX translocon components vary

Since the *ptex88*⁻ and *trx2*⁻ lines as well as the 5'*exp2::tag* and 5'*ptex150::tag* parasites express mCherry under the control of the endogenous promoters, an assessment of the levels of red fluorescence allowed an approximation of their respective promoter activities. Microscopical examination revealed a clear difference in mCherry intensity between the different parasite lines in all different blood stages (Figure 4A). We confirmed the observed differences through flow cytometric quantification of the fluorescence intensity (Figure 4B). The mCherry signals revealed a similar promoter activity (25th to 75th percentile, relative to the mean *HSP70* promoter activity) for *EXP2* (21-46%) and *PTEX150* (19-41%). The value for *PTEX88* is clearly lower at 8-17%, while the *TRX2* promoter seems the least active (3-7%). Comparison with *PfHSP70* normalized transcription data of *P. falciparum*³⁵ revealed a similar trend though with much lower levels of *PfPTEX150*

and *PfPTEX88* transcription.

Localization of *PTEX88* and *TRX2*

Finally, we generated parasites expressing endogenous *PTEX88* and *TRX2* fused to an mCherry-3xMyc tag (Supplementary Figure S8A). The absence of WT parasites in the isogenic recombinant lines was confirmed by diagnostic PCR (Supplementary Figure S8B). Western blot analysis using anti-mCherry antibodies revealed the presence of both full-length tagged proteins in mixed blood stages thus ruling out that the proteins are processed (Supplementary Figure S8C and F). To further support that the observed localization is physiologically relevant, blood stage development was evaluated using the intravital competition assay.

The growth curves of co-injected *trx2::tag* and Beryellow parasites overlapped substantially (Supplementary Figure S8D), thus providing evidence for, at least partial, functional complementation. Parasites expressing *TRX2::tag* exhibited a

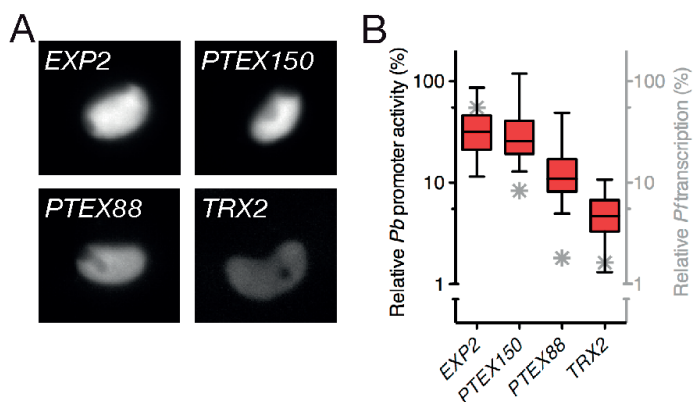


Figure 4 | Promoter activity in isogenic recombinant parasites. (A) Live fluorescence micrographs of trophozoites expressing mCherry under the control of the endogenous promoter regions of the targeted genes. *EXP2* and *PTEX150* promoter activities were monitored in the isogenic 5' *exp2::tag* and 5' *pTEX150::tag* lines. *PTEX88* and *TRX2* promoter activities were monitored in the isogenic gene deletion mutants. These representative images were recorded using identical exposure times. (B) Quantification of the respective promoter activities based on fluorescence intensity as measured by flow cytometry. All data were normalized to *HSP70* promoter activity determined by measuring Berred parasite fluorescence. Shown are whisker plots with 5th and 95th percentiles of 300-500 parasites. Stars indicate published relative transcription levels, normalized to *PfHSP70* transcript levels, of cultured blood stage *P. falciparum*.³⁵

very consistent staining throughout blood stage development (Figure 5A and Supplementary Figure S8E). The protein localizes to a distinct peripheral focus in free merozoites and mature schizonts. The punctate staining remains throughout ring and trophozoite development and in gametocytes. The number of TRX2::tag-positive structures varies and appears loosely associated with the developmental stage of the parasite. Ring stages usually display one or two of these structures, whereas the number of foci in trophozoites is more variable (Figure 5A).

In contrast to the null-mutants, the *ptex88::tag* grew indistinguishable from co-injected Beryellow (Supplementary Figure S8G), thus providing evidence for a functional complementation and simultaneously ruling out aberrant localization of the tagged protein. Live imaging revealed that PTEX88::tag predominantly localizes to regions in the parasites cytoplasm of both asexual (Figure 5B) and sexual (Supplementary Figure S8H) blood stages. Similar to TRX2::tag, a singular

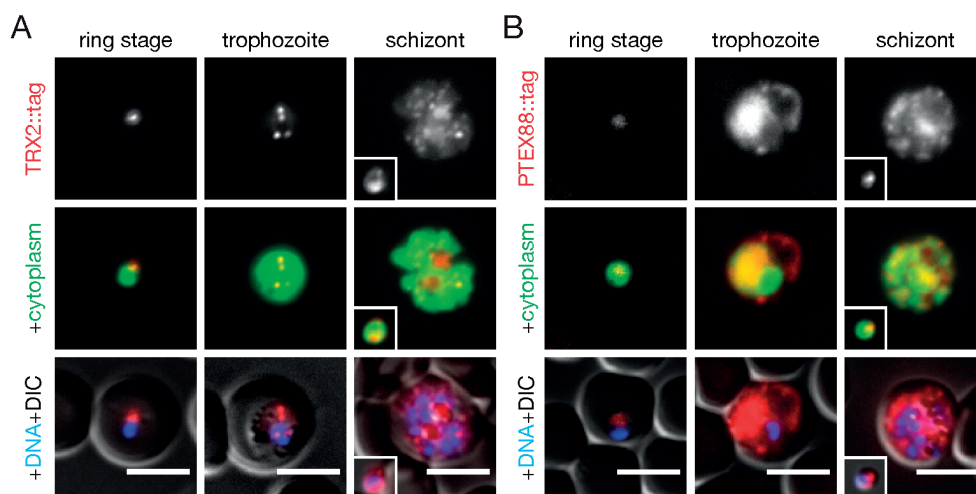


Figure 5 | Live imaging of PTEX88::tag and TRX2::tag in blood stage parasites. Representative images of ring, trophozoite, and schizont stage parasites reveal low-level expression throughout asexual blood stage development. The small inset shows a free merozoite. Bars, 5 μ m. (A) TRX2::tag consistently localizes to one or more intraparasitic vesicle-like structures that regularly appear to associate with the parasite periphery. (B) PTEX88::tag showed a diffuse intraparasitic staining with singular, peripheral dots in free merozoites and mature schizonts. In trophozoites, PTEX88::tag also localized to dynamic protrusions extending far into the red blood cell cytoplasm (see also Supplementary Figure S9).

punctate structure was observed, which localizes to the periphery of the parasite in mature schizonts and free merozoites. In ring and trophozoite stages and gametocytes, the intraparasitic PTEX88::tag pattern is more diffuse. In the majority of the maturing trophozoites and young schizonts, we observed that PTEX88::tag also localizes to thin, dynamic extensions, which reach from the parasite surface into the erythrocyte cytoplasm (Figure 5B and Supplementary Figure S9). These extensions only appeared when parasites had matured and were never evident in ring stages or sexual stages. Typically, a single extension emerges from one end of the parasite and extends far into the host cell, often following the shape of the red blood cell membrane towards the other end of the parasite. Sometimes two extensions emerged from opposite ends of a parasite. Infrequently, PTEX88::tag localized to multiple smaller extensions (Supplementary Figure S9). The structures appeared dynamic in all cases, displaying whipping- and folding-like motions.

DISCUSSION

Initially identified by pull-down of HA-tagged *Pf*PTEX150 and *Pf*HSP101, the actual localization of *Pf*PTEX88 and *Pf*TRX2 has remained elusive. Very recent immunofluorescence data for tagged PTEX88 in fixed ring stage parasites suggested a PV/PVM residency.³⁶ Here, we provide the first live localization data for PTEX88. We were able to localize *Pb*PTEX88 to intra- and extraparasitic structures of *P. berghei*. In mature schizonts and free merozoites, the protein resides in peripheral foci. This is in agreement with the storage of the PTEX components in dense granules during these developmental stages.²⁷ Following invasion, PTEX88 can be observed in undefined structures in the parasite cytoplasm. This staining could arise from ER-resident protein, since PTEX88 possesses an amino-terminal signal sequence and is transported to the PVM via the secretory pathway. Unfortunately, a complementary set of tools to perform an adequate co-localization of the tagged protein with the ER, either by antibodies or subcellular fluorescent markers, is currently not available for *P. berghei*.

Surprisingly, the extraparasitic PTEX88 we observed in maturing parasites did not display a circumferential staining as expected for a typical PVM localization, but accumulated in elongated and dynamic protrusions emerging from the parasite surface and reaching far into the red blood cell cytoplasm. This finding is consistent

with the observation that other elements of the PTEX complex localize to specific translocation foci at the parasite periphery.³⁷ Thus far, localization to similar extensions has not been reported for any of the PTEX components, suggesting that perhaps PTEX88 has a role downstream of the translocon. Alternatively, it is conceivable that the extensions might have escaped observation as previously PTEX components, with the exception of tagged *PfTRX2*, have been visualized in fixed parasites only. Live imaging, as performed in this study, will be required to gain a better understanding of the temporal and spatial dynamics of these previously unrecognized structures in *P. berghei*-infected erythrocytes. Indeed, our own attempts to conserve the structures by standard fixation methods³⁸ failed (data not shown).

Assuming a function in protein export, it would be interesting to explore any possible roles of the dynamic extensions in the translocation of proteins to the red blood cell plasma membrane directly or to parasite derived structures, such as the dynamic, punctate structures recently identified in *P. berghei*-infected red blood cells.^{39,40} Alternatively, parasite protein-filled vesicles might bud off from the extensions,⁴¹ though this appears less likely, since we failed to detect PTEX88-positive vesicles. We are currently exploring the composition of these protrusions and their potential roles, if any, in protein export.

The residency of *PfTRX2* remains controversial. Overexpressed chimeric *PfTRX2::GFP* fusion protein localized to the parasite mitochondrion.⁴² When under the control of the chloroquine resistance transporter (*CRT*) promoter, which drives blood stage expression levels comparable to *PfTRX2*,³⁵ the *PfTRX2::GFP* fusion protein localized to non-dividing and membrane bound organelles.⁴³ In addition, a PV-like staining was observed in ring stages.⁴³ An antibody raised against recombinant TRX2 demonstrated a similar staining at the parasite periphery.⁴⁴ Unfortunately, the specificity of the anti-TRX2 antibody remains unclear in the absence of experimental confirmation. Our own observations are most consistent with compartmentalization and localization to an unidentified parasite organelle, as suggested previously,⁴³ although low-level dual localization in PV and/or mitochondrion cannot be ruled out. The very recent immunofluorescence data with tagged *PbTRX2* from fixed blood stage parasites are also consistent with our own observations.³⁶ Near recovery of WT blood stage growth of the *trx2::tag* parasites suggests that an important fraction of the protein is localized and functioning correctly.

Considering the importance of many conserved *P. berghei* genes encoding exported proteins,^{22,25} we anticipated that the majority, if not all, of the PTEX translocon components would be refractory to gene deletion. Recent data suggest a relatively small PEXEL exportome in the murine malaria parasite but emphasize the likeliness of a very broad range of PNEPs in the *P. berghei* genome.²⁵ Also, export-related processes, such as sequestration,⁴⁵ immune evasion⁴⁶ and host actin remodeling⁴⁷ have been demonstrated for *P. berghei*, suggesting an important role of protein export pathways in murine malaria parasites and their pathogenesis.

Therefore, we were initially surprised to find drug-insensitive, GFP-positive parasites with one or two integration-positive PCR bands for all targeted genes but *HSP101*. As we demonstrated, two of the obtained mutant lines had retained the targeted genes and were merely the result of a rare event of single homologous recombination followed by non-homologous end-joining. Homologous recombination is likely to be the dominant form of DNA double strand break repair in unicellular eukaryotes including yeast, as opposed to non-homologous end-joining, which is more common in multicellular eukaryotes.^{48,49} The isolation of these rare mutants and more importantly of the *ptex88*⁻ line demonstrates the power of the applied methods while simultaneously providing additional, albeit indirect, proof of the essentiality of *EXP2* and *PTEX150*.

P. falciparum transcription levels of *PTEX88* and *TRX2* are less abundant than those of the other three components,³⁵ which led to the suggestion that these might function as protein export regulators.⁵⁰ We confirmed the lower expression levels by demonstrating a reduced *P. berghei* promoter activity and disproved an essential role for both proteins through the successful deletion of both putative PTEX components. Perhaps these factors are not required for the export of essential proteins. Alternatively, they may increase overall protein export efficiency to different degrees, which could explain the growth differences we observed with our novel intravital competition assay. Considering the localization of the protein and the mild growth defect of the null-mutant, the involvement of *TRX2* in the translocation process remains puzzling. Our data could support functions elsewhere in the parasite as well as a minor role in protein export, either through small quantities of PV-resident *TRX2* or through the interaction of multiple macromolecular structures, *i.e.* the *TRX2* delineated foci, the PTEX core translocon, and the *PTEX88*-positive extensions.

To analyze the blood stage development of our mutant parasite lines, we

developed an intravital competition assay based on flow cytometry. Conventional determination of blood stage parasitemia using Giemsa-stained thin blood films, though cheap and requiring little specialized instrumentation, is labor-intensive and subjective. Flow cytometry offers higher precision in parasitemia measurements (especially at low parasitemia) through the sheer number of red blood cells that can be analyzed, while simultaneously increasing the objectivity of parasite identification.

Flow cytometric methods used to determine parasite numbers in infected mice are continuously being improved but are typically based on differentiation of parasites by DNA dyes.⁵¹⁻⁵⁶ These methods cannot differentiate between parasites with different genetic backgrounds. The availability of the three Bercolor reference parasite lines and the use of different fluorophores allow for an *in vivo* analysis of blood stage development of parasites growing in direct competition. This significantly reduces experimental variation as well as animal usage per experimental replicate. Furthermore, the method can assist the identification of mild phenotypes in a competitive setting and might also be applied as a more reliable approach to perform *in vivo* drug screening.

ACKNOWLEDGEMENTS

We would like to thank Markus Ganter for critically reading the manuscript, Sanketha Kenthirapalan for fruitful discussions, and Carolin Nahar and Manuel Rauch for technical assistance. We would also like to acknowledge the assistance of the Flow Cytometry Core Facility at the Deutsches Rheuma-Forschungszentrum (Berlin), with special thanks to Toralf Kaiser and Jenny Kirsch for expert advice. This work was supported by the Max Planck Society and the European Union's Seventh Framework Programme (FP7/2007-2013) under grant agreement n°242095: EVIMalaR - Towards the establishment of a permanent European Virtual Institute dedicated to Malaria Research.

REFERENCES

- 1 Mbengue A, Yam XY, Braun-Breton C. Human erythrocyte remodelling during *Plasmodium falciparum* malaria parasite growth and egress. *Br J Haematol*. 2012; 157:171–9.
- 2 Spielmann T, Montagna GN, Hecht L, Matuschewski K. Molecular make-up of the *Plasmodium* parasitophorous vacuolar membrane. *Int J Med Microbiol*. 2012;302:179–86.
- 3 Boddey JA, Cowman AF. *Plasmodium* nesting: Remaking the erythrocyte from the inside out. *Annu Rev Microbiol*. 2013;67:243–69.
- 4 Marti M, Spielmann T. Protein export in malaria parasites: many membranes to cross. *Curr Opin Microbiol*. 2013;16:445–51.
- 5 Baruch DI, Pasloske BL, Singh HB, Bi X, Ma XC, Feldman M, *et al*. Cloning the *P. falciparum* gene encoding PfEMP1, a malarial variant antigen and adherence receptor on the surface of parasitized human erythrocytes. *Cell*. 1995;82:77–87.
- 6 Smith JD, Chitnis CE, Craig AG, Roberts DJ, Hudson-Taylor DE, Peterson DS, *et al*. Switches in expression of *Plasmodium falciparum* var genes correlate with changes in antigenic and cytoadherent phenotypes of infected erythrocytes. *Cell*. 1995;82:101–10.
- 7 Su XZ, Heatwole VM, Wertheimer SP, Guinet F, Herrfeldt JA, Peterson DS, *et al*. The large diverse gene family var encodes proteins involved in cytoadherence and antigenic variation of *Plasmodium falciparum*-infected erythrocytes. *Cell*. 1995;82:89–100.
- 8 Maier AG, Rug M, O'Neill MT, Brown M, Chakravorty SJ, Szeszak T, *et al*. Exported proteins required for virulence and rigidity of *Plasmodium falciparum*-infected human erythrocytes. *Cell*. 2008;134:48–61.
- 9 Cyrklaff M, Sanchez CP, Kilian N, Bisseye C, Simpore J, Frischknecht F, *et al*. Hemoglobins S and C interfere with actin remodeling in *Plasmodium falciparum*-infected erythrocytes. *Science*. 2011;334:1283–6.
- 10 Nguitragool W, Bokhari AAB, Pillai AD, Rayavara K, Sharma P, Turpin B, *et al*. Malaria parasite *clag3* genes determine channel-mediated nutrient uptake by infected red blood cells. *Cell*. 2011;145:665–77.
- 11 Marti M, Good RT, Rug M, Knuepfer E, Cowman AF. Targeting malaria virulence and remodeling proteins to the host erythrocyte. *Science*. 2004;306:1930–3.
- 12 Hiller NL, Bhattacharjee S, van Ooij C, Liolios K, Harrison T, Lopez-Estraño C, *et al*. A host-targeting signal in virulence proteins reveals a secretome in malarial infection. *Science*. 2004;306:1934–7.
- 13 Bhattacharjee S, Stahelin RV, Speicher KD, Speicher DW, Haldar K. Endoplasmic reticulum PI(3)P lipid binding targets malaria proteins to the host cell. *Cell*. 2012;148: 201–12.
- 14 Boddey JA, Hodder AN, Günther S, Gilson PR, Patsiouras H, Kapp EA, *et al*. An aspartyl protease directs malaria effector proteins to the host cell. *Nature*. 2010;463: 627–31.
- 15 Russo I, Babbitt S, Muralidharan V, Butler T, Oksman A, Goldberg DE. Plasmepsin V licenses *Plasmodium* proteins for export into the host erythrocyte. *Nature*. 2010;463:

- 632–6.
- 16 Chang HH, Falick AM, Carlton PM, Sedat JW, DeRisi JL, Marletta MA. N-terminal processing of proteins exported by malaria parasites. *Mol Biochem Parasitol.* 2008; 160:107–15.
 - 17 Grüring C, Heiber A, Kruse F, Flemming S, Franci G, Colombo SF, *et al.* Uncovering common principles in protein export of malaria parasites. *Cell Host Microbe.* 2012;12: 717–29.
 - 18 Heiber A, Kruse F, Pick C, Grüring C, Flemming S, Oberli A, *et al.* Identification of new PNEPs indicates a substantial non-PEXEL exportome and underpins common features in *Plasmodium falciparum* protein export. *PLoS Pathog.* 2013;9:e1003546.
 - 19 Kooij TWA, Carlton JM, Bidwell SL, Hall N, Ramesar J, Janse CJ, *et al.* A *Plasmodium* whole-genome synteny map: indels and synteny breakpoints as foci for species-specific genes. *PLoS Pathog.* 2005;1:e44.
 - 20 Carlton JM, Adams JH, Silva JC, Bidwell SL, Lorenzi H, Caler E, *et al.* Comparative genomics of the neglected human malaria parasite *Plasmodium vivax*. *Nature.* 2008; 455:757–63.
 - 21 Sargeant TJ, Marti M, Caler E, Carlton JM, Simpson KM, Speed TP, *et al.* Lineage-specific expansion of proteins exported to erythrocytes in malaria parasites. *Genome Biol.* 2006;7:R12.
 - 22 van Ooij C, Tamez PA, Bhattacharjee S, Hiller NL, Harrison T, Liolios K, *et al.* The malaria secretome: from algorithms to essential function in blood stage infection. *PLoS Pathog.* 2008;4:e1000084.
 - 23 Pick C, Ebersberger I, Spielmann T, Bruchhaus I, Burmester T. Phylogenomic analyses of malaria parasites and evolution of their exported proteins. *BMC Evol Biol.* 2011; 11:167.
 - 24 Fonager J, Pasini EM, Braks JAM, Klop O, Ramesar J, Remarque EJ, *et al.* Reduced CD36-dependent tissue sequestration of *Plasmodium*-infected erythrocytes is detrimental to malaria parasite growth *in vivo*. *J Exp Med.* 2012;209:93–107.
 - 25 Pasini EM, Braks JA, Fonager J, Klop O, Aime E, Spaccapelo R, *et al.* Proteomic and genetic analyses demonstrate that *Plasmodium berghei* blood stages export a large and diverse repertoire of proteins. *Mol Cell Proteomics.* 2013;12:426–48.
 - 26 de Koning-Ward TF, Gilson PR, Boddey JA, Rug M, Smith BJ, Papenfuss AT, *et al.* A newly discovered protein export machine in malaria parasites. *Nature.* 2009;459:945–9.
 - 27 Bullen HE, Charnaud SC, Kalanon M, Riglar DT, Dekiwadia C, Kangwanrangsan N, *et al.* Biosynthesis, localization, and macromolecular arrangement of the *Plasmodium falciparum* translocon of exported proteins (PTEx). *J Biol Chem.* 2012;287:7871–84.
 - 28 Haase S, de Koning-Ward TF. New insights into protein export in malaria parasites. *Cell Microbiol.* 2010;12:580–7.
 - 29 Bullen HE, Crabb BS, Gilson PR. Recent insights into the export of PEXEL/HTS-motif containing proteins in *Plasmodium* parasites. *Curr Opin Microbiol.* 2012;15:699–704.
 - 30 Gehde N, Hinrichs C, Montilla I, Chapien S, Lingelbach K, Przyborski JM. Protein unfolding is an essential requirement for transport across the parasitophorous vacuolar membrane of *Plasmodium falciparum*. *Mol Microbiol.* 2009;71:613–28.
 - 31 Kooij TWA, Rauch MM, Matuschewski K. Expansion of experimental genetics

- approaches for *Plasmodium berghei* with versatile transfection vectors. Mol Biochem Parasitol. 2012;185:19–26.
- 32 Kenthirapalan S, Waters AP, Matuschewski K, Kooij TWA. Flow cytometry-assisted rapid isolation of recombinant *Plasmodium berghei* parasites exemplified by functional analysis of aquaglyceroporin. Int J Parasitol. 2012;42:1185–92.
 - 33 Janse CJ, Franke-Fayard BMD, Mair GR, Ramesar J, Thiel C, Engelmann S, *et al.* High efficiency transfection of *Plasmodium berghei* facilitates novel selection procedures. Mol Biochem Parasitol. 2006;145:60–70.
 - 34 Haussig JM, Matuschewski K, Kooij TWA. Inactivation of a *Plasmodium* apicoplast protein attenuates formation of liver merozoites. Mol Microbiol. 2011;81:1511–25.
 - 35 Le Roch KG, Zhou Y, Blair PL, Grainger M, Moch JK, Haynes JD, *et al.* Discovery of gene function by expression profiling of the malaria parasite life cycle. Science. 2003;301:1503–8.
 - 36 Matthews K, Kalanon M, Chisholm SA, Sturm A, Goodman CD, Dixon MWA, *et al.* The *Plasmodium* translocon of exported proteins (PTEX) component thioredoxin-2 is important for maintaining normal blood-stage growth. Mol Microbiol. 2013;89:1167–86.
 - 37 Riglar DT, Rogers KL, Hanssen E, Turnbull L, Bullen HE, Charnaud SC, *et al.* Spatial association with PTEX complexes defines regions for effector export into *Plasmodium falciparum*-infected erythrocytes. Nat Commun. 2013;4:1415.
 - 38 Tonkin CJ, van Dooren GG, Spurck TP, Struck NS, Good RT, Handman E, *et al.* Localization of organellar proteins in *Plasmodium falciparum* using a novel set of transfection vectors and a new immunofluorescence fixation method. Mol Biochem Parasitol. 2004;137:13–21.
 - 39 Ingmundson A, Nahar C, Brinkmann V, Lehmann MJ, Matuschewski K. The exported *Plasmodium berghei* protein IBIS1 delineates membranous structures in infected red blood cells. Mol Microbiol. 2012;83:1229–43.
 - 40 Haase S, Hanssen E, Matthews K, Kalanon M, de Koning-Ward TF. The exported protein PbCP1 Localises to cleft-like structures in the rodent malaria parasite *Plasmodium berghei*. PLoS ONE. 2013;8:e61482.
 - 41 Currà C, Pace T, Franke-Fayard BMD, Picci L, Bertuccini L, Ponzi M. Erythrocyte remodeling in *Plasmodium berghei* infection: the contribution of SEP family members. Traffic. 2012;13:388–99.
 - 42 Boucher IW, McMillan PJ, Gabrielsen M, Akerman SE, Brannigan JA, Schnick C, *et al.* Structural and biochemical characterization of a mitochondrial peroxiredoxin from *Plasmodium falciparum*. Mol Microbiol. 2006;61:948–59.
 - 43 Kehr S, Sturm N, Rahlfs S, Przyborski JM, Becker K. Compartmentation of redox metabolism in malaria parasites. PLoS Pathog. 2010;6:e1001242.
 - 44 Sharma A, Sharma A, Dixit S, Sharma A. Structural insights into thioredoxin-2: a component of malaria parasite protein secretion machinery. Sci Rep. 2011;1:179.
 - 45 Franke-Fayard B, Fonager J, Braks A, Khan SM, Janse CJ. Sequestration and tissue accumulation of human malaria parasites: can we learn anything from rodent models of malaria? PLoS Pathog. 2010;6:e1001032.
 - 46 Jemmely NY, Niang M, Preiser PR. Small variant surface antigens and *Plasmodium* evasion of immunity. Future Microbiol. 2010;5:663–82.
 - 47 Gomes-Santos CSS, Itoe MA, Afonso C, Henriques R, Gardner R, Sepúlveda N, *et al.*

- Highly dynamic host actin reorganization around developing *Plasmodium* inside hepatocytes. PLoS ONE. 2012;7:e29408.
- 48 Kass EM, Jasin M. Collaboration and competition between DNA double-strand break repair pathways. FEBS Lett. 2010;584:3703–8.
 - 49 Mladenov E, Iliakis G. Induction and repair of DNA double strand breaks: the increasing spectrum of non-homologous end joining pathways. Mutat Res. 2011;711: 61–72.
 - 50 Crabb BS, de Koning-Ward TF, Gilson PR. Protein export in *Plasmodium* parasites: from the endoplasmic reticulum to the vacuolar export machine. Int J Parasitol. 2010; 40:509–13.
 - 51 Janse CJ, van Vianen PH, Tanke HJ, Mons B, Ponnudurai T, Overdulve JP. *Plasmodium* species: flow cytometry and microfluorometry assessments of DNA content and synthesis. Exp Parasitol. 1987;64:88–94.
 - 52 Barkan D, Ginsburg H, Golenser J. Optimisation of flow cytometric measurement of parasitaemia in *Plasmodium*-infected mice. Int J Parasitol. 2000;30:649–53.
 - 53 Jiménez-Díaz MB, Rullas J, Mulet T, Fernández L, Bravo C, Gargallo-Viola D, *et al.* Improvement of detection specificity of *Plasmodium*-infected murine erythrocytes by flow cytometry using autofluorescence and YOYO-1. Cytometry A. 2005;67:27–36.
 - 54 Bhakdi SC, Sratongno P, Chiumma P, Rungruang T, Chuncharunee A, Neumann HPH, *et al.* Re-evaluating acridine orange for rapid flow cytometric enumeration of parasitemia in malaria-infected rodents. Cytometry A. 2007;71:662–7.
 - 55 Jiménez-Díaz MB, Mulet T, Gómez V, Viera S, Alvarez A, Garuti H, *et al.* Quantitative measurement of *Plasmodium*-infected erythrocytes in murine models of malaria by flow cytometry using bidimensional assessment of SYTO-16 fluorescence. Cytometry A. 2009;75:225–35.
 - 56 Gerena Y, Gonzalez-Pons M, Serrano AE. Cytofluorometric detection of rodent malaria parasites using red-excited fluorescent dyes. Cytometry A. 2011;79:965–72.

Supplementary Information for:

Two putative protein export regulators promote *Plasmodium* blood stage development *in vivo*

Matz JM, Matuschewski K, Kooij TWA. Mol. Biochem. Parasitol. 2013; 191:44–52.

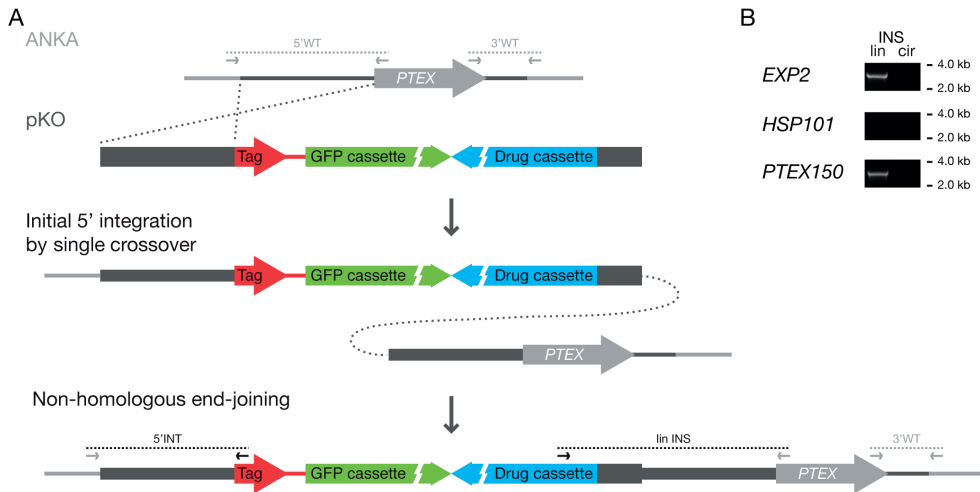
3

Content:

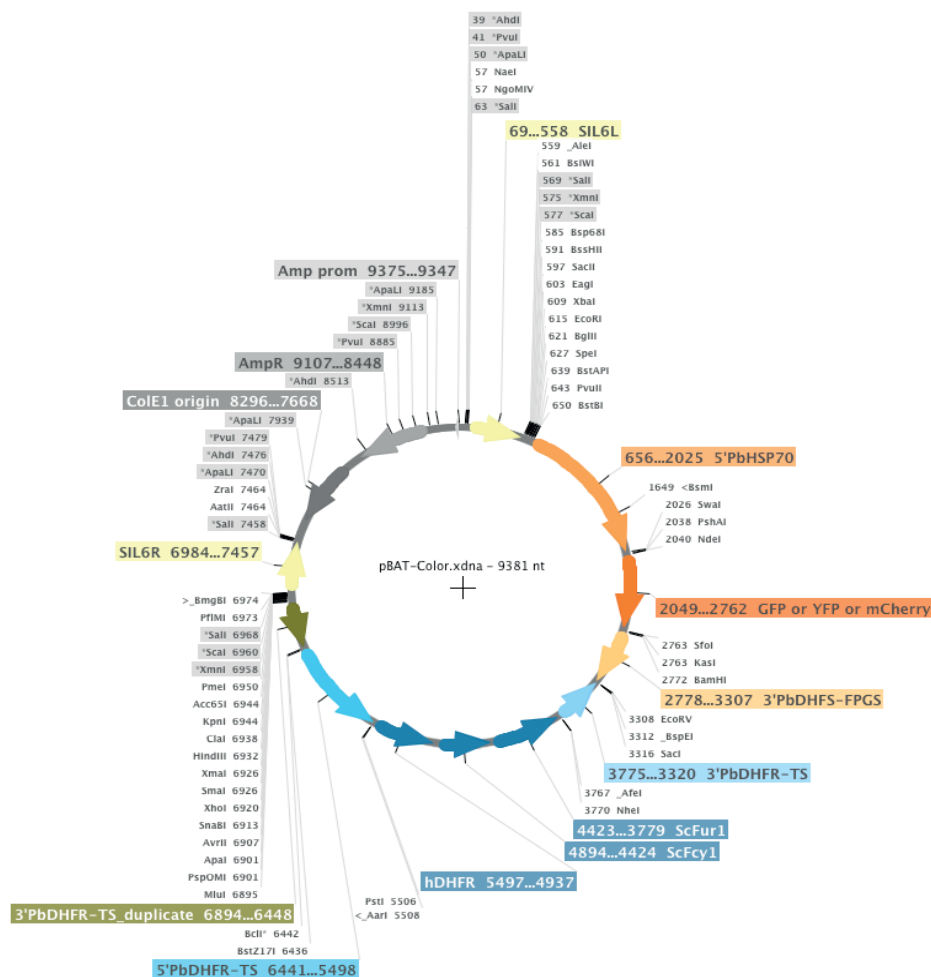
- Supplementary Figure S1** | *Plasmodium* PTEX component identities
- Supplementary Figure S2** | Insertion of linearized transfection constructs through single homologous recombination followed by non-homologous end-joining
- Supplementary Figure S3** | Detailed map of pBAT-Color
- Supplementary Figure S4** | Generation of the Bergreen, Beryellow, and Berred reference lines
- Supplementary Figure S5** | Gating strategy for quantification of fluorescent malaria parasites
- Supplementary Figure S6** | Validation of the intravital competition assay
- Supplementary Figure S7** | Natural transmission of *ptex88*⁻ and *trx2*⁻ is not affected
- Supplementary Figure S8** | Generation of *trx2::tag* and *ptex88::tag* parasites
- Supplementary Figure S9** | Live fluorescence micrographs of mature *ptex88::tag* trophozoites
- Supplementary Table S1** | Primer sequences

	Pf	Pv	Pk	Pcy	Pch	Py	Pb
PbEXP2	65	70	67	62	83	94	100
PyEXP2	66	69	67	60	83	100	
PchEXP2	65	70	68	63	100		
PcyEXP2	67	87	83	100			
PkEXP2	75	92	100				
PvEXP2	77	100					
PfEXP2	100						
	Pf	Pv	Pk	Pcy	Pch	Py	Pb
PbHSP101	82	82	81	82	94	98	100
PyHSP101	81	82	81	82	94	100	
PchHSP101	82	83	82	82	100		
PcyHSP101	88	97	96	100			
PkHSP101	88	97	100				
PvHSP101	88	100					
PfHSP101	100						
	Pf	Pv	Pk	Pcy	Pch	Py	Pb
PbPTEX150	33	33	33	34	68	82	100
PyPTEX150	34	34	33	34	71	100	
PchPTEX150	32	34	33	34	100		
PcyPTEX150	38	82	76	100			
PkPTEX150	38	75	100				
PvPTEX150	40	100					
PfPTEX150	100						
	Pf	Pv	Pk	Pcy	Pch	Py	Pb
PbPTEX88	46	46	48	47	76	84	100
PyPTEX88	46	47	48	47	75	100	
PchPTEX88	46	46	46	46	100		
PcyPTEX88	50	90	84	100			
PkPTEX88	52	84	100				
PvPTEX88	52	100					
PfPTEX88	100						
	Pf	Pv	Pk	Pcy	Pch	Py	Pb
PbTRX2	49	58	54	56	78	91	100
PyTRX2	46	53	50	53	78	100	
PchTRX2	54	61	59	61	100		
PcyTRX2	64	94	90	100			
PkTRX2	62	90	100				
PvTRX2	64	100					
PfTRX2	100						

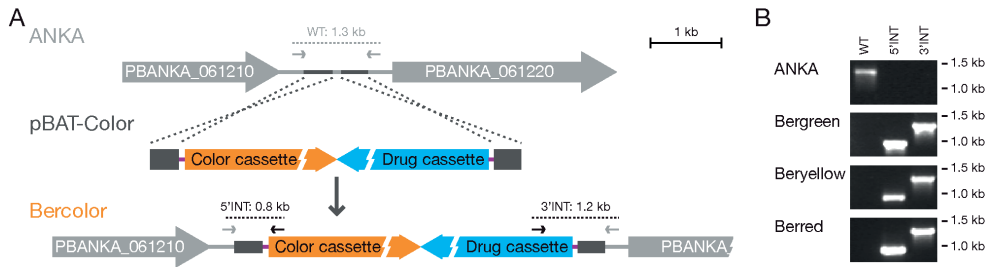
Supplementary Figure S1 | *Plasmodium* PTEX component identities. Protein identity matrices of the five putative PTEX translocon components generated using ClustalΩ alignment (<http://www.ebi.ac.uk/Tools/msa/clustalo/>) of the amino acid sequences of three rodent *Plasmodium* spp. (Pb, *P. berghei* ANKA; Py, *P. y. yoelii* 17xnl; Pch, *P. c. chabaudi* AS) and four spp. infecting primates and humans (Pcy, *P. cynomolgi* B; Pk, *P. knowlesi* H; Pv, *P. vivax* Sall; Pf, *P. falciparum* 3D7). Sequences were retrieved from GeneDB (<http://www.genedb.org/>).



Supplementary Figure S2 | Insertion of linearized transfection constructs through single homologous recombination followed by non-homologous end-joining. (A) Schematic representation of the proposed mechanism of insertion of linear transfection vectors targeting essential genes through single homologous recombination followed by non-homologous end-joining. After integration, the endogenous promoter drives expression of the mCherry-3xMyc tag while the targeted gene locus remains intact. Recombinant parasites have also acquired pyrimethamine-resistance (blue) and high-expressing GFP (green) cassettes for positive selection of recombinant parasites. (B) PCR diagnostic for insertion of linear transfection vector by non-homologous end-joining (lin INS) in recombinant isogenic parasite lines transfected with pEXP2-KO and pPTEX150-KO. These parasites also show 5' integration and 3' WT PCR reactions (Fig 1). A second reaction demonstrating the potential insertion of an undigested, circular plasmid (cir INS) through single crossover/ends in homologous recombination into the 5' integration region remained negative in all selected parasite lines.

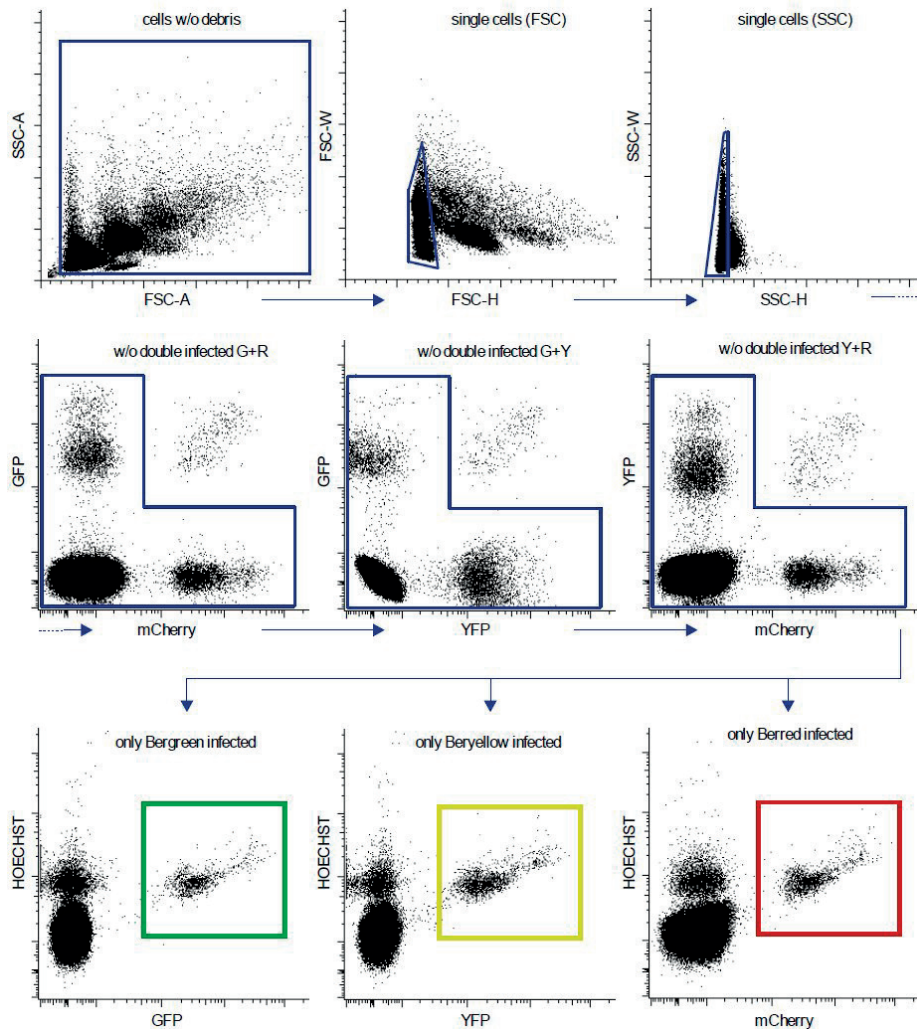


Supplementary Figure S3 | Detailed map of pBAT-Color. Shown are all vector elements, including unique REase recognition sites (no shading) and vector linearization Rease recognition sites (grey shading). The fluorescent protein cassette (orange) contains sequences encoding one of the following: GFP (pBAT-G6), YFP (pBAT-Y6), or mCherry (pBAT-M6) under the control of the *PbHSP70* promoter. Olive colored bars indicate the duplicated sequences that facilitate recombination following negative selection. Note that the *Pst*I site is not unique in pBAT-Y6 as it also appears in the sequence encoding YFP.



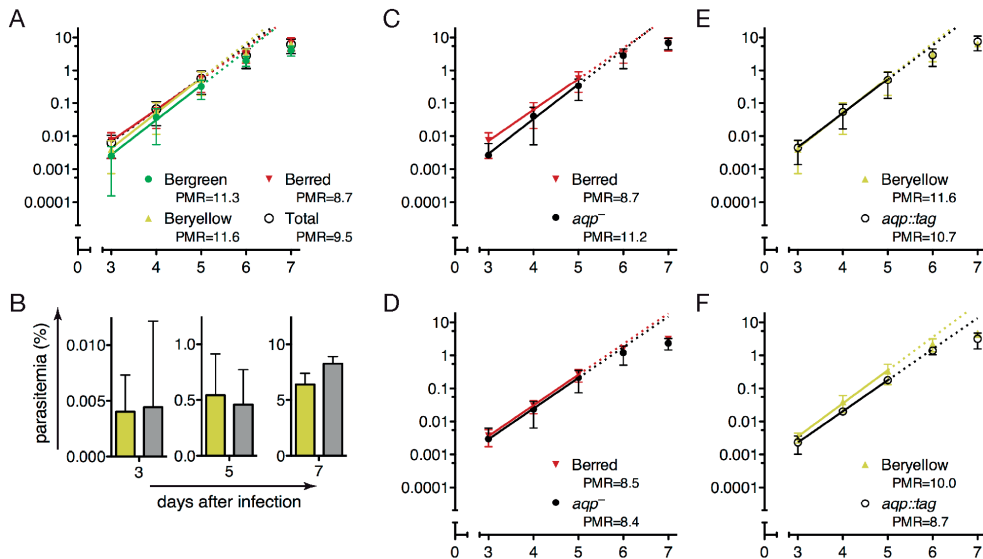
Supplementary Figure S4 | Generation of the Bergreen, Beryellow, and Berred reference lines.

(A) Schematic representation of the integration of linearized “pBAT-Color” into *P. berghei* chromosome 6. Isogenic lines were generated by flow cytometry-assisted isolation and contained the drug-selectable cassette (blue) as well as a high-expressing fluorescent protein cassette (orange). (B) Genotyping of the recombinant Bergreen, Beryellow, and Berred parasite lines. Using integration- specific primer combinations, the successful replacement events were verified. Absence of the WT signal from isogenic parasites confirmed purity of the isogenic parasite lines.

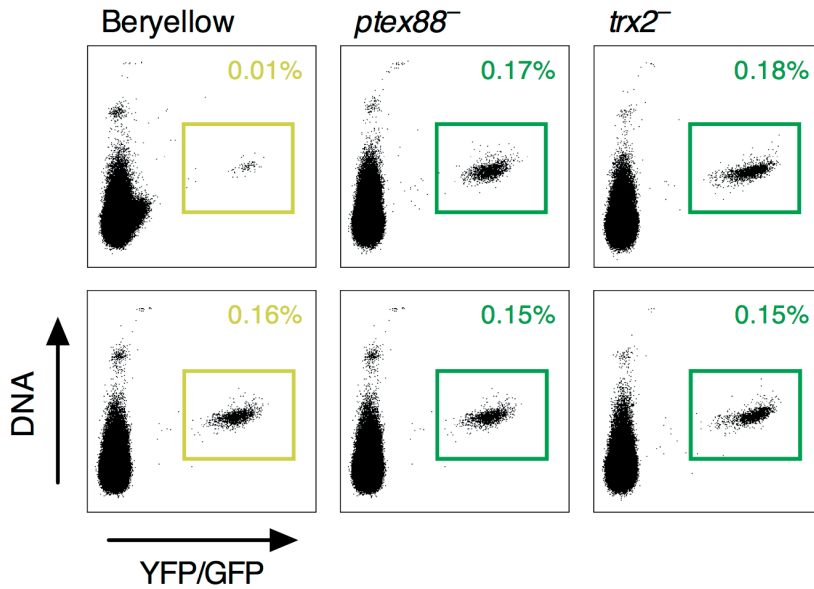


Supplementary Figure S5 | Gating strategy for quantification of fluorescent malaria parasites.

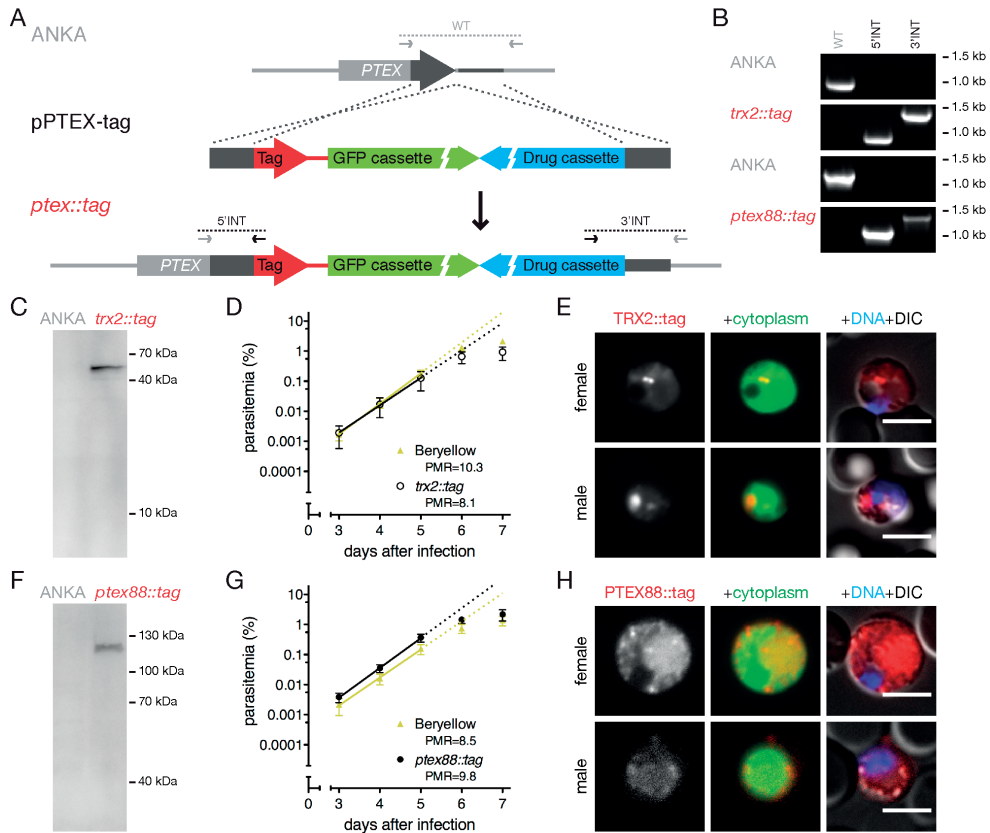
Recombinant malaria parasites expressing high levels of fluorescent protein markers and stained with Hoechst 33342 were quantified using flow cytometry. First, small particles and debris were excluded using the forward and side scatter plot. Singlets were selected using the forward width vs. height and side width vs. height scatter plots. Erythrocytes infected with two or more differently labeled parasites were also excluded from the analysis by gating out double positive cells. Finally, cells positive for Hoechst and GFP-, YFP-, or mCherry, *i.e.* erythrocytes infected by a single parasite line, were quantified. Note that, for analysis of double fluorescent parasite lines the appropriate double colored cells need to be gated for.



Supplementary Figure S6 | Validation of the intravital competition assay. In three independent experiments, parasitemia of mice infected with a total of 1,000 parasites were established using flow cytometry (see Materials and Methods and Supplementary Figure S5 for further details). Data from the exponential growth phase, *i.e.* with parasitemia <1%, fitted a linear regression well ($r^2 \geq 0.995$) and allowed the calculation of the parasite multiplication rate (PMR). (A) Blood stage development in mice infected with a single reference strain (Bergreen, Beryellow, or Berred) did not differ significantly from each other or from total parasitemia of mice infected with all three reference lines simultaneously ($P > 0.05$; two-way ANOVA). (B) Flow cytometric (yellow bars) and Giemsa-stained blood film-based (gray bars) determination of parasitemia at days 3, 5, and 7 after inoculation did not differ significantly for mice infected with Beryellow only ($P > 0.05$; paired, two-tailed student's T-test). The competitive quantification method was tested with two previously established recombinant parasite lines³² Growth in mice infected with a single parasite line (C and E), and in mice infected with a mutant and reference strain simultaneously, *i.e.* using the intravital competition assay (D and F), were compared. (C and D) Green fluorescent *aqpr*⁻ parasites³² and the Berred reference strain did not grow significantly different in single or double infections ($P > 0.05$; two-way ANOVA). (E and F) Green and red double fluorescent *aqpr::tag* parasites³² and the Beryellow reference strain did not grow significantly different in single or double infections ($P > 0.05$; two-way ANOVA).

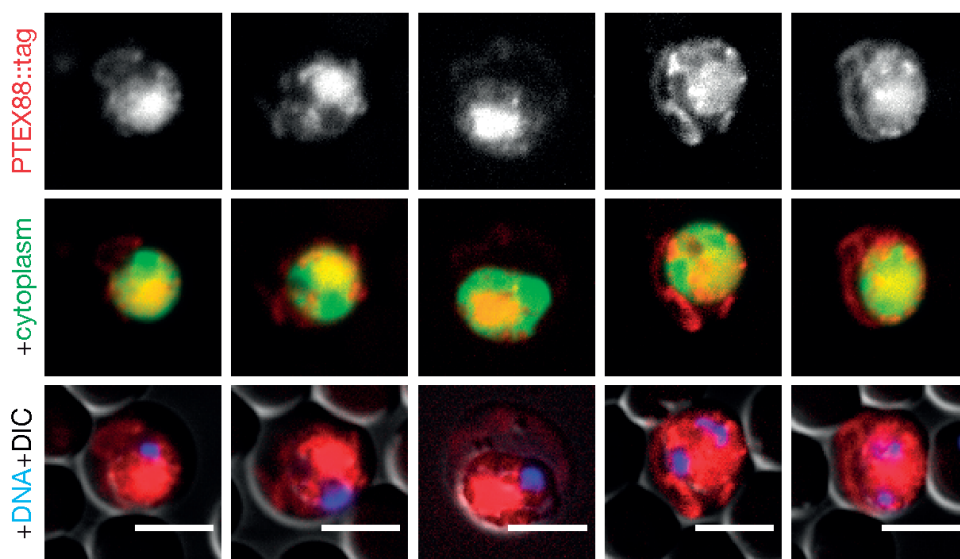


Supplementary Figure S7 | Natural transmission of *ptex88*⁻ and *trx2*⁻ is not affected. Flow cytometric analysis of blood from C57BL/6 mice ($n=2$ each) 3 days after natural sporozoite transmission by exposure to mosquitoes infected with Beryellow, *ptex88*⁻, or *trx2*⁻ parasites. Parasitemia of all knockout mutants were comparable to WT, indicating that *in vivo* liver stage development is not delayed. Note that one Beryellow-infected mice apparently received a lower inoculation dose.



Supplementary Figure S8 | Generation of *trx2::tag* and *ptex88::tag* parasites. (A) Replacement strategy to generate stable parasite lines with endogenous *TRX2* and *PTEX88* fused to an mCherry-3xMyc tag (red). In addition, recombinant parasites contain the high-expressing GFP cassette (green) and the drug-selectable *hDHFR-yFcu* cassette (blue). Primer combinations specific for integration (5' and 3'INT) and WT are indicated. (B) Diagnostic PCR of the loci of WT (ANKA) and isolated *trx2::tag* and *ptex88::tag* parasites. (C) Western blot analysis using anti-mCherry antibodies reveals a single band of the predicted size for tagged TRX2 (48 kDa). (D) Intravital competition assay for Beryellow and *trx2::tag* parasites. Linear regressions ($r^2 \geq 0.999$) and the parasite multiplication rates (PMR) did not differ significantly ($P > 0.05$). However, overall blood stage development was significantly different ($P < 0.05$, two-way ANOVA). This difference was attributable to the final, high-parasitemia stages of infection. (E) Live fluorescent imaging of *trx2::tag* sexual stages revealed low expression levels. In female gametocytes, TRX2::tag typically localized to a single intraparasitic vesicle-like structure. TRX2::tag staining in males appeared predominantly at the parasite periphery. Bars, 5 μ m. (F) Western blot analysis using anti-mCherry antibodies reveals a single band of the predicted size for tagged PTEX88 (118 kDa). (G) The intravital competition

assay revealed no significant difference in blood infection ($P>0.05$, two-way ANOVA) or PMR ($r^2\geq 0.999$, $P>0.05$) between Beryellow and *ptex88::tag* parasites. (H) Live fluorescent imaging of *ptex88::tag* sexual stages revealed low expression levels. In female gametocytes, PTEX88::tag showed a diffuse intraparasitic staining with some brighter foci at the periphery of the cell. In males, PTEX88::tag localized mainly to the parasite periphery. Bars, 5 μm .



Supplementary Figure S9 | Live fluorescence micrographs of mature *ptex88::tag* trophozoites.

Live fluorescent imaging of *ptex88::tag* asexual blood stages revealed low expression levels. PTEX88::tag displayed a diffuse intraparasitic staining and localized to previously unrecognized protrusions extending far into the red blood cell cytoplasm in trophozoites. Bars, 5 μm .

Supplementary Table S1 | Primer sequences.

Primer Name	Primer Sequence (restriction sites underlined)	Size WT (bp) ^a	Size INT (bp) ^b	Use ^c Target	Reference
mCherry-F-PstAI	TTTGACATATGCTCTGTGAGCAAGGGCGAGG	738		TV mCherry	
mCherry-R-BamHI	ATTGGATCCCTTAGGCGCCCTTATACAGCTCGTCATTCC			TV mCherry	
YFP-F-PstAI	AATTAATTGACATATGCTCTGTGAGCAAGGGCGAGGAG	751		TV YFP	
YFP-R-BamHI	ATTGGATCCCTTAGGCGCCCTTGTACAGCTCGTCCATGC			TV YFP	
SIL6F	GACAGCGCATATGATGGATG		847	GT PbSIL6	(Kenthirapalan, 2012)
SIL6R	TACGAATACGCAATTTCTCAAC	1315	1247	GT PbSIL6	(Kenthirapalan, 2012)
5'HSP70rev	CAATTTGTGTACATAAAATAGGCAG			GT 5'PbHSP70	(Kenthirapalan, 2012)
5'DHFRrev	ATGAAATACCGCTCCATTTTTCC			GT 5'PbDHFR-TS	(Kenthirapalan, 2012)
mCherryRev	CCCTCGATGTGAACCTTGAAG			GT mCherry	(Kenthirapalan, 2012)
PbHSP70-F	GCTAACGCAAAAGCAAAGC			RT PbHSP70	(Haussig, 2011)
PbHSP70-R	TCGGTAAAGCTACATAGGATG	164		RT PbHSP70	(Haussig, 2011)
5'EXP2-F-SacII	TTATTACCGCGGGTTTAGAGACATGATATGTGCGC	1593		TV 5'PbEXP2	
5'EXP2-R-HpaI	GGCACGGTTAACAATGTTAAAAATAATATACATAAAATCGGTAATAC			TV 5'PbEXP2	
3'EXP2-F-XhoI	AGTCCACCTCGAGCTAAATAGAGAAACAATGGTGTATTAAGC	606		TV 3'PbEXP2	
3'EXP2-R-KpnI	AGGGCTGTGATCCCTTATTATGAAATGCAAAATAACGAAATAGC			TV 3'PbEXP2	
5'EXP2-F	CATATATGTATGTTTACTTTTGTGTTTGAATG		2077	GT 5'PbEXP2	
5'EXP2-R	TTGCTGTCAATCACTATATGCG	2073		GT 5'PbEXP2	
3'EXP2-F	ATTATTTGAAGAGCAAGAACTGATTC			GT 3'PbEXP2	
3'EXP2-R	TGGCATGTGGCAATAAGCATAC	1096	1475	GT 3'PbEXP2	
5'HSP101-F-SacII	AGTACCGCGCGGATAAATAGAAATAGATGCTTGCTTCG	1578		TV 5'PbHSP101	
5'HSP101-R-HpaI	ATCAGGGTTAACTAAATTTATAGTAAATAGATATAATTTTATCTTCATC			TV 5'PbHSP101	
3'HSP101-F-XhoI	AGATGTCTCGAGTTAAATAAAACAACACGATATGTTGCATG	848		TV 3'PbHSP101	
3'HSP101-R-KpnI	TACTTGCTGCTTATTTATCACACACTTTTTCATAGATATTGC			TV 3'PbHSP101	
5'HSP101-F	GATTATGACAAAAGGTTTAAATTTTATTTG		1948	GT 5'PbHSP101	
5'HSP101-R	GCACAGACAATACAAAACGATGAC	1902		GT 5'PbHSP101	
3'HSP101-F	TGATGATATGGATGATATGTTGATTACAAC			GT 3'PbHSP101	
3'HSP101-R	CGTGTGGGCATAGATCAATGA	1026	1547	GT 3'PbHSP101	
5'PTX150-F-SacII	TTGCTCCGCGGATATATAAGTGTAAATAGTGTTTTTTTGTGC	1467		TV 5'PbPTX150	
5'PTX150-R-HpaI	CTTGCCGTTAACTTTATTTATCTTAATTTATTTATTTCTGTTCTTTTG			TV 5'PbPTX150	
3'PTX150-F-XhoI	AACGTTCTCGAGTAGCATAGGTGCGCGAGTC	790		TV 3'PbPTX150	
3'PTX150-R-KpnI	TTAGTGGGTACCGGTAAAGACAAGAAACAAAATGCAATTATC			TV 3'PbPTX150	
5'PTX150-F	GGTGTTTAAAGTACGACCTAAATAGG		1727	GT 5'PbPTX150	
5'PTX150-R	CAATTTTTGTTGATCGCGTCACAC			GT 5'PbPTX150	
3'PTX150-F	TTTGCAACGATGGCAACAGTG			GT 3'PbPTX150	
3'PTX150-R	TGCAAGCATTTGTACCAATTAATCC	1054	1486	GT 3'PbPTX150	
5'PTX88-F-SacII	ACGATACCGCGGGCATAAAGGCTATTGCGGGCTA	1345		TV 5'PbPTX88	
5'PTX88-R-HpaI	TACGCTGTTAACTCGCAATTTTGGGGATTCAATCTTTTAAAG			TV 5'PbPTX88	
CT-PTX88-F-SacII	AACACTCCGCGGGATTTACCACAACCATTTGGATTAAAG	699		TV CT-PbPTX88	
CT-PTX88-R-HpaI	ACTAATGTTAACTTCATGCAAAATAGTAACCTATTGTG			TV CT-PbPTX88	
3'PTX88-F-XhoI	GTCCTTCTCGAGTTTAGAAAACCCAAATCAACGCTACTGG	498		TV 3'PbPTX88	
3'PTX88-R-KpnI	GTGTACGGTACCGGCATCAAGATGCGTGGAGA			TV 3'PbPTX88	
5'PTX88-F	GTGAAAAGTGACAAATGAAGAATTATATG		1890	GT 5'PbPTX88	
5'PTX88-R	CAATGCAACCAATGCACAAC	1826		GT 5'PbPTX88	
CT-PTX88-F	GCTTGATGAAATATGCTATTATGATTCTC	1196	1002	GT CT-PbPTX88	
3'PTX88-F	ACCACAACCATTTGGATTAAACGATAG	974		GT 3'PbPTX88	
3'PTX88-R	GTGACTTGATTTCAGATTAATAATGCA		1285	GT 3'PbPTX88	
5'TRX2-F-SacII	ATCCTACCGCGGTTTCTTGCTTCCTTTTGTGTATTTTG	1094		TV 5'PbTRX2	
5'TRX2-R-HpaI	GACGACGTTAACTTTCTATTATAGTTTATTAATAATAGATATCAGG			TV 5'PbTRX2	
CT-TRX2-F-SacII	ACTCGTCCGCGGTTTGTTTTGTATTCTATGCCAAATGG	652		TV CT-PbTRX2	
CT-TRX2-R-HpaI	ACTAATGTTAACTAAATGCTTCTAATAGTTGATGTTAATTC			TV CT-PbTRX2	
3'TRX2-F-XhoI	ATCTTCTCGAGAGTTGTGTTTAAATTTTCATACACTTTTCG	531		TV 3'PbTRX2	
3'TRX2-R-KpnI	ATCTCCGTTACCAATCGAATTAACCAATATCATAGCTTATTC			TV 3'PbTRX2	
5'TRX2-F	TGAAAGACAAATAGCACTACCGG		1381	GT 5'PbTRX2	
5'TRX2-R	GTGCTGCTTTGTCCAATCTTG	1456		GT 5'PbTRX2	
CT-TRX2-F	TGCACGTAGAAATAATACCAATCCG	950	857	GT CT-PbTRX2	
3'TRX2-F	TGATGGGTGTGAGCATGTAATGG			GT 3'PbTRX2	
3'TRX2-R	GTTGTATTTGTACGCCGAATTAAG	1004	1302	GT 3'PbTRX2	

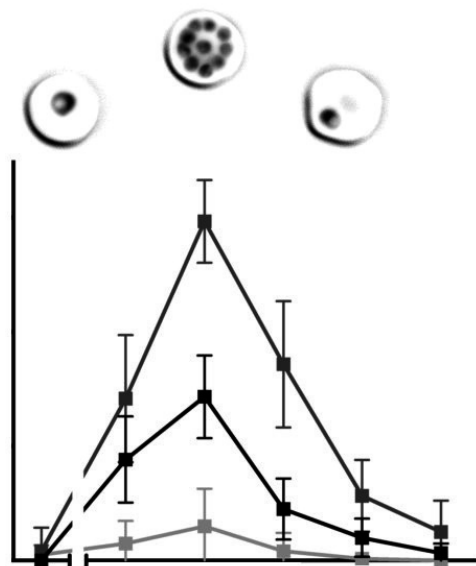
^a Sizes of the PCR products of forward and reverse primers on WT gDNA; carboxy-terminal *ptex88::tag* and *trx2::tag* integration-specific primers combined with their respective reverse 3' gene-specific primers. ^b Sizes of the respective integration-specific PCR products; forward 5' and carboxy-terminal gene-specific primers combined with 5'HSP70rev (Bercoler lines) or mCherryRev (PTEX lines) and reverse 3' gene-specific primers combined with 5'DHFRrev. ^c TV, primers used for construction of Transfection Vectors; GT, primers used for GenoTyping; RT, primers used for RT-PCR.

Chapter 4

In vivo function of PTEX88 in malaria parasite sequestration and virulence

Matz JM, Ingmundson A, Costa Nunes J, Stenzel W, Matuschewski K, Kooij TWA. Eukaryot. Cell. 2015; 14:528–534.

(cover image)



ABSTRACT

Malaria pathology is linked to remodeling of red blood cells by eukaryotic *Plasmodium* parasites. Central to host-cell refurbishment is the trafficking of parasite-encoded virulence factors through the *Plasmodium* translocon of exported proteins (PTEX). Much of our understanding of its function is based on experimental work with cultured *Plasmodium falciparum*, yet direct consequences of PTEX impairment during an infection remain poorly defined. Using the murine malaria model parasite *Plasmodium berghei*, it is shown here that efficient sequestration to the pulmonary, adipose, and brain tissue vasculature is dependent on the PTEX components thioredoxin 2 (TRX2) and PTEX88. While *TRX2*-deficient parasites remain virulent, *PTEX88*-deficient parasites no longer sequester in the brain correlating with abolishment of cerebral complications in infected mice. However, an apparent trade-off for virulence attenuation was spleen enlargement, which correlates with a strongly reduced schizont-to-ring-stage transition. Strikingly, general protein export is unaffected in *PTEX88*-deficient mutants that mature normally *in vitro*. Thus, PTEX88 is pivotal for tissue sequestration *in vivo*, parasite virulence, and preventing exacerbation of spleen pathology, but these functions do not correlate with general protein export to the host erythrocyte. The presented data suggest that the protein export machinery of *Plasmodium* parasites and their underlying mechanistic features are considerably more complex than previously anticipated and indicate potential challenges for targeted intervention strategies.

INTRODUCTION

The asexual replication inside the red blood cell is the sole phase of a malaria parasite infection that leads to pathological symptoms.¹ Within the host cell, the eukaryotic pathogen hides and replicates in a niche of its own making, termed the parasitophorous vacuole (PV).² In order to accommodate the parasite's needs, the erythrocytes are extensively refurbished through the translocation of parasite proteins across the PV membrane into the host cell.^{3,4} As a consequence, parasite-derived proteins that are exported to the host cell surface enable the binding to endothelial ligands, thereby preventing free circulation of the infected erythrocytes.¹ Through sequestration, the parasite avoids passing the spleen, which could otherwise destroy the infected red blood cell, due to the *Plasmodium*-induced changes in rigidity and deformability.⁵ Sequestration of *Plasmodium falciparum*-infected erythrocytes and the resulting vascular obstruction are responsible for the more severe complications of malaria, including edema, ischemia, and coma.^{1,6}

The identification of a protein export element (PEXEL) or vacuolar transport signal (VTS) in *P. falciparum*,^{7,8} revealed a large set of exported *Plasmodium* proteins that likely contribute to erythrocyte remodeling and, at least partly, to parasite virulence. The signature PEXEL/VTS motif is strictly conserved among different malaria parasite species. In addition, a growing list of PEXEL/VTS-negative exported proteins (PNEP) is being recognized in *P. falciparum* and other malaria parasite species.^{9,10} A corresponding *Plasmodium* translocon of exported proteins (PTEX)¹¹ is present in all mammalian *Plasmodium* parasites. This specialized multiprotein complex consists of three essential core components,^{12,13} two of which have recently been demonstrated to be directly involved in active export of both PEXEL/VTS-containing proteins and PNEPs.^{14,15} In the murine malaria model parasite, *Plasmodium berghei*, two additional PTEX constituents, thioredoxin 2 (TRX2) and PTEX88, appear to fulfill auxiliary roles.^{12,13} While parasites deficient in TRX2 display only minor alterations in growth rate and virulence, PTEX88-deficient parasites could only be selected using advanced experimental genetics approaches.^{13,16}

In this study, we systematically investigate the pathology caused by asexual blood-stage *P. berghei* lacking PTEX88 (PBANKA_094130) in comparison to TRX2 (PBANKA 135800)-deficient parasites.

MATERIALS AND METHODS

Ethics statement

This study was carried out in strict accordance with the German 'Tierschutzgesetz in der Fassung vom 22. Juli 2009' and the Directive 2010/63/EU of the European Parliament and Council 'On the protection of animals used for scientific purposes'. The protocol was approved by the ethics committee of the Berlin state authority (Landesamt für Gesundheit und Soziales Berlin, permit number G0469/09). Female NMRI and C57BL/6 mice were purchased from Charles River Laboratories (Sulzfeld, Germany). NMRI mice were used for blood-stage growth assays and spleen weight measurements. Sporozoite inoculations as well as experimental cerebral malaria (ECM) and sequestration experiments were performed using C57BL/6 mice.

Plasmodium berghei in vivo and ex vivo blood-stage development

For *ex vivo* cultivation of *P. berghei*, blood from highly infected mice (2–5%) was collected and incubated in *Pb* culture medium (RPMI 1640 complemented with 20% heat-inactivated fetal calf serum). The cultures were incubated in a low-oxygen atmosphere (5%) at 37 °C under constant shaking (77 rpm). In order to obtain a synchronized *P. berghei* infection, schizont purification was performed 18 h after inoculation by a one-step Nycodenz density gradient centrifugation.¹⁷ The obtained schizont pellets were resuspended in medium and intravenously injected into recipient mice for highly synchronized *in vivo* infections. To obtain tightly synchronized *ex vivo* cultures, blood from these mice was collected one hour after schizont injection and incubated once more in *Pb* culture medium. Stage determination of synchronized *ex vivo* cultures and *in vivo* infections of WT (Berggreen),¹³ *trx2*⁻, and *ptex88*⁻ parasites was performed by microscopic examination of Giemsa-stained thin films.

In order to measure the stage conversion efficiency of tightly synchronized, *ex vivo* cultured schizonts, NMRI donor mice were infected with both *ptex88*⁻ parasites and YFP-expressing WT (Beryellow) parasites.¹³ The parasitemias of the two parasite populations were measured by flow cytometry prior to inoculation of an *ex vivo* blood culture for schizont or merozoite purification. Two hours following the injection of the mixed purified schizonts or released merozoites into recipient mice,

the parasitemias were measured again to compare stage conversion of the two parasite lines.

Mouse pathogenesis and histology

In order to determine the outcome of a blood-stage infection, 1,000 WT (Berggreen), 1,000 *trx2*⁻, 5,000 *trx2*⁻, 1,000 *ptex88*⁻, or 100,000 *ptex88*⁻ parasites were injected intravenously into naïve C57BL/6 mice. Development of cerebral complications was monitored daily by assessing behavioral and functional abnormalities.¹⁸ Upon the diagnosis of a minimum of three neurological symptoms, usually between 7 and 9 days after injection, mice were classified as suffering from ECM and sacrificed. For quantification of the parasite burden by real-time PCR and histology, highly infected C57BL/6 mice were sacrificed 7 days after injection. The animals were perfused intracardially with isotonic NaCl solution. Brains, lungs, and adipose tissue were harvested and either fixed for 48 hours in 4% buffered formaldehyde or homogenized in trizol for RNA isolation and subsequent cDNA synthesis and real time PCR. After paraffin embedding, 4 µm tissue sections were stained with Giemsa (adipose tissue), an anti-GFP antibody (Abcam, UK; lungs and brains), or hematoxylin and eosin (H&E; brain). Microglial cells were visualized by using an anti-ionized calcium-binding adapter molecule 1 (IBA1) antibody (WAKO, Japan). Astrocytes were stained with an anti-glial fibrillary acidic protein (GFAP) antibody (DAKO, Germany). The immunohistochemical staining procedures were performed by using the iView-Ventana diaminobenzidine (DAB) Detection Kit (Ventana, Tucson, AZ, USA) with appropriate biotinylated secondary antibodies and DAB visualization of the peroxidase reaction product with a Benchmark XT immunostainer (Ventana). Omission of primary antibodies resulted in the absence of any cellular labeling. Photomicrographs were taken with a Leica DMR microscope equipped with a Jenoptik ProgRes SpeedXT Core 3 CCD camera. For spleen weight measurements, NMRI mice were sacrificed one week after the injection of 1,000 parasites. Splenectomies for the *in vivo* growth assay were performed in NMRI mice, several weeks before parasite injection.

Assessment of protein export

Surface antigen labeling of infected erythrocytes was performed using serum from

a naïve mouse or from a mouse immunized with blood-stage parasites.^{15,19} A single drop of tail blood was taken from a WT- (Bergreen) or *ptex88*⁻-infected mouse. Erythrocytes were briefly washed in RPMI 1640 (Gibco) and blocked in *Pb* culture medium (20% FCS) for 45 min before 3 h of incubation with 20% semi- or non-immune serum in RPMI. After repeated washing with *Pb* culture medium, the cells were incubated for 2 h with secondary antibody (Alexa Fluor 546 goat anti-mouse, 1:250; Life Technologies). After thorough washing, fluorescence was detected with a Zeiss AxioObserver Z1 epifluorescence microscope. A similar protocol was used for flow cytometric analysis, using blood from a double-infected mouse (WT [Beryellow] and *ptex88*⁻ parasites) and a different secondary antibody (Alexa Fluor 633 goat anti-mouse, 1:250; Life Technologies). Fluorescence of infected cells was measured by flow cytometry using a BD Biosciences LSR Fortessa analyzer. All incubations were carried out at room temperature.

For live localization of cargo proteins, transgenic parasite lines were generated by single crossover homologous recombination (Supplementary Figure S1A and Supplementary Table S1). Transfection constructs were made by introducing the PCR-amplified carboxy-terminal sequences (in some cases including the adjacent 5' flanking sequence) into the b3D+mCherry vector,²⁰ using the SacII and SpeI/NheI recognition sites (Supplementary Table S1). Vectors were linearized in the coding sequence, using BstBI (PBANKA_144540), BsmI (PBANKA_083680), PmlI (PBANKA_021540), PacI (PBANKA_010060), XbaI (PBANKA_132730), or SpeI (PBANKA_140030) and transfected into *P. berghei* strain ANKA parasites, using the standard procedure.¹⁷ After successful transfection, the parasites harbored a carboxy-terminal mCherry-tag in the respective endogenous locus. Successful integration was confirmed by fluorescence and diagnostic PCR (Supplementary Figure S1B and Supplementary Table S1). For live localization studies of PBANKA_136550, the *IBIS1-mCherry* parasite line was used.²¹ All seven parasite lines expressing mCherry-tagged cargo proteins were crossed *in vivo* with the *ptex88*⁻ parasites. Single and double mutants were imaged live following bite back feeding to C57BL/6 mice.

Statistical analysis

All data were obtained from at least 3 independent experiments, shown are mean values \pm SD. The statistical analyses were performed using GraphPad Prism 5.0

software. All parasite blood-stage development experiments were analyzed using two-way ANOVA. Data from the exponential growth phase, *i.e.* with parasitemia <1%, fitted a linear regression well ($r^2 \geq 0.99$) and allowed the calculation and comparison of the parasite multiplication rates. Differences in time to development of ECM-symptoms were analyzed using the Mantel-Cox test. Schizont nuclei were compared with an unpaired two-tailed Student's *t*-test of the $n_{\geq 8}$ cohorts. All other data sets were analyzed with a one-way ANOVA followed by Tukey's multiple comparison test. P-values <0.05 were considered statistically significant.

RESULTS

Absence of PTEX88 and thioredoxin 2 impairs tissue sequestration of Plasmodium berghei-infected erythrocytes

Upon inspection of the parasitemias of infected mice, we observed that *ptex88*⁻ parasites displayed elevated numbers of schizonts in the peripheral blood (Figure 1A). This prompted us to carefully monitor the course of synchronized *in vivo* blood

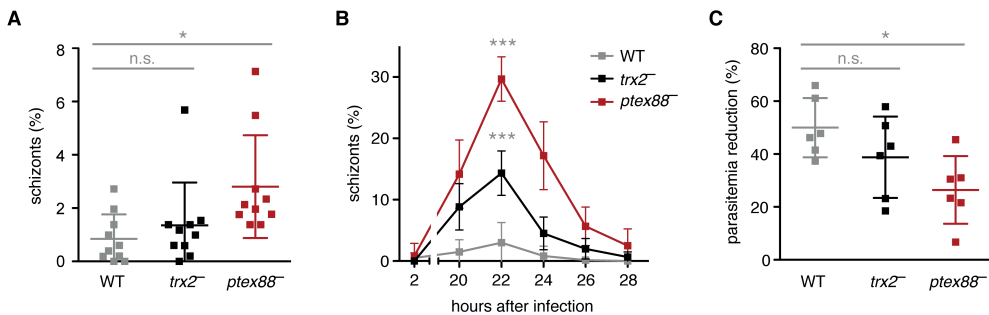


Figure 1 | Ablations of *PTEX88* and *TRX2* lead to enhanced schizont circulation *in vivo*. (A) Proportion of schizont-infected erythrocytes in peripheral blood during asynchronous infections with WT (gray), *trx2*⁻ (black), and *ptex88*⁻ (red) parasites (n.s., non-significant; *, P<0.05; one-way ANOVA and Tukey's multiple comparison test, n=10). (B) Proportion of schizont-infected erythrocytes in peripheral blood during tightly synchronized infections with WT (gray), *trx2*⁻ (black), and *ptex88*⁻ (red) parasites (***, P<0.001; two-way ANOVA, n=6). (C) Parasitemias of tightly synchronized infections were measured 2h (all rings) and 20h (all mature stages) after injection of WT (gray), *trx2*⁻ (black), and *ptex88*⁻ schizonts. The reduction of parasitemia coincides with the dominance of mature stages and the absence of ring-stage parasites (n.s., non-significant; *, P<0.05; one-way ANOVA and Tukey's multiple comparison test, n=6).

infections (Figure 1B). We detected a remarkably high (30%) percentage of schizonts in the peripheral blood of *ptex88*⁻-infected animals as compared to WT infections (3%). This phenomenon was most pronounced 22 h after infection and coincided with a reduced sequestration-dependent drop in parasitemia during parasite maturation (Figure 1C). In comparison, *trx2*⁻ parasites displayed an intermediate phenotype.

Previous work established that *P. berghei* schizonts typically sequester to adipose and lung tissue,^{22,23} which was recently also documented in *P. falciparum*-infected patients.²⁴ To test whether the large proportion of circulating *ptex88*⁻ schizonts correlates with a defect in sequestration, we performed histological organ sections of infected mice adjusted to similar parasitemia levels (Figure 2A). The number of sequestered parasites in the pulmonary vessels was an order of magnitude lower during an infection with *ptex88*⁻ parasites, compared to WT infections (Figure 2B). This defect is even more pronounced in adipose tissue, where only very few *ptex88*⁻ schizonts were detected (Figure 2C). As expected, ablation of *TRX2* resulted in a more moderate reduction of the parasite burden in vessels of lung and adipose tissue (Figure 2B and C). Molecular analysis of parasite rRNA by qPCR reflects the results of the histological quantification (Supplementary Figure S2A and B), although incomplete perfusion, for instance of fat tissue, renders the differences less prominent than in histology, which permits cell-type specific quantifications.

ptex88⁻ parasites do not cause experimental cerebral malaria

A lethal outcome of infections with virulent *P. berghei* (strain ANKA) is ECM.²⁵ Though a link between sequestration of infected erythrocytes in the brain and ECM is plausible, experimental evidence for such a correlation remains controversial.^{22,26} Histological sections of infected C57BL/6 mice seven days after infection revealed a 6-fold reduction in sequestration of *ptex88*⁻-infected erythrocytes in the brain capillaries (Figure 3A and B). In contrast, *trx2*⁻ parasites displayed a less striking deficit, resulting in a substantial, albeit non-significant, reduction in parasite burden in the cerebral vessels (Figure 3A and B). Differences in cerebral parasite burden could not be confirmed using real-time PCR, probably due to remaining blood in hemorrhages and larger vessels (Supplementary Figure S2C).

To establish a potential link between the striking sequestration deficit of the *ptex88*⁻ mutant and parasite virulence, we investigated the infection outcome by monitoring

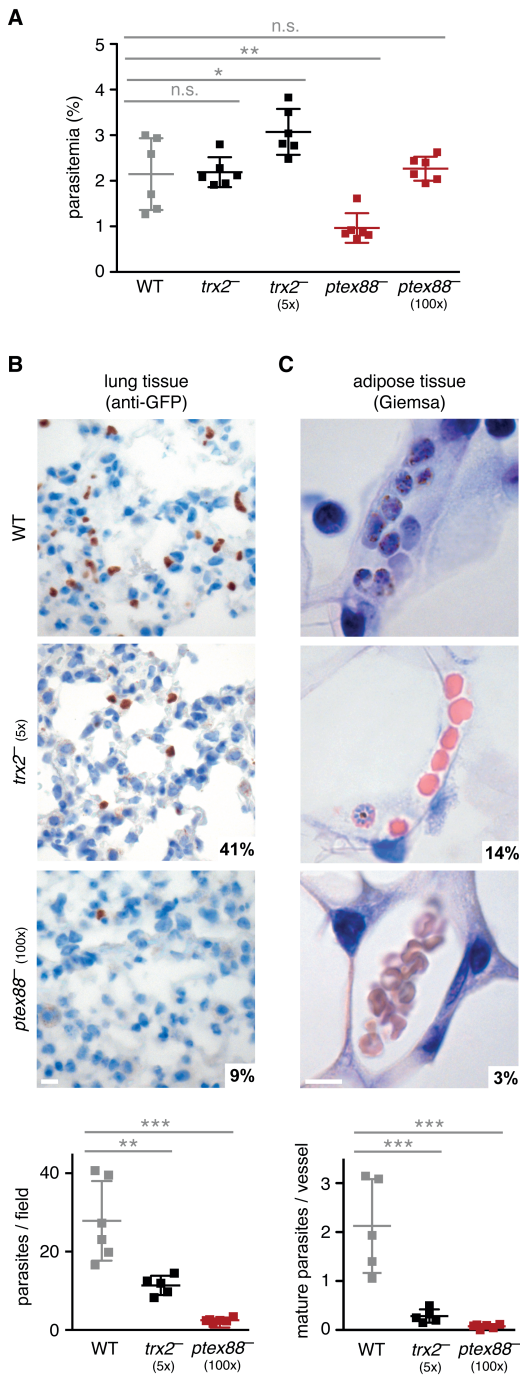


Figure 2 | PTEX88 and TRX2 are important for efficient sequestration to lung and adipose tissue. (A) Parasitemias on day 7 after intravenous injection of 1,000, 5,000 (5x), or 100,000 (100x) parasites (n.s., non-significant; *, $P < 0.05$; **, $P < 0.01$; one-way ANOVA and Tukey's multiple comparison test, $n = 6$). Representative micrographs of lung (B) and adipose (C) tissue infected with WT (left), *trx2*⁻ (center), and *ptex88*⁻ (right) parasites. Parasites were visualized by immunohistochemistry using an anti-GFP antibody (lung tissue) or stained with Giemsa (adipose tissue) and quantified microscopically (graphs; **, $P < 0.01$; ***, $P < 0.001$; one-way ANOVA and Tukey's multiple comparison test, $n \geq 5$). Bar, 10 μ m.

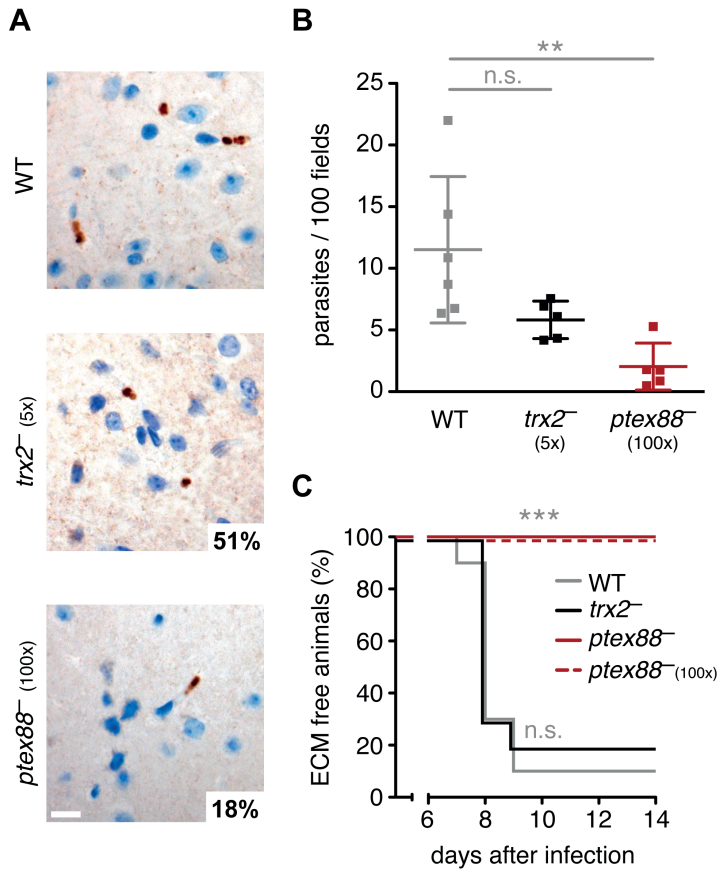


Figure 3 | Reduced cerebral sequestration of *ptex88*⁻ parasites correlates with absence of experimental cerebral malaria. (A) Representative micrographs of brain tissue infected with WT (top), *trx2*⁻ (center), and *ptex88*⁻ (bottom) parasites. Parasites were visualized by immunohistochemistry using an anti-GFP antibody. Bar, 10 μ m. (B) Microscopic quantification of sequestered parasites in cerebral vessels (n.s., non-significant; **, $P < 0.01$; one-way ANOVA and Tukey's multiple comparison test, $n \geq 5$). (C) Kaplan-Meier analysis of time to development of signature experimental cerebral malaria (ECM) symptoms. C57BL/6 mice were infected by intravenous injection of 1,000 WT (gray), *trx2*⁻ (black), or *ptex88*⁻ blood-stage parasites (red solid line), or by injection of 100,000 *ptex88*⁻ (100x, red dashed line) parasites (***, $P < 0.001$; Mantel-Cox test, $n = 10$).

the development of ECM in C57BL/6 mice following the intravenous injection of 1,000 parasites. We compared the development of cerebral complications during infections with WT, *ptex88*⁻, and *trx2*⁻ parasites (Figure 3C). Strikingly, all *ptex88*⁻ infected mice remained ECM-free and continued to develop hyperparasitemia and anemia during the later phase of infection. Even when a 100-fold excess of *ptex88*⁻ parasites was injected, no signature ECM symptoms were observed. In contrast, 80% of *trx2*⁻ infected animals displayed symptoms of cerebral complications.

Next, we performed histological analysis of cerebral bleeding and activation of microglia and astrocytes (Supplementary Figure S3). We note that histological samples from *ptex88*⁻, *trx2*⁻, and WT-infected mice were indistinguishable seven days after infection. Apparently, continuous parasite replication in the peripheral blood elicits damage to the host, including tissue injury. This finding is reminiscent of asymptomatic infections of A/J mice with either virulent (ANKA) or avirulent (NK65) *P. berghei*, which in both cases leads to cerebral hemorrhages, but not ECM.²⁶

*General export of parasite proteins is unaffected in *ptex88*⁻ parasites*

Sequestration and virulence might be dependent on a functioning protein export machinery. Therefore, we tested whether *ptex88*⁻ parasites displayed defects in export of virulence factors to the red blood cell surface by staining with serum from an immunized mouse. Surprisingly, we did not detect any significant differences in antigen exposure between WT- and *ptex88*⁻ infected erythrocytes (Figure 4A and B). To obtain independent support for our finding, we also analyzed the localization of seven exported proteins representing four known classes, *i.e.* proteins with a PEXEL/VTs motif, PNEPs, with, and without transmembrane domains (Figure 4C and Supplementary Figure S1). In agreement with the results from the surface labelling, no deficits in export were observed. All cargo proteins were targeted to the cytoplasm or to the periphery of the erythrocyte, including the schizont membrane-associated cytoadherence protein (SMAC), which is required for efficient tissue sequestration.²⁷

It has previously been demonstrated that inhibition of protein export by conditional knockdown of PTEX core components resulted in a growth arrest during asexual blood-stage propagation.^{14,15} Therefore, we tested whether the overall slower blood-stage development of the *ptex88*⁻ mutant can be attributed to delayed

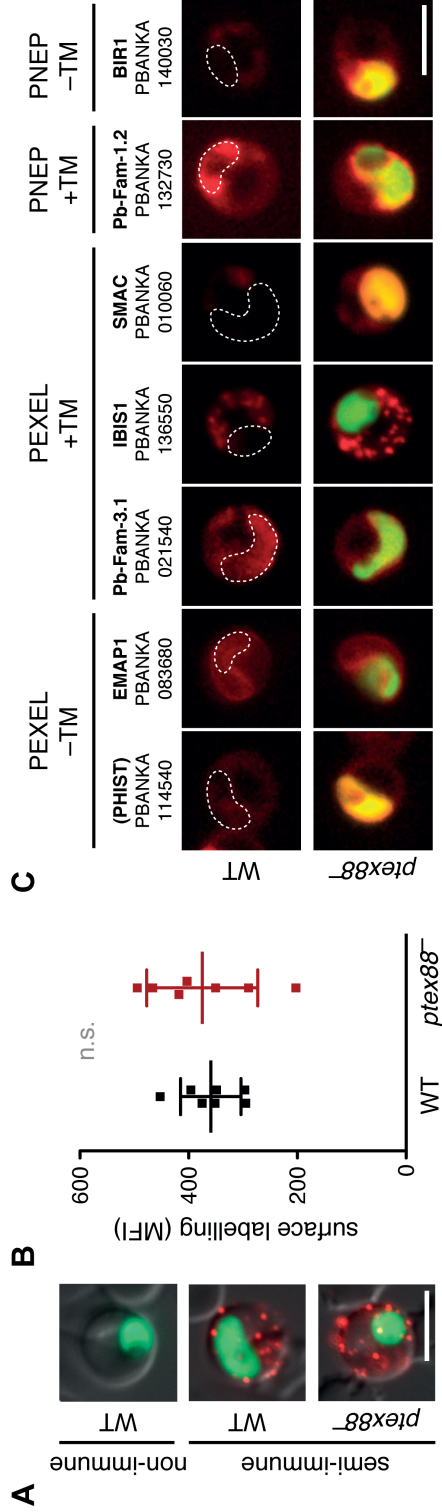


Figure 4 | General export of parasite proteins is unaffected in *ptex88⁻* parasites. (A) Surface labeling of parasite-derived antigens on WT- (top) and *ptex88⁻* - (bottom) infected erythrocytes by live immunofluorescence using sera of non-immune and semi-immune mice. Depicted is a merge of the stained antigens (red), the parasite cytoplasm (green) and a differential interference contrast image. Bar, 5 μ m. (B) Quantification of parasite-derived antigens on the surface of WT- and *ptex88⁻*-infected erythrocytes. Shown is the mean fluorescence intensity (MFI) as determined by flow cytometric analysis after staining with semi-immune serum (n.s., non-significant; paired Student's *t*-test, *n*=7). (C) Live imaging of representative mCherry-tagged cargo proteins (red signal) in WT- (top) and *ptex88⁻* (bottom) infected erythrocytes. The white outline marks the position of the non-fluorescent mCherry-tagged cargo proteins (red) can be recognized by their cytoplasmic GFP fluorescence. Note that *ptex88⁻* parasites display a certain degree of cytoplasmic mCherry fluorescence due to promoter tagging in the original loss-of-function mutant.¹³ Names and accession numbers of the exported proteins are shown. PEXEL, *Plasmodium* export element; PNEP, PEXEL-negative exported protein; TM, transmembrane domain; Bar, 5 μ m.

parasite maturation. We inoculated synchronized *ex vivo* blood cultures and assessed the parasite stages by microscopic analysis of Giemsa-stained culture smears (Figure 5A and Supplementary Figure S4). There were no detectable differences in the stage distribution of WT and *ptex88*⁻ parasites, further strengthening the notion of general protein export competence in the *PTEX88*-deficient mutant. In contrast, *trx2*⁻ parasites developed significantly slower and displayed prolonged persistence of trophozoites and fewer nuclei per schizont, which is in good agreement with its slightly reduced blood-stage propagation rate^{12,13} and protein export deficiency.¹⁵

Splenomegaly in ptex88⁻-infected mice

During organ extractions, we observed a remarkable swelling of the spleen in *ptex88*⁻-infected mice. We quantified this by measuring the splenic mass of NMRI mice seven days after intravenous injection of 1,000 infected erythrocytes (Figure 5B). *ptex88*⁻-infected mice displayed clear signs of exacerbated splenomegaly. Notably, this pathology coincides with the two-fold lower parasitemias of *ptex88*⁻-infected mice as compared to WT-infected animals at this time point (Figure 2A).

Splenic clearance is considered the principal mechanism to remove infected erythrocytes and non-viable parasites from the circulation and frequently results in splenomegaly.⁵ To investigate the possibility that the growth deficit observed in *ptex88*⁻ parasites might be directly due to enhanced splenic clearance of circulating mature parasite stages, we infected splenectomized animals (Figure 5C). Blood-stage development of both *ptex88*⁻ and WT parasites was not significantly affected by splenectomy, corroborating earlier findings with *P. berghei* parasites lacking the exported protein SMAC.²⁷

Spleen swelling could be due to recognition of non-viable *ptex88*⁻ parasites. Since we did not observe enhanced mortality during parasite maturation (Figure 5A), we looked for deficiencies during the schizont-to-ring-stage transition by injection of purified schizonts (Figure 5D). We observed a two-fold drop in relative *ptex88*⁻ parasitemia, suggesting that reduced parasite multiplication can be largely attributed to this step of the asexual replication cycle. Since a similar drop in stage-conversion efficiency was observed when purified merozoites were injected, a potential defect in parasite egress is unlikely.

DISCUSSION

In this study, we provide the first *in vivo* evidence for a function of a PTEX component in the sequestration of infected erythrocytes to multiple organs. The reduced presence of *ptex88*⁻ parasites in cerebral vessels correlates with the complete loss of ECM symptoms and lends additional support to the critical interrelation of tissue sequestration and parasite virulence. In contrast, *trx2*⁻-infected mice were prone to a lethal disease outcome, underlining an earlier study, which reported incomplete levels of protection from ECM in *trx2*⁻-infected animals.¹²

These differences in clinical outcome match our data on tissue sequestration, which is only moderately reduced for *trx2* parasites and much more pronounced in *ptex88*⁻ mutants. However, whereas *trx2*⁻ parasites were shown to exhibit suboptimal protein export,¹⁵ we were not able to detect such a defect in parasites lacking PTEX88. Our finding that protein export remains unaffected in *ptex88*⁻ parasites casts considerable doubt that this protein is involved in the actual translocation process. To date, the only supporting evidence for this has been biochemical data from co-immunoprecipitation experiments.¹¹ Still, the defects in parasite sequestration and virulence upon PTEX88 deletion are striking, suggesting important, albeit undisclosed, roles in erythrocyte remodeling. We note that we cannot formally exclude that translocation of a few selected cargo proteins strictly depends on PTEX88. We consider this scenario rather unlikely since exported proteins share common features, regardless of their targeting motives.^{9,28} An alternative, but highly speculative, explanation is that PTEX88 might act primarily in modifying, and thereby functionalizing, proteins prior to export without affecting translocation itself.

We also show, that PTEX88-deficient parasites mature normally and display a defect in schizont-to-ring stage conversion. One explanation is that the merozoites might suffer from a specific invasion defect. This would be difficult to reconcile with the original identification as part of the PTEX translocon. A second explanation could be that the microenvironment created during sequestration is directly beneficial for parasite replication²⁹ or reinvasion by bringing mature merozoites in close proximity to new host erythrocytes in a more static setting. Based on our observations, we favor the hypothesis that PTEX88 performs more specialized functions, particularly around the time of sequestration, that in turn affect the

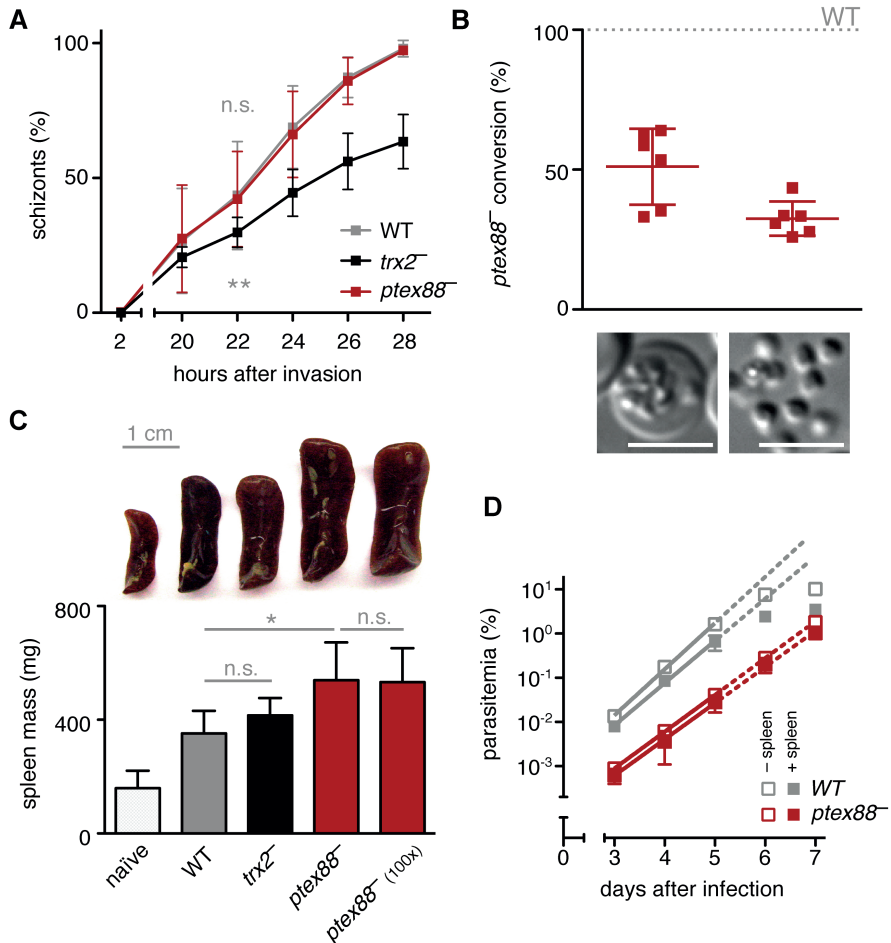


Figure 5 | Impaired schizont-to-ring stage transition of *ptex88*⁻ parasites correlates with exacerbated splenomegaly in infected mice. (A) *ptex88*⁻ parasites develop normally *ex vivo*, while *trx2*⁻ parasites display a continuous growth delay (n.s., non-significant; **, P<0.01; two-way ANOVA, n=6). (B) Representative photographs of spleens (top, from left to right) from a naïve mouse, a WT-infected mouse, a *trx2*⁻ infected mouse, and two *ptex88*⁻ infected mice (1x and 100x inoculum). Shown below is spleen weight (mg) according to infections. Spleens were removed 7 days after intravenous injection of 1,000 or 100,000 (100x) parasites (n.s., non-significant; *, P<0.05; one-way ANOVA, Tukey's multiple comparison test, n=5). (C) *In vivo* parasite growth of WT (gray) and *ptex88*⁻ (red) parasites in normal (filled squares) or splenectomized (open squares) mice (non-significant; two-way ANOVA, n=3). Parasite multiplication rates – WT, normal mice: 9.1; WT, splenectomized mice: 11.0; *ptex88*⁻, normal mice: 6.6; *ptex88*⁻, splenectomized mice: 6.8. (D) *In vivo* schizont-to-ring stage conversion of *ex vivo* cultured *ptex88*⁻ parasites relative to an internal WT control after mixed inoculations of schizonts (left) or free merozoites (right). Bars, 5 μ m.

mature parasite stages and, thereby, merozoite viability. Circulating non-viable merozoites may well be the cause for the shift in pathology to splenomegaly. Indeed, our inability to recover WT-like multiplication rates in splenectomized mice suggests that spleen swelling in *ptex88*⁻-infected mice is not associated with clearance of viable non-sequestering *ptex88*⁻ parasites.

Splenomegaly is a hallmark of malaria in human and murine infections that remains understudied.^{1,5} Therefore, our *in vivo* model might also offer research opportunities towards a better understanding of the pathophysiology of splenomegaly observed in persisting human malaria.

Our findings in the murine malaria model show that complete virulence attenuation and a clinical benefit against severe disease progression can be achieved by ablating PTEX88 function. The associated increase in spleen pathology, however, warrants a cautionary note; tailored intervention strategies that target the malaria parasite's PTEX components might be more difficult to develop than previously anticipated, since partial parasite survival might give rise to unforeseen complications.

ACKNOWLEDGEMENTS

We thank Carolin Rauch, Manuel Rauch, Petra Matylewski, and Silke Bandermann for technical assistance. We also acknowledge the assistance of the Flow Cytometry Core Facility at the Deutsches Rheuma-Forschungszentrum (Berlin), particularly Toralf Kaiser and Jenny Kirsch for expert advice. This work was supported by the Max Planck Society and partly the European Commission through the EVIMalaR network (partner 34).

REFERENCES

- 1 Haldar K, Murphy SC, Milner DA, Taylor TE. 2007. Malaria: mechanisms of erythrocytic infection and pathological correlates of severe disease. *Annu. Rev. Pathol.* 2007;2: 217–249.
- 2 Spielmann T, Montagna GN, Hecht L, Matuschewski K. Molecular make-up of the *Plasmodium* parasitophorous vacuolar membrane. *Int. J. Med. Microbiol.* 2012;302: 179–186.
- 3 Boddey JA, Cowman AF. *Plasmodium* nesting: remaking the erythrocyte from the inside out. *Annu. Rev. Microbiol.* 2013;67:243–269.
- 4 Maier AG, Rug M, O'Neill MT, Brown M, Chakravorty S, Szestak T, *et al.* Exported proteins required for virulence and rigidity of *Plasmodium falciparum*-infected human erythrocytes. *Cell.* 2008;134:48–61.
- 5 del Portillo HA, Ferrer M, Brugat T, Martin-Jaular L, Langhorne J, Lacerda MVG. The role of the spleen in malaria. *Cell. Microbiol.* 2012;14:343–355.
- 6 Ponsford MJ, Medana IM, Prapansilp P, Hien TT, Lee SJ, Dondorp AM, *et al.* Sequestration and microvascular congestion are associated with coma in human cerebral malaria. *J. Infect. Dis.* 2012;205:663–671.
- 7 Hiller NL, Bhattacharjee S, van Ooij C, Liolios K, Harrison T, Lopez-Estraño C, *et al.* A host-targeting signal in virulence proteins reveals a secretome in malarial infection. *Science.* 2004;306:1934–1937.
- 8 Marti M, Good RT, Rug M, Knuepfer E, Cowman AF. Targeting malaria virulence and remodeling proteins to the host erythrocyte. *Science.* 2004;306:1930–1933.
- 9 Grüning C, Heiber A, Kruse F, Flemming S, Franci G, Colombo SF, *et al.* Uncovering common principles in protein export of malaria parasites. *Cell Host Microbe.* 2012;12: 717–729.
- 10 Pasini EM, Braks JA, Fonager J, Klop O, Aime E, Spaccapelo R, *et al.* Proteomic and genetic analyses demonstrate that *Plasmodium berghei* blood stages export a large and diverse repertoire of proteins. *Mol. Cell. Proteomics.* 2013;12:426–448.
- 11 de Koning-Ward TF, Gilson PR, Boddey JA, Rug M, Smith BJ, Papenfuss AT, *et al.* A newly discovered protein export machine in malaria parasites. *Nature.* 2009;459:945–949.
- 12 Matthews K, Kalanon M, Chisholm SA, Sturm A, Goodman CD, Dixon MWA, *et al.* The *Plasmodium* translocon of exported proteins (PTEX) component thioredoxin-2 is important for maintaining normal blood-stage growth. *Mol. Microbiol.* 2013;89:1167–1186.
- 13 Matz JM, Matuschewski K, Kooij TWA. Two putative protein export regulators promote *Plasmodium* blood stage development *in vivo*. *Mol. Biochem. Parasitol.* 2013; 191:44–52.
- 14 Beck JR, Muralidharan V, Oksman A, Goldberg DE. PTEX component HSP101 mediates export of diverse malaria effectors into host erythrocytes. *Nature.* 2014;511: 592–595.
- 15 Elsworth B, Matthews K, Nie CQ, Kalanon M, Charnaud SC, Sanders PR, *et al.* PTEX is an essential nexus for protein export in malaria parasites. *Nature.* 2014;511:587–

- 591.
- 16 Matz JM, Kooij TWA. Towards genome-wide experimental genetics in the *in vivo* malaria model parasite *Plasmodium berghei*. *Pathog. Glob. Health*. 2015;109:46–60.
- 17 Janse C, Franke-Fayard B, Mair GR, Ramesar J, Thiel C, Engelmann S, *et al.* High efficiency transfection of *Plasmodium berghei* facilitates novel selection procedures. *Mol. Biochem. Parasitol.* 2006;145:60–70.
- 18 Lackner P, Beer R, Heussler V, Goebel G, Rudzki D, Helbok R, *et al.* Behavioural and histopathological alterations in mice with cerebral malaria. *Neuropathol. Appl. Neurobiol.* 2006;32:177–188.
- 19 de Koning-Ward TF, O'Donnell RA, Drew DR, Thomson R, Speed TP, Crabb BS. A new rodent model to assess blood stage immunity to the *Plasmodium falciparum* antigen merozoite surface protein 1₉ reveals a protective role for invasion inhibitory antibodies. *J. Exp. Med.* 2003;198:869–875.
- 20 Silvie O, Goetz K, Matuschewski K. A sporozoite asparagine-rich protein controls initiation of *Plasmodium* liver stage development. *PLoS Pathog.* 2008;4:e1000086.
- 21 Ingmundson A, Nahar C, Brinkmann V, Lehmann MJ, Matuschewski K. The exported *Plasmodium berghei* protein IBIS1 delineates membranous structures in infected red blood cells. *Mol. Microbiol.* 2012;83:1229–1243.
- 22 Franke-Fayard BMD, Janse C, Cunha-Rodrigues M, Ramesar J, Büscher P, Que I, *et al.* Murine malaria parasite sequestration: CD36 is the major receptor, but cerebral pathology is unlinked to sequestration. *Proc. Natl. Acad. Sci. U.S.A.* 2005;102:11468–11473.
- 23 Franke-Fayard B, Fonager J, Braks A, Khan SM, Janse C. Sequestration and tissue accumulation of human malaria parasites: can we learn anything from rodent models of malaria? *PLoS Pathog.* 2010; 6:e1001032.
- 24 Milner DA, Whitten RO, Kamiza S, Carr R, Liomba G, Dzamalala C, *et al.* The systemic pathology of cerebral malaria in African children. *Front Cell Infect Microbiol.* 2014;4: 104.
- 25 Engwerda C, Belnoue E, Grüner AC, Rénia L. Experimental models of cerebral malaria. *Curr. Top. Microbiol. Immunol.* 2005;297:103–143.
- 26 Nacer A, Movila A, Baer K, Mikolajczak SA, Kappe SHI, Frevert U. Neuroimmunological blood brain barrier opening in experimental cerebral malaria. *PLoS Pathog.* 2012;8:e1002982.
- 27 Fonager J, Pasini EM, Braks JAM, Klop O, Ramesar J, Remarque EJ, *et al.* Reduced CD36-dependent tissue sequestration of *Plasmodium*-infected erythrocytes is detrimental to malaria parasite growth *in vivo*. *J. Exp. Med.* 2012;209:93–107.
- 28 Heiber A, Kruse F, Pick C, Grüning C, Flemming S, Oberli A, *et al.* Identification of new PNEPs indicates a substantial non-PEXEL exportome and underpins common features in *Plasmodium falciparum* protein export. *PLoS Pathog.* 2013;9:e1003546.
- 29 Sherman IW, Eda S, Winograd E. Cytoadherence and sequestration in *Plasmodium falciparum*: defining the ties that bind. *Microbes Infect.* 2003;5:897–909.

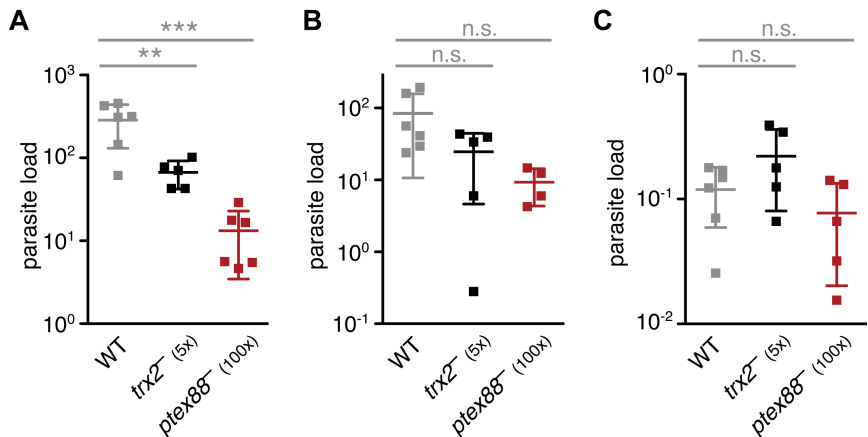
Supplementary Information for:

In vivo function of PTEX88 in malaria parasite sequestration and virulence

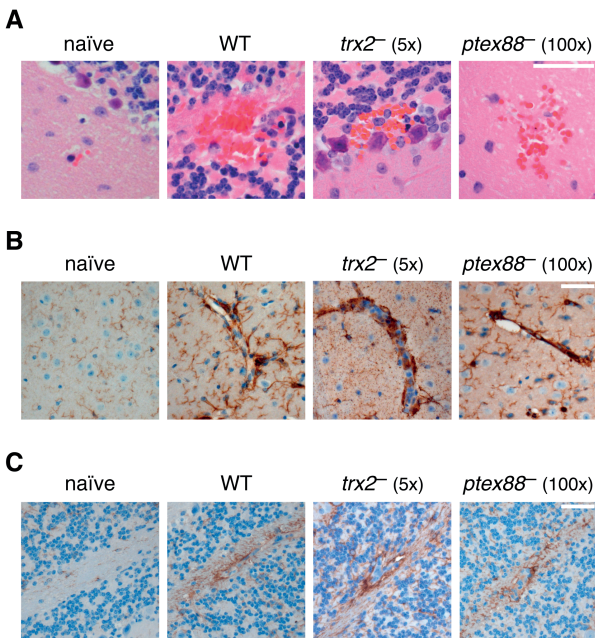
Matz JM, Ingmundson A, Costa Nunes J, Stenzel W, Matuschewski K, Kooij TWA.
Eukaryot. Cell. 2015; 14:528–534.

Content:

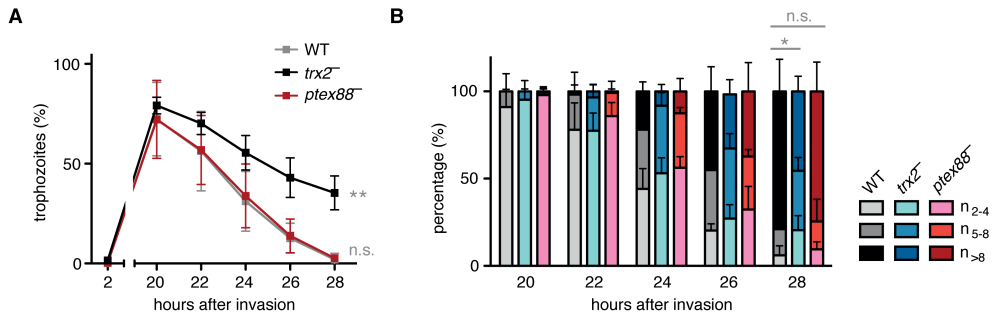
- Supplementary Figure S1** | Generation of parasite lines expressing mCherry-tagged cargo proteins
- Supplementary Figure S2** | Quantification of sequestered parasites by real-time PCR
- Supplementary Figure S3** | Cerebral hemorrhages and cell activation remain unaltered upon infection with *ptex88*⁻ or *trx2*⁻ parasites
- Supplementary Figure S4** | Development of *ptex88*⁻ and *trx2*⁻ blood stages *in vitro*.
- Supplementary Table S1** | Primer sequences



Supplementary Figure S2 | Quantification of sequestered parasites by real-time PCR. Burden of WT (gray), *trx2*⁻ (black), and *ptex88*⁻ (red) parasites in lung (A), adipose tissue (B), and brain (C) was determined by quantification of *P. berghei* 18S ribosomal RNA relative to mouse *GAPDH* mRNA (n.s., non-significant; **, P<0.01; ***, P<0.001; one-way ANOVA and Tukey's multiple comparison test, n≥5).



Supplementary Figure S3 | Cerebral hemorrhages and cell activation remain unaltered upon infection with *ptex88*⁻ or *trx2*⁻ parasites. (A) Intracerebral bleedings are present in WT, *ptex88*⁻, and *trx2*⁻-infected animals. (B) Systemic activation and association of microglial cells with cerebral vessels was visualized by immunohistochemistry using an anti-iba-1 antibody. (C) Astrocyte activation in the white matter of the cerebellum was visualized by immunohistochemistry using an anti-gfap antibody. Brains were extracted seven days after infection. Bars, 50 µm.



Supplementary Figure S4 | Development of *ptex88*⁻ and *trx2*⁻ blood stages *in vitro*. (A) Proportion of trophozoite-infected erythrocytes during synchronized *in vitro* cultures of WT (gray), *trx2*⁻ (black), and *ptex88*⁻ (red) parasites (n.s., non-significant; **, P<0.01; two-way ANOVA, n=6). (B) Number of schizont nuclei during synchronized *in vitro* cultures of WT (grays), *trx2*⁻ (blues), and *ptex88*⁻ (reds) parasites. Schizonts were classified by harboring 2 to 4, 5 to 8, or more than 8 nuclei (n.s., non-significant; *, P<0.05; two-tailed unpaired Student's *t*-test of the n>8 cohorts, n=6).

Supplementary Table S1 | Primer sequences.

Primer Name	Primer Sequence (restriction sites underlined)	Size WT (bp) ^a	Size INT (bp) ^b	Use ^c	Target
mCherryRev (A152)	TTCAGCTTGGCGGTCTGGGTGCCCTCG			GT	mCherry
5'PBANKA_114540-F-SacII	TATAATCCGCGGTGAACAACATATTGCACCCAC	1829		TV	5'PBANKA_114540
CT-PBANKA_114540-R-SpeI	TTAATACTAGTAGCAGCAGCGCTTTGTATGTCCTTCAAAAACG			TV	CT-PBANKA_114540
5'PBANKA_114540-F	TACAAAACCCCTCATGATAATAGC	1896	2005	GT	5'PBANKA_114540
3'PBANKA_114540-R	AAGAAAGACTAAATGGATACATATGC		1895	GT	3'PBANKA_114540
NT-PBANKA_083680-F-SacII	ATTTAACCGCGGGCTGTAAACTTGTTCTATACCTAAAGTG	1731		TV	NT-PBANKA_083680
CT-PBANKA_083680-R-SpeI	TTAATTACTAGTAGCAGCAGCTTTAAAACTATTTTTTAATAAATCGATCAAATATAGC			TV	CT-PBANKA_083680
NT-PBANKA_083680-F	CTCAGACAATGGTTAAAAATACATATAG		1906	GT	NT-PBANKA_083680
3'PBANKA_083680-R	AGTGATAAAGAATTATGTGGGG	1776	1776	GT	3'PBANKA_083680
5'PBANKA_021540-F-SacII	AATAAACCGCGGAATACAAAAGCGCTTTAACATCTG	1752		TV	5'PBANKA_021540
CT-PBANKA_021540-R-NheI	AACCTAGCTAGCAGCAGCAGCTTTAATTAAAGCGATTATTTCTGGATTC			TV	CT-PBANKA_021540
5'PBANKA_021540-F	TTTCTATATGGTGAATCTCTATTATAAC	1952	1978	GT	5'PBANKA_021540
3'PBANKA_021540-R	CAAGCAATTAATCATATTTTCATTGTTG		1901	GT	3'PBANKA_021540
5'PBANKA_132730-F-SacII	AATAATCCGCGGCTAATTAATGATATAGAGAATAAAACGC	1859		TV	5'PBANKA_132730
CT-PBANKA_132730-R-SpeI	AATAACTACTAGTAGCAGCAGCCTTTTAAAAATATCCTTTAATTTTACAAGAG			TV	CT-PBANKA_132730
5'PBANKA_132730-F	CATAATTAATAGCTAACATTTAAGGAG	1979	2028	GT	5'PBANKA_132730
3'PBANKA_132730-R	AATAAAATTAGTATCATGCAACAATAATTC		1985	GT	3'PBANKA_132730
5'PBANKA_140030-F-SacII	AATCATCCGCGGGTTTAAACCGTGGGAAATATGTGC	1861		TV	5'PBANKA_140030
CT-PBANKA_140030-R-NheI	TCTATTGCTAGCAGCAGCAGCATAATTCATTTCTCTTTATATTTTTAACGTTTC			TV	CT-PBANKA_140030
5'PBANKA_140030-F	TACGGTTTTAGTGCTAATTGCC		2017	GT	5'PBANKA_140030
3'PBANKA_140030-R	CTGAAATAGTCACTCTCTTTGAATC	1883	1902	GT	3'PBANKA_140030
5'PBANKA_010060-F-NotI	AGACGCGCGCCCTTATAAATCGATGTAGTGATTACTTCTCTCC	1839		TV	5'PBANKA_136550
CT-PBANKA_010060-R-SpeI	TATGACTAGTTATGGAAGTGAATAGCGAGTACAGCAG			TV	CT-PBANKA_136550
5'PBANKA_010060-F	TTATCTCTCTCTCAAAGTGC	2087	2105	GT	5'PBANKA_136550
3'PBANKA_010060-R	CTGAAATAGTCATCTCTTTTGAATC		2004	GT	3'PBANKA_136550

^a Sizes of the PCR products of forward and reverse primers on WT gDNA. ^b Sizes of the respective integration-specific PCR products; forward 5' gene-specific primers combined with mCherryRev and reverse 3' gene-specific primers combined with T7. ^c TV, primers used for construction of Transfection Vectors; GT, primers used for Genotyping.

Chapter 5

The *Plasmodium berghei* translocon of
exported proteins reveals spatiotemporal
dynamics of tubular extensions

Matz JM, Goosmann C, Brinkmann V, Grützke J, Ingmundson A,
Matuschewski K, Kooij TWA. Sci. Rep. 2015; 5:12532.



ABSTRACT

The erythrocyte is an extraordinary host cell for intracellular pathogens and requires extensive remodelling to become permissive for infection. Malaria parasites modify their host red blood cells to acquire nutrients and evade immune responses. Endogenous fluorescent tagging of three signature proteins of the *Plasmodium berghei* translocon of exported proteins (PTEX), heat shock protein 101, exported protein 2, and PTEX88, revealed motile, tubular extensions that protrude from the parasite far into the red blood cell. EXP2 displays a more prominent presence at the periphery of the parasite, consistent with its proposed role in pore formation. The tubular compartment is most prominent during trophozoite growth. Distinct spatiotemporal expression of individual PTEX components during sporogony and liver-stage development indicates additional functions and tight regulation of the PTEX translocon during parasite life cycle progression. Together, live cell imaging and correlative light and electron microscopy permitted previously unrecognized spatiotemporal and subcellular resolution of PTEX-containing tubules in murine malaria parasites. These findings further refine current models for *Plasmodium*-induced erythrocyte makeover.

INTRODUCTION

The pathogenic features of a malaria infection are caused exclusively by repeated asexual blood-stage replication of *Plasmodium* parasites.¹ Within the erythrocyte, the parasite resides inside a membrane-bound compartment called the parasitophorous vacuole (PV), which is both protective and restrictive. Host cell remodelling is most prominent during asexual intra-erythrocytic development,^{2,3} but occurs in all intracellular life cycle stages, including gametocytes and liver stages,⁴ Since the erythrocyte is devoid of organelles, vesicular transport, and some essential nutrients, the malaria parasite needs to perform extensive remodelling to render its new home permissive for successful intracellular replication.⁵

Early morphological evidence for erythrocyte remodelling in human malarial parasites⁶⁻⁸ inspired extensive research to gain a better molecular and cellular understanding of the underlying mechanisms. It was not until nearly a century later that confocal microscopy allowed the visualization of a tubovesicular network forming extensive membranous structures that originate from the PV.^{9,10} These structures have been implicated in nutrient acquisition and protein trafficking,^{11,12} but the subsequent identification of a signature sequence in exported virulence factors, termed vacuolar transport signal (VTS)¹³ or *Plasmodium* export element (PEXEL),¹⁴ implied the presence of a protein translocon.

A candidate protein transport complex has been identified in *Plasmodium falciparum* and was termed the *Plasmodium* translocon of exported proteins (PTEX).¹⁵ Five components are thought to form a macromolecular complex. Exported protein 2 (EXP2, PBANKA_133430) is a small membrane-associated protein¹⁶ that likely forms the membrane-spanning pore by multimerization.¹⁷ Heat shock protein 101 (HSP101, PBANKA_093120) is a member of the ClpA/B chaperone family and might unfold cargo proteins, a process required for *Plasmodium* protein export,¹⁸ thereby feeding them into the central channel using the energy generated by its two AAA+ ATPase domains. The biochemical functions of the three additional factors, PTEX150 (PBANKA_100850), PTEX88 (PBANKA_094130), and thioredoxin 2 (TRX2, PBANKA_135800), are less obvious.

Experimental genetics in the murine malaria model parasite *Plasmodium berghei* consistently showed that EXP2, HSP101, and PTEX150 are refractory to targeted

gene deletion.^{19,20} Using advanced knock-down technology, two studies recently reported compelling evidence for direct roles of HSP101 and PTEX150 in protein export in *P. berghei* *in vivo* and cultured *P. falciparum* parasites.^{21,22} Together, all available data are consistent with a role of the PTEX complex in trafficking of virulence factors. However, the spatiotemporal development of the translocon during asexual blood infection and life cycle progression during transmission of the malaria parasite by live imaging remains to be characterized.

We previously employed live imaging of fluorescently tagged, endogenous PTEX88 to localize this component to extraparasitic protrusions.²⁰ This finding opened the intriguing possibility that by tracing more abundant PTEX components, parasite-induced structures can be visualized throughout blood merogony and other phases of the *Plasmodium* life cycle. In this study, we performed live imaging of endogenously tagged, functional EXP2 and HSP101, and present intriguing dynamic tubular processes initiated by a eukaryotic pathogen in a terminally differentiated host cell.

RESULTS

Live imaging of the Plasmodium berghei PTEX component HSP101 reveals dynamic tubular extensions

We initiated our analysis by generating a transgenic *P. berghei* line that contains a fluorescent mCherry-3xMyc tag fused to endogenous HSP101 (Figure 1a and Supplementary Figure S1). Since *HSP101* is refractory to targeted gene deletion,^{19,20} successful selection of recombinant parasites with the desired gene replacement (Supplementary Figure S1) and a normal parasite multiplication rate of *hsp101-mCherry* parasites during blood infection (Figure 1b) provide direct proof for normal functioning of tagged HSP101. In addition, Western blot analysis revealed expression of the tagged protein at the expected size (Figure 1c). Live imaging of *hsp101-mCherry*-infected erythrocytes revealed that HSP101-mCherry switches its localization from peripheral accumulations in ring stage to one or more tubular structures during the trophozoite stage (Figure 1d). These tubular structures emerge from the surface of the parasite and arch across the erythrocyte cytoplasm displaying vivid motility and exerting undirected folding movements (Supplementary Video S1). In mature schizonts, HSP101-mCherry

localizes to peripheral foci of daughter merozoites (Figure 1d), in good agreement with previous immunofluorescence data.^{15,17}

To assess the development of the tubular structures *in vivo*, we first synchronized infections and quantified the structures by epifluorescence microscopy of tail blood samples fixed immediately following collection (Figure 2a). Since the structures were not preserved following standard fixation protocols using methanol, acetone, or 4% paraformaldehyde, we explored a variety of different procedures and found that the structures observed during live cell imaging were preserved best following fixation with 2.5% glutaraldehyde and 4% paraformaldehyde in PBS. Several attempts to enhance the signal using anti-mCherry or anti-c-Myc antibodies were unsuccessful under these conditions, thus rendering immuno-fluorescence and -electron microscopical analyses impossible. Systematic epifluorescence analysis of the endogenously tagged HSP101 revealed that length and frequency of the tubular compartment increase during the maturation of trophozoites, peaking 18 h after invasion, and eventually decrease when reaching the schizont stage (Figure 2).

HSP101 is trafficked by the parasite secretory pathway

We postulated that the dynamic structures stained by HSP101-mCherry are motile evaginations of the PV, while the intraparasitic proportion of tagged protein (Figure 1d) localizes to the endoplasmic reticulum (ER). We confirmed these findings using double mutant *P. berghei* strains that were generated by two rounds of advanced genetic manipulation. We first generated parasites with fluorescently labelled endogenous HSP101 that lack both GFP and drug-selectable cassette (Supplementary Figure S1). In this *hsp101-mCherry* line, we introduced a transgenic GFP marker fused to the signal peptide and ER-retention sequences of *PbHSP70-2/BiP* (PBANKA_081890), which labels the parasite's ER (GFP^{ER}; Supplementary Figure S2). Live imaging of the resulting *hsp101-mCherry/GFP^{ER}* line revealed co-localization of GFP^{ER} with internal HSP101-mCherry signal (Supplementary Figure S3a).

To further test whether localization of HSP101-mCherry to the tubular structures depends on the parasite's secretory pathway, we inhibited transport from the ER onward with brefeldin A (BFA), an ARF guanine nucleotide exchange inhibitor (Supplementary Figure S3b). As expected, inhibition of infected erythrocytes with

BFA resulted in accumulation of the fluorescent signal inside the parasite, presumably the ER.

HSP101-positive tubules originate from the parasitophorous vacuole

Since HSP101 harbours a signal peptide and is trafficked by the parasite's secretory pathway, we postulated that the dynamic structures are motile evaginations of the PV. In order to test this hypothesis, we introduced a different transgenic GFP marker fused only to the HSP70-2/BiP signal peptide sequence, which labels the parasite's PV (GFP^{PV}), into *hsp101-mCherry* parasites (Supplementary Figure S2). Live imaging revealed near-perfect co-localization of

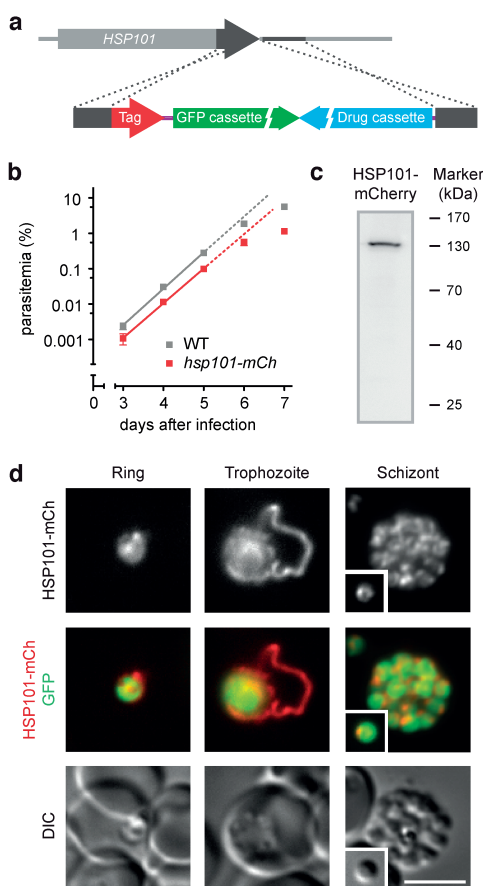


Figure 1 | Live fluorescent imaging of *Plasmodium berghei* HSP101 during asexual blood-stage development. (a) Recombination strategy for the endogenous tagging of HSP101. Double crossover integration into the wild-type locus yields recombinant parasites with their endogenous locus tagged by mCherry-3xMyc. For details see Supplementary Figure S1 and Supplementary Table S1. (b) Intravital competition assay of WT and *hsp101-mCherry* parasites. Parasite multiplication rates for WT and *hsp101-mCherry* parasites were 10.7 and 9.6, respectively (non-significant). (c) Western blot analysis of *hsp101-mCherry* parasites. The predicted size for tagged HSP101 is 133 kDa and was identified correctly using an anti-mCherry antibody. (d) Fluorescent micrographs of live *hsp101-mCherry*-infected red blood cells. Shown are representative images of the fluorescent signal of HSP101-mCherry (top), a merge of HSP101-mCherry and cytoplasmic GFP (middle), and differential interference contrast images (DIC, bottom) for three asexual developmental stages. Inset, free merozoite; scale bar, 5 μ m.

GFP^{PV} with tubular HSP101-mCherry (Figure 3a). As anticipated, the PV marker is not restricted to the tubular extension but also shows a typical peripheral distribution around the parasite, from which HSP101-mCherry is excluded in mature blood stages. In addition, we observed low-level signal from the erythrocyte cytoplasm indicating some leaking of this abundant marker protein. Though the typical appearance of double labelled mature trophozoites constituted a single GFP^{PV}- and HSP101-mCherry-positive tubule, we observed a diversity of less regular patterns (Figure 3a). HSP101-positive protrusions occasionally formed

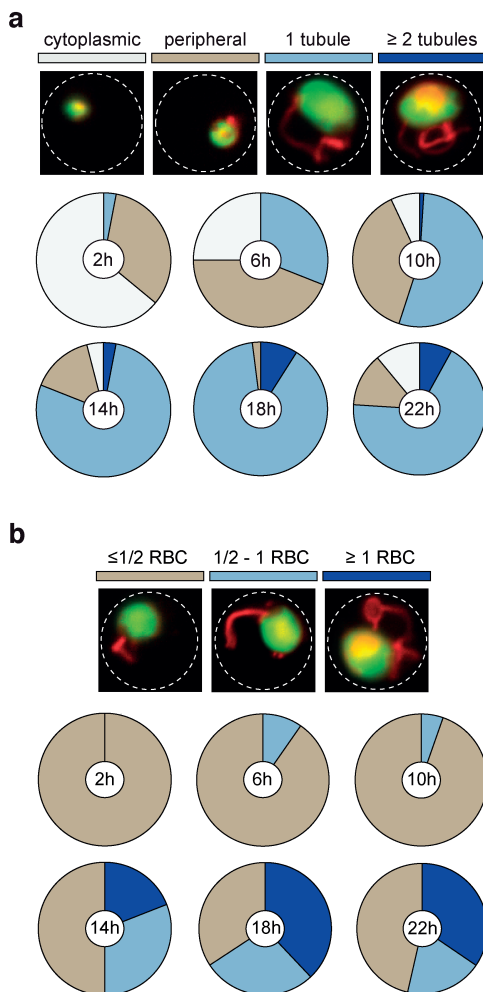


Figure 2 | Spatiotemporal analysis of extra-parasitic HSP101. (a) Quantification of HSP101-mCherry localization throughout a synchronized infection at 4 h intervals according to four categories indicated by representative images (top). The localization categories are: punctate cytoplasmic (white), additional periphery (light brown), one tubular extension (light blue), and two or more tubular extensions (dark blue). White outlines, erythrocyte; green, parasite cytoplasm; red, HSP101-mCherry. The proportions of extraparasitic HSP101-mCherry are indicated for six time points ($n=100$ per time point) of the 24 h asexual blood-stage cycle. (b) Quantification of tubular length in relation to the red blood cell (RBC) diameter indicated by representative images (top). The length categories are: ≤ 0.5 RBC diameter (light brown), $0.5 - 1$ RBC diameter (light blue), and ≥ 1 RBC diameter (dark blue). White outlines, erythrocyte; green, parasite cytoplasm; red, HSP101-mCherry. Length distributions of extraparasitic HSP101-mCherry are indicated for the same six time points ($n=100$ per time point) as in (a).

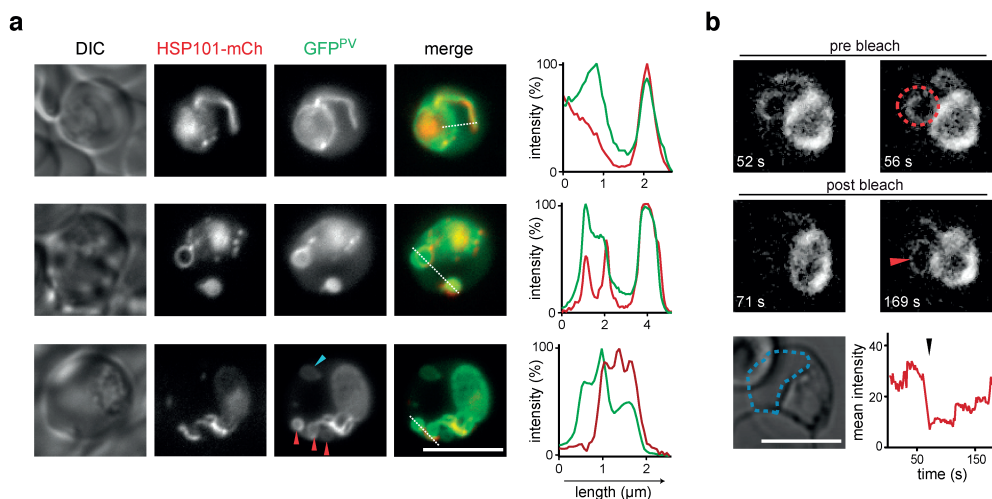


Figure 3 | HSP101 delineates a tubular subcompartment of the parasitophorous vacuole. (a) Live co-localization of HSP101-mCherry (centre left) with a marker protein of the parasitophorous vacuole (GFP^{PV}, centre). The line in the merge (centre right) indicates profiling of the fluorescent signal (right). Shown are three representative trophozoites demonstrating vacuolar tubules, loops, and vesicles. The blue arrowhead denotes a detached, vacuole-derived, and HSP101-mCherry negative lumen. The red arrowheads denote budding structures at the site of a vacuolar tubule. Note that HSP101-mCherry is excluded from these compartments. (b) FRAP analysis reveals free diffusion from the parasitophorous vacuole to the tubular extensions. Erythrocytes infected with *mCherry*^{PV} parasites were analysed by confocal microscopy before (pre bleach) and after (post bleach) photo bleaching (red area, bleach location). Shown is a representative trophozoite and the respective temporal fluorescence analysis in the erythrocyte cytoplasm (blue dotted line); black arrowhead indicates time of the bleaching pulse. White outlines, erythrocyte; scale bar, 5 μ m.

large loops, which in some cases were filled with GFP^{PV} signal. These dually labelled vesicles were also observed detached, suggesting that the tubular extensions might act as sites of membrane budding. Moreover, we captured loops and vesicles that were stained with the PV marker, but which were negative for HSP101-mCherry, suggestive of potential sub-compartmentalization of the PV-derived extensions.

Free protein exchange between the PV and tubules

To better understand the connectivity between the PV and the tubular extensions, we examined the ability of a *P. berghei* PV-marker to diffuse between these

compartments by fluorescence recovery after photobleaching (FRAP). For such an analysis, the *hsp101-mCherry* parasite line was not suitable due to its exclusive localization to the tubular extensions. As an alternative, we employed a parasite line, which, like *GFP^{PV}*, localizes to the extraparasitic tubular extensions and peripheral to the blood-stage parasites. The reporter consists of an amino-terminal fragment of the exported protein IBIS1 (PBANKA_136550),²³ which is insufficient for export into the host cell, fused to mCherry (Supplementary Figure S2). The *mCherry^{PV}* line was preferred over the *GFP^{PV}* line due to its stronger and more stable fluorescence signal, rendering it particularly suited for confocal imaging. When the mCherry^{PV} signal was bleached in the tubules, we consistently observed signal recovery (Figure 3b, Supplementary Figure S4, and Supplementary Videos S2 and S3). We conclude that (i) the lumen of the tubular extensions is contiguous with the PV and (ii) the tubular structures contain a specific protein composition, distinct from the residual PV.

HSP101-positive tubules are membrane-bound and present in wild-type parasites

To characterize the tubular ultrastructure in *P. berghei*-infected erythrocytes, we employed correlative light and electron microscopy (CLEM) using *hsp101-mCherry*-infected erythrocytes (Figure 4a and b). We were able to correlate the fluorescent HSP101-mCherry signal with continuous extended membrane evaginations (Figure 4a), which are distinct from intra-erythrocytic *P. berghei*-induced structures (IBIS), previously identified by correlative light and electron microscopy of *IBIS1-mCherry*-infected erythrocytes.²³ While the latter could be assigned to punctate structures that correlate with short membranous tubules found scattered across the erythrocyte cytoplasm, the tubules appeared much more elongated and wider in diameter.

3D reconstruction of the micrographs revealed a tubular compartment with a variable diameter of ~100 nm (75 -125 nm; Figure 4a and b and Supplementary Video S4). The protrusions appear to be confined by a singular membrane. Close examination of the tubular lumen revealed a uniform transparent appearance, indicative of soluble rather than filamentous content.

To further exclude the contribution of a cytoskeleton to the motility of the tubules, we tested a range of inhibitors of tubulin and actin filament polymerization, *i.e.*

nocodazole, cytochalasin D, and jasplakinolide, as well as motility inhibitors, *i.e.* blebbistatin, erythro-9-(2-hydroxy-3-nonyl)adenine (EHNA), and vanadate. None of the tested inhibitors affected motility or appearance of the HSP101-positive extensions (Supplementary Table S2).

Previous work showed that the dye BODIPY TR ceramide delineates a tubovesicular network (TVN) in *P. falciparum*.⁹ In order to test whether this dye displays a similar signal in *P. berghei*-infected erythrocytes, we added BODIPY TR ceramide to erythrocytes infected with *GFP^{PV}* parasites (Supplementary Figure S5). We detected, albeit irregular and weak, signals, which occasionally coincided with *GFP^{PV}*-positive structures. This co-localization was particularly prominent in loop

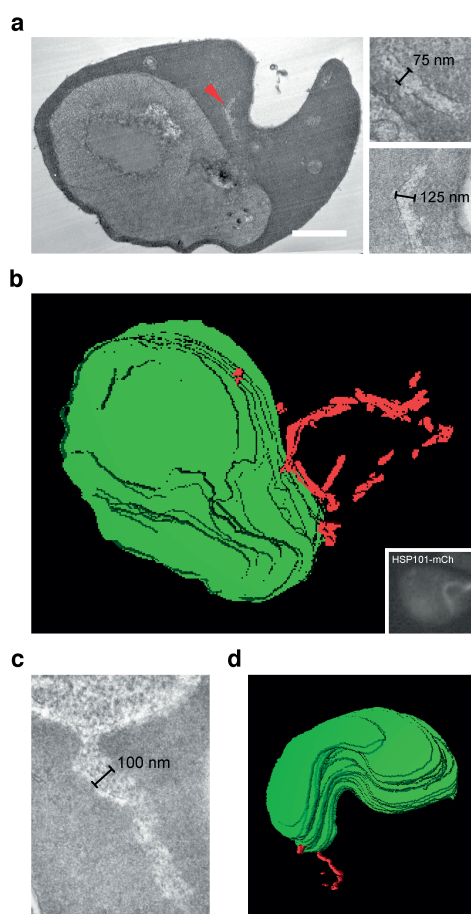


Figure 4 | Ultrastructure of the vacuolar tubules. (a) Representative transmission electron micrograph (TEM) of an *hsp101-mCherry*-infected erythrocyte, obtained by correlative light and electron microscopy (left). The red arrowhead denotes a tubular extension. Two representative high magnification images of the compartment are shown (right). Scale bar, 1 μ m. (b) Tubules were visualized by fluorescence microscopy (inset) and correlated with multiple transmission electron microscopic (TEM) sections of the same cell. The 3D-reconstruction was generated by parasite membrane alignment of 29 consecutive TEM sections. Green, parasite surface; red, tubule. (c) TEM section of a WT-infected erythrocyte. Shown is a representative high magnification image of a vacuolar tubule. (d) 3D-reconstruction generated by parasite membrane alignment of 19 TEM sections of a WT-infected erythrocyte. Green, parasite surface; red, tubule.

structures (Supplementary Figure S5). The TVN-specific inhibitor DL-*threo*-1-Phenyl-2-palmitoylamino-3-morpholino-1-propanol (PPMP)²⁴ did neither affect appearance nor motility of the protrusions in *P. berghei* parasites (Supplementary Table S2). Despite apparent differences, the overall striking similarities suggest that the HSP101-positive structures observed *ex vivo* in *P. berghei*-infected erythrocytes might share aspects of the TVN described in cultured *P. falciparum*-infected erythrocytes.⁹⁻¹²

In order to confirm the presence of a membrane-bound tubular compartment in wild-type (WT)-infected erythrocytes, we synchronized a *P. berghei* culture and scanned trophozoite-infected erythrocytes by transmission electron microscopy (Figure 4c and d, Supplementary Figure S6, and Supplementary Video S5). The presence of translucent membranous tubules extending from the PV further corroborated the physiological relevance of the structures detected in the *hsp101-mCherry* parasites. 3D-reconstruction of consecutive thin sections demonstrated a close association of the tubules with the PV (Figure 4d), lending additional ultrastructural support for this tubular compartment and its connectivity to the PV in parasite-infected erythrocytes.

Vacuolar tubules harbour at least three PTEX components

To test whether tubular localization is a unifying feature of all *P. berghei* PTEX core components and PTEX88, we employed a strategy equivalent to the one used for HSP101. We generated recombinant parasites expressing a fluorescently labelled endogenous EXP2 protein (Figure 5a and Supplementary Figure S1b). A normal parasite multiplication rate of *exp2-mCherry* parasites (Figure 5b) together with the reported refractoriness of *EXP2* to targeted gene deletion^{19,20} and detection of a tagged protein of the expected size by Western blot analysis (Figure 5c) indicate normal functions of this fusion protein. We also confirmed that EXP2-mCherry is only solubilized after treatment of membranes with Triton X-100, indicating that the large tag does not interfere with EXP2 insertion into membranes (Figure 5d).

Repeated attempts to endogenously tag PTEX150 were unsuccessful, indicating that the mCherry-3xMyc tag interferes with protein function (Supplementary Figure S1b).

We next performed live imaging of *exp2-mCherry*-infected erythrocytes and

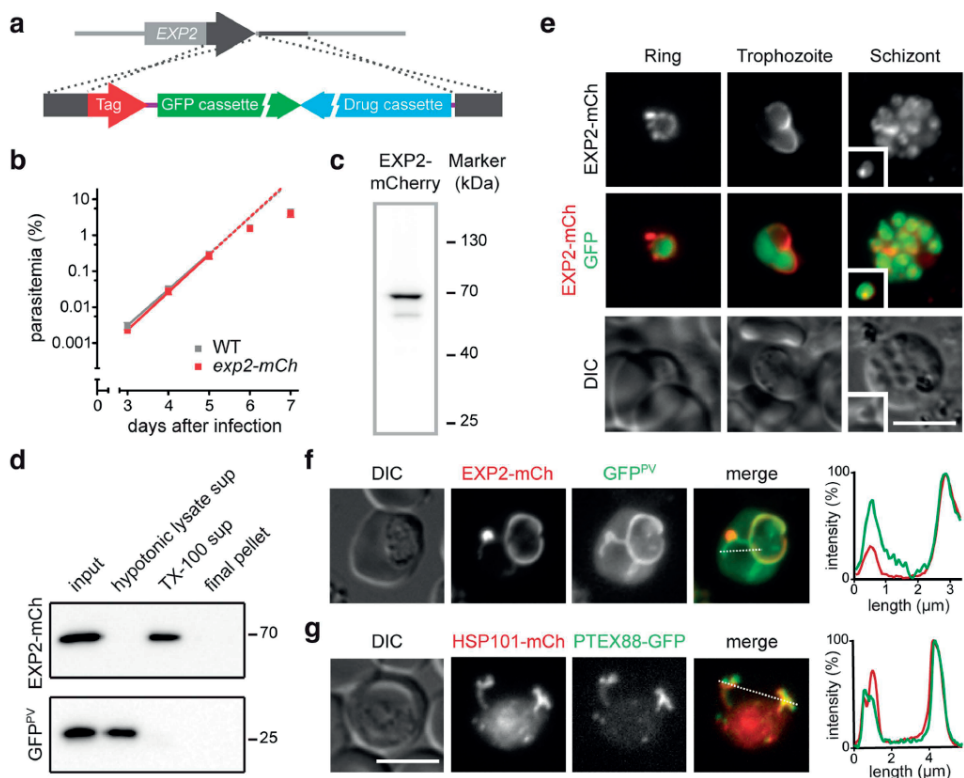


Figure 5 | Live fluorescent imaging of the PTEX components EXP2 and PTEX88. (a)

Recombination strategy for the endogenous tagging of EXP2. Double crossover integration into the wild-type locus yields recombinant parasites with their endogenous locus tagged by mCherry-3xMyc. (b) Intravital competition assay of WT and *exp2-mCherry* parasites. Parasite multiplication rates for WT and *exp2-mCherry* parasites were 10.0 and 11.2, respectively (non-significant). (c) Western blot analysis of *exp2-mCherry* parasites. The predicted size for tagged EXP2 is 62 kDa and was identified correctly using an anti-mCherry antibody. (d) Purified *exp2-mCherry* × *GFP^{PV}*-infected erythrocytes were lysed with hypotonic buffer (input) and spun at 100 000 × *g*. The supernatant (hypotonic lysate sup) along with proteins released from the pellet after Triton X-100 treatment (TX-100 sup) and the remaining insoluble pellet were analyzed by SDS-PAGE and Western blotting using anti-mCherry (EXP2-mCh) and anti-GFP (*GFP^{PV}*) antibodies. (e) Micrographs of live *exp2-mCherry*-infected erythrocytes. Shown are representative images for three asexual developmental stages including the fluorescent EXP2-mCherry signal (top), a merge of EXP2-mCherry and cytoplasmic GFP (middle), and differential interference contrast images (DIC, bottom). Inset, free merozoite. (f) Co-localization of EXP2-mCherry (top left) with the parasitophorous vacuole (*GFP^{PV}*, top right). The line in the merge (bottom left) indicates profiling of the fluorescent signal (bottom right). (g) Co-localization of HSP101-mCherry (top left) with PTEX88-GFP (top right). The line in the merge (bottom left) indicates profiling of the fluorescent signal (bottom right). Scale bars, 5 μm.

compared the signal to GFP markers of the parasite cytoplasm (Figure 5e) and the PV (Figure 5f). In good agreement with previous findings,^{15-17,19} we detected a circumferential staining pattern delineating the developing parasite during early blood-stage development (Figure 5e). In maturing stages, the signal is concentrated to one or two particular zones, which often appear to form blebs extending away from the parasite (Figure 5e), but always matches the pattern of the GFP^{PV} marker indicating a distribution throughout the entire PV including the vacuolar tubules where HSP101 resides (Figure 5f). We note that both signals also label vesicles, frequently observed in the erythrocyte cytoplasm during the trophozoite stage (Supplementary Figure S7 and Supplementary Video S6). Confirmation that the PTEX88-positive extensions, which we reported earlier,²⁰ are indeed the vacuolar tubules harbouring HSP101 and EXP2 was obtained through a genetic cross of *hsp101-mCherry* and *ptex88-GFP*, a parasite line expressing PTEX88 endogenously tagged with GFP (Supplementary Figure S1). The double fluorescent parasites displayed the exact same extraparasitic protein distribution (Figure 5g). The exclusion from the remainder of the PV, with the exception of a few smaller foci, further strengthens the notion that the tubules are distinct from the PV. Therefore, PTEX88 forms a second signature protein of this compartment, while live imaging of EXP2-mCherry reveals two distinct localizations of this putative PTEX pore protein.

Spatiotemporal dynamics of PTEX components during Plasmodium berghei life cycle progression

Transcription profiling of the genes believed to encode the *P. berghei* PTEX components has demonstrated that these are active almost throughout the entire life cycle.¹⁹ Encouraged by the dynamic spatiotemporal expression and localization in live blood stage parasites, we performed a systematic analysis of the timing and localization of the four endogenously tagged proteins, HSP101, EXP2, PTEX88, and TRX2²⁰ (Figure 6).

When we examined midguts from infected *Anopheles stephensi* mosquitoes, we noted abundant expression and uniform distribution of TRX2 (Figure 6a). EXP2-mCherry also displayed a uniform, though barely detectable red fluorescent signal, while *ptex88-mCherry* oocysts never reached levels above background seen in WT parasites (Figure 6a). HSP101 was also readily detectable and displayed a distinct

circumferential pattern in addition to uniform cytoplasmic distribution inside developing oocysts (Figure 6a).

In mature, salivary gland sporozoites, the distinct temporal expression essentially remained, *i.e.* PTEX88 was not detectable and EXP2 showed an extremely faint, diffuse accumulation barely above background, whereas TRX2 and HSP101 signals were clearly present in individual sporozoites (Figure 6b). Strikingly, HSP101 localized to the apical tip of sporozoites, reminiscent of the peripheral localization in free merozoites (Figure 1d), while TRX2 localized to punctate structures inside sporozoites, as reported previously for blood-stage parasites.^{20,25}

PTEX expression displayed a rather different pattern during liver-stage development. EXP2 and PTEX88 were continuously expressed during liver-stage maturation and localized to the periphery of the developing parasite, most likely the PV (Figure 6c and d). TRX2 continued to be expressed in this phase of the life cycle and localized initially to multiple, intraparasitic foci, but in more mature stages also to the parasite-host interface. In marked contrast and despite its presence during development in the definitive mosquito host, HSP101 expression was completely switched off during the first two days of intrahepatic growth (Figure 6c and d). As expected, all four PTEX components were expressed in merozoites derived from *in vitro* liver-stage cultures in preparation of a new blood infection (Supplementary Figure S8).

Together, the distinct patterns of all four PTEX components indicate that the constellation of the translocon may vary considerably during *Plasmodium* life cycle progression. Furthermore, the different components may also fulfil additional functions unrelated to the multimeric protein complex described for asexual intra-erythrocytic propagation, *e.g.* during mosquito-stage development.

DISCUSSION

Plasmodium parasites have the remarkable ability to remodel their host cell by membrane and protein trafficking. Most of our understanding of parasite-induced erythrocyte manipulation has come from studies of the human malaria parasite *P. falciparum*.^{2,26-28} Detailed electron microscopic analyses have revealed a close functional and physical association of parasite derived membranous structures,

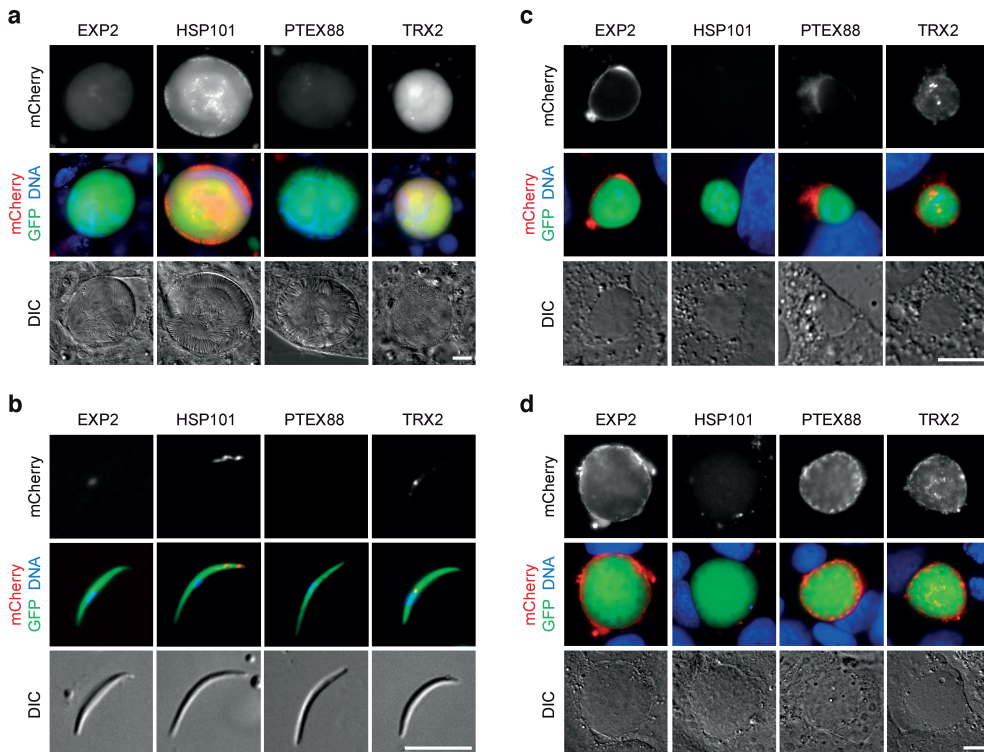


Figure 6 | Live imaging of four PTEX components during *Plasmodium berghei* life cycle progression. Micrographs of live midgut-associated oocysts (a), salivary gland sporozoites (b), and liver stages 24 h (c) and 48 h after infection (d). Shown are representative images including the fluorescent signal of the tagged protein (top), a merge of tagged protein, cytoplasmic GFP, and Hoechst 33342 DNA dye (middle) and differential interference contrast images (DIC, bottom). Scale bars, 10 μm.

such as the Maurer's clefts, and the cytoadhesion complex in *P. falciparum*.^{29,30} Despite our growing insights, it remains unclear how protein export mechanisms and parasite-induced membrane-structures in the erythrocyte cytoplasm relate.

In this work, we demonstrate that components of the putative protein export translocon localize to a specific, perhaps even specialized, tubular compartment of the PV. We identified HSP101 and PTEX88, two components of the proposed *Plasmodium* translocon, as signature proteins that localize to this tubular lumen of the PV. Thus far, localization data of the PTEX components have been consistently

obtained using immunofluorescence in fixed ring-stage parasites and mature schizonts or merozoites.^{15,17,19,31} Our data are consistent with the reported apical localization in merozoites and the specific peripheral foci in ring stages. With the exception of our own live imaging of PTEX88-mCherry,²⁰ which revealed a similar though much weaker staining pattern as described here for HSP101-mCherry (Figure 1), none of the previous studies reported tubular extensions. There are two reasons that may explain why the structures have remained elusive. Firstly, the tubules are fixation-sensitive and collapse unless high glutaraldehyde concentrations are applied, something that might even contribute to the previously observed “beads-on-a-string” staining pattern. Secondly, none of the published data show parasites at the second half of their intra-erythrocytic development when the tubular structures are largest and most prevalent.

Whereas the function of HSP101 in protein export has been demonstrated convincingly in both human and rodent malaria parasites,^{21,22} PTEX88 does not appear to play a direct role in protein translocation despite being pivotal to parasite virulence.³² However, the striking co-localization of HSP101 and PTEX88 strengthens the hypothesis that both components fulfil functions as part of the protein export complex. One open question that remains is how this co-localization is achieved at these very specific loci, particularly considering the apparent absence of filamentous structures.

EXP2, which has been hypothesized to build the membrane-spanning pore of the translocon, was also found in the PV-tubules, though not exclusively. In addition, we observed EXP2 along the parasite periphery not limited to a few specific foci, arguing for multiple functions. This pattern resembles immuno-electron microscopic observations of exported protein 1 (EXP1) that localized to the PV and extraparasitic, tubular loops in *P. falciparum*-infected erythrocytes.¹¹ Our observation that EXP2 also localizes to vesicles in the erythrocyte cytoplasm is supported by a concurrent publication, reporting similar vesicular EXP2-positive structures, primarily in reticulocytes infected with human or rodent malaria species.³³ Collectively, these data support the notion that a tubular network originates from the PV of the developing intra-erythrocytic parasite. The multiple localizations and differential transcription profile, render it conceivable that an EXP2-formed channel module may fulfil several transport functions, e.g. in protein export, waste disposal, as well as nutrient acquisition, depending on its location, protein interaction partners, or post-translational modifications.

Together with the recent identification in the rodent malaria model parasite *P. berghei* of small cleft-like structures, to which exported proteins are specifically trafficked,^{23,34} the present characterization of dynamic PV membrane tubules highlights the universal capacity of malaria parasites to extensively remodel host erythrocytes. The presence of an extensive membranous network originating from the parasitophorous vacuole that is implicated in protein trafficking compares in many respects with the description of the *P. falciparum* TVN.⁹⁻¹² Indeed, the first observation of a *P. berghei* TVN was made following the expression of GFP fused to a *P. falciparum* signal peptide sequence, which led the authors speculate that these tubular structures may facilitate protein export.³⁵ In the context of a high-resolution localization study of *P. falciparum* PTEX components, whorl-like structures were also described that were devoid of any such components.³¹ However, these structures appear within minutes of invasion and disappear soon after, whereas we observe tubular motile PV extensions predominantly in maturing trophozoites. In *P. falciparum*, the TVN has been shown to release double membrane vesicles.¹² We observed HSP101-delineated tubular loops, where the enclosed space was marked by GFP^{PV}, which is consistent with the genesis of double membrane compartments. Furthermore, the TVN was described as a site in which parasite-derived proteins can be specifically enriched,⁹ as demonstrated for HSP101 and PTEX88 in the present study.

Several of our observations set the described vacuolar tubules apart from the original description of the *P. falciparum* TVN: (i) the HSP101-, EXP2-, PTEX88-, and GFP^{PV}-positive tubular compartment is highly dynamic, whereas the TVN was described as a rather static membrane network;¹⁰ (ii) fixation with formaldehyde preserved membrane morphology of the TVN in *P. falciparum*-infected erythrocytes,⁹ while the tubular compartment of *P. berghei* was only conserved when employing fixation with 2.5% glutaraldehyde; (iii) the sphingomyelin synthase inhibitor PPMP blocks TVN assembly in *P. falciparum*,^{11,24} but not the development of the *P. berghei* PV-tubules, and (iv) the lipid marker BODIPY TR ceramide, which visualizes TVN membranes in *P. falciparum*, did not consistently stain the PV-tubules, despite clear visibility of the derived vesicular structures. Though many of these differences may be attributed to species-specific characteristics, additional work is necessary to confidently label the tubular protrusions as TVN. The absence of a population of HSP101-negative tubular structures as detected by CLEM supports the notion that a detailed characterization of the TVN development in *P. falciparum*-infected erythrocytes, as described herein for the murine parasite, will

further highlight the parallels between mechanisms of host-cell remodeling of both species. We favour the hypothesis that the tubules along with a limited number of peripheral foci define (sub)compartments of the interconnected PV/TVN space that might have evolved to specifically serve protein export to remodel the erythrocyte, while the EXP2-positive sites devoid of HSP101 or PTEX88 specialized in other functions, *e.g.* nutrient acquisition.

In a previous study, transcripts of all PTEX translocon components were detected by non-quantitative RT-PCR throughout the entire life cycle of *P. berghei*.¹⁹ Our live imaging analysis, however, demonstrated that several of the PTEX components were not or barely detectable at the protein level during several phases of the life cycle. Most striking is the inverse correlation of the expression levels of the two components co-localizing perfectly in blood-stage parasites, HSP101 and PTEX88. The apparent absence of HSP101 during liver-stage growth contrasts with abundant expression during parasite propagation in the *Anopheles* vector, where PTEX88 expression is not evident. EXP2, like PTEX88, is expressed in the PV of the developing liver-stage parasites, while signals in mosquito stages are only marginally above background levels. The observed protein expression levels in liver-stage parasites largely reflect the transcription levels.¹⁹ In developing oocysts, *PTEX88* and *HSP101* transcription levels are equivalent and those of *EXP2* are even much higher, contrasting with our protein expression data. A simple explanation for the discrepancies could be the detection of leaky transcription by the sensitive PCR-based method. It is also important to note that the transcription data are not quantitative, which is reflected by different transcription levels of the *P. yoelii* orthologues in these stages.^{36,37} Together, these data could also be indicative of post-transcriptional silencing of *PTEX* gene expression, with striking distinct patterns. Systematic studies of candidate mechanisms, such as translational repression during host switch,^{38,39} will be important to assign functions to PTEX components throughout the *Plasmodium* life cycle. While interpretations remain speculative without functional evidence using stage-specific knock-downs, the tight and exclusive regulation of distinct PTEX components already justify the notion that these proteins fulfil additional and distinct functions in other parasite life cycle stages. Based on our data, we postulate that the apparent absence of HSP101 protein during liver-stage development offers a plausible molecular explanation for the observed retention of PEXEL/VTs proteins inside the PV during intrahepatic parasite propagation.^{40,41}

In conclusion, this study establishes that PTEX components, which function in a macromolecular complex and primarily in protein translocation across the PV membrane, are signature proteins of PV tubules that might reflect an evolutionary conserved protein trafficking tubular system.

METHODS

Ethics statement

This study was carried out in strict accordance with the German 'Tierschutzgesetz in der Fassung vom 22. Juli 2009' and the Directive 2010/63/EU of the European Parliament and Council 'On the protection of animals used for scientific purposes'. The protocol was approved by the ethics committee of the Berlin state authority (Landesamt für Gesundheit und Soziales Berlin, permit number G0469/09). Female NMRI and C57BL/6 mice were purchased from Charles River Laboratories (Sulzfeld, Germany). NMRI mice were used for blood-stage growth assays and parasite cultivation. Sporozoite transmission was performed using C57BL/6 mice.

Generation and isolation of recombinant Plasmodium berghei parasite lines

Recombinant parasite lines were generated and isolated as described.⁴²⁻⁴⁴ Transfection plasmids designed for endogenous tagging were based on the pBAT vector⁴⁵ and constructed following a similar strategy as described previously²⁰ (Supplementary Figure S1 and Supplementary Table S1). In a first cloning step, the 3' flanking regions of *EXP2* (606 bp) and *HSP101* (848 bp) were amplified from genomic DNA and inserted into the pBAT vector, using the XhoI and KpnI restriction sites. The resultant intermediate constructs (pEXP2-IM and pHSP101-IM) were digested with SacII and HpaI prior to insertion of the carboxy-terminal coding sequences of *EXP2* (703 bp) and *HSP101* (638 bp). In the final pEXP2-mCh and pHSP101-mCh plasmids, the carboxy-terminal sequences of the genes were thus fused in frame to an mCherry-3xMyc-tag, allowing for live protein localization in the resulting *exp2-mcherry* (*exp2-mCh^{GFP, res}*) and *hsp101-mCherry* (*hsp101-mCh^{GFP, res}*) parasite lines (Supplementary Figure S1). For co-localization purposes with GFP-coupled proteins, the high-fluorescent GFP expression

cassette was removed by PvuII/EcoRV digestion and plasmid re-ligation. A transfection plasmid for the generation of a parasite line expressing the endogenous *PTEX88* fused in-frame to *GFP* was generated by digesting the pPTEX88-tag plasmid²⁰ with Swal and AgeI, followed by Klenow fill-in and plasmid re-ligation.

For the generation of two novel reference strains with GFP marker proteins staining either the parasitophorous vacuole (*GFP^{PV}*) or the endoplasmic reticulum (*GFP^{ER}*), the GFP coding sequence of the pBAT-SIL6 plasmid was equipped with the BiP signal peptide at the amino-terminal, either alone (*GFP^{PV}*, 818 bp) or in combination with a carboxy-terminal *BiP* ER retention signal (*GFP^{ER}*, 830 bp). Inserted coding sequences were confirmed by commercial Sanger sequencing. All pBAT-based plasmids were linearized with ApaLI and AhdI prior to transfection and integration into the genome of *P. berghei* ANKA parasites through stable double crossover homologous recombination.

For the mCherry^{PV} plasmid, the first 484 bp of the coding sequence of *IBIS1* and 1,282 bp of the 5' flanking region were cloned into the b3D+mCherry vector,⁴⁶ using the SacII and SpeI restriction sites. Following linearization, the mCherry^{PV} transfection vector was integrated into the genome of *P. berghei* GFPcon⁴² through single crossover homologous recombination. The lack of a spacer between the IBIS1 PEXEL/VTs motif and mCherry prevents export of the fusion protein. Successful integration of all transfection vectors into the endogenous *EXP2*, *HSP101*, *PTEX88*, and *IBIS1* loci or into the silent intergenic locus on *P. berghei* chromosome 6 (SIL6) was confirmed by diagnostic PCR (Supplementary Figure S1 and S2 and Supplementary Table S1).

Strategies for the generation of parasite double mutants

We followed two different strategies to generate double mutant parasite lines. (1) The isogenic pyrimethamine-insensitive but *GFP*-negative *hsp101-mCherry* (*hsp101-mCh^{res}*) line was subjected to negative selection with 5-fluorocytosine, yielding *hsp101-mCh^{sens}* parasites that are accessible for a subsequent round of genetic manipulation due to the loss of their drug-selectable resistance cassette. The clonal *hsp101-mCh^{sens}* line was transfected with the pGFP^{PV} and pGFP^{ER} plasmids and images were recorded directly from the parental populations. (2) In a complementary approach, we infected NMRI mice with two parasite lines of

different genetic backgrounds and fed these mice to *Anopheles stephensi* mosquitoes. Sporozoite transmission was achieved by bite back feeding of C57BL/6 mice. Cross-fertilization and chromosomal recombination during mosquito stage development yielded a mixed population of single and double mutant blood-stage parasites. This method was employed to generate genetic crosses of *exp2-mCherry* × *GFP^{PV}* and *hsp101-mCherry* × *ptex88-GFP*.

Plasmodium berghei in vivo and ex vivo blood-stage development

For the *in vitro* cultivation of *P. berghei*, blood from highly infected mice (2–5%) was collected and incubated in *Pb* culture medium (RPMI 1640 complemented with 20% heat-inactivated foetal calf serum). The cultures were incubated in a low-oxygen atmosphere (5%) at 37 °C under constant shaking (77 rpm). In order to obtain a synchronized *P. berghei* infection, schizont purification was performed 18 hours after inoculation by a one-step Nycodenz density gradient centrifugation.⁴² The obtained schizont pellets were resuspended in medium and intravenously injected into recipient mice for highly synchronized *in vivo* infections. To obtain highly synchronized *ex vivo* cultures, blood from these mice was collected and incubated once more in *Pb* culture medium supplemented with or without different concentrations of Brefeldin A.

Blood-stage propagation of the *exp2-mCherry* (*exp2-mCh^{GFP, res}*) and *hsp101-mCherry* (*hsp101-mCh^{GFP, res}*) parasite lines was measured by the intravital competition assay as described²⁰. This method relies on the co-injection of a double fluorescent mutant line with the YFP-expressing WT (Beryellow) parasite,²⁰ and their subsequent analysis by flow cytometry.

Biochemical fractionation and Western blot analysis

Differential solubilisation of *exp2-mCherry* × *GFP^{PV}*-infected erythrocytes was performed as described previously.²³ In short, infected erythrocytes were purified on a Nycodenz gradient⁴⁷ and lysed hypotonically for 1 h on ice in 1 mM TRIS-HCl, pH 7.5. Lysates were spun 50 min at 100,000 × *g*. The pellet was resuspended in 1% Triton X-100 in PBS and spun 50 min at 100,000 × *g*.

Equal amounts of each of these fractions or whole protein extracts of mixed blood

stages of parasites expressing endogenously tagged proteins, *hsp101-mCherry* (*hsp101-mCh^{GFP,res}*) and *exp2-mCherry* (*exp2-mCh^{GFP,res}*), were separated on SDS-polyacrylamide and transferred onto a PVDF membrane. Western blotting was performed using a rat monoclonal anti-mCherry antibody (1:5,000; ChromoTek) or a chicken polyclonal anti-GFP antibody (1:5,000; Abcam) and followed by a horseradish peroxidase coupled goat anti-rat/chicken antibody (1:5,000; Jackson ImmunoResearch).

Light microscopy of live and fixed parasites

Images for live protein localization were recorded on a Zeiss AxioObserver Z1 epifluorescence microscope, equipped with a Zeiss AxioCam MRm camera, and processed minimally with FIJI.⁴⁸ Live protein localization was performed only minutes after blood sampling using either conventional slides and coverslips or concanavalin A-coated ibidi μ -Dishes (35 mm, low; Grid500) with pre-warmed *Pb* culture medium. For the assessment of HSP101-mCherry localization during blood-stage development, peripheral blood from a tightly synchronized *hsp101-mCherry* (*hsp101-mCh^{GFP,res}*) infection was taken every four hours and diluted 1:50 with *Pb* culture medium. The dilution was then transferred onto a poly-L-lysine coated coverslip. The RBCs were allowed to settle for five minutes at 37 °C prior to fixation with 2.5% glutaraldehyde and 4% paraformaldehyde in PBS for 20 minutes. After repeated washing with PBS, the coverslip was mounted onto a glass slide and protein localization was analysed for 100 parasites per time point. Three-dimensional reconstruction of the EXP2-mCherry signal was performed by optical sectioning with a Zeiss ApoTome.2 using structured illumination technology. Fluorescent membrane labelling was achieved by inoculating an *ex vivo* blood culture with 0.5 mM BODIPY TR ceramide for several hours.

Photobleaching experiments were conducted using *mCherry^{PV}*-infected erythrocytes. Red blood cells were suspended in *Pb* culture medium and seeded on a concanavalin A-coated ibidi μ -Dish (35 mm, low; Grid500). After 15 min of incubation at 37 °C, the cells were imaged with a Leica TCS-SP5 confocal microscope at 37 °C using the non-resonant scanner at 1000 Hz. mCherry was excited with the 561 nm laser line. The indicated areas were bleached for 200 ms with the 405 nm laser, before scanning was resumed.

Electron microscopy

Correlative light and electron microscopy was performed with the *hsp101-mCherry* (*hsp101-mCh^{GFP,res}*) parasite line. Infected blood was diluted 1:300 in pre-warmed *Pb* culture medium and the cell suspension was transferred to a concanavalin A coated ibidi μ -Dish (35 mm, low; Grid500) and incubated at 37 °C for 15 minutes. Infected RBCs were continuously imaged with a Zeiss Axiovert 200M wide field microscope, equipped with a Hamamatsu Orca CCD camera, until subsequent *in situ* fixation with 2.5% glutaraldehyde and washed with PBS. WT ANKA strain parasites were fixed in solution with 2.5% glutaraldehyde in PBS and, after washing with PBS, were embedded in agarose beads. Both WT and *hsp101-mCherry* preparations were contrasted with 0.5% osmium-tetroxide, tannic acid, and 2% uranyl-acetate, dehydrated in a graded ethanol series, cleared in styrene (WT samples only), and infiltrated gradually in several changes of epoxy resin for several hours. The samples were embedded in epoxy on the microscopy dish, using inverted microcentrifuge tubes as moulds, or in standard flat embedding moulds (WT samples), and heat-cured overnight. Sections were made using a diamond knife on a Leica Ultracut-R ultramicrotome. After retrieval on copper grids, the sections were visualized and recorded with a Zeiss LEO 906 or 912 transmission electron microscope, equipped with an SIS-Olympus Morada side mounted or Cantega bottom mount digital camera. For high-resolution modelling, grids of digital images from consecutive sections were stitched and aligned using the TrakEM2 plugin in the FIJI software package.⁴⁸⁻⁵¹ Membranous borders were segmented and aligned interactively and subsequently exported as 3D views.

ACKNOWLEDGEMENTS

We thank Carolin Rauch and Manuel Rauch, for technical assistance. We also acknowledge the assistance of the Flow Cytometry Core Facility at the Deutsches Rheuma-Forschungszentrum (Berlin), particularly Toralf Kaiser and Jenny Kirsch for expert advice.

This work was supported by the Max Planck Society and partly by the European Commission through the EVIMalaR network (partner 34).

AUTHOR CONTRIBUTIONS

J.M.M., C.G., V.B., J.G., A.I., and T.W.A.K. performed the experiments. J.M.M., K.M., and T.W.A.K. conceived the study, designed all experiments, analysed the data, and wrote the manuscript.

ADDITIONAL INFORMATION

Competing financial interests: The authors declare no competing financial interests.

REFERENCES

- 1 Haldar K, Murphy SC, Milner DA, Taylor TE. Malaria: mechanisms of erythrocytic infection and pathological correlates of severe disease. *Annu. Rev. Pathol.* 2007;2: 217–249.
- 2 Marti M, Spielmann T. Protein export in malaria parasites: many membranes to cross. *Curr. Opin. Microbiol.* 2013;16:445–451.
- 3 Elsworth B, Crabb BS, Gilson PR. Protein export in malaria parasites: an update. *Cell. Microbiol.* 2014;16:355–363.
- 4 Ingmundson A, Alano P, Matuschewski K, Silvestrini F. Feeling at home from arrival to departure: protein export and host cell remodelling during *Plasmodium* liver stage and gametocyte maturation. *Cell. Microbiol.* 2014;16:324–333.
- 5 Baumeister S, Winterberg M, Przyborski JM, Lingelbach K. The malaria parasite *Plasmodium falciparum*: cell biological peculiarities and nutritional consequences. *Protoplasma.* 2010;240:3–12.
- 6 Schüffner W. Beitrag zur Kenntnis der Malaria. *Dtsch. Arch. Klin. Med.* 1899;64:428–449.
- 7 Maurer G. Die malaria perniciosa. *Zentralbl. Bakteriол. Parasitenk.* 1902;21:695–719.
- 8 Ziemann H. Über eigenartige Malariaparasitenformen. *Zentralbl. Bakt.* 1915;76:384–391.
- 9 Behari R, Haldar K. *Plasmodium falciparum*: protein localization along a novel, lipid-rich tubovesicular membrane network in infected erythrocytes. *Exp. Parasitol.* 1994;79: 250–259.
- 10 Elmendorf HG, Haldar K. *Plasmodium falciparum* exports the Golgi marker sphingomyelin synthase into a tubovesicular network in the cytoplasm of mature erythrocytes. *J. Cell Biol.* 1994;124:449–462.
- 11 Lauer SA, Rathod PK, Ghori N, Haldar K. A membrane network for nutrient import in red cells infected with the malaria parasite. *Science.* 1997;276:1122–1125.
- 12 Adisa A, Rug M, Klonis N, Foley M, Cowman AF, Tilley L. The signal sequence of exported protein-1 directs the green fluorescent protein to the parasitophorous vacuole of transfected malaria parasites. *J. Biol. Chem.* 2003;278:6532–6542.
- 13 Hiller NL, Bhattacharjee S, van Ooij C, Liolios K, Harrison T, Lopez-Estraño C, *et al.* A host-targeting signal in virulence proteins reveals a secretome in malarial infection. *Science.* 2004;306:1934–7.
- 14 Marti M, Good RT, Rug M, Knuepfer E, Cowman AF. Targeting malaria virulence and remodeling proteins to the host erythrocyte. *Science.* 2004;306:1930–1933.
- 15 de Koning-Ward TF, Gilson PR, Boddey JA, Rug M, Smith BJ, Papenfuss AT, *et al.* A newly discovered protein export machine in malaria parasites. *Nature.* 2009;459:945–949.
- 16 Johnson D, Günther K, Ansorge I, Benting J, Kent A, Bannister L, *et al.* Characterization of membrane proteins exported from *Plasmodium falciparum* into the host erythrocyte. *Parasitology.* 1994;109:1–9.
- 17 Bullen HE, Charnaud SC, Kalanon M, Riglar DT, Dekiwadia C, Kangwanrangsan N, *et al.* Biosynthesis, localization, and macromolecular arrangement of the *Plasmodium*

- falciparum* translocon of exported proteins (PTEX). J Biol Chem. 2012;287:7871–84.
- 18 Gehde N, Hinrichs C, Montilla I, Chappian S, Lingelbach K, Przyborski JM. Protein unfolding is an essential requirement for transport across the parasitophorous vacuolar membrane of *Plasmodium falciparum*. Mol Microbiol. 2009;71:613–28.
 - 19 Matthews K, Kalanon M, Chisholm SA, Sturm A, Goodman CD, Dixon MWA, *et al.* The *Plasmodium* translocon of exported proteins (PTEX) component thioredoxin-2 is important for maintaining normal blood-stage growth. Mol Microbiol. 2013;89:1167–86.
 - 20 Matz JM, Matuschewski K, Kooij TWA. Two putative protein export regulators promote *Plasmodium* blood stage development *in vivo*. Mol. Biochem. Parasitol. 2013; 191:44–52.
 - 21 Beck JR, Muralidharan V, Oksman A, Goldberg DE. PTEX component HSP101 mediates export of diverse malaria effectors into host erythrocytes. Nature. 2014;511: 592–595.
 - 22 Elsworth B, Matthews K, Nie CQ, Kalanon M, Charnaud SC, Sanders PR, *et al.* PTEX is an essential nexus for protein export in malaria parasites. Nature. 2014;511:587–91.
 - 23 Ingmundson A, Nahar C, Brinkmann V, Lehmann MJ, Matuschewski K. The exported *Plasmodium berghei* protein IBIS1 delineates membranous structures in infected red blood cells. Mol. Microbiol. 2012;83:1229–1243.
 - 24 Lauer SA, Ghori N, Haldar K. Sphingolipid synthesis as a target for chemotherapy against malaria parasites. Proc. Natl. Acad. Sci. U.S.A. 1995;92:9181–9185.
 - 25 Kehr S, Sturm N, Rahlfs S, Przyborski JM, Becker K. Compartmentation of redox metabolism in malaria parasites. PLoS Pathog. 2010;6:e1001242.
 - 26 Bhattacharjee S, Stahelin RV, Haldar K. Host targeting of virulence determinants and phosphoinositides in blood stage malaria parasites. Trends Parasitol. 2012;28:555–562.
 - 27 Boddey JA, Cowman AF. *Plasmodium* nesting: remaking the erythrocyte from the inside out. Annu. Rev. Microbiol. 2013;67:243–269.
 - 28 Desai SA. Why do malaria parasites increase host erythrocyte permeability? Trends Parasitol. 2014;30:151–159.
 - 29 Hanssen E, Sougrat R, Frankland S, Deed S, Klonis N, Lippincott-Schwartz J, *et al.* Electron tomography of the Maurer's cleft organelles of *Plasmodium falciparum*-infected erythrocytes reveals novel structural features. Mol. Microbiol. 2008;67:703–718.
 - 30 Cyrklaff M, Sanchez CP, Kilian N, Bisseye C, Simpore J, Frischknecht F, *et al.* Hemoglobins S and C interfere with actin remodeling in *Plasmodium falciparum*-infected erythrocytes. Science. 2011;334:1283–6.
 - 31 Riglar DT, Rogers KL, Hanssen E, Turnbull L, Bullen HE, Charnaud SC, *et al.* Spatial association with PTEX complexes defines regions for effector export into *Plasmodium falciparum*-infected erythrocytes. Nat Commun. 2013;4:1415.
 - 32 Matz JM, Ingmundson A, Costa Nunes J, Stenzel W, Matuschewski K, Kooij TWA. *In vivo* function of PTEX88 in malaria parasite sequestration and virulence. Eukaryot. Cell. 2015;14:528–534.
 - 33 Meibalan E, Comunale MA, Lopez AM, Bergman LW, Mehta A, Vaidya AB, *et al.* Host erythrocyte environment influences the localization of exported protein 2, an essential component of the *Plasmodium* translocon. Eukaryot. Cell. 2015;14:371–384.

- 34 Haase S, Hanssen E, Matthews K, Kalanon M, de Koning-Ward TF. The exported protein PbCP1 localises to cleft-like structures in the rodent malaria parasite *Plasmodium berghei*. PLoS ONE. 2013;8:e61482.
- 35 MacKenzie JJ, Gómez ND, Bhattacharjee S, Mann S, Haldar K. A *Plasmodium falciparum* host-targeting motif functions in export during blood stage infection of the rodent malarial parasite *Plasmodium berghei*. PLoS ONE. 2008;3:e2405.
- 36 Tarun AS, Peng X, Dumpit RF, Ogata Y, Silva-Rivera H, Camargo N, *et al.* A combined transcriptome and proteome survey of malaria parasite liver stages. Proc. Natl. Acad. Sci. U.S.A. 2008;105:305–310.
- 37 Zhou Y, Ramachandran V, Kumar KA, Westenberger S, Refour P, Zhou B, *et al.* Evidence-based annotation of the malaria parasite's genome using comparative expression profiling. PLoS ONE. 2008;3:e1570.
- 38 Mair GR, Braks JA, Garver LS, Wiegant JC, Hall N, Dirks RW, *et al.* Regulation of sexual development of *Plasmodium* by translational repression. Science. 2006;313:667–669.
- 39 Silvie O, Briquet S, Müller K, Manzoni G, Matuschewski K. Post-transcriptional silencing of *UIS4* in *Plasmodium berghei* sporozoites is important for host switch. Mol. Microbiol. 2014;91:1200–1213.
- 40 Grützke J, Rindte K, Goosmann C, Silvie O, Rauch C, Heuer D, *et al.* The spatiotemporal dynamics and membranous features of the *Plasmodium* liver stage tubovesicular network. Traffic. 2014;15:362–382.
- 41 Montagna GN, Beigier-Bompadre M, Becker M, Kroczeck RA, Kaufmann SH, Matuschewski K. Antigen export during liver infection of the malaria parasite augments protective immunity. mBio. 2014;5:e01321–14.
- 42 Janse CJ, Franke-Fayard BMD, Mair GR, Ramesar J, Thiel C, Engelmann S, *et al.* High efficiency transfection of *Plasmodium berghei* facilitates novel selection procedures. Mol Biochem Parasitol. 2006;145:60–70.
- 43 Kenthirapalan S, Waters AP, Matuschewski K, Kooij TWA. Flow cytometry-assisted rapid isolation of recombinant *Plasmodium berghei* parasites exemplified by functional analysis of aquaglyceroporin. Int. J. Parasitol. 2012;42:1185–1192.
- 44 Matz JM, Kooij TWA. Towards genome-wide experimental genetics in the *in vivo* malaria model parasite *Plasmodium berghei*. Pathog. Glob. Health. 2015;109:46–60.
- 45 Kooij TWA, Rauch MM, Matuschewski K. Expansion of experimental genetics approaches for *Plasmodium berghei* with versatile transfection vectors. Mol. Biochem. Parasitol. 2012;185:19–26.
- 46 Silvie O, Goetz K, Matuschewski K. A sporozoite asparagine-rich protein controls initiation of *Plasmodium* liver stage development. PLoS Pathog. 2008;4:e1000086.
- 47 Janse C, Waters AP. *Plasmodium berghei*: the application of cultivation and purification techniques to molecular studies of malaria parasites. Parasitol. Today. 1995;11:138–143.
- 48 Schindelin J, Arganda-Carreras I, Frise E, Kaynig V, Longair M, Pietzsch T, *et al.* Fiji: an open-source platform for biological-image analysis. Nat. Methods. 2012;9:676–682.
- 49 Kaynig V, Fischer B, Müller E, Buhmann JM. Fully automatic stitching and distortion correction of transmission electron microscope images. J. Struct. Biol. 2010;171:163–173.

- 50** Saalfeld S, Cardona A, Hartenstein V, Tomančák P. As-rigid-as-possible mosaicking and serial section registration of large ssTEM datasets. *Bioinformatics*. 2010;26:i57–63.
- 51** Cardona A, Saalfeld S, Schindelin J, Arganda-Carreras I, Preibisch S, Longair M, *et al.* TrakEM2 software for neural circuit reconstruction. *PLoS ONE*. 2012;7:e38011.

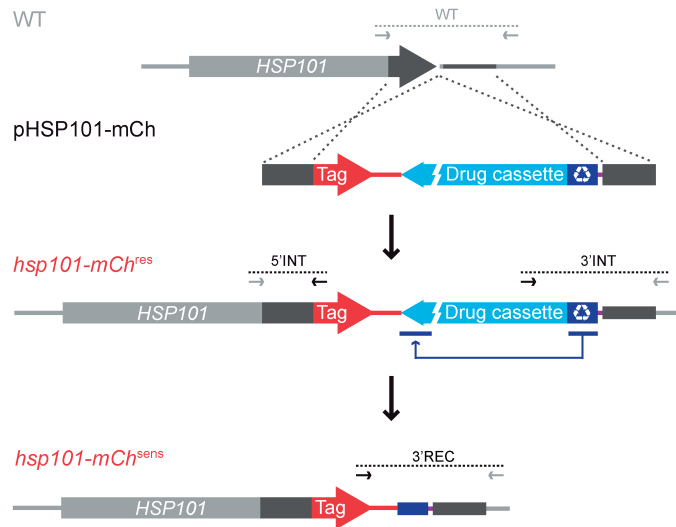
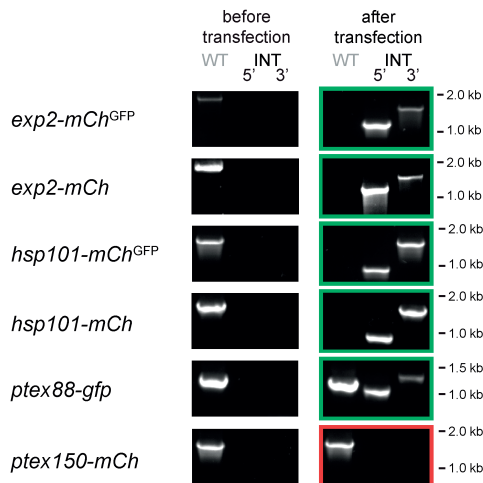
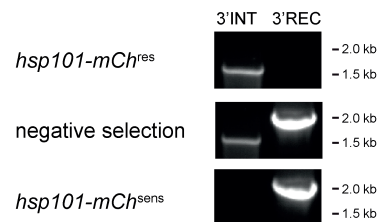
Supplementary Information for:

The *Plasmodium berghei* translocon of exported proteins reveals spatiotemporal dynamics of tubular extensions

Matz JM, Goosmann C, Brinkmann V, Grützke J, Ingmundson A, Matuschewski K, Kooij TWA. Sci. Rep. 2015; 5:12532

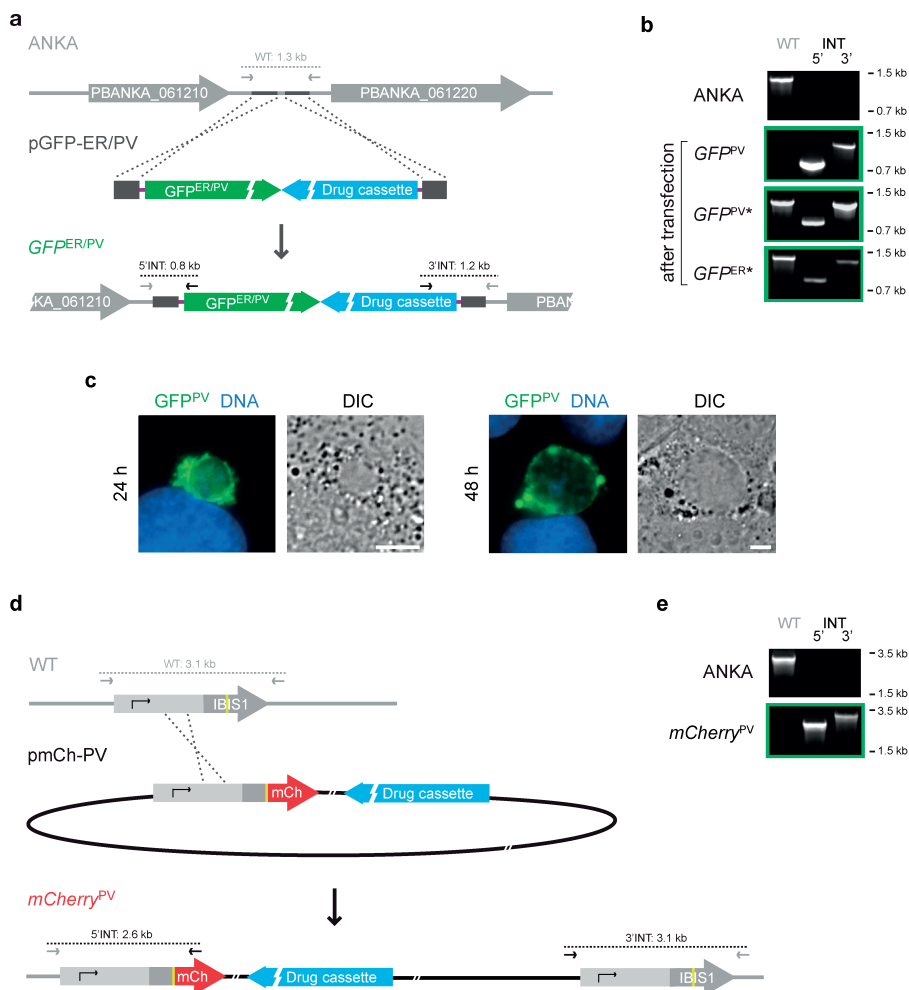
Content:

- Supplementary Figure S1** | Generation of transgenic parasite lines for protein localization
- Supplementary Figure S2** | Generation of transgenic parasite lines with fluorescent proteins in the parasitophorous vacuole and endoplasmic reticulum
- Supplementary Figure S3** | HSP101 is trafficked by the parasite's secretory pathway
- Supplementary Figure S4** | FRAP analysis reveals free diffusion from the parasitophorous vacuole to the tubular extensions
- Supplementary Figure S5** | Partial co-localization of motile tubules highlighted by GFP^{PV} and a membrane marker
- Supplementary Figure S6** | Ultrastructure of the vacuolar tubules
- Supplementary Figure S7** | EXP2 localizes to extraparasitic vesicular structures
- Supplementary Figure S8** | Live imaging of four PTEX components in merosomes
- Supplementary Table S1** | Primer sequences.
- Supplementary Table S2** | The effect of different inhibitors on HSP101-mCherry localization

a**b****c****Supplementary Figure S1 | Generation of transgenic parasite lines for protein localization.**

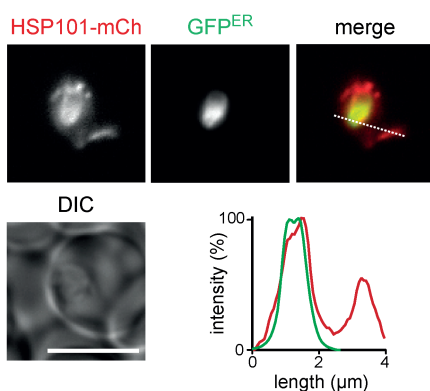
(a) Recombination strategies for endogenous tagging exemplified by the targeting of *HSP101*. Double crossover integration into the wild-type locus yields transgenic parasites with their endogenous locus tagged by mCherry-3xMyc (red). Recombinant parasites harbour the drug-selectable hDHFR-yFcu cassette (blue) and in some cases a high-expressing GFP-cassette (not shown). Subsequent

negative selection with 5-fluorocytosine removes large parts of the drug-selectable cassette. Primer combinations specific for the wild-type locus (WT), integration (5' and 3'INT), and drug cassette recombination (3'REC) are indicated. (b) Diagnostic PCR of the WT loci and integration sites before and after transfection with PTEX component targeting plasmids. Primer combinations were specific for WT, 5' and 3' integration, as indicated in (a). Green and red frames indicate successful and non-successful endogenous tagging, respectively. Note that all generated lines were isolated successfully using flow cytometry with the exception of *ptex88-gfp*, which lacks the highly expressed fluorescent cassette. (c) Genotyping of the *hsp101-mCherry* parasite line before (res, pyrimethamine-resistant) and after negative selection, and after subsequent clonal isolation (sens, pyrimethamine-sensitive). Primer combinations were specific for 3' integration and drug cassette recombination, as indicated in (a).

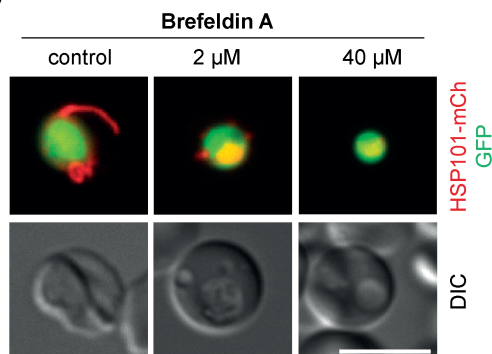


Supplementary Figure S2 | Generation of transgenic parasite lines with fluorescent proteins in the parasitophorous vacuole and endoplasmic reticulum. (a) Recombination strategy for double crossover stable integration of green fluorescent markers of the parasitophorous vacuole (GFP^{PV}; GFP fused to the BiP signal peptide) and the endoplasmic reticulum (GFP^{ER}; GFP fused to the BiP signal peptide and ER retention signal) into the silent intergenic locus on *P. berghei* chromosome 6. In addition to the high-expressing fluorescent protein cassette (green), the recombinant parasites harbour the drug-selectable hDHFR-yFcu cassette (blue). Primer combinations specific for the wild-type locus (WT) and integration (5' and 3'INT) are indicated. (b) Diagnostic PCRs of transgenic parasites. The asterisk marks transfectants for live co-localization, using pyrimethamine-sensitive *hsp101-mCherry* parasites as the recipient strain. (c) Live fluorescent imaging of the GFP^{PV} marker protein reveals a circumferential staining pattern in maturing liver stage parasites, confirming localization to the parasitophorous vacuole. Scale bars, 10 μ m. (d-e) Recombination strategy for single crossover integration of a red fluorescent marker of the parasitophorous vacuole (mCherry^{PV}) and diagnostic PCRs. Integration yields a fusion of the *IBIS1* N-terminal sequence and the fluorescent mCherry-3xMyc tag. The tag is fused directly adjacent to the PEXEL/VTS motif (yellow) without including a spacer, thereby preventing export.

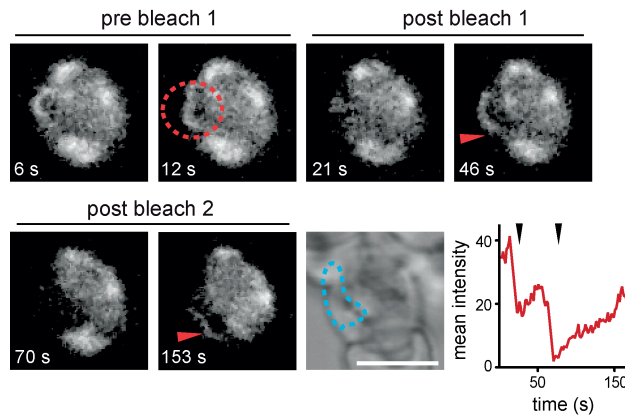
a



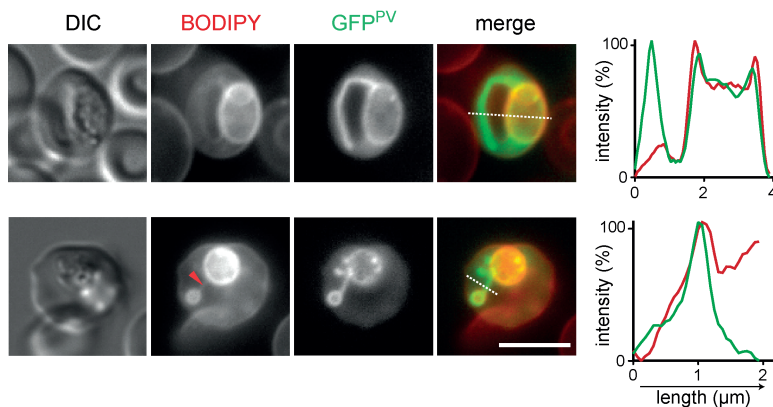
b



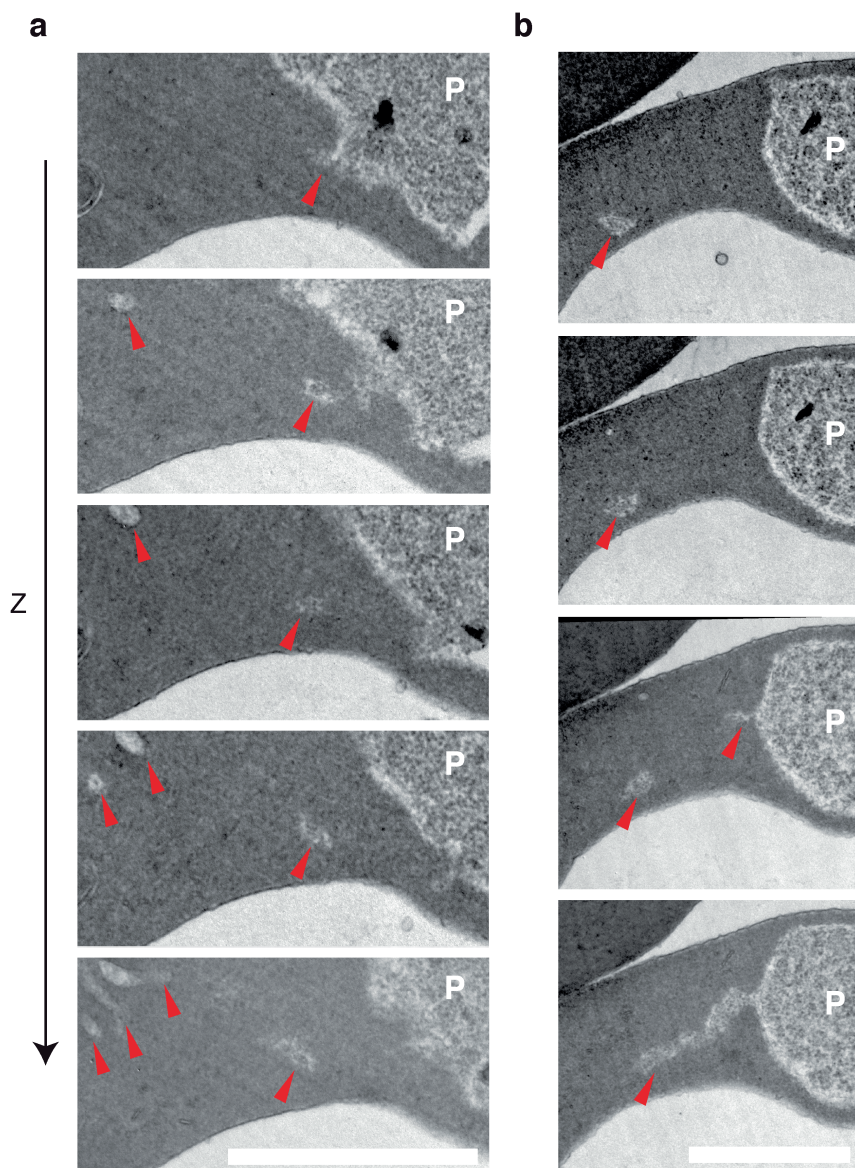
Supplementary Figure S3 | HSP101 is trafficked by the parasite's secretory pathway. (a) Live co-localization of HSP101-mCherry (left) and ER-resident GFP (GFP^{ER}, centre). The line in the merge (right) indicates profiling of the fluorescent signals (bottom left). (b) Localization of HSP101-mCherry and cytoplasmic GFP after treatment with Brefeldin A. Secretion of tagged HSP101 to the tubules is inhibited in a concentration-dependent manner. Synchronized *in vitro* cultures of the *hsp101-mCherry* line were grown in the presence of Brefeldin A and analysed 18 h later. Scale bars, 5 μ m.



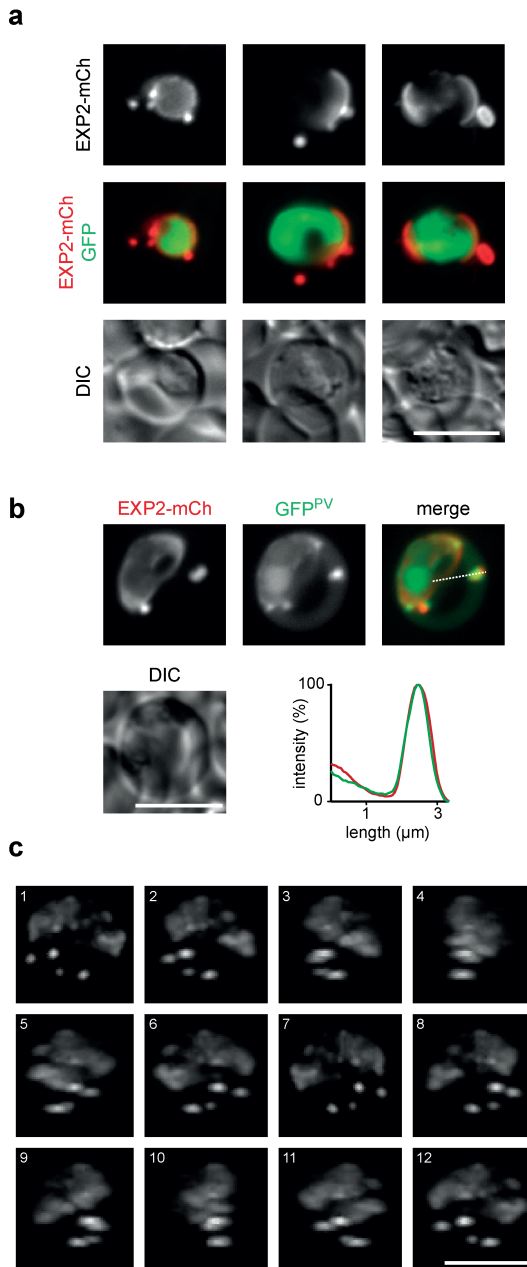
Supplementary Figure S4 | FRAP analysis reveals free diffusion from the parasitophorous vacuole to the tubular extensions. Erythrocytes infected with *mCherry^{PV}* parasites were analysed by confocal microscopy before (pre bleach) and after repeated (post bleach 1 and 2) photo bleaching (red area, bleach location). Shown is a representative trophozoite and the respective temporal fluorescence analysis in the erythrocyte cytoplasm (blue dotted line); black arrowheads indicate times of the bleaching pulses. Scale bar, 5 μm .



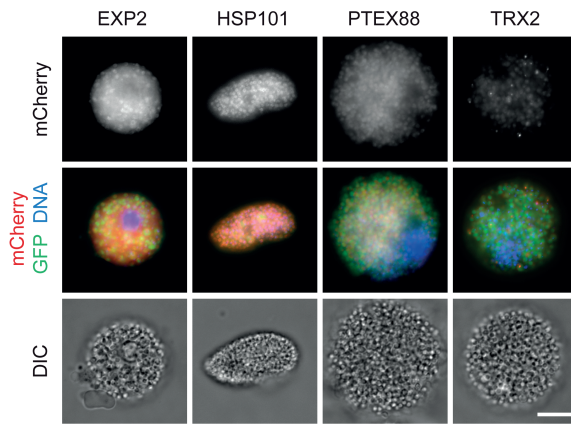
Supplementary Figure S5 | Partial co-localization of motile tubules highlighted by *GFP^{PV}* and a membrane marker. Co-localization of the lipid marker BODIPY TR ceramide (centre left) and *GFP^{PV}* (centre). The indicated lines in the merge (centre right) denote profiling of the fluorescent signals (right). Shown are two representative trophozoites. The red arrowhead denotes a vacuolar tubule stained by BODIPY TR ceramide. Scale bar 5 μm .



Supplementary Figure S6 | Ultrastructure of the vacuolar tubules. (a,b) Representative high magnification transmission electron micrographs of two WT-infected erythrocytes. The sequential sections show vacuolar tubules (red arrowheads) that emerge from the parasite (P) surface. Scale bars, 1 μm .



Supplementary Figure S7 | EXP2 localizes to extraparasitic vesicular structures. (a) Fluorescent images of EXP2-mCherry (top) and merge of EXP2-mCherry and cytoplasmic GFP (middle). Three representative trophozoites are shown. (b) Live co-localization of EXP2-mCherry (top left) with a marker protein of the parasitophorous vacuole (GFP^{PV}; top centre). The indicated line in the merge (top right) denotes profiling of the fluorescent signals (bottom right). (c) 12 frames of Supplementary Video S6 showing a 3D-reconstruction of EXP2-mCherry, obtained by optical sectioning of a fixed *exp2-mCherry* parasite-infected erythrocyte. Scale bars, 5 μm.



Supplementary Figure S8 | Live imaging of four PTEX components in merosomes. Micrographs of the merozoite containing merosomes derived from *in vitro* cultured liver stage parasites 72 h after infection. Shown are representative images including the fluorescent signal of the tagged protein (top), a merge of tagged protein, cytoplasmic GFP, and Hoechst 33342 DNA dye (middle) and differential interference contrast images (DIC, bottom). Scale bar, 10 μ m.

Supplementary Table S1 | Primer sequences.

Primer Name	Primer Sequence (restriction sites underlined)	Size WT (bp) ^a	Size INT (bp) ^b	Use ^c	Target	Reference
SIL6F	GACAGCGCATATGATGGATG	1315	847	GT	PbSIL6	(Kenthirapalan, 2012)
SIL6R	TACGAATACGCAATTTCTCAAAC		1247	GT	PbSIL6	(Kenthirapalan, 2012)
mCherryFor	CTATACCATCGTGGGAACAGTAC			GT	mCherry	
mCherryRev1	CCCTCCATGTGAACCTTGAAG			GT	mCherry	(Haussig, 2011)
mCherryRev2	GATCCTTACTTGTACAGC			GT	mCherry	
GFPv	TGTGCCCATTAACATCACCATC			GT	GFP	(Haussig, 2013)
5'HSP70rev	CAATTTGTTGATACATAAAATAGGCAG			GT	5'PbHSP70	(Kenthirapalan, 2012)
5'DHFRrev	ATGAAATACCGCTCCATTTTCC			GT	5'PbDHFR-TS	(Kenthirapalan, 2012)
BiP-SP-GFP-F-SwaI	GGGATTTAAATATGGGAAATTCAAAGGCATTGTTTGTAGTATTATTGTATCCCTGTGAAATTTATAAGCGCCGGACATATGCTGTGAGTAAAGG	830		TV	GFP	
BiP-RS-GFP-R-BamHI	ATTGGATCCTTATAATTCATCACTGGCGCCTTGTATAGTTCATC			TV	GFP	
GFP-R-BamHI-KasI	CTAGGATCCTTAGGCGCCTTTGTATAGTTCATCCATGCCATGTGTAATCCTGCTGCTG	818		TV	GFP	
CT-EXP2-F-SacII	AATAATCCGCGGTTAAGGTGGTCTCGTATGTTGGTGG	703		TV	CT-PbEXP2	
CT-EXP2-R-HpaI	AATAATGTTAACAGCCTCATTAGAATCAGTTTCTTGC			TV	CT-PbEXP2	
3'EXP2-F-XhoI	AGTCCACTCGAGCTAAATAGAGAAACAATGGTGTTTTATAAGC	606		TV	3'PbEXP2	(Matz, 2013)
3'EXP2-R-KpnI	AGGGCTGGTACCTTTATTGAAAAATGCAAAAATACGAAAAATAGC			TV	3'PbEXP2	(Matz, 2013)
CT-EXP2-F	GATTTAGCAGCAACCACTGCC	1998	1049	GT	CT-PbEXP2	
3'EXP2-R	TTGGCATGTGGCAATAAGCATAC		1475	GT	3'PbEXP2	(Matz, 2013)
CT-HSP101-F-SacII	ATTATCCGCGGGACCTCATTCTGTTGTCTATTGTATG	638		TV	CT-PbHSP101	
CT-HSP101-R-NaeI	ACACTTGCCGGCTGACAATGAAAGGTTAATAACAATGTTGTG			TV	CT-PbHSP101	
3'HSP101-F-XhoI	AGATGTCTCGAGTTAAATAAAACAACACGATATGTTGCATG	848		TV	3'PbHSP101	(Matz, 2013)
3'HSP101-R-KpnI	TTACTTGGTACCTTATTATCACACACTTTTTCATAGATATTGC			TV	3'PbHSP101	(Matz, 2013)
CT-HSP101-F	GTCAGAATTACAGAAGCACATTACG		828	GT	CT-PbHSP101	
3'HSP101-R	CGTGTGGGCATAGATCAGTGA	1674	1547 (res) 2058 (sens)	GT	3'PbHSP101	(Matz, 2013)
CT-PTEX88-F	GCTTGATGAAATATGCTATTATGATTCTC	1196	1025	GT	CT-PbPTEX88	(Matz, 2013)
3'PTEX88-R	GTGACTTGGATTACAGATTAAAAATGCA		1285	GT	3'PbPTEX88	(Matz, 2013)
CT-PTEX150-F-SacII	ACCATACCGCGGCTATTATCATCAAGCACACAGTTG	622		TV	CT-PbPTEX150	
CT-PTEX150-R-HpaI	TTATTGTTAACTTCATCTTCATCTTCATCCTCTGG			TV	CT-PbPTEX150	
3'PTEX150-F-XhoI	AACGTTTCTCGAGTAGCATAGGTGCGCGAGTC	790		TV	3'PbPTEX150	(Matz, 2013)
3'PTEX150-R-KpnI	TTAGTGGGTACCGGTAAGAACAAAGAACAAAAATGCAATTATC			TV	3'PbPTEX150	(Matz, 2013)
CT-PTEX150-F	GATGAAAACTTTACGATGCTTACAAAC	1645	770	GT	CT-PbPTEX150	
3'PTEX150-R	TGCAAGCAITGTGACCATTATAACC		1486	GT	3'PbPTEX150	(Matz, 2013)
5'IBIS1-F-SacII	GCATCCGCGCGGATTTTAAATCATACACTATACGTTTTTCC	1784		TV	5'PbIBIS1	
IBIS1-PEXEL-R-SpeI	GGACTAGTCCCACTCTGATAATATTCTGCTTTTTCC			TV	PEXEL-PbIBIS1	
5'IBIS1-F	GATCCTTACTGTTACAGC	3147	2579	GT	5'PbIBIS1	
3'IBIS1-R	TCCAACCTCTGATAATATTCTGCTTTTTCC		3086	GT	3'PbIBIS1	

^a Sizes of the PCR products of forward and reverse primers on WT gDNA. ^b Sizes of the respective integration-specific PCR products; forward 5' gene-specific primers combined with 5'HSP70rev, mCherryRev1/2, or GFPprev and reverse 3' gene-specific primers combined with 5'DHFRrev (pyrimethamine-resistant lines), mCherryFor (pyrimethamine-sensitive lines), or T7 (*mCherryPV*). ^c TV, primers used for construction of Transfection Vectors; GT, primers used for GenoTyping.

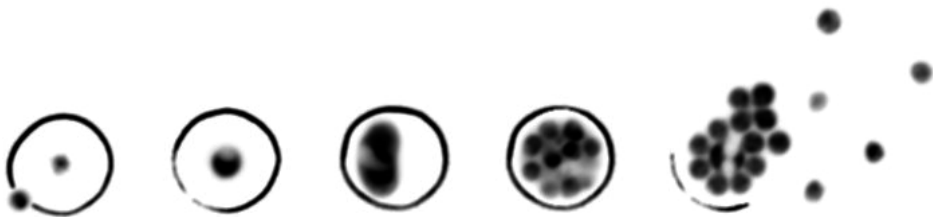
Supplementary Table S2 | The effect of different inhibitors on HSP101-mCherry localization.

Inhibitor	Target	Concentrations	HSP101-mCh in tubule	Tubular motility	Developmental delay
cytochalasin D	actin polymerization (▼)	200 nM	+	+	–
		20 µM	+	+	–
		50 µM	+	+	+/-
jasplakinolide	actin polymerization (▲)	1 nM	+	+	–
		10 nM	+	+	–
		500 nM	+	+	+/-
blebbistatin	myosin	2 nM	+	+	–
		200 nM	+	+	–
		20 µM	+	+	–
nocodazole	tubulin polymerization	300 nM	+	+	–
		30 µM	+	+	+/-
		300 µM	+	+	+
EHNA	dynein	20 nM	+	+	–
		200 nM	+	+	+/-
		2 µM	+	+	+
vanadate	ATPase domains	20 nM	+	+	+/-
		200 nM	+	+	+
		2 µM	+	+	+
PPMP	sphingomyelin synthase	500 nM	+	+	+/-
		5 µM	+	+	+
		50 µM	+	+	+

EHNA, erythro-9-(2-hydroxy-3-nonyl)adenine; PPMP, DL-threo-1-Phenyl-2-palmitoylamino-3-morpholino-1-propanol. Experiments have been performed with synchronized and unsynchronized *in vitro* cultures of the *hsp101-mCherry* parasite line.

Chapter 6

General discussion



LIVING IN A VACUOLE – AN EVOLUTIONARY PERSPECTIVE

The intravacuolar niche

It is worthwhile to consider the adaptations of other intracellular pathogens, in order to better understand the challenges of living inside a vacuole. While host cell physiology differs considerably between *Plasmodium* and other pathogens, universal features of the intravacuolar niche might provide some insights into the function of the plasmodial PV.

There are two fundamental life styles during host cell infection: (1) residing in the cytoplasm and (2) thriving inside of a vacuolar compartment. Both locations hold several threats to the survival of the intruder: in the cytoplasm, endogenous pattern recognition receptors are able to start a signalling cascade that can directly or indirectly lead to the elimination of the pathogen, either by inducing host cell apoptosis or by immune-mediated clearance.¹⁻⁴ Furthermore, cytosolic proteases may adversely affect the development of the pathogen and direct ubiquitination of its surface can lead to the induction of autophagy.^{5,6} Intuitively, hiding inside a membrane-bound compartment appears to be the favorable option. However, there are many disadvantages to the intravacuolar niche. As protective as an enveloping membrane might seem, the dangers of degradation and recognition remain significant. Most pathogen-containing vacuoles are formed during endocytic uptake. Therefore, these compartments are tightly interlinked with the host endosomal pathway and are in constant danger of lysosomal fusion and subsequent pathogen lysis.⁷ Additionally, several pattern recognition receptors localize to the membranes of the host vesicular pathway and can mount efficient immune responses if fusion is not inhibited.⁸

Therefore, the intracellular pathogen can either exit from its vacuole and face different adversities in the cytoplasm,^{9,10} or adapt to the dangers it holds. Indeed, the apicomplexan parasite *Toxoplasma gondii* exhibits the latter strategy by manipulating its PV so that it does not fuse with the lysosomes of the host cell.^{11,12} Similarly, many bacteria are able to secrete effectors which interfere with phagosome maturation.¹³⁻¹⁶ In marked contrast, *Leishmania* amastigotes reside in a phagosome-derived compartment which readily fuses with host cell lysosomes. Consequently, its lumen is highly acidic and displays elevated hydrolase activity.¹⁷ It is believed that the parasite's robustness towards these stresses correlates with

the presence of a dense glycocalyx on the plasma membrane, demonstrating a strategy that is characterized by an active coping mechanism rather than avoidance.¹⁸⁻²⁰

Hiding inside an isolated membranous compartment may help to evade host cell defenses. Yet, this life style has major nutritional consequences. While cytoplasmic pathogens are conveniently immersed in the nutrient-rich cytosol, vacuolar pathogens need to arrange for special uptake mechanisms. *T. gondii* has been shown to sequester host cell lysosomes as a means of nutrient acquisition.²¹ Additionally, an intimate contact of the PV with host mitochondria and ER is indicative of nutrient transfer processes at this highly specialized host-pathogen interface.²² The sexually transmitted bacterium *Chlamydia trachomatis* has also been shown to exploit host cell organelles, by actively importing lipid droplets into the lumen of its vacuole.²³ Additionally, nutrients may be acquired by fusion of the pathogen-containing vacuole with host cell vesicles. For instance, *Chlamydia* reroutes Golgi-derived vesicles destined to the plasma membrane in order to scavenge host-synthesized sphingomyelin.²⁴

While the recruitment of host cell organelles and vesicles may account for a substantial degree of nutrient delivery, it is imperative, that the pathogen-containing vacuole remains permeable to ions and organic low molecular weight compounds. This is achieved by the activity of membrane-resident channels and transporters. While apicomplexan parasites have been shown to insert their own proteinaceous pores,^{25,26} the general view on bacterial solute permeation favors the involvement of host-derived transporters in the vacuolar membrane.²⁷⁻²⁹

The adaptations of all these phylogenetically diverse organisms clearly demonstrate the constant trade-off between stealth and host cell access, underlining the ambivalent functions of a pathogen-induced compartment that is both protective and restrictive.

Cytoskeletal interactions of vacuolar processes

A recurring phenomenon of intravacuolar pathogens is the radiation of membrane extensions into the host cell cytoplasm, and experimental evidence suggests that these membranous processes are often sites of cytoskeletal interactions. *T. gondii* induces membrane protuberances on its PV, which can reach far into the cytoplasm and are mostly oriented towards the host cell nucleus.³⁰⁻³⁵ Interestingly,

these extensions are dependent on the microtubular network of the host, since nocodazole treatment leads to aberrations in their length and morphology (Isabelle Coppens, personal communication). Indeed, it is known that *T. gondii* efficiently recruits microtubule organizing centers (MTOCs) upon infection, thereby tightly tethering its PVM to the cytoskeleton of the host cell.²¹ It is possible, that the extensions of the *T. gondii* PVM are merely a byproduct of this close association. Within 30 minutes after invasion the vacuole is transported to the perinuclear region in a microtubule-dependent manner.³⁶ The transport of the PV towards the MTOCs might generate a pulling-force along the microtubules, by which the PV becomes passively deformed, leading to the formation of long PVM strands. Conversely, the extensions might actively move along the filaments in order to recruit the MTOCs. Evidently, interactions of the PVM with the host cytoskeleton are of high importance for *T. gondii*. Not only the microtubules, but also the vimentin network of the host is recruited to the PVM.³⁷ Furthermore, the aforementioned apposition of host mitochondria and the salvaging of lysosomes were demonstrated to depend on microtubule-mediated transport mechanisms.^{21,38} If the vacuolar extensions are actually involved in the cytoskeletal recruitment to the PVM or if they are a consequence thereof, remains a matter of speculation.

It is believed, that many pathogen-containing vacuoles depend on cytoskeletal stabilization.^{38,40} The inclusion bodies containing *C. trachomatis* bacteria are stabilized by actin and intermediate filaments, and inhibition of filamentous actin formation results in leakage of the vacuolar contents into the host cell cytoplasm.⁴¹ Furthermore, the secreted chlamydial protease-like activity factor (CPAF) is able to process the intermediate filament network in order to support the expansion of the *Chlamydia*-containing vacuole during intracellular replication.⁴² Similar observations have been made for *Salmonella enterica*.⁴³ In a manner analogous to *T. gondii*, the *Salmonella*-containing vacuole associates with host microtubules and is transported to a juxtanuclear, Golgi-associated region.^{44,45} Shortly after the initial uptake, thin membrane strands emerge from the surface of the vacuole. Several of these protrusions display distinct protein compositions and they have been categorized by the localization of different host and pathogen markers.⁴⁶

Most of our knowledge about bacterial vacuole tubulation stems from the well-characterized *Salmonella*-induced filaments (SIFs). Their biogenesis is dependent on the microtubular cytoskeleton of the host, which serves as a scaffold for their emergence.^{47,48} Interestingly, SIF formation is abolished in the absence of the

secreted *Salmonella* virulence factor SifA, and this loss of tubulation correlates with a reduced vacuolar stability. Consequently, the vacuole disintegrates and the bacteria spill into the cytoplasm.⁴⁹ Though it is tempting to suggest a direct causal link between membrane tubulation and vacuolar stability, it is more likely that it is the intimate contact of the membrane and its protrusions with the microtubular network that promotes the integrity of the vacuole. Indeed, SifA has been shown to interact with the SifA and kinesin-interacting protein (SKIP), an adapter that tightly associates with kinesin and thereby with the microtubules. Consequently, loss of SifA is likely to lead to an impaired cytoskeletal attachment and simultaneously to the loss of SIF formation and vacuolar integrity.⁵⁰⁻⁵²

Due to the overwhelming differences in host cell physiology, it is rather unlikely that the tubulation of the plasmodial PVM is linked to the maintenance of vacuolar integrity in a manner similar to *Salmonella*, *Chlamydia* and *Toxoplasma*. Though the host cytoskeleton is extensively manipulated during invasion,⁵³ and even more so during intraerythrocytic development,⁵⁴ there are no indications, that the PV of *Plasmodium* is stabilized by host-derived filaments. The detailed CLEM analysis shown in the previous chapter did not reveal the presence of filamentous structures in or around the tubular compartment. Furthermore, I could demonstrate, that cytoskeletal inhibitors did not significantly affect the morphology of the PV. Due to their inability to synthesize *de novo* proteins, erythrocytes have a static pool of cytoskeletal filaments, which cannot be renewed. Therefore, recruitment of the subpellicular cytoskeleton would very likely impair RBC integrity and result in the lysis of the host cell. Any potential PV-stabilizing mechanism must therefore be restricted to the PVM itself.

Protein and lipid-mediated membrane tubulation

Since tubulation of the plasmodial vacuole is independent of cytoskeletal interactions, membrane morphogenesis is likely to be regulated by lipid and protein determinants of the PVM. In *Salmonella*, the secreted virulence factor SseJ is able to esterify cholesterol and thereby change the lipid contents of the pathogen-containing vacuole,⁵⁵⁻⁵⁷ and it has been suggested, that the SseJ-mediated regulation of membrane fluidity might contribute to the tubulation process.⁵⁵ It is possible, that the malaria parasite also actively influences the fluidity and tubulation capacity of its vacuole by regulating the composition of the PVM. Unfortunately, not

much is known about the exact lipid determinants of the plasmodial PVM. It is a well-accepted fact, that the parasite-containing vacuole is first formed from an invagination of the RBC membrane and that most of its lipid content is derived from the erythrocytic surface.⁵⁸ However, during asexual parasite development the PV grows in both volume and morphological complexity, suggesting the incorporation of newly synthesized or scavenged lipids. Indeed, upon erythrocyte infection, the lipid contents and composition of the infected RBC change dramatically.^{59,60} While the machinery for *de novo* fatty acid synthesis has been identified in *Plasmodium*, the enzymes of this pathway were shown to be dispensable for asexual blood stage propagation *in vivo*.⁶¹ Conversely, *Plasmodium* efficiently salvages free fatty acids and lipids derived from lipoproteins.^{62,63} In the parasite, imported fatty acids are readily desaturated, elongated and incorporated into phospholipids, which can be interconverted by the parasite.^{64,65} *Plasmodium* seems to have retained a certain degree of metabolic plasticity, since a combination of palmitic acid, stearic acid and oleic acid can fully replace the serum supplementation in *P. falciparum* cultures.^{65,66}

Evidently, the *Plasmodium* parasite has the capacity for extensive membrane biogenesis and remodeling, which may influence membrane fluidity and support the tubulation of the PVM. It is indeed known, that the malaria parasite accumulates large quantities of sphingolipids in the membranes of the TVN.⁶⁷ Inhibition of the parasite's sensitive sphingomyelin synthase by PPMP treatment resulted in an aberrant morphology of the *P. falciparum* TVN, suggesting an important function of lipid trafficking in the regulation of vacuolar ultrastructure.⁶⁸ However, there remains doubt about the specificity of PPMP. Addition of the inhibitor significantly impairs the development of the parasite (as was also shown in the previous chapter), allowing the possibility, that the structural changes in TVN morphology are indeed a secondary effect.

While lipids define membrane morphology on a nanoscopic level,⁶⁹ curvature of larger membrane areas is usually promoted by protein factors.⁷⁰ Indeed, a vast multitude of proteins has been shown to influence membrane curvature, tubulation and budding by several different mechanisms.⁷¹ A very striking example can be observed in the closely related coccidian *T. gondii*. The parasite generates an extensive network of highly convoluted membrane tubules inside its spacious vacuole.⁷² It has been suggested, that this network might facilitate nutrient uptake by enhancing the effective exchange area between host and parasite.⁷³ Interestingly, *T. gondii* secretes several proteins from its dense granules, that are

essential for the formation of this nanotubular network.^{72,73} Genetic ablation of the dense granule proteins GRA2 and GRA6 leads to an accumulation of membrane lamellae at the posterior end of the parasite and to the absence of tubular structures in the PV.⁷³ This phenotype coincides with a reduced virulence *in vivo*.⁷⁴ Reintroduction of the respective GRA protein-encoding genes reverted the membrane morphology to its natural tubular state.⁷³ Notably, several GRA protein homologues have been identified amongst intravacuolar apicomplexans, suggesting specific functions inside this compartment.⁷⁵ *Plasmodium* parasites harbor a GRA17-like protein that is believed to be related to *T. gondii* GRA17 and GRA23. Most strikingly, this homologue is the PTEX component EXP2. Both EXP2 in *Plasmodium* and the GRA17-like proteins in *T. gondii* have been implied in permeation across the PV.⁷⁵ While these proteins are likely uninvolved in membrane curvature, this observation opens the possibility, that other membrane-shaping GRA homologues are yet to be discovered in the plasmodial genome.

PLASMODIUM-INDUCED TUBULES AND THEIR POTENTIAL FUNCTIONS

A P. berghei TVN involved in nutrient uptake?

In the previous chapter, I used a combination of advanced *P. berghei* experimental genetics and an array of microscopic techniques to identify and characterize a tubular subcompartment of the PV. It is evident, that parallels to other intravacuolar pathogens must be drawn with caution, due to the overwhelming differences in host cell physiology. Especially the lack of cytoskeletal recruitment by the malaria parasite renders it difficult to assess the potential origin and function of the tubules.⁷⁶ Even the comparison between different *Plasmodium* species does not offer major functional insights, since it remains unclear, if the PVM protrusions in *P. berghei*-infected RBCs are indeed homologous to the TVN of *P. falciparum*.

In a preliminary experiment, I transfected *in vitro* cultured *P. falciparum* strain 3D7 parasites with a plasmid containing a GFP^{PV} construct, similar to the one used for *P. berghei*. Intriguingly, tubules of vivid motility were observed after transfection, albeit at rare occasions (Figure 1). The extremely low frequency of these tubules in 3D7 parasites can possibly be attributed to suboptimal culturing conditions. It has been shown, that *P. falciparum* displays alterations in protein export and host cell remodeling during cultivation with serum supplements.⁷⁸ Indeed, prolonged *in vitro*

cultivation of the human malaria parasite often leads to the loss of entire chromosomal regions and in consequence to the abolishment of *PfEMP1* display and cytoadhesion.^{79,80} These observations call into question, if the unphysiological conditions of *ex vivo* *P. falciparum* cultivation are sufficient to support correct membrane morphogenesis. Furthermore, they underline the importance of suitable *in vivo* model systems to evaluate specific aspects of erythrocyte remodeling.

Though I detected motile protrusions in the transfected 3D7 parasites, these observations are not sufficient to determine, if the tubular PV extensions of *P. berghei* are indeed the equivalent of the *P. falciparum* TVN. While the presence of *Plasmodium*-induced membrane structures has been recognized already decades ago,⁸¹⁻⁸³ our knowledge of the TVN is almost entirely derived from a handful of studies, using fluorescent lipid probes and electron microscopy.^{67,68,84} The significance of these efforts notwithstanding, the identification of specific protein markers of the TVN is a prerequisite for understanding the evolutionary conservation or divergence in PVM morphology. Future work on protein distribution and subcompartmentalization in the PV will aid in this mission. So far, only the TVN-junctional protein 1 (TVN-JP1) has been localized to the TVN of *P. falciparum*, where it specifically accumulates at junctional sites between different vesicular regions.⁸⁵ Intriguingly, an orthologue of TVN-JP1 is present in *P. berghei*, and it would be highly interesting to assess its localization relative to the HSP101-positive tubules and their derived vesicular compartments.

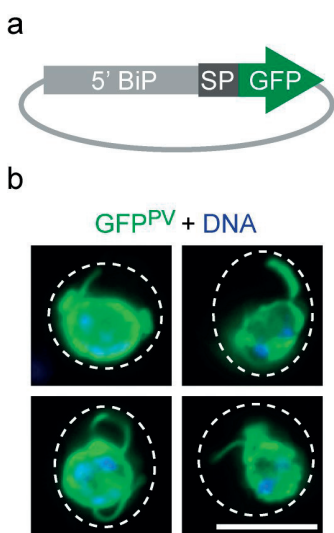


Figure 1 | The parasitophorous vacuole of *Plasmodium falciparum* displays tubular features. (a) Schematic representation of the plasmid used for transfection of *P. falciparum* 3D7 parasites. The GFP^{PV} construct is a fusion of the *PfBiP* promoter (5' BiP), the sequence of the *PfBiP* signal peptide (SP), and GFP. The plasmid is derived from the pARL2-GFP vector⁷⁷ and was maintained episomally. (b) Live fluorescence micrographs of four early *P. falciparum* schizonts transfected with the GFP^{PV} construct, showing tubular extensions of the parasitophorous vacuole. Note, that these features were only observed occasionally. The images are a merge of the GFP^{PV} signal and the nuclear dye Hoechst 33342. White outlines, erythrocyte. Bar, 5 μ m.

It was suggested that the TVN of *P. falciparum* serves as a site of nutrient uptake, since inhibition with PPMP blocked both the TVN assembly and import of several nutrients and fluorescent reporters.⁶⁸ A function in the uptake of nutrients appears plausible due to the surface-enhancing properties of the tubules and the TVN, respectively. While it was argued that the TVN might temporarily contact the RBC periphery to enhance permeability,⁶⁸ it is not clear, why it would retain such a highly structured morphology for this purpose. Instead, the complex shape of the TVN suggests a function in surface enlargement and permeation inside the RBC. It is possible, that nutrients imported by the activity of exported transporters^{86,87} are taken up from the RBC cytosol across the entire TVN membrane. The highly complex nature of the TVN would increase the exchange area and enhance the flux of nutrients to the parasite. This scenario bears some resemblance to the nanotubular network inside the *T. gondii*-containing vacuole.⁷³

The tubular nature of the protrusions observed in *P. berghei* implies the possibility of bridging the PV with another otherwise isolated compartment. One could therefore argue, that the tubular extensions might function as the ominous parasitophorous duct by connecting the PV lumen with the extracellular milieu and facilitating the access to nutrients from the serum.⁸⁸ However, I could never detect a permanent or transient association of the tubular compartments with the RBC membrane. While speculations about nutrient import are justified, the data presented in this thesis do neither support nor discard the possibility that the tubules may enhance nutrient permeation. It is however noteworthy, that the EXP2 orthologues, GRA17 and GRA23 mediate the movement of small molecules across the PVM of *T. gondii*, and defects in the respective *T. gondii* loss of function mutants could be completely restored by expression of the plasmodial EXP2.⁷⁵ It is therefore possible that EXP2, apart from acting as the pore-forming translocation channel, might independently facilitate nutrient import. However, the uniform distribution of EXP2 in the PVM would suggest, that import does not preferentially occur at the site of the tubules.

Membrane fusion and fission

While the tubular extensions were never observed to connect with the erythrocyte surface, it remains possible that they display an inherent capacity of fusion with other parasite-derived membrane structures. In *Salmonella*, the SIFs of the

pathogen-containing vacuole have been shown to fuse with vesicles of the host endosomal pathway, thereby acquiring nutrients and gaining membrane material for their expansion.^{89,90} While residual organelle remnants of the erythrocyte could theoretically merge with the *Plasmodium*-induced tubules, the vast majority of vesicular membrane bodies in the infected RBC are derived from the parasite. Indeed, Ingmundson and colleagues (2012) identified punctate vesicles in *P. berghei*-infected RBCs, called intra-erythrocytic *P. berghei*-induced structures (IBIS).⁹¹ Specific IBIS targeting of the two PEXEL-containing transmembrane proteins IBIS1 and *P. berghei* cleft-like protein 1 (*PbCP1*) has been demonstrated by fluorescence microscopy.^{91,92} Though fusion of IBIS vesicles with the tubules is conceivable, the signature protein IBIS1 is absent from the parasite periphery and neither IBIS1 nor *PbCP1* have been detected in any tubular structures.^{91,92}

While experimental support for a function in membrane fusion is currently lacking, I could demonstrate that the tubules can serve as a budding site, delivering detached membrane bodies into the RBC cytoplasm. Interestingly, colocalization of the GFP^{PV} marker with HSP101-mCherry revealed an incomplete overlap of the signals in many cases, especially during the budding of PV-derived lumina. In several instances, forming vesicular compartments were positive for the vacuole marker, but negative for HSP101, suggesting that compartments of distinct protein composition can be formed at these tubular sites. Interestingly, the formation of lariat structures appears to be common and while prolonged live imaging would be necessary to provide definitive proof, the current data suggest the formation of loops at the PV and their subsequent detachment (Figure 2a). The distinct distributions of the GFP^{PV} marker and HSP101-mCherry in detaching loops imply the involvement of multiple membranes during this process. Indeed, similar observations have been made for TVN-derived vesicles of *P. falciparum*.⁹³

The function of these PVM fission events remains elusive. Though frequently observed, the limited number of such compartments in the infected erythrocyte might imply minor functions in host cell remodeling. A recent report demonstrated the presence of EXP2 positive vesicles in *P. yoelii* and *P. berghei*-infected RBCs,⁹⁴ for which I obtained independent experimental support. Surprisingly, the frequency of such vesicles was shown to depend on the maturity of the infected RBCs. Due to the presence of residual host cell trafficking components, it was suggested that reticulocytic SNARE (soluble N-ethylmaleimide-sensitive-factor attachment receptor), Rab (Ras-related in brain) and VAMP (vesicle associated membrane

proteins) proteins might be involved in the enhanced vesiculation activity.⁹⁴ It remains a matter of speculation, if the observed loop formation and detachment are restricted to *P. berghei*-infected reticulocytes. It is however possible that such membrane fission events represent specific adaptations towards the developmental status of the host cell.

Recent insights into vesicle-mediated inter-parasite communication might further imply the tubular PV extensions in the delivery of messenger particles. Two complementing reports claim that *Plasmodium* parasites induce the production and release of microvesicles from the infected erythrocyte.^{95,96} These microvesicles are thought to mediate inter-parasite communication in a process analogous to the well-characterized quorum sensing of bacteria and other single cell eukaryotes, thereby promoting gametocytogenesis. To that end, microvesicles are released by an unknown mechanism and then internalized into the recipient infected RBC, ultimately ending up inside a compartment in the parasite's perinuclear region.⁹⁵ The authors have demonstrated that only a subpopulation of infected RBCs is receptive for this uptake process, even at unphysiologically high concentrations of purified microvesicles. After uptake into the RBC cytoplasm, labeled microvesicles were still detectable as distinct punctate foci, suggesting that they are internalized in their original conformation.⁹⁵ Intuitively, this would suggest an endocytosis-like uptake mechanism at the RBC membrane. Indeed, infected erythrocytes have been shown to display coated pits on their surface, which might promote an endocytosis-related process.⁹⁷⁻¹⁰⁰ Fusion of the hypothetical RBC-derived uptake compartment with the PVM would result in the release of the microvesicles into the PV lumen, from where they can be internalized even further. In the light of these observations, it is possible that the vividly moving PVM tubules act as an uptake organelle for parasite-induced microvesicles. Since the import of the putative messenger particles into the RBC was shown to be rather inefficient,⁹⁵ the parasite might compensate by reaching far out into the cytoplasm, essentially 'fishing' for the few internalized microvesicles. The vivid motility of the tubules could aid in the establishment of initial binding prior to membrane fusion.

The concept of microvesicle-mediated communication between *Plasmodium*-infected RBCs is relatively new and its biological relevance remains to be determined. Proteomic data suggest, that the microvesicles harbor abundant cytoplasmic and cytoskeletal proteins of both parasite and the host cell, as well as components of the parasite-induced protein export pathway.⁹⁵ Indeed, the pattern

of identified proteins is more or less suggestive of an infected RBC lysate rather than a specific subcompartment, raising the question, if this protein composition is indeed of physiological nature or influenced by sample impurities. *In vitro* cultivation of *P. falciparum* parasites is often accompanied by spontaneous parasite mortality,^{101,102} and membrane blebbing during parasite disintegration might have contributed to the outcome of the proteomic measurements. In any case, it is noteworthy that the two tubule-resident proteins EXP2 and HSP101 were amongst the putative microvesicle constituents.⁹⁵

The observation of endocytosis-like microvesicle uptake has far-reaching implications for multiple aspects of parasite biology and host cell remodeling. On the one hand, it provides another potential mechanism of nutrient acquisition by means of erythrocytic endocytosis and vesicular trafficking. On the other hand, it implies the presence of a novel parasite-derived compartment in the infected RBC and potential interactions with other induced membrane lumina, including the vacuolar tubules. However, more research is warranted to determine if the process of microvesicle-mediated communication is indeed occurring during infection. The relatively low efficiency of microvesicle uptake by the RBC raises doubts about the biological relevance of this process *in vivo*.⁹⁵

Implications for protein export

I was able to show that the tubular evaginations of the PV are home to at least three components of the plasmodial protein export machinery. More importantly, HSP101 and PTEX88 specifically localize to the tubular extensions and are almost absent from the remainder of the PV. It can therefore be concluded that the PV tubules are specialized subcompartments with a distinct protein composition. Furthermore, the specific residence of two PTEX components implies the tubules in the process of protein translocation (Figure 2a and b). I initially hypothesized that the tubules might act as motile syringe-like translocators which directly insert transmembrane cargo proteins into the RBC membrane *in situ*. This scenario appeared highly attractive for several reasons: (1) the tubules could serve as a lipid pool, in which transmembrane cargo proteins remain properly folded prior to translocation. (2) Transmembrane proteins could easily be trafficked across the host cell without the need of additional solubilization factors like chaperones and heat shock proteins, by physically bridging the RBC cytoplasm. (3) Since the

tubules are home to the PTEX translocon, the transmembrane cargo proteins could actively be translocated at specific membrane contact zones, while soluble proteins are translocated at the remaining tubular surface. (4) Ablation of the signature tubule protein PTEX88 significantly impaired the parasite's ability to sequester to peripheral tissues, suggestive of an altered surface proteome of the infected RBC.

However attractive the hypothesis may be, several lines of evidence argue against this scenario. Even though the phenotype of the PTEX88 gene deletion mutant suggests a defect in protein export, I could not detect any impairment in the trafficking of surface antigens. More importantly, the tubules appear to undergo a developmental process, during which they grow in length and complexity. However, transmembrane proteins need to be inserted from very early on, almost immediately after invasion,¹⁰³ and at that point the tubules have yet to emerge from the PV. Furthermore, the vacuolar extensions were never observed to make intimate contact with the surface of the infected RBC. Instead, they rather passively follow the shape of the erythrocyte and appeared disconnected from the RBC membrane in all cases.

The spatiotemporal analysis of the PTEX translocon presented in this thesis reveals novel insights into the morphogenesis, behavior, protein composition, and ultrastructure of the tubular PVM processes. Unfortunately, I was not able to specifically inhibit the genesis or morphology of these tubules. Previous studies demonstrated that the compound PPMP specifically interferes with the formation of the TVN in *P. falciparum*.^{68,104} However, during my experiments, treatment with PPMP and other inhibitors did neither affect the presence nor the morphology of the tubular extensions, hampering the functional examination of the vacuolar protrusions in *P. berghei*-infected cells. Consequently, a direct causal link between the tubules and protein export remains to be demonstrated.

REFINING THE PTEX PARADIGM

Protein translocation across pathogen-containing vacuoles is by no means an exclusive feature of *Plasmodium* parasites. Indeed, several intravacuolar pathogens have been shown to manipulate their environment by transporting virulence factors to distinct locations in the host cell cytoplasm. For that purpose, many bacteria use highly complex secretion systems, which often take the form of

a 'molecular needle'.^{105,106} For example, most subspecies of *Salmonella enterica* express a type III secretion system in response to the acidic and nutrient-poor conditions in the pathogen-containing vacuole.^{107,108} In contrast to the PTEX translocon, this complex directly bridges the cytoplasm of the pathogen and the host cell by making contact with the vacuolar membrane. Through this molecular channel, *Salmonella* transports multiple effectors into the host cell, in order to modulate its intracellular environment.^{109,110} Bacterial secretion systems have long been the focus of extensive research and their protein composition and organization proved to be highly complex.¹¹¹ In contrast, the current model of the PTEX translocon appears rather simplistic. It remains questionable if such a humble complex could accommodate for the enormous array of effector proteins, that *Plasmodium* parasites do so desperately depend upon, and future research will likely reveal, that the protein export machinery is more complicated than previously anticipated.

The PTEX translocon has first been identified by combining biochemical approaches with the application of five specific criteria:¹¹² (1) It was argued, that a putative PEXEL protein translocating machinery must be restricted to the genus of *Plasmodium*, since other organisms do not display this protein export motif.^{113,114} (2) The translocon requires the incorporation of an energy source, which couples an exergonic reaction to the unfolding and translocation of the cargo.¹¹⁵ (3) The components of the translocon should display an apical localization in merozoites and a PVM localization during the ring stage and should also be expressed during the liver stage of infection. (4) The components should be essential during asexual blood merogony and (5) should specifically bind to exported cargo proteins.

Interestingly, only one of these five criteria has actually been employed to identify a candidate component of the protein export translocon. Analysis of the detergent-resistant membrane proteome of *Plasmodium* ring stage parasites revealed a putative power source for the complex, the AAA+ ATPase containing chaperone HSP101. Identification of PTEX150 was based on a similar transcription profile and the presence of both HSP101 and PTEX150 in the same distinct high molecular weight bands during proteomic analysis.^{112,116} Subsequent pull-downs using HA-tagged HSP101 and PTEX150 as a bait, led to the identification of the remaining three PTEX components.¹¹² A thorough biochemical analysis established that the PTEX translocon exists as a complex of approximately 1,230 kDa. Furthermore, it provided evidence for the sequential organization of the three core components,

with PTEX150 bridging the membrane-associated EXP2 and the more distal HSP101.¹¹⁷ In addition, recent biochemical evidence suggests the association of three previously unreported proteins with the PTEX translocon.¹¹⁸ However, further experimental evidence is needed to unravel the nature of their association and their involvement in protein export.

Recent reports progressively refute the premises of the employed criteria. Indeed, not all PTEX components appear to be restricted to *Plasmodium*, since EXP2 was shown to be a homologue of the GRA17-like proteins of *T. gondii*.⁷⁵ Furthermore, the presence of PEXEL-related export motives is not restricted to *Plasmodium*. Indeed, a PEXEL-like motif (termed TEXEL) and a corresponding processing peptidase have recently been identified in *T. gondii*.¹¹⁹⁻¹²¹ The results presented in this thesis also disprove many of the initially proposed features of the PTEX components with regards to their localization, liver stage expression and essentiality, questioning the robustness of the employed identification criteria.

Heat shock protein 101 and PTEX150

Two recent reports provide strong support for a function of the two initially identified PTEX components HSP101 and PTEX150 in the translocation of exported proteins.^{122,123} Elsworth and colleagues (2015) showed, that inducible knockdown of HSP101 in *P. berghei* and PTEX150 in *P. falciparum* greatly affect the export of PEXEL positive and negative cargo proteins, causing them to colocalize with EXP2 in the periphery of the parasite. In consequence, the mutants displayed an arrested maturation, underlining the essentiality of these two PTEX core components.¹²² Unfortunately, the exact function of PTEX150 remains unknown. Blue native electrophoresis and immuno-precipitation experiments suggest that this protein serves as a bridging component between HSP101 and EXP2, and that it possibly displays a similar stoichiometry as HSP101, which is predicted to form a hexameric ring.¹¹⁷ Truncation of the carboxy-terminus of PTEX150 was shown to cause a reduced association with the remaining PTEX components, however without measurably affecting parasite viability or protein export.¹¹⁸ These data suggest a function of the PTEX150 carboxy-terminus in supporting translocon stability. Yet, the unimpaired blood stage development of the respective mutant suggests this function to be of secondary importance.

Beck and colleagues (2015) employed a different strategy to unravel the role of

HSP101 in *P. falciparum*.¹²³ They fused the endogenous HSP101 to a DHFR destabilization domain, that disrupts any protein interactions of HSP101 in the absence of trimethoprim. Indeed, upon withdrawal of the compound, HSP101 was demonstrated to display decreased interactions with EXP2 and PTEX150, while interactions of EXP2 with PTEX150 remained undisturbed. In consequence, many cargo proteins became trapped in the PV, suggesting that the association of HSP101 with the remaining PTEX components is pivotal for efficient protein export. Indeed, during HSP101 dissociation from the complex, binding to the cargo protein ring-infected erythrocyte surface antigen (RESA) was significantly enhanced, supporting the idea of HSP101-mediated cargo unfolding.¹²³ As of yet, it remains unknown, how HSP101 recognizes the secreted proteins, but multiple different scenarios have been proposed.¹²⁴

Interestingly, the authors also employed an osmolytic lysis assay to demonstrate a reduction in NPP activity, convincingly showing for the first time a direct functional link between PTEX function and enhanced erythrocytic nutrient permeation. It is however noteworthy, that the only exported protein known to date to enhance RBC permeability, the cytoadherence-linked asexual protein 3 (CLAG3),¹²⁵ was still efficiently exported to the red blood cell surface when HSP101 was dissociated from the translocon. The authors conclude that CLAG3 might traffic by an HSP101-independent pathway or is merely deposited into the RBC membrane during the invasion process, similar to other rhoptry-resident proteins.¹²³ However, the loss of NPP activity and the unaltered presence of CLAG3 upon HSP101 dissociation, suggest multiple exported proteins in the establishment of the NPP.

While the involvement of HSP101 in protein translocation is evident, its catalytical properties as a chaperone and unfoldase have not been demonstrated yet. A recent review points out the unorthodox role of HSP101 in the translocation process.¹²⁶ The AAA+ ATPases that drive translocation in other systems are usually localized at the *trans* site of the membrane, where they exert a pulling force across the translocation channel.^{127,128} However, HSP101 is localized at the *cis* site. The authors suggest, that HSP101 might be involved in the pulling of transmembrane cargo proteins from the parasite plasma membrane into the translocation channel, since HSP101 would localize at their *trans* site.¹²⁶ While there is no evidence for this scenario, it also does not provide a satisfying explanation for the translocation of soluble proteins. So far, the source of the threading force has only been hypothesized to be HSP101,¹¹² and it remains possible, that a yet unidentified

protein fulfills this function, probably localizing to the surface of the PVM.

Indeed, PTEX pull-downs revealed a marked enrichment in human HSP70, suggesting that host-derived ATPases might be involved in pulling the cargo proteins across the PVM and catalyze their refolding.¹¹² It should also be noted, that *P. falciparum* has been shown to export an HSP70/HSP40 chaperone complex, which localizes to dynamic punctate structures known as J-dots.^{129,130} J-dots have been implied in protein trafficking across the RBC cytosol¹³⁰ and might transiently contact the PV in order to pick up cargo proteins. It is conceivable that during such a transient contact, protein translocation is powered by the HSP70/HSP40 chaperone complex in *cis*. Consequently, HSP101 might just be involved in the unfolding and recruitment to the translocation site.

Until now, it remains a matter of speculation, by which mechanism cargo protein translocation is energized. HSP101 has been hypothesized to deliver the necessary energy for this process due to the presence of its AAA+ ATPase domains. However, a detailed biochemical characterization of HSP101 will be necessary to obtain prove for this rather premature assumption.

Exported protein 2

The evidence for EXP2 serving as the pore-forming component was initially based on two observations: (1) EXP2 has been demonstrated to be associated with the PVM and displays a high resistance towards carbonate extraction, and (2) it is predicted to fold in a similar manner as the pore-forming toxin hemolysin E from *Escherichia coli*.¹¹² While initial studies merely suggested a membrane association *via* an amino-terminal amphipathic helix,^{131,132} recent evidence from cross-species complementation experiments provides additional support for EXP2 as a pore-forming protein. As discussed above, expression of *P. falciparum* EXP2 in *T. gondii* rescued the defects caused by deletion of GRA17, a protein that has convincingly been shown to enable the permeation of small fluorophores across the PVM and to enhance the membrane conductivity in *Xenopus* oocytes.⁷⁵

Pull-down analysis using transgenic *P. falciparum* parasites suggest that HA-tagged PTEX150 and HSP101 maintain a close association with EXP2, and initial immunofluorescence analysis demonstrated substantial overlap of the PTEX150 signal with EXP2.¹¹² PTEX150 proved to be inaccessible for carboxy-terminal

tagging with mCherry-3xMyc during my experiments, and consequently no colocalization experiments with EXP2 could be performed. However, life cell imaging revealed a uniform distribution of EXP2 across the entire PVM, in stark contrast to other PTEX components that only localized to the tubular extensions. If the PTEX translocon does indeed comprise EXP2, HSP101, and PTEX88, then (1) EXP2 is either not functional in the non-tubular fraction of the PVM, or (2) it may translocate cargo independent of HSP101 and PTEX88, or (3) it fulfills additional functions independent of protein translocation. Indeed, the localization pattern of EXP2 and the potential implication of this protein in solute transport might suggest channeling functions, which strictly depend on its localization and protein interaction partners. In such a scenario, the PV tubules could serve as sites of protein translocation, due to the specific targeting of the other translocon components and their interactions with EXP2. In the remainder of the PV, different interaction partners or the absence thereof might facilitate solute uptake or other permeation-related functions (Figure 2c).⁷⁵

Thioredoxin 2

The biochemical characterization of the PTEX core components EXP2, PTEX150 and HSP101 by Bullen and colleagues (2012) established PTEX as a *bona fide* complex and provided the first insights into the stoichiometry and arrangement of the translocon.¹¹⁷ However, due to the lack of specific antibodies, knowledge about PTEX88 and TRX2 was scarce. The two putative regulators have initially been identified by pull down analysis¹¹² and these results have been confirmed repeatedly.^{117,133} It was however clear from the beginning that PTEX88 and TRX2 are significantly less abundant at the complex or that their association is less stable.¹¹² As discussed in chapter 3, the localization of TRX2 has been a matter of controversy, since a multitude of studies, including my own, have ascribed the protein to intraparasitic structures.^{134,135} Experimental evidence suggesting a peripheral localization reminiscent of the PV(M), has been obtained by ectopic expression of a TRX2-GFP fusion protein under the control of an unphysiological promoter or by immunofluorescence analysis with antibodies of unspecified reactivity.^{135,136} Previous attempts to reconcile these contradictory results by claiming a dual localization to the cytoplasm and the periphery of the parasite remain unconvincing.¹³³

The data presented in this thesis show, that TRX2 localizes to intraparasitic structures and not to the periphery of blood stage parasites. This localization analysis is based on live microscopy of the genome-encoded TRX2 protein fused to an mCherry-3xMyc tag. Consequently, the fluorescent signal reflects the natural expression of the protein. Western blot analysis and intravital competition assay ruled out the possibility of incorrect processing or dysfunctionality of the fusion protein, confirming that the obtained localization pattern is indeed physiological.

The nature of the intraparasitic structures is unknown. A combination of differential solubilization and thermolysin digestion supports the idea, that TRX2 localizes to a membrane-bound parasite organelle.¹³⁵ However, the varying number of TRX2-positive foci already early during development and the absence of a branching morphology suggest that these organelles are neither the mitochondrion nor the apicoplast. Correlative light and electron microscopy as performed in the previous chapter may facilitate the identification and morphological analysis of the TRX2-positive organelles.

Given the nature of TRX2 localization, it remains unclear, what role, if any, this protein and its home compartment play in protein export. Irregardless of the localization issue, it has been argued that TRX2 might be involved in the hydrolysis of disulphide bonds during translocation or could be involved in some sort of translocon redox-regulation.^{124,137} However, experimental evidence for such a scenario is currently lacking. Interestingly, it has been shown that *P. berghei* TRX2 knockout parasites display a reduced amount of parasite antigens at the RBC surface, suggestive of a function in protein export.¹²² Indeed, I could demonstrate that the loss of TRX2 correlates with a slightly reduced sequestration efficiency and with delayed parasite maturation *in vivo* and *in vitro*. These results strengthen the notion of TRX2 involvement in the export of virulence factors. However, I attempted to reproduce the findings of Elsworth and colleagues (2015)¹²² by staining TRX2-deficient parasites with the semi-immune serum that was used to assess the protein export capacity of PTEX88 knockout parasites. Strikingly, no quantitative difference was observed in the surface staining of wildtype and *trx2*-infected RBCs (data not shown). Due to the elusive specificity of the semi-immune sera, quantitative microscopy of individual cargo proteins, as performed for the PTEX88 knockout parasites, is imperative in order to assess the importance of TRX2 for the export of virulence factors.

The last word about the involvement of TRX2 in the PTEX translocon has not yet

been spoken. However contradictory the molecular data might be, the phenotype of the gene deletion mutant suggests some function in protein export. It is conceivable that the TRX2-positive compartments could be transient stations for cargo proteins *en route* to the PVM during the secretion process, where they might be folded, processed, or made translocation-competent by any other means. Quite possibly, prolonged interactions with the cargo proteins during secretion may be the cause for the repeated detection of TRX2 during immuno-precipitation experiments (Figure 2a and d).^{112,117,133}

It is a well-established fact, that cargo proteins are primed for export already inside the parasite. The ER-resident protease Plasmepsin V has been shown to recognize and cleave the PEXEL motif, which is essential for the export of these proteins.¹³⁸⁻¹⁴⁰ Further processing might very well occur in more downstream locations of the parasite's secretory pathway. The distribution of the TRX2-positive compartments is reminiscent of the Golgi apparatus, which has previously been characterized in *P. falciparum*. Transgenic parasites expressing the Golgi re-assembly stacking protein (GRASP) fused to GFP displayed a punctate pattern in the parasite cytoplasm similar to that of TRX2.¹⁴¹ Indeed, exported proteins are believed to traffic *via* the Golgi apparatus.¹⁴² Co-localization with markers of the *cis* and *trans* Golgi network will help to elucidate the identity of the TRX2-positive compartments and might uncover yet another checkpoint in the export of parasite virulence factors.

PTEX88

It is remarkable that depletions of both TRX2 and PTEX88 lead to similar phenotypes during *in vivo* infection, despite their distinct localization patterns. The sequestration defect in PTEX88 knockout parasites is very pronounced and has major consequences for parasite virulence and infection outcome. The TRX2-deficient mutant replicates this phenotype, though to a lesser degree. These observations might suggest, that both PTEX88 and TRX2 act in the same pathway, which may include different compartments, such as the ER, Golgi apparatus, PV, and several locations in the RBC.

Remarkably, the *in vivo* consequences of ablating PTEX88 did not correlate with a general protein export deficiency, as revealed by immunofluorescent surface

staining and live cell imaging of cargo proteins. Nonetheless, it remains possible that PTEX88 is essential for the export of a limited subset of proteins. Alternatively, one might speculate that PTEX88 somehow functionalizes cargo proteins during the translocation process. Both scenarios would explain the comparable exposure of *P. berghei*-derived virulence factors in wildtype and PTEX88-deficient parasites. The methods I employed do not allow for a comprehensive overview of the exportome, and detailed biochemical analysis is warranted to assess the potential roles of PTEX88 in protein export. However, the data suggest more specialized contributions during this process.

While the molecular functions of PTEX88 are yet to be uncovered, the *in vivo* analysis of the corresponding gene deletion mutant offers important new insights into several features of malaria parasite pathogenesis. In particular, the functional implications and consequences of parasite sequestration appear more complex than previously anticipated. Although the gene deletion mutant fails to sequester to the peripheral tissues, viable parasites are not removed by means of splenic clearance, irregardless of the pronounced splenomegaly. This observation raises some important questions about the significance of the spleen in the clearance of malaria parasites and simultaneously demands an alternative explanation for why *Plasmodium* parasites sequester in the first place. Interestingly, the reduced sequestration capacity of the PTEX88-deficient parasites was linked to a defect during the transition from schizont to ring stage. Purified merozoites lacking PTEX88 were less invasive than WT merozoites in an *in vivo* setting. It remains unclear, if and how the two specific deficiencies in sequestration and RBC reinvasion correlate.

A recent study provides additional evidence for the importance of PTEX88 during *in vivo* growth, sequestration and virulence, using a conditional knockdown system in both *P. berghei* and *P. falciparum*.¹⁴³ Interestingly, our finding of overall protein export competence was corroborated by immunofluorescence analysis in PTEX88-deficient *P. berghei* and *P. falciparum* parasites. However, the authors misinterpret some of their results, seemingly contradicting my previously published findings. They demonstrate normal blood stage development of PTEX88 knockdown *P. berghei* and *P. falciparum* parasites *in vitro*, and show that the conversion from schizont to ring stage was not impaired during inducible knockdown of PTEX88 in *P. falciparum*. However, they fail to convincingly reconcile these observation with the marked growth defect observed during *in vivo* infection. The authors claim, that

the non-sequestering parasites are cleared by the spleen, since they measured an elevated splenic parasite burden by qPCR. However, these measurements might be caused by the filtration of non-viable parasites,¹⁴⁴ e.g. merozoites, which we already suggested as a potential reason for the observed splenomegaly. My results obtained from the infection of splenectomized animals clearly show that splenic clearance is not the mediator of the delayed growth during infection and point towards a parasite defect during schizont-to-ring stage transition *in vivo*. The observation that *P. falciparum* can efficiently enter fresh erythrocytes during inducible knockdown of PTEX88 is highly interesting, since it demonstrates that this protein is not directly involved in the invasion process under *in vitro* conditions.

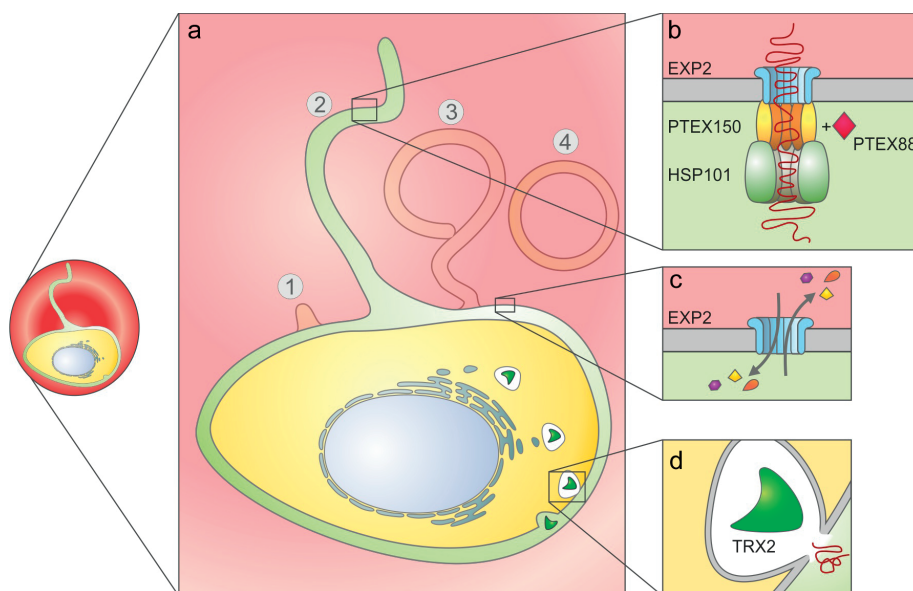


Figure 2 | Revised model of the PTEX translocon and its spatio-temporal organization. (a) During asexual growth, the *Plasmodium* parasite induces extensive tubulation of the parasitophorous vacuole (PV, green). During maturation, the tubules start to bud from the PV (1) and grow in size (2). In several cases, the PV extensions form lariat structures (3), which often detach from the parasite surface (4). (b) The tubules are home to the protein export translocon, consisting of the pore-forming exported protein 2 (EXP2), the central adapter PTEX150, the AAA+ ATPase heat shock protein 101 (HSP101), and the regulator PTEX88, which promote the transposition of cargo proteins (red thread) across the PV membrane (gray) into the host cell. (c) EXP2 is also abundant in the remainder of the PV, where it might enhance solute permeation. (d) Thioredoxin 2 (TRX2) is found in organelles of unknown identity, which might represent a central hub during cargo protein secretion (a).

However, the marked differences between the observations *in vivo* and *in vitro* point towards host factors affecting efficient reinvasion, and perhaps PTEX88-dependent functions can be bypassed in a cultivation setting.

DIFFERENT STAGES – DIFFERENT FUNCTIONS

PTEX during mosquito stages

Cumulating evidence suggests that the protein export machinery is a highly specialized adaptation towards the desolate host cell environment during blood stage propagation.¹²⁴ Consequently, the PTEX translocon is expected to be absent during other life cycle stages of the malaria parasite. A previous study has shown that EXP2, HSP101 and PTEX150 are internalized into the parasite cytoplasm during gametocytogenesis, suggesting the disassembly and degradation of a complex that is dispensable for mosquito infection.¹³³ Indeed, I observed an association of tagged EXP2, HSP101, and PTEX88 with the granular contents of *in vitro* cultivated ookinetes during preliminary experiments (Figure 3). It appears that the protein export translocon is degraded upon mosquito infection, underlining its specific functions during blood stage development.

Surprisingly, I found distinct expression and localization patterns of the PTEX components during oocyst development and sporogony. Both HSP101 and TRX2 were efficiently expressed in the oocyst stage, whereas EXP2 and PTEX88 protein levels were negligible. Particularly interesting is the apical localization of HSP101 in sporozoites, suggestive of a storage in the rhoptries or micronemes.¹⁴⁵ During

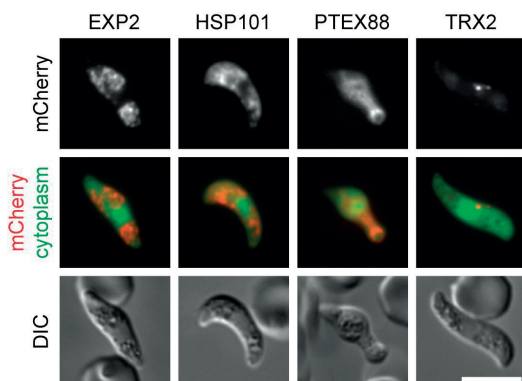


Figure 3 | Live localization of four PTEX components in *Plasmodium berghei* ookinetes. Parasites expressing endogenous PTEX components fused to a carboxy-terminal mCherry-3xMyc tag were imaged during ookinete development *in vitro*. Shown are the mCherry signal (top), a merge of cytoplasmic GFP and mCherry (middle) and differential interference contrast images (DIC, bottom). Bar, 5µm.

blood stage development, EXP2 and PTEX150 were shown to localize to the apical end of purified *P. falciparum* merozoites¹¹⁷ and it is believed, that the translocon is instantly inserted into the PVM by means of dense granule secretion. Consequently, EXP2 and HSP101 were found in the parasite periphery only moments after RBC invasion.¹⁴⁶ Detailed microscopic analysis will help uncover, if such an organelle discharge scenario also applies during liver cell invasion. Perhaps, HSP101 is secreted from the apical organelles of the sporozoite and is directly inserted into the early liver stage PVM. However, the function of HSP101 would then be restricted to the very early stage of liver cell infection, since the protein is not expressed 24 hours post invasion and remains absent from the PV throughout the rest of liver stage development.

The distinct distribution and expression levels of the individual components suggest, that PTEX does not function as a composite protein translocon during mosquito and liver stage infection. However, some of the PTEX components might fulfill translocon-independent functions during these life cycle stages.

Protein export during liver stage development

Initially, it was claimed that all PTEX components should also be expressed during liver stage development.¹¹² Semi-quantitative RT-PCR analysis suggested efficient expression of all five PTEX components, at least during the later phase of intrahepatic growth.¹³³ I was able to show protein localization of *P. berghei* EXP2 and PTEX88 to the periphery of the developing liver stage parasite and a previous report using liver-chimeric mice reported a similar protein distribution for *P. falciparum* EXP2 and PTEX150.¹⁴⁷ Interestingly, I could also detect TRX2 in the parasite periphery, convincingly showing for the first time, that endogenous TRX2 can efficiently be secreted across the parasite plasma membrane. Additionally, intraparasitic TRX2-positive foci were abundant in the parasite cytoplasm, as was the case during all other investigated life cycle stages. The presence of these four PTEX components in the periphery of the parasite has been interpreted as an indication that the protein export translocon might also be active during intrahepatic growth.¹³³ However, the absence of HSP101 protein at the parasite-hepatocyte interface, as demonstrated in this thesis, suggests otherwise.

Indeed the evidence for *bona fide* protein export during liver stage development is highly controversial. The first reports of parasite antigens in the hepatocyte

cytoplasm stem from early immunofluorescence studies using antibodies directed against sporozoites.¹⁴⁸ And since circumsporozoite protein (CSP) is the most abundant and immunodominant antigen of the sporozoite, its localization has been extensively investigated. In most studies, the majority of CSP was detected on the surface of the developing parasite. However, a fraction of the protein localizes to distinct foci in the host cell cytoplasm during the early phase of liver infection.¹⁴⁹⁻¹⁵² Interestingly, the amino-terminus of CSP entails two putative PEXEL motives. Singh and colleagues (2007) found that the transport of CSP into the hepatocyte cytoplasm is dependent on these PEXEL motives.¹⁵³ However, in a later study, Cockburn and colleagues (2011) could not reproduce this finding.¹⁵² Indeed, the presence of CSP in the hepatocyte cytoplasm is not necessarily due to protein translocation, but might be a byproduct of sporozoite surface shedding. Analysis of the membranous features of the liver stage TVN clearly demonstrated vesiculation of the vacuolar membrane,¹⁵⁴ suggesting another mode by which CSP might enter the host cell cytoplasm.

More relevant insights stem from a protein that has actually been shown to be exported during blood stage development. IBIS1 is a PEXEL-positive trans-membrane protein, which localizes to distinct structures in the RBC cytoplasm, which are believed to be the *P. berghei* equivalent of the MCs.^{91,155} The protein is also expressed during liver stage development, thereby offering a physiologically relevant comparison between protein export during the two intracellular stages of the plasmodial life cycle. Strikingly, IBIS1 was retained in the PV during liver stage development and localized to different dynamic features of the PVM.^{91,154} Additionally, the protein was detected in detached vesicles.¹⁵⁴

It is highly problematic to assess the liver stage parasite's capacity for protein export by localizing membrane-associated cargo, like CSP and IBIS1, since localization to membranous features does not easily allow for a discrimination between host or parasite contributions. Indeed, the presence of a vesicular trafficking pathway in the hepatocyte renders these distinctions very problematic. Therefore, meaningful data can only be obtained through the observation of soluble protein cargo. The liver specific protein 2 (LISP2) is a soluble protein expressed exclusively during intrahepatic growth. Immunofluorescence and western blot analysis suggest that one part of the protein is exported into the cytoplasm and nucleus of the hepatocyte after cleavage by an unknown enzyme, while the other part is retained in the PV.¹⁵⁶ Indeed, *P. berghei* LISP2 contains an atypically placed

PEXEL motif, however this sequence is not conserved in *P. falciparum*. While this report is the first to convincingly demonstrate the export of a soluble parasite-derived protein into the hepatocyte, it does not answer the question, if protein export mechanisms are similar in blood and liver stages of infection. A recent report has finally provided some desperately needed insights into this issue. Kalanon and colleagues (2015) used a fusion of the *P. falciparum* KAHRP PEXEL motif and GFP to demonstrate efficient export during *P. berghei* blood stage development.¹⁵⁷ Upon hepatocyte infection, the protein accumulated in large membrane bulges of the PV and was not detected in the host cell cytoplasm. This reporter retention clearly demonstrates two distinct modes of protein translocation during blood and liver stage development.

Indeed, the absence of HSP101 in the periphery of the liver stage parasite provides a potential explanation for why PEXEL proteins accumulate inside the PV. However, this hypothesis remains to be tested by ectopic expression of HSP101 during liver stage development in combination with protein localization of PEXEL-containing reporters.

ULTIMATE FUNCTIONS OF THE PARASITOPHOUS VACUOLE

Vacuolar compartments can be of great benefit for intracellular pathogens, since they provide a protective hiding spot for the intruder, yet allow for interactions with the host cell.¹⁵⁸ However, *Plasmodium* parasites have no obvious reason for hiding inside a vacuole. They are replicating in a terminally differentiated cell, that is almost entirely filled with hemoglobin and which is devoid of any organelles, pathogen recognition pathways or defense mechanisms. With these observations in mind, it seems puzzling, why the malaria parasite even remains inside the PV during red blood cell infection. While one might appreciate the intricate formation of membranous features and the establishment of a protein export machinery, these aspects of parasite biology seem overly complicated when compared to a intracytosolic life style. Most functions attributed to the PV and its proteins, like nutrient acquisition, protein translocation and merozoite egress, are simply complex mechanisms of coping with the existence of such a restrictive compartment. The formation of the PV could be regarded as a mere byproduct of the merozoite invasion process.¹⁵⁹ However, staying inside the PV is not

imperative, since other closely related pathogens are known to leave their vacuolar compartment after initial uptake. Indeed, the piroplasmid parasites *Babesia* and *Theileria* are known to initially form a PV. However, upon invasion of the host cell, both parasites degrade their temporal envelop and thrive in the RBC cytoplasm.^{76,160,161} A recent time-lapse imaging study has revealed, that the breakdown of the *Babesia*-containing vacuole occurs already ten minutes after RBC invasion.¹⁶² It would be an easy alternative for the malaria parasite to simply disrupt the vacuolar envelope and reside in the RBC cytosol, which neither possesses the capacity to recognize nor to lyse the parasite. In such a scenario, default protein secretion by the parasite could deliver virulence factors directly into the host cell cytoplasm for further trafficking, as was shown for *Babesia*.¹⁶³ One is therefore left to wonder, what the actual benefit of the plasmodial PV might be.

It is conceivable that the PV serves as an essential membrane pool, which is needed for the genesis of other budding compartments like the MCs. Indeed, a central trafficking hub like the MCs could be a prerequisite for correct protein sorting and export, and budding from the PV might be the only means of generating enough membrane material for this purpose. However, MCs are already established very early during intraerythrocytic development, which would still allow for parasite egress from the PV.^{103,164} Furthermore, alterations of MC organization do not substantially impair the viability of *in vitro* cultured *P. falciparum* parasites.^{165,166}

In theory, membranous features could also be generated by parasite secretion, as was shown for the closely related coccidian *T. gondii*, which is known to secrete membrane material from its apical organelles during host cell invasion.³¹ Also, many other *Plasmodium* parasites do not develop MC-like structures, suggesting that the genesis of vacuole-derived membrane lumina is not the ultimate reason for *Plasmodium* to reside inside the PV. Furthermore, *Babesia* parasites have been shown to replicate many aspects of *Plasmodium*-induced host cell remodeling despite the lack of a PV or MCs, including the specific trafficking of virulence factors, rigidification of the RBC, induction of knob-like protrusions called 'ridges' and even cytoadhesion and sequestration.¹⁶⁷

As discussed previously, the membrane processes of the PVM might fulfill a very important function in nutrient acquisition by connecting the parasite to the extracellular milieu. Indeed, this was suggested to be the function of the TVN and the 'parasitophorous duct', and in extension one might speculate that this is the

ultimate function of the entire PV.^{68,88} A constant or temporary connection with the host serum might represent a direct and highly efficient way of nutrient transfer, much more so than the activity of exported transporters in the RBC membrane. But as already stated, evidence for such a continuity is far from conclusive.

The PV of the malaria parasite might also fulfill a protective function. Due to its role in oxygen transport, erythrocytes are continuously exposed to endogenous and exogenous sources of reactive oxygen species.¹⁶⁸ While the RBC exhibits a complex network of enzymatic and non-enzymatic redox-regulators,¹⁶⁹ one might speculate that a growing and fast replicating organism like *Plasmodium* requires a more fundamental protection from the harsh conditions in the host cell cytosol. The PV and its contained proteins might provide an effective shielding mechanism against redox-stress and potential toxicity of the RBC cytosol. As is obvious from the permeability limit of ~1.4 kDa, reactive oxygen species can easily diffuse across the PVM.²⁶ It is however possible that a very strict redox-buffering system in the PV provides sufficient protection for the parasite. Indeed, the highly abundant and PVM-resident exported protein 1 (EXP1) was shown to act as a glutathion transferase, providing support for a potential function of the PV in redox-protection.¹⁷⁰ However, *Babesia* and *Theileria* are able to withstand the adverse conditions in the RBC cytosol without any additional redox-buffer, suggesting potential coping mechanisms. As of yet, the ultimate function of the plasmodial PV remains elusive.

THE VACUOLAR PROTEOME

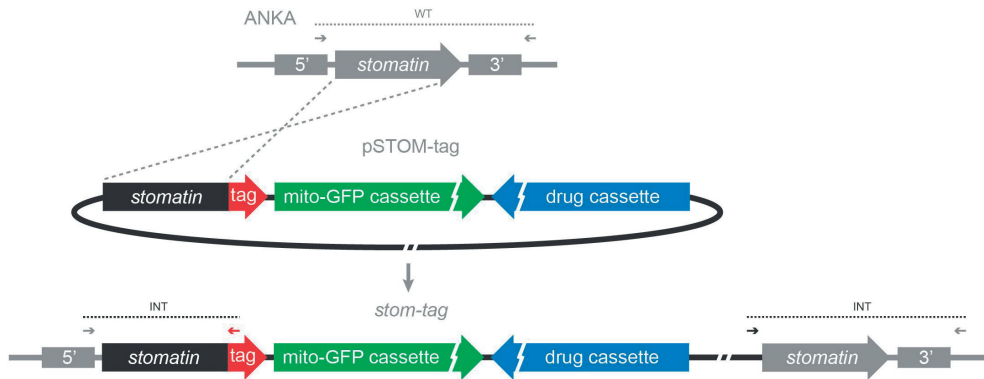
We are left to speculate what the ultimate function of the PV is, other than compensating for the inconvenience of its own existence. Though many different scenarios are imaginable, there is no way of understanding the functional and evolutionary relevance of the plasmodial PV without detailed knowledge of its proteome. Nyalwidhe & Lingelbach (2006) attempted to identify soluble proteins of the PV by labeling streptolysin-O-treated infected RBCs with a biotin derivative.¹⁷¹ This compound is thought to traverse the lysed RBC membrane and the PVM but not the parasite plasma membrane, thereby only labeling the contents of the PV.¹⁷² However, the presented evidence suggests otherwise: even though several known PV proteins were identified, protein labeling also implied the presence of multiple

cytoplasmic and ER-resident parasite proteins in the PV lumen, including heat shock proteins, enzymes of central carbon metabolism and components of the parasite cytoskeleton, despite the lack of any recognizable targeting information. The authors argue that the biotinylation must have been restricted to the PV, since labeling of other equally abundant cytoplasmic parasite proteins was not detected. This argumentation is solely based on negative data and disregards the possibility that parasite proteins might display different susceptibilities for labeling with this biotin derivative. Furthermore, several highly expressed PV proteins were not identified with this approach, including the components of the PTEX translocon. In the absence of appropriate controls, the presented proteomic data remain inconclusive. Apart from this ambitious yet unconvincing attempt, no systematic effort of characterizing the proteome of the plasmodial PV has been undertaken, and knowledge on PV resident proteins is exemplary and incomplete.

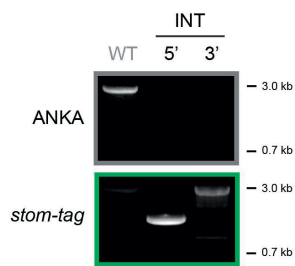
Interestingly, many proteins of the merozoite rhoptries can be detected in the early ring stage PV,^{173,174} but the functional relevance of this localization remains questionable, since these proteins might just passively diffuse into the PV(M) during the invasion process. For instance, a stomatin orthologue was shown to localize to the rhoptries of *P. falciparum* merozoites, where it resides in detergent-resistant membranes and from which it is released into the nascent PVM.¹⁷⁵ Surprisingly, our own preliminary data suggest that the *Plasmodium* stomatin resides in the membranes of the parasite's mitochondrion, contradicting the immunofluorescence data from Hiller and colleagues (2003).¹⁷⁵ We successfully generated transgenic *P. berghei* parasites expressing the endogenous stomatin fused to a carboxy-terminal mCherry-3xMyc tag (Figure 4a and b). Co-localization with an additional marker consisting of the promoter and amino-terminus of the mitochondrial heat shock protein 70-3 fused to GFP, convincingly revealed the mitochondrial localization of the *P. berghei* stomatin (Figure 4c). Repeated attempts to delete the stomatin-encoding gene were unsuccessful, suggesting essential functions during asexual development and corroborating the physiological nature of its mitochondrial localization (Figure 4d and e).

Most identified proteins of the *Plasmodium*-containing vacuole are membrane-associated. Apart from the aforementioned EXP1, members of the early transcribed membrane proteins (ETRAMPs) are highly abundant in the PVM and are transcribed at high levels during different stages of intraerythrocytic growth.¹⁷⁶

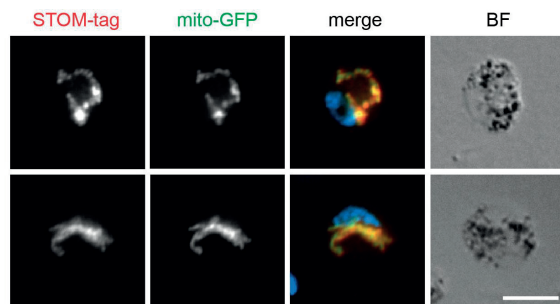
a



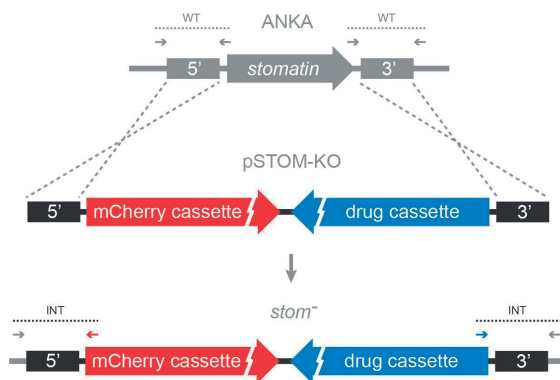
b



c



d



e

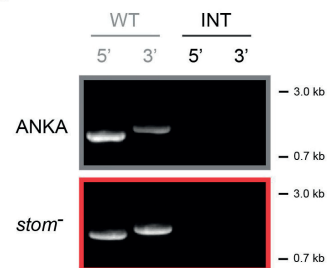


Figure 4 | Stomatin localizes to the mitochondrion of *P. berghei* and is essential during blood stage development. (a) Recombination strategy for the endogenous tagging of stomatin. Single crossover integration into the wild-type locus yields recombinant parasites with their endogenous locus tagged by mCherry-3xMyc (red). The plasmid contains a drug-selectable cassette (blue) and a mitochondrial marker cassette consisting of the promoter and amino-terminus of the mitochondrial HSP70-3 fused to GFP (green). Primer combinations specific for integration (INT) and wildtype (WT) as well as the expected fragments are indicated. (b) Diagnostic PCRs of *P. berghei* parasites before and after transfection with the pSTOM-tag vector. Primer combinations were used as indicated in (a). (c) Immunofluorescence analysis using anti-mCherry and anti-GFP antibodies reveal substantial co-localization of stomatin (STOM-tag) and the mitochondrial marker (mito-GFP). Depicted are two representative gametocytes. BF, brightfield. Bar, 5µm. (d) Replacement strategy to delete the *P. berghei* stomatin gene. The respective locus was targeted with a replacement plasmid containing the 5' and 3' region flanking the stomatin open reading frame, a high-expressing mCherry cassette (red), and the drug-selectable cassette (blue). Primer combinations specific for integration (INT) and wildtype (WT) as well as the expected fragments are indicated. (e) Diagnostic PCRs of *P. berghei* parasites before and after transfection with the pSTOM-KO vector. Primer combinations were used as indicated in (d).

ETRAMPs form homo-oligomers and their highly variable carboxy-termini are exposed to the host cell cytosol.¹⁷⁷ It was suggested that ETRAMPs might be involved in the formation of specific PVM microdomains that are involved in protein export. However, this assumption lacks any experimental support.¹⁷⁸ Less is known about the soluble proteins of the plasmodial PV, though some factors like the serine repeat antigens have been implicated in host cell egress during blood stage development.¹⁷⁹ While some other soluble factors have been localized to the PV, their functional role remains unknown, as is the case for the highly abundant parasitophorous vacuolar protein 1.^{171,180}

Our understanding of the PV and the proteins contained therein is very limited. It is likely that the *Plasmodium* parasite has evolved a multitude of peculiar and highly specialized proteins, that carry out functions, which are distinct from other known cellular processes, hampering their functional assignment. The PTEX translocon is a perfect example for a genus-specific and highly specialized machinery that has evolved to meet the challenges of RBC infection. Advanced experimental genetics, as demonstrated in this thesis, are a powerful tool box that allows for detailed insights into the structure and function of the PV, and will continue to enhance our understanding of the intravacuolar niche of the malaria parasite.

REFERENCES

1. Grassmé H, Jendrossek V, Gulbins E. Molecular mechanisms of bacteria induced apoptosis. *Apoptosis*. 2001;6(6):441-5.
2. von Moltke J, Ayres JS, Kofoed EM, Chavarría-Smith J, Vance RE. Recognition of bacteria by inflammasomes. *Annu Rev Immunol*. 2013;31:73-106.
3. Abdullah Z, Knolle PA. Scaling of immune responses against intracellular bacterial infection. *EMBO J*. 2014;33(20):2283-94.
4. Motta V, Soares F, Sun T, Philpott DJ. NOD-like receptors: versatile cytosolic sentinels. *Physiol Rev*. 2015;95(1):149-78.
5. Fujita N, Yoshimori T. Ubiquitination-mediated autophagy against invading bacteria. *Curr Opin Cell Biol*. 2011;23(4):492-7.
6. Shibutani ST, Yoshimori T. Autophagosome formation in response to intracellular bacterial invasion. *Cell Microbiol*. 2014;16(11):1619-26.
7. Sarantis H, Grinstein S. Subversion of phagocytosis for pathogen survival. *Cell Host Microbe*. 2012;12(4):419-31.
8. Moretti J, Blander JM. Insights into phagocytosis-coupled activation of pattern recognition receptors and inflammasomes. *Curr Opin Immunol*. 2014;26:100-10.
9. Ray K, Marteyn B, Sansonetti PJ, Tang CM. Life on the inside: the intracellular lifestyle of cytosolic bacteria. *Nat Rev Microbiol*. 2009;7(5):333-40.
10. Fredlund J, Enninga J. Cytoplasmic access by intracellular bacterial pathogens. *Trends Microbiol*. 2014;22(3):128-37.
11. Jones TC, Hirsch JG. The interaction between *Toxoplasma gondii* and mammalian cells. II. The absence of lysosomal fusion with phagocytic vacuoles containing living parasites. *J Exp Med*. 1972;136(5):1173-94.
12. Mordue DG, Håkansson S, Niesman I, Sibley LD. *Toxoplasma gondii* resides in a vacuole that avoids fusion with host cell endocytic and exocytic vesicular trafficking pathways. *Exp Parasitol*. 1999;92(2):87-99.
13. Armstrong JA, Hart PD. Response of cultured macrophages to *Mycobacterium tuberculosis*, with observations on fusion of lysosomes with phagosomes. *J Exp Med*. 1971;134(3 Pt 1):713-40.
14. Horwitz MA. The Legionnaires' disease bacterium (*Legionella pneumophila*) inhibits phagosome-lysosome fusion in human monocytes. *J Exp Med*. 1983;158(6):2108-26.
15. Ishibashi Y, Arai T. Specific inhibition of phagosome-lysosome fusion in murine macrophages mediated by *Salmonella typhimurium* infection. *FEMS Microbiol Immunol*. 1990;2(1):35-43.
16. Mehra A, Zahra A, Thompson V, Sirisaengtaksin N, Wells A, Porto M, *et al.* *Mycobacterium tuberculosis* type VII secreted effector EsxH targets host ESCRT to impair trafficking. *PLoS Pathog*. 2013;9(10):e1003734.
17. Antoine JC, Prina E, Jouanne C, Bongrand P. Parasitophorous vacuoles of *Leishmania amazonensis*-infected macrophages maintain an acidic pH. *Infect Immun*. 1990;58(3):779-87.
18. McConville MJ, Blackwell JM. Developmental changes in the glycosylated

- phosphatidylinositols of *Leishmania donovani*. Characterization of the promastigote and amastigote glycolipids. J Biol Chem. 1991;266(23):15170-9.
19. Späth GF, Garraway LA, Turco SJ, Beverley SM. The role(s) of lipophosphoglycan (LPG) in the establishment of *Leishmania major* infections in mammalian hosts. Proc Natl Acad Sci U S A. 2003;100(16):9536-41.
 20. Lodge R, Diallo TO, Descoteaux A. *Leishmania donovani* lipophosphoglycan blocks NADPH oxidase assembly at the phagosome membrane. Cell Microbiol. 2006;8(12):1922-31.
 21. Coppens I, Dunn JD, Romano JD, Pypaert M, Zhang H, Boothroyd JC, *et al.* *Toxoplasma gondii* sequesters lysosomes from mammalian hosts in the vacuolar space. Cell. 2006;125(2):261-74.
 22. Sinai AP, Webster P, Joiner KA. Association of host cell endoplasmic reticulum and mitochondria with the *Toxoplasma gondii* parasitophorous vacuole membrane: a high affinity interaction. J Cell Sci. 1997;110 (Pt 17):2117-28.
 23. Cocchiari JL, Kumar Y, Fischer ER, Hackstadt T, Valdivia RH. Cytoplasmic lipid droplets are translocated into the lumen of the *Chlamydia trachomatis* parasitophorous vacuole. Proc Natl Acad Sci U S A. 2008;105(27):9379-84.
 24. Hackstadt T, Rockey DD, Heinzen RA, Scidmore MA. *Chlamydia trachomatis* interrupts an exocytic pathway to acquire endogenously synthesized sphingomyelin in transit from the Golgi apparatus to the plasma membrane. EMBO J. 1996;15(5):964-77.
 25. Schwab JC, Beckers CJ, Joiner KA. The parasitophorous vacuole membrane surrounding intracellular *Toxoplasma gondii* functions as a molecular sieve. Proc Natl Acad Sci U S A. 1994;91(2):509-13.
 26. Desai SA, Rosenberg RL. Pore size of the malaria parasite's nutrient channel. Proc Natl Acad Sci U S A. 1997;94(5):2045-9.
 27. Das P, Lahiri A, Sen M, Iyer N, Kapoor N, Balaji KN, *et al.* Cationic amino acid transporters and *Salmonella typhimurium* ArgT collectively regulate arginine availability towards intracellular *Salmonella* growth. PLoS One. 2010;5(12):e15466.
 28. Price CT, Richards AM, Abu Kwaik Y. Nutrient generation and retrieval from the host cell cytosol by intra-vacuolar *Legionella pneumophila*. Front Cell Infect Microbiol. 2014; 4:111.
 29. Price CT, Abu Kwaik Y. The transcriptome of *Legionella pneumophila*-infected human monocyte-derived macrophages. PLoS One. 2014;9(12):e114914.
 30. Dubremetz JF, Achbarou A, Bermudes D, Joiner KA. Kinetics and pattern of organelle exocytosis during *Toxoplasma gondii* / host-cell interaction. Parasitol Res. 1993;79(5):402-8.
 31. Håkansson S, Charron AJ, Sibley LD. *Toxoplasma* evacuoles: a two-step process of secretion and fusion forms the parasitophorous vacuole. EMBO J. 2001;20(12):3132-44.
 32. Rome ME, Beck JR, Turetzky JM, Webster P, Bradley PJ. Intervacuolar transport and unique topology of GRA14, a novel dense granule protein in *Toxoplasma gondii*. Infect Immun. 2008;76(11):4865-75.
 33. Dunn JD, Ravindran S, Kim SK, Boothroyd JC. The *Toxoplasma gondii* dense granule protein GRA7 is phosphorylated upon invasion and forms an unexpected association with the rhoptry proteins ROP2 and ROP4. Infect Immun. 2008;76(12):5853-61.

34. Lige B, Romano JD, Bandaru VV, Ehrenman K, Levitskaya J, Sampels V, *et al.* Deficiency of a Niemann-Pick, type C1-related protein in *Toxoplasma* is associated with multiple lipidoses and increased pathogenicity. *PLoS Pathog.* 2011;7(12):e1002410.
35. Romano JD, de Beaumont C, Carrasco JA, Ehrenman K, Bavoil PM, Coppens I. Fierce competition between *Toxoplasma* and *Chlamydia* for host cell structures in dually infected cells. *Eukaryot Cell.* 2013;12(2):265-77.
36. Walker ME, Hjort EE, Smith SS, Tripathi A, Hornick JE, Hinchcliffe EH, *et al.* *Toxoplasma gondii* actively remodels the microtubule network in host cells. *Microbes Infect.* 2008;10(14-15):1440-9.
37. Halonen SK, Weidner E. Overcoating of *Toxoplasma* parasitophorous vacuoles with host cell vimentin type intermediate filaments. *J Eukaryot Microbiol.* 1994;41(1):65-71.
38. Pernas L, Adomako-Ankomah Y, Shastri AJ, Ewald SE, Treeck M, Boyle JP, *et al.* *Toxoplasma* effector MAF1 mediates recruitment of host mitochondria and impacts the host response. *PLoS Biol.* 2014;12(4):e1001845.
39. Roy CR. Vacuolar pathogens value membrane integrity. *Proc Natl Acad Sci U S A.* 2012;109(9):3197-8.
40. Creasey EA, Isberg RR. Maintenance of vacuole integrity by bacterial pathogens. *Curr Opin Microbiol.* 2014;17:46-52.
41. Kumar Y, Valdivia RH. Actin and intermediate filaments stabilize the *Chlamydia trachomatis* vacuole by forming dynamic structural scaffolds. *Cell Host Microbe.* 2008;4(2):159-69.
42. Jorgensen I, Bednar MM, Amin V, Davis BK, Ting JP, McCafferty DG, *et al.* The *Chlamydia* protease CPAF regulates host and bacterial proteins to maintain pathogen vacuole integrity and promote virulence. *Cell Host Microbe.* 2011;10(1):21-32.
43. Méresse S, Unsworth KE, Habermann A, Griffiths G, Fang F, Martínez-Lorenzo MJ, *et al.* Remodelling of the actin cytoskeleton is essential for replication of intravacuolar *Salmonella*. *Cell Microbiol.* 2001;3(8):567-77.
44. Salcedo SP, Holden DW. SseG, a virulence protein that targets *Salmonella* to the Golgi network. *EMBO J.* 2003;22(19):5003-14.
45. Abrahams GL, Hensel M. Manipulating cellular transport and immune responses: dynamic interactions between intracellular *Salmonella enterica* and its host cells. *Cell Microbiol.* 2006;8(5):728-37.
46. Schroeder N, Mota LJ, Méresse S. *Salmonella*-induced tubular networks. *Trends Microbiol.* 2011;19(6):268-77.
47. Brumell JH, Goosney DL, Finlay BB. SifA, a type III secreted effector of *Salmonella typhimurium*, directs *Salmonella*-induced filament (Sif) formation along microtubules. *Traffic.* 2002;3(6):407-15.
48. Kuhle V, Jäckel D, Hensel M. Effector proteins encoded by *Salmonella* pathogenicity island 2 interfere with the microtubule cytoskeleton after translocation into host cells. *Traffic.* 2004;5(5):356-70.
49. Beuzón CR, Méresse S, Unsworth KE, Ruiz-Albert J, Garvis S, Waterman SR, *et al.* *Salmonella* maintains the integrity of its intracellular vacuole through the action of SifA. *EMBO J.* 2000;19(13):3235-49.
50. Ohlson MB, Huang Z, Alto NM, Blanc MP, Dixon JE, Chai J, *et al.* Structure and

- function of *Salmonella* SifA indicate that its interactions with SKIP, SseJ, and RhoA family GTPases induce endosomal tubulation. *Cell Host Microbe*. 2008;4(5):434-46.
51. Diacovich L, Dumont A, Lafitte D, Soprano E, Guilhon AA, Bignon C, *et al.* Interaction between the SifA virulence factor and its host target SKIP is essential for *Salmonella* pathogenesis. *J Biol Chem*. 2009;284(48):33151-60.
 52. Dumont A, Boucrot E, Drevensek S, Daire V, Gorvel JP, Poüs C, *et al.* SKIP, the host target of the *Salmonella* virulence factor SifA, promotes kinesin-1-dependent vacuolar membrane exchanges. *Traffic*. 2010;11(7):899-911.
 53. Zuccala ES, Baum J. Cytoskeletal and membrane remodelling during malaria parasite invasion of the human erythrocyte. *Br J Haematol*. 2011;154(6):680-9.
 54. Shi H, Liu Z, Li A, Yin J, Chong AG, Tan KS, *et al.* Life cycle-dependent cytoskeletal modifications in *Plasmodium falciparum* infected erythrocytes. *PLoS One*. 2013;8(4):e61170.
 55. Nawabi P, Catron DM, Haldar K. Esterification of cholesterol by a type III secretion effector during intracellular *Salmonella* infection. *Mol Microbiol*. 2008;68(1):173-85.
 56. Lossi NS, Rolhion N, Magee AI, Boyle C, Holden DW. The *Salmonella* SPI-2 effector SseJ exhibits eukaryotic activator-dependent phospholipase A and glycerophospholipid : cholesterol acyltransferase activity. *Microbiology*. 2008;154(Pt 9):2680-8.
 57. Christen M, Coye LH, Hontz JS, LaRock DL, Pfuetzner RA, Megha, *et al.* Activation of a bacterial virulence protein by the GTPase RhoA. *Sci Signal*. 2009;2(95):ra71.
 58. Ward GE, Miller LH, Dvorak JA. The origin of parasitophorous vacuole membrane lipids in malaria-infected erythrocytes. *J Cell Sci*. 1993;106 (Pt 1):237-48.
 59. Lawrence CW, Cenedella RJ. Lipid content of *Plasmodium berghei*-infected rat red blood cells. *Exp Parasitol*. 1969;26(2):181-6.
 60. Holz GG. Lipids and the malarial parasite. *Bull World Health Organ*. 1977;55(2-3):237-48.
 61. Vaughan AM, O'Neill MT, Tarun AS, Camargo N, Phuong TM, Aly AS, *et al.* Type II fatty acid synthesis is essential only for malaria parasite late liver stage development. *Cell Microbiol*. 2009;11(3):506-20.
 62. Moll GN, Vial HJ, Ancelin ML, Op den Kamp JA, Roelofsen B, van Deenen LL. Phospholipid uptake by *Plasmodium knowlesi* infected erythrocytes. *FEBS Lett*. 1988; 232(2):341-6.
 63. Krishnegowda G, Gowda DC. Intraerythrocytic *Plasmodium falciparum* incorporates extraneous fatty acids to its lipids without any structural modification. *Mol Biochem Parasitol*. 2003;132(1):55-8.
 64. Palacpac NM, Hiramane Y, Mi-ichi F, Torii M, Kita K, Hiramatsu R, *et al.* Developmental-stage-specific triacylglycerol biosynthesis, degradation and trafficking as lipid bodies in *Plasmodium falciparum*-infected erythrocytes. *J Cell Sci*. 2004;117(Pt 8):1469-80.
 65. Mi-Ichi F, Kita K, Mitamura T. Intraerythrocytic *Plasmodium falciparum* utilize a broad range of serum-derived fatty acids with limited modification for their growth. *Parasitology*. 2006;133(Pt 4):399-410.
 66. Mi-Ichi F, Kano S, Mitamura T. Oleic acid is indispensable for intraerythrocytic proliferation of *Plasmodium falciparum*. *Parasitology*. 2007;134(Pt 12):1671-7.
 67. Elmendorf HG, Haldar K. *Plasmodium falciparum* exports the Golgi marker sphingomyelin synthase into a tubovesicular network in the cytoplasm of mature

- erythrocytes. *J Cell Biol.* 1994;124(4):449-62.
68. Lauer SA, Rathod PK, Ghori N, Haldar K. A membrane network for nutrient import in red cells infected with the malaria parasite. *Science.* 1997;276(5315):1122-5.
 69. Cooke IR, Deserno M. Coupling between lipid shape and membrane curvature. *Biophys J.* 2006;91(2):487-95.
 70. Zimmerberg J, Kozlov MM. How proteins produce cellular membrane curvature. *Nat Rev Mol Cell Biol.* 2006;7(1):9-19.
 71. McMahon HT, Boucrot E. Membrane curvature at a glance. *J Cell Sci.* 2015;128(6):1065-70.
 72. Sibley LD, Niesman IR, Parmley SF, Cesbron-Delauw MF. Regulated secretion of multi-lamellar vesicles leads to formation of a tubulo-vesicular network in host-cell vacuoles occupied by *Toxoplasma gondii*. *J Cell Sci.* 1995;108 (Pt 4):1669-77.
 73. Mercier C, Dubremetz JF, Rauscher B, Lecordier L, Sibley LD, Cesbron-Delauw MF. Biogenesis of nanotubular network in *Toxoplasma* parasitophorous vacuole induced by parasite proteins. *Mol Biol Cell.* 2002;13(7):2397-409.
 74. Mercier C, Howe DK, Mordue D, Lingnau M, Sibley LD. Targeted disruption of the GRA2 locus in *Toxoplasma gondii* decreases acute virulence in mice. *Infect Immun.* 1998;66(9):4176-82.
 75. Gold DA, Kaplan AD, Lis A, Bett GC, Rosowski EE, Cirelli KM, *et al.* The *Toxoplasma* dense granule proteins GRA17 and GRA23 mediate the movement of small molecules between the host and the parasitophorous vacuole. *Cell Host Microbe.* 2015;17(5):642-52.
 76. Repnik U, Gangopadhyay P, Bietz S, Przyborski JM, Griffiths G, Lingelbach K. The apicomplexan parasite *Babesia divergens* internalizes band 3, glycophorin A and spectrin during invasion of human red blood cells. *Cell Microbiol.* 2015;17(7):1052-68.
 77. Przyborski JM, Miller SK, Pfahler JM, Henrich PP, Rohrbach P, Crabb BS, *et al.* Trafficking of STEVOR to the Maurer's clefts in *Plasmodium falciparum*-infected erythrocytes. *EMBO J.* 2005;24(13):2306-17.
 78. Tilly AK, Thiede J, Metwally N, Lubiana P, Bachmann A, Roeder T, *et al.* Type of *in vitro* cultivation influences cytoadhesion, knob structure, protein localization and transcriptome profile of *Plasmodium falciparum*. *Sci Rep.* 2015;5:16766.
 79. Barnes DA, Thompson J, Triglia T, Day K, Kemp DJ. Mapping the genetic locus implicated in cytoadherence of *Plasmodium falciparum* to melanoma cells. *Mol Biochem Parasitol.* 1994;66(1):21-9.
 80. Bourke PF, Holt DC, Sutherland CJ, Kemp DJ. Disruption of a novel open reading frame of *Plasmodium falciparum* chromosome 9 by subtelomeric and internal deletions can lead to loss or maintenance of cytoadherence. *Mol Biochem Parasitol.* 1996;82(1):25-36.
 81. Trager W, Rudzinska MA, Bradbury PC. The fine structure of *Plasmodium falciparum* and its host erythrocytes in natural malarial infections in man. *Bull World Health Organ.* 1966;35(6):883-5.
 82. Langreth SG, Jensen JB, Reese RT, Trager W. Fine structure of human malaria *in vitro*. *J Protozool.* 1978;25(4):443-52.
 83. Stenzel DJ, Kara UA. Sorting of malarial antigens into vesicular compartments within the host cell cytoplasm as demonstrated by immunoelectron microscopy. *Eur J Cell*

- Biol. 1989;49(2):311-8.
84. Behari R, Haldar K. *Plasmodium falciparum*: protein localization along a novel, lipid-rich tubovesicular membrane network in infected erythrocytes. *Exp Parasitol*. 1994;79(3):250-9.
 85. van Ooij C, Tamez P, Bhattacharjee S, Hiller NL, Harrison T, Liolios K, *et al*. The malaria secretome: from algorithms to essential function in blood stage infection. *PLoS Pathog*. 2008;4(6):e1000084.
 86. Baumeister S, Winterberg M, Duranton C, Huber SM, Lang F, Kirk K, *et al*. Evidence for the involvement of *Plasmodium falciparum* proteins in the formation of new permeability pathways in the erythrocyte membrane. *Mol Microbiol*. 2006;60(2):493-504.
 87. Nguitragool W, Bokhari AA, Pillai AD, Rayavara K, Sharma P, Turpin B, *et al*. Malaria parasite clag3 genes determine channel-mediated nutrient uptake by infected red blood cells. *Cell*. 2011;145(5):665-77.
 88. Pouvelle B, Spiegel R, Hsiao L, Howard RJ, Morris RL, Thomas AP, *et al*. Direct access to serum macromolecules by intraerythrocytic malaria parasites. *Nature*. 1991;353(6339):73-5.
 89. Brumell JH, Tang P, Mills SD, Finlay BB. Characterization of *Salmonella*-induced filaments (Sifs) reveals a delayed interaction between *Salmonella*-containing vacuoles and late endocytic compartments. *Traffic*. 2001;2(9):643-53.
 90. Krieger V, Liebl D, Zhang Y, Rajashekar R, Chlanda P, Giesker K, *et al*. Reorganization of the endosomal system in *Salmonella*-infected cells: the ultrastructure of *Salmonella*-induced tubular compartments. *PLoS Pathog*. 2014;10(9):e1004374.
 91. Ingmundson A, Nahar C, Brinkmann V, Lehmann MJ, Matuschewski K. The exported *Plasmodium berghei* protein IBIS1 delineates membranous structures in infected red blood cells. *Mol Microbiol*. 2012;83(6):1229-43.
 92. Haase S, Hanssen E, Matthews K, Kalanon M, de Koning-Ward TF. The exported protein PbCP1 localises to cleft-like structures in the rodent malaria parasite *Plasmodium berghei*. *PLoS One*. 2013;8(4):e61482.
 93. Adisa A, Rug M, Klonis N, Foley M, Cowman AF, Tilley L. The signal sequence of exported protein-1 directs the green fluorescent protein to the parasitophorous vacuole of transfected malaria parasites. *J Biol Chem*. 2003;278(8):6532-42.
 94. Meibalan E, Comunale MA, Lopez AM, Bergman LW, Mehta A, Vaidya AB, *et al*. Host erythrocyte environment influences the localization of exported protein 2, an essential component of the *Plasmodium* translocon. *Eukaryot Cell*. 2015;14(4):371-84.
 95. Mantel PY, Hoang AN, Goldowitz I, Potashnikova D, Hamza B, Vorobjev I, *et al*. Malaria-infected erythrocyte-derived microvesicles mediate cellular communication within the parasite population and with the host immune system. *Cell Host Microbe*. 2013;13(5):521-34.
 96. Regev-Rudzki N, Wilson DW, Carvalho TG, Sisqueira X, Coleman BM, Rug M, *et al*. Cell-cell communication between malaria-infected red blood cells via exosome-like vesicles. *Cell*. 2013;153(5):1120-33.
 97. Aikawa M, Miller LH, Rabbege J. Caveola-vesicle complexes in the plasmalemma of erythrocytes infected by *Plasmodium vivax* and *P. cynomolgi*. Unique structures related to Schüffner's dots. *Am J Pathol*. 1975;79(2):285-300.

98. Burns ER, Pollack S. *P. falciparum* infected erythrocytes are capable of endocytosis. In *Vitro Cell Dev Biol*. 1988;24(5):481-6.
99. Trelka DP, Schneider TG, Reeder JC, Taraschi TF. Evidence for vesicle-mediated trafficking of parasite proteins to the host cell cytosol and erythrocyte surface membrane in *Plasmodium falciparum* infected erythrocytes. *Mol Biochem Parasitol*. 2000;106(1):131-45.
100. Taraschi TF, O'Donnell M, Martinez S, Schneider T, Trelka D, Fowler VM, *et al*. Generation of an erythrocyte vesicle transport system by *Plasmodium falciparum* malaria parasites. *Blood*. 2003;102(9):3420-6.
101. Mutai BK, Waitumbi JN. Apoptosis stalks *Plasmodium falciparum* maintained in continuous culture condition. *Malar J*. 2010;9 Suppl 3:S6.
102. Engelbrecht D, Coetzer TL. Sunlight inhibits growth and induces markers of programmed cell death in *Plasmodium falciparum* *in vitro*. *Malar J*. 2015;14:378.
103. Grüning C, Heiber A, Kruse F, Ungefehr J, Gilberger TW, Spielmann T. Development and host cell modifications of *Plasmodium falciparum* blood stages in four dimensions. *Nat Commun*. 2011;2:165.
104. Lauer SA, Ghori N, Haldar K. Sphingolipid synthesis as a target for chemotherapy against malaria parasites. *Proc Natl Acad Sci U S A*. 1995;92(20):9181-5.
105. Kubori T, Matsushima Y, Nakamura D, Uralil J, Lara-Tejero M, Sukhan A, *et al*. Supramolecular structure of the *Salmonella typhimurium* type III protein secretion system. *Science*. 1998;280(5363):602-5.
106. Loquet A, Sgourakis NG, Gupta R, Giller K, Riedel D, Goosmann C, *et al*. Atomic model of the type III secretion system needle. *Nature*. 2012;486(7402):276-9.
107. Rappl C, Deiwick J, Hensel M. Acidic pH is required for the functional assembly of the type III secretion system encoded by *Salmonella* pathogenicity island 2. *FEMS Microbiol Lett*. 2003;226(2):363-72.
108. Löber S, Jäckel D, Kaiser N, Hensel M. Regulation of *Salmonella* pathogenicity island 2 genes by independent environmental signals. *Int J Med Microbiol*. 2006;296(7):435-47.
109. Figueira R, Holden DW. Functions of the *Salmonella* pathogenicity island 2 (SPI-2) type III secretion system effectors. *Microbiology*. 2012;158(Pt 5):1147-61.
110. Burkinshaw BJ, Strynadka NC. Assembly and structure of the T3SS. *Biochim Biophys Acta*. 2014;1843(8):1649-63.
111. Costa TR, Felisberto-Rodrigues C, Meir A, Prevost MS, Redzej A, Trokter M, *et al*. Secretion systems in Gram-negative bacteria: structural and mechanistic insights. *Nat Rev Microbiol*. 2015;13(6):343-59.
112. de Koning-Ward TF, Gilson PR, Boddey JA, Rug M, Smith BJ, Papenfuss AT, *et al*. A newly discovered protein export machine in malaria parasites. *Nature*. 2009;459(7249):945-9.
113. Hiller NL, Bhattacharjee S, van Ooij C, Liolios K, Harrison T, Lopez-Estraño C, *et al*. A host-targeting signal in virulence proteins reveals a secretome in malarial infection. *Science*. 2004;306(5703):1934-7.
114. Marti M, Good RT, Rug M, Knuepfer E, Cowman AF. Targeting malaria virulence and remodeling proteins to the host erythrocyte. *Science*. 2004;306(5703):1930-3.
115. Gehde N, Hinrichs C, Montilla I, Chappian S, Lingelbach K, Przyborski JM. Protein

- unfolding is an essential requirement for transport across the parasitophorous vacuolar membrane of *Plasmodium falciparum*. Mol Microbiol. 2009;71(3):613-28.
116. Sanders PR, Cantin GT, Greenbaum DC, Gilson PR, Nebel T, Moritz RL, *et al.* Identification of protein complexes in detergent-resistant membranes of *Plasmodium falciparum* schizonts. Mol Biochem Parasitol. 2007;154(2):148-57.
 117. Bullen HE, Charnaud SC, Kalanon M, Riglar DT, Dekiwadia C, Kangwanrangsan N, *et al.* Biosynthesis, localization, and macromolecular arrangement of the *Plasmodium falciparum* translocon of exported proteins (PTEX). J Biol Chem. 2012;287(11):7871-84.
 118. Elsworth B, Sanders PR, Nebel T, Batinovic S, Kalanon M, Nie CQ, *et al.* Proteomic analysis reveals novel proteins associated with the *Plasmodium* protein exporter PTEX and a loss of complex stability upon truncation of the core PTEX component, PTEX150. Cell Microbiol. 2016. Accepted article. DOI: 10.1111/cmi.12596.
 119. Hammoudi PM, Jacot D, Mueller C, Di Cristina M, Dogga SK, Marq JB, *et al.* Fundamental roles of the Golgi-associated *Toxoplasma* aspartyl protease, ASP5, at the host-parasite interface. PLoS Pathog. 2015;11(10):e1005211.
 120. Coffey MJ, Sleebs BE, Uboldi AD, Garnham A, Franco M, Marino ND, *et al.* An aspartyl protease defines a novel pathway for export of *Toxoplasma* proteins into the host cell. Elife. 2015;4.
 121. Curt-Varesano A, Braun L, Ranquet C, Hakimi MA, Bougdour A. The aspartyl protease TgASP5 mediates the export of the *Toxoplasma* GRA16 and GRA24 effectors into host cells. Cell Microbiol. 2016;18(2):151-67.
 122. Elsworth B, Matthews K, Nie CQ, Kalanon M, Charnaud SC, Sanders PR, *et al.* PTEX is an essential nexus for protein export in malaria parasites. Nature. 2014;511(7511):587-91.
 123. Beck JR, Muralidharan V, Oksman A, Goldberg DE. PTEX component HSP101 mediates export of diverse malaria effectors into host erythrocytes. Nature. 2014;511(7511):592-5.
 124. Boddey JA, Cowman AF. *Plasmodium* nesting: remaking the erythrocyte from the inside out. Annu Rev Microbiol. 2013;67:243-69.
 125. Nguitragool W, Rayavara K, Desai SA. Proteolysis at a specific extracellular residue implicates integral membrane CLAG3 in malaria parasite nutrient channels. PLoS One. 2014;9(4):e93759.
 126. Spillman NJ, Beck JR, Goldberg DE. Protein export into malaria parasite-infected erythrocytes: mechanisms and functional consequences. Annu Rev Biochem. 2015;84:813-41.
 127. Vembar SS, Brodsky JL. One step at a time: endoplasmic reticulum-associated degradation. Nat Rev Mol Cell Biol. 2008;9(12):944-57.
 128. Li HM, Chiu CC. Protein transport into chloroplasts. Annu Rev Plant Biol. 2010;61:157-80.
 129. Külzer S, Rug M, Brinkmann K, Cannon P, Cowman A, Lingelbach K, *et al.* Parasite-encoded Hsp40 proteins define novel mobile structures in the cytosol of the *P. falciparum*-infected erythrocyte. Cell Microbiol. 2010;12(10):1398-420.
 130. Külzer S, Charnaud S, Dagan T, Riedel J, Mandal P, Pesce ER, *et al.* *Plasmodium falciparum*-encoded exported hsp70/hsp40 chaperone/co-chaperone complexes within

- the host erythrocyte. *Cell Microbiol.* 2012;14(11):1784-95.
131. Johnson D, Günther K, Ansorge I, Benting J, Kent A, Bannister L, *et al.* Characterization of membrane proteins exported from *Plasmodium falciparum* into the host erythrocyte. *Parasitology.* 1994;109 (Pt 1):1-9.
 132. Fischer K, Marti T, Rick B, Johnson D, Benting J, Baumeister S, *et al.* Characterization and cloning of the gene encoding the vacuolar membrane protein EXP-2 from *Plasmodium falciparum*. *Mol Biochem Parasitol.* 1998;92(1):47-57.
 133. Matthews K, Kalanon M, Chisholm SA, Sturm A, Goodman CD, Dixon MW, *et al.* The *Plasmodium* translocon of exported proteins (PTEX) component thioredoxin-2 is important for maintaining normal blood-stage growth. *Mol Microbiol.* 2013;89(6):1167-86.
 134. Boucher IW, McMillan PJ, Gabrielsen M, Akerman SE, Brannigan JA, Schnick C, *et al.* Structural and biochemical characterization of a mitochondrial peroxiredoxin from *Plasmodium falciparum*. *Mol Microbiol.* 2006;61(4):948-59.
 135. Kehr S, Sturm N, Rahlfs S, Przyborski JM, Becker K. Compartmentation of redox metabolism in malaria parasites. *PLoS Pathog.* 2010;6(12):e1001242.
 136. Sharma A, Dixit S. Structural insights into thioredoxin-2: a component of malaria parasite protein secretion machinery. *Sci Rep.* 2011;1:179.
 137. Elsworth B, Crabb BS, Gilson PR. Protein export in malaria parasites: an update. *Cell Microbiol.* 2014;16(3):355-63.
 138. Russo I, Babbitt S, Muralidharan V, Butler T, Oksman A, Goldberg DE. Plasmepsin V licenses *Plasmodium* proteins for export into the host erythrocyte. *Nature.* 2010;463(7281):632-6.
 139. Boddey JA, Hodder AN, Günther S, Gilson PR, Patsiouras H, Kapp EA, *et al.* An aspartyl protease directs malaria effector proteins to the host cell. *Nature.* 2010;463(7281):627-31.
 140. Sleebs BE, Lopatnicki S, Marapana DS, O'Neill MT, Rajasekaran P, Gazdik M, *et al.* Inhibition of Plasmepsin V activity demonstrates its essential role in protein export, PfEMP1 display, and survival of malaria parasites. *PLoS Biol.* 2014;12(7):e1001897.
 141. Struck NS, de Souza Dias S, Langer C, Marti M, Pearce JA, Cowman AF, *et al.* Redefining the Golgi complex in *Plasmodium falciparum* using the novel Golgi marker PfGRASP. *J Cell Sci.* 2005;118(Pt 23):5603-13.
 142. Saridaki T, Sanchez CP, Pfahler J, Lanzer M. A conditional export system provides new insights into protein export in *Plasmodium falciparum*-infected erythrocytes. *Cell Microbiol.* 2008;10(12):2483-95.
 143. Chisholm SA, McHugh E, Lundie R, Dixon MW, Ghosh S, O'Keefe M, *et al.* Contrasting inducible knockdown of the auxiliary PTEX component PTEX88 in *P. falciparum* and *P. berghei* unmasks a role in parasite virulence. *PLoS One.* 2016;11(2):e0149296.
 144. Chotivanich K, Udomsangpetch R, McGready R, Proux S, Newton P, Pukrittayakamee S, *et al.* Central role of the spleen in malaria parasite clearance. *J Infect Dis.* 2002; 185(10):1538-41.
 145. Kudryashev M, Lepper S, Stanway R, Bohn S, Baumeister W, Cyrklaff M, *et al.* Positioning of large organelles by a membrane-associated cytoskeleton in *Plasmodium* sporozoites. *Cell Microbiol.* 2010;12(3):362-71.
 146. Riglar DT, Rogers KL, Hanssen E, Turnbull L, Bullen HE, Charnaud SC, *et al.* Spatial

- association with PTEX complexes defines regions for effector export into *Plasmodium falciparum*-infected erythrocytes. *Nat Commun.* 2013;4:1415.
147. Vaughan AM, Mikolajczak SA, Wilson EM, Grompe M, Kaushansky A, Camargo N, *et al.* Complete *Plasmodium falciparum* liver-stage development in liver-chimeric mice. *J Clin Invest.* 2012;122(10):3618-28.
 148. Hollingdale MR, Leland P, Leef JL, Leef MF, Beaudoin RL. Serological reactivity of *in vitro* cultured exoerythrocytic stages of *Plasmodium berghei* in indirect immunofluorescent or immunoperoxidase antibody tests. *Am J Trop Med Hyg.* 1983;32(1):24-30.
 149. Hamilton AJ, Suhrbier A, Nicholas J, Sinden RE. Immunoelectron microscopic localization of circumsporozoite antigen in the differentiating exoerythrocytic trophozoite of *Plasmodium berghei*. *Cell Biol Int Rep.* 1988;12(2):123-9.
 150. Khan ZM, Ng C, Vanderberg JP. Early hepatic stages of *Plasmodium berghei*: release of circumsporozoite protein and host cellular inflammatory response. *Infect Immun.* 1992;60(1):264-70.
 151. Hügel FU, Pradel G, Frevert U. Release of malaria circumsporozoite protein into the host cell cytoplasm and interaction with ribosomes. *Mol Biochem Parasitol.* 1996;81(2):151-70.
 152. Cockburn IA, Tse SW, Radtke AJ, Srinivasan P, Chen YC, Sinnis P, *et al.* Dendritic cells and hepatocytes use distinct pathways to process protective antigen from *Plasmodium* *in vivo*. *PLoS Pathog.* 2011;7(3):e1001318.
 153. Singh AP, Buscaglia CA, Wang Q, Levay A, Nussenzweig DR, Walker JR, *et al.* *Plasmodium* circumsporozoite protein promotes the development of the liver stages of the parasite. *Cell.* 2007;131(3):492-504.
 154. Grützke J, Rindte K, Goosmann C, Silvie O, Rauch C, Heuer D, *et al.* The spatiotemporal dynamics and membranous features of the *Plasmodium* liver stage tubovesicular network. *Traffic.* 2014;15(4):362-82.
 155. Petersen W, Matuschewski K, Ingmundson A. Trafficking of the signature protein of intra-erythrocytic *Plasmodium berghei*-induced structures, IBIS1, to *P. falciparum* Maurer's clefts. *Mol Biochem Parasitol.* 2015;200(1-2):25-9.
 156. Orito Y, Ishino T, Iwanaga S, Kaneko I, Kato T, Menard R, *et al.* Liver-specific protein 2: a *Plasmodium* protein exported to the hepatocyte cytoplasm and required for merozoite formation. *Mol Microbiol.* 2013;87(1):66-79.
 157. Kalanon M, Bargieri D, Sturm A, Matthews K, Ghosh S, Goodman CD, *et al.* The *Plasmodium* translocon of exported proteins component EXP2 is critical for establishing a patent malaria infection in mice. *Cell Microbiol.* 2016;18(3):399-412.
 158. Kumar Y, Valdivia RH. Leading a sheltered life: intracellular pathogens and maintenance of vacuolar compartments. *Cell Host Microbe.* 2009;5(6):593-601.
 159. Weiss GE, Crabb BS, Gilson PR. Overlaying molecular and temporal aspects of malaria parasite invasion. *Trends Parasitol.* 2016;32(4):284-95.
 160. Rudzinska MA, Trager W, Lewengrub SJ, Gubert E. An electron microscopic study of *Babesia microti* invading erythrocytes. *Cell Tissue Res.* 1976;169(3):323-34.
 161. Shaw MK, Tilney LG, Musoke AJ. The entry of *Theileria parva* sporozoites into bovine lymphocytes: evidence for MHC class I involvement. *J Cell Biol.* 1991;113(1):87-101.
 162. Asada M, Goto Y, Yahata K, Yokoyama N, Kawai S, Inoue N, *et al.* Gliding motility of

- Babesia bovis* merozoites visualized by time-lapse video microscopy. PLoS One. 2012; 7(4):e35227.
163. Pellé KG, Jiang RH, Mantel PY, Xiao YP, Hjelmqvist D, Gallego-Lopez GM, *et al.* Shared elements of host-targeting pathways among apicomplexan parasites of differing lifestyles. Cell Microbiol. 2015;17(11):1618-39.
164. McMillan PJ, Millet C, Batinovic S, Maiorca M, Hanssen E, Kenny S, *et al.* Spatial and temporal mapping of the PfEMP1 export pathway in *Plasmodium falciparum*. Cell Microbiol. 2013;15(8):1401-18.
165. Spycher C, Rug M, Pachlatko E, Hanssen E, Ferguson D, Cowman AF, *et al.* The Maurer's cleft protein MAHRP1 is essential for trafficking of PfEMP1 to the surface of *Plasmodium falciparum*-infected erythrocytes. Mol Microbiol. 2008;68(5):1300-14.
166. Hanssen E, Hawthorne P, Dixon MW, Trenholme KR, McMillan PJ, Spielmann T, *et al.* Targeted mutagenesis of the ring-exported protein-1 of *Plasmodium falciparum* disrupts the architecture of Maurer's cleft organelles. Mol Microbiol. 2008;69(4):938-53.
167. Gohil S, Kats LM, Sturm A, Cooke BM. Recent insights into alteration of red blood cells by *Babesia bovis*: moovin' forward. Trends Parasitol. 2010;26(12):591-9.
168. Edwards CJ, Fuller J. Oxidative stress in erythrocytes. Comp Hematol Int. 1996;6:24-31.
169. Cimen MY. Free radical metabolism in human erythrocytes. Clin Chim Acta. 2008;390(1-2):1-11.
170. Lisewski AM, Quiros JP, Ng CL, Adikesavan AK, Miura K, Putluri N, *et al.* Super-genomic network compression and the discovery of EXP1 as a glutathione transferase inhibited by artesunate. Cell. 2014;158(4):916-28.
171. Nyalwidhe J, Lingelbach K. Proteases and chaperones are the most abundant proteins in the parasitophorous vacuole of *Plasmodium falciparum*-infected erythrocytes. Proteomics. 2006;6(5):1563-73.
172. Nyalwidhe J, Baumeister S, Hibbs AR, Tawill S, Papakrivos J, Volker U, *et al.* A nonpermeant biotin derivative gains access to the parasitophorous vacuole in *Plasmodium falciparum*-infected erythrocytes permeabilized with streptolysin O. J Biol Chem. 2002;277(42):40005-11.
173. Ling IT, Florens L, Dluzewski AR, Kaneko O, Grainger M, Yim Lim BY, *et al.* The *Plasmodium falciparum* clag9 gene encodes a rhoptry protein that is transferred to the host erythrocyte upon invasion. Mol Microbiol. 2004;52(1):107-18.
174. Richard D, Kats LM, Langer C, Black CG, Mitri K, Boddey JA, *et al.* Identification of rhoptry trafficking determinants and evidence for a novel sorting mechanism in the malaria parasite *Plasmodium falciparum*. PLoS Pathog. 2009;5(3):e1000328.
175. Hiller NL, Akompong T, Morrow JS, Holder AA, Halder K. Identification of a stomatin orthologue in vacuoles induced in human erythrocytes by malaria parasites. A role for microbial raft proteins in apicomplexan vacuole biogenesis. J Biol Chem. 2003;278(48):48413-21.
176. Spielmann T, Ferguson DJ, Beck HP. etramps, a new *Plasmodium falciparum* gene family coding for developmentally regulated and highly charged membrane proteins located at the parasite-host cell interface. Mol Biol Cell. 2003;14(4):1529-44.
177. Spielmann T, Gardiner DL, Beck HP, Trenholme KR, Kemp DJ. Organization of ETRAMPs and EXP-1 at the parasite-host cell interface of malaria parasites. Mol

- Microbiol. 2006;59(3):779-94.
178. Spielmann T, Montagna GN, Hecht L, Matuschewski K. Molecular make-up of the *Plasmodium* parasitophorous vacuolar membrane. Int J Med Microbiol. 2012;302(4-5):179-86.
 179. Blackman MJ. Malarial proteases and host cell egress: an 'emerging' cascade. Cell Microbiol. 2008;10(10):1925-34.
 180. Chu T, Lingelbach K, Przyborski JM. Genetic evidence strongly support an essential role for *Pf*PV1 in intra-erythrocytic growth of *P. falciparum*. PLoS One. 2011;6(3):e18396.

ABSTRACT

Malaria parasites have the remarkable ability to propagate inside red blood cells. To make up for the absence of organelles, trafficking pathways and certain nutrients, the parasite desperately needs to remodel the erythrocyte by delivering both proteins and lipids to distinct locations in the host cell. During blood stage development, the parasite resides in a parasitophorous vacuole, and secreted virulence factors *en route* to the erythrocyte need to cross its membranous boundary. This process is thought to be facilitated by the *Plasmodium* translocon of exported proteins (PTEX). In this thesis, development and application of advanced experimental genetics techniques for the rodent malaria model parasite *Plasmodium berghei* served to uncover novel features of the protein export machinery. In depth phenotyping of two loss-of-function mutants revealed dispensable roles for the putative translocon regulators PTEX88 and thioredoxin 2. Strikingly, their ablation resulted in decreased sequestration of infected erythrocytes to peripheral tissues. In consequence, deletion of PTEX88 caused the alleviation of cerebral complications, for the first time linking the protein export machinery with parasite sequestration and virulence *in vivo*. Microscopic and flow cytometric assessment of the parasite exportome suggests specialized functions of PTEX88 in the translocation process. Furthermore, detailed life cycle analysis revealed distinct spatio-temporal patterns of the putative translocon constituents. During asexual development in the blood, two components exclusively localized to tubular protrusions emerging from the parasite surface. A combination of live fluorescence microscopy, photo bleaching and correlative light and electron microscopy revealed insights into the protein composition, development, ultrastructure, and behavior of this vacuolar subcompartment. The data presented in this thesis significantly refine our current understanding of parasite-induced protein and lipid trafficking and shed light on the interconnection of host cell refurbishment and malaria pathology.

SAMENVATTING

Malariaparasieten hebben de merkwaardige eigenschap dat ze zich in rode bloedcellen vermenigvuldigen. Om de afwezigheid van organellen, transportroutes en bepaalde voedingsstoffen te compenseren, moet de parasiet de erythrocyt bewerken door eiwitten en vetten te leveren aan verschillende locaties in de gastheercel. Gedurende de ontwikkeling in de bloedstadia bevindt de parasiet zich in een vacuole. Uitgescheiden virulente factoren en route naar de erythrocyt moeten dit membraan passeren. Men vermoedt dat dit proces mogelijk wordt gemaakt door de Plasmodium translocon van geëxporteerde eiwitten (PTEX). In deze thesis wordt de ontwikkeling en toepassing van geavanceerde experimentele genetische technieken op de knaagdier malaria modelparasiet *Plasmodium berghei* gebruikt om nieuwe eigenschappen van het eiwit export mechanisme te ontdekken. De fenotypering van twee loss-of-function mutanten liet een niet-essentiële rol zien voor de putatieve translocon regulatoren PTX88 en thioredoxine 2. Opvallend was dat uitschakeling van deze regulatoren resulteerde in een verminderde sekwestratie van geïnfecteerde erythrocyten in perifere weefsels. Als gevolg hiervan leidde uitschakeling van PTX88 tot verlichting van cerebrale complicaties. Dit verbond voor het eerst het eiwit export mechanisme met sekwestratie van parasieten en virulentie in vivo. Microscopische en flow cytometrische lokalisatie van geëxporteerde eiwitten suggereerde een gespecialiseerde functie van PTX88 in het translocatie proces. Daarnaast liet gedetailleerde bestudering van de levenscyclus een verschillend tijd-ruimte patroon van de vermeende translocon componenten zien. Twee componenten waren exclusief gelokaliseerd in tubulaire uitstulpingen ontstaan vanuit het oppervlak van de parasiet gedurende de asexuele ontwikkeling. Een combinatie van live fluorescentie microscopie, fotobleking en correlatieve licht- en elektronenmicroscopie gaf inzicht in de eiwit compositie, ontwikkeling, ultrastructuur en gedrag van dit vacuolaire subcompartiment. De data gepresenteerd in deze thesis geven ons meer inzicht in parasiet-geïnduceerde eiwit en vet transport en belicht de connectie tussen gastheer bewerkingen en malaria pathologie.

ZUSAMMENFASSUNG

Malariaparasiten besitzen die erstaunliche Fähigkeit, sich in roten Blutzellen zu vermehren. Aufgrund der Abwesenheit von Organellen, Transportmechanismen und von diversen Nährstoffen, muss der Parasit seine Wirtszelle extensiv verändern, indem er sowohl Lipide als auch Proteine zu verschiedenen Orten im Erythrocyten transportiert. Während seiner Entwicklung im Blut, wächst der Parasit in einer parasitophoren Vakuole heran. Virulenzfaktoren, die in die Wirtszelle exportiert werden, müssen daher zunächst die Membran der Vakuole passieren. Dieser Prozess wird durch das *Plasmodium* Translokons für exportierte Proteine (PTEX) katalysiert. Die vorliegende Arbeit demonstriert, wie die Entwicklung und Anwendung experimentell-genetischer Methoden für den murinen Modellparasiten *Plasmodium berghei* neue Einsichten über die Proteinexportmaschinerie gewährt. Die detaillierte Phänotypisierung zweier Gendelektionsmutanten offenbart die Entbehrlichkeit der zwei potentiellen Translokonsregulatoren PTEX88 und Thioredoxin 2. Die Abwesenheit dieser Komponenten verursacht markante Defekte bei der Sequestrierung infizierter Erythrozyten zu peripheren Geweben. Infolgedessen verursachen PTEX88-defiziente Parasiten keinerlei zerebrale Komplikationen. Diese Beobachtungen stellen zum ersten Mal eine überzeugende funktionelle Verbindung zwischen der Proteinexportmaschinerie und der Virulenz von Malariaparasiten her. Des weiteren legt die mikroskopische und durchflusszytometrische Untersuchung von Kargoproteinen spezialisierte Funktionen von PTEX88 im Translokationsprozess nahe. Eine detaillierte Analyse des Lebenszyklus gewährt Einsichten in die temporalen und räumlichen Aspekte des PTEX Translokons. Während der asexuellen Merogonie im Blut lokalisieren zwei Komponenten ausschließlich zu tubulären Protuberanzen auf der Parasitenoberfläche. Eine Kombination aus Lebend-Fluoreszenzmikroskopie, Photobleichung und korrelativer Licht- und Elektronenmikroskopie gewährt Einsichten in die Proteinzusammensetzung, Entwicklung, Ultrastruktur und das Verhalten dieses vakuolären Subkompartiments. Die vorliegenden Daten erweitern unser Wissen über Parasiten-induzierten Protein- und Lipidtransport und enthüllen die enge Verknüpfung zwischen Wirtszellremodellierung und Parasitenvirulenz.

ACKNOWLEDGEMENTS

The publication of this thesis would not have been possible without the contributions of several colleagues, collaborators, and funding parties. I am especially thankful for the competent supervision and guidance by Dr. Taco W.A. Kooij and Prof. Dr. Robert W. Sauerwein from the Radboud University Medical Center in Nijmegen, and by Prof. Dr. Kai Matuschewski from the Max Planck Institute for Infection Biology / Humboldt University in Berlin. Independently designing and conducting my own curiosity-driven research has been a strong motivator throughout my doctoral studies, and I am very grateful that my supervisors have provided me with the opportunity to do so. Furthermore, the expertise and kind advice of my colleagues and collaborators have inspired me immensely during my research. The technical assistance by Manuel and Carolin Rauch, Christian Goosmann, Silke Bandermaann, Petra Matylewski, Marga van de Vegte-Bolmer and Geert-Jan van Geemert has been a major contribution to my work. Furthermore, I highly appreciate the expert advice of Dr. Volker Brinkmann during light and electron microscopy and of Prof. Dr. Werner Stenzel during analysis of histological organ sections. I also acknowledge the assistance of the Flow Cytometry Core Facility at the Deutsches Rheuma-Forschungszentrum in Berlin, particularly Toralf Kaiser and Jenny Kirsch, and the assistance and advice of Rob Woestenenk from the Flow Cytometry Technology Center at the Radboud University Medical Center in Nijmegen. I am also thankful for the personal support that I have experienced from the members of both laboratories, not all of which can be named here. Special thanks go to Dr. Alyssa Ingmundson, Josefine Dunst, Dr. Juliane Schaer and Dr. Isaie Reuling for inspiring and fruitful discussion. Furthermore, I acknowledge the help of Laura de Vries with the Dutch translation of the abstract. Diane Schad contributed to the figure design. I am thankful for the permission of Springer, Elsevier, the Nature Publishing Group, and the Rockefeller University Press to use previously published figures and schematics in the introduction of the thesis.

I am very grateful for the opportunity to obtain my doctoral degree from both the Radboud University in Nijmegen and the Humboldt University in Berlin according to the *cotutelle de thèse* procedure. Hence, special thanks go out to Martina Sick, Jana Lahmer and Hannelies Linders for their work on the cotutelle agreement. I thank the manuscript committee, consisting of Prof. Dr. Mike S.M. Jetten, Prof. Dr.

Andreas Herrmann and Prof. Dr. Mike J. Blackman for the critical evaluation of my doctoral thesis. Furthermore, I am very grateful for the funding of my research by the Max Planck Society and the Netherlands Organization for Scientific Research. Additional funding for participation in symposia and international meetings was provided by the Zentrum für Infektionsbiologie und Immunität (ZIBI) graduate school in Berlin.

LIST OF PUBLICATIONS

1. **Matz JM**, Matuschewski K, Kooij TWA. Two putative protein export regulators promote *Plasmodium* blood stage development *in vivo*. Mol. Biochem. Parasitol. 2013; 191:44–52. (cover image)
2. **Matz JM**, Ingmundson A, Costa Nunes J, Stenzel W, Matuschewski K, Kooij TWA. *In vivo* function of PTEX88 in malaria parasite sequestration and virulence. Eukaryot. Cell. 2015; 14:528–534. (cover image)
3. **Matz JM**, Kooij TWA. Towards genome-wide experimental genetics in the *in vivo* malaria model parasite *Plasmodium berghei*. Pathog. Glob. Health. 2015; 109:46–60. (invited review, cover image, editor's choice)
4. **Matz JM**, Goosmann C, Brinkmann V, Grützke J, Ingmundson A, Matuschewski K, Kooij TWA. The *Plasmodium berghei* translocon of exported proteins reveals spatiotemporal dynamics of tubular extensions. Sci. Rep. 2015; 5:12532.
5. Rijpma SR, van der Velden M, Annoura T, **Matz JM**, Kenthirapalan S, Kooij TW, Matuschewski K, van Gemert GJ, van de Vegte-Bolmer M, Siebelink-Stoter R, Graumans W, Ramesar J, Klop O, Russel FG, Sauerwein RW, Janse CJ, Franke-Fayard BM, Koenderink JB. Vital and dispensable roles of *Plasmodium* multidrug resistance transporters during blood- and mosquito-stage development. Mol. Microbiol. 2016; 101:78–91

COVER IMAGES

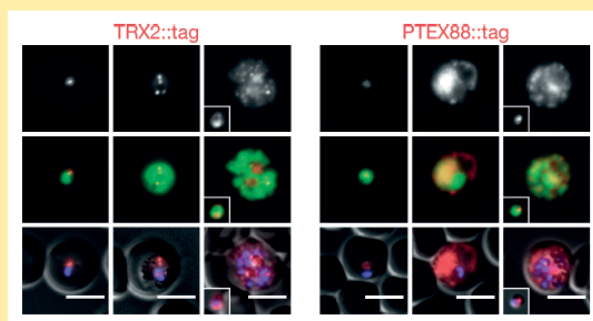
(following pages)



Volume 191, Issue 1, September 2013

ISSN 0166-6851
191 (1) 1–52 (2013)

MOLECULAR & BIOCHEMICAL PARASITOLOGY



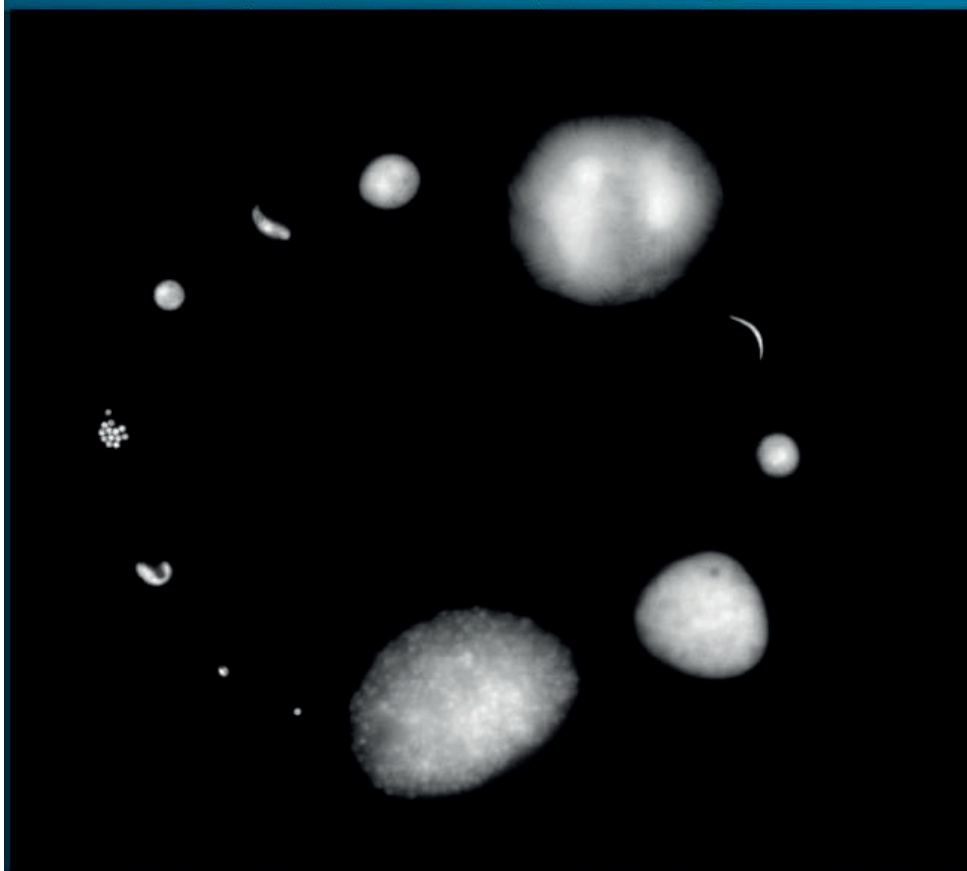
E-submission available:
<http://ees.elsevier.com/molbio/>

Volume 109 Number 2 March 2015

ISSN 2047-7724

Pathogens and Global Health

Experimental genetics in the rodent malaria parasite *Plasmodium berghei*

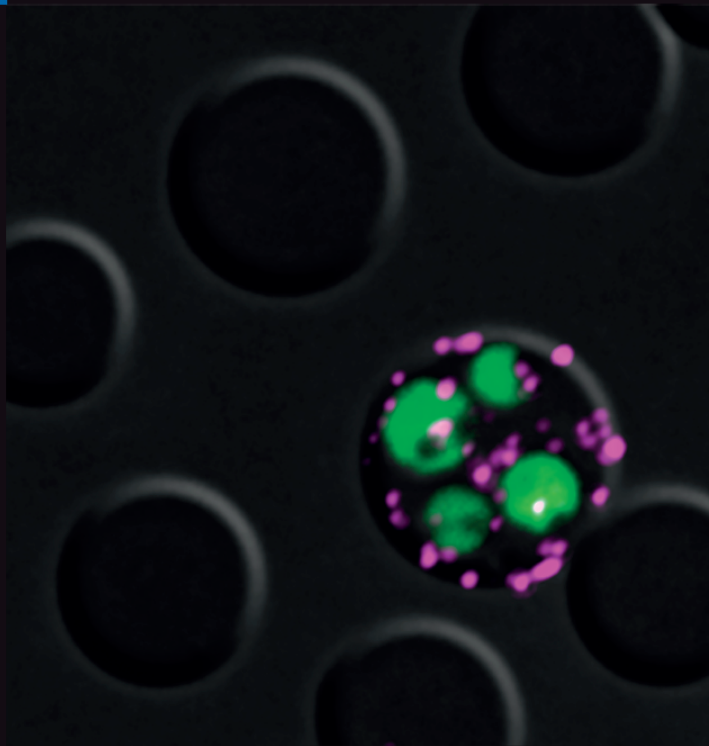


 Maney
Publishing

JUNE 2015

VOLUME 14 | NUMBER 6

Eukaryotic Cell



published monthly by



AMERICAN
SOCIETY FOR
MICROBIOLOGY